UNIVERSIDAD NACIONAL AUTÓNOMA DE MÉXICO

PROGRAMA DE MAESTRÍA Y DOCTORADO

EN INGENIERÍA AMBIENTAL – RESIDUOS SOLIDOS

**DEVELOPMENT AND LOCALIZATION OF
THE INNOVATIVE BIOREFINERY SCHEME FOR BIOBUTANOL PRODUCTION
FROM LIGNOCELLULOSIC BIOMASS IN MEXICO**

TESIS

QUE PARA OPTAR POR EL GRADO DE:

DOCTOR EN INGENIERÍA

PRESENTA

M. en C. Karol Adam Dudek

TUTORA PRINCIPAL

Dra. Idania Valdez Vazquez, Instituto de Ingeniería

COMITÉ TUTORAL

Dr. Germán Buitón Méndez, Instituto de Ingeniería

Dra. Lorena Amaya Delgado, CIATEJ Unidad Zapopan

Santiago de Querétaro, Querétaro, 2023

JURADO ASIGNADO:

Presidente:	Dr. Edson Baltazar Estrada Arriaga
Secretario:	Dr. Germán Buitrón Méndez
1er. Vocal:	Dr. Héctor Arturo Ruiz Leza
2do. Vocal:	Dra. Lorena Amaya Delgado
3er. Vocal:	Dra. Idania Valdez Vazquez

Lugar donde se realizó la tesis: Laboratorio de Investigación de Procesos Avanzados de Tratamiento de Aguas, Unidad Académica Juriquilla-Querétaro, Instituto de Ingeniería, UNAM.

TUTORA DE TESIS:

Dra. Idania Valdez Vazquez

_____

FIRMA

Agradecimientos Académicos

Agradecimientos Personales

Content

Summary

This doctoral dissertation was related to an innovative biorefinery scheme for biofuel production that consists of two cascading consolidated bioprocesses for biological pretreatment of lignocellulosic biomass and acetone-butanol-ethanol (ABE) fermentation from cellulose. Each consolidated bioprocess is mediated by specialized microbiotas. The proposed scheme is characterized by the absence of chemical usages such as acids and bases (except for pH adjustment) and does not apply any physicochemical (high-energy demand) pretreatment. The work was divided into two parts – experimental and simulation.

The first experimental part was dedicated to the solubilization of hemicellulosic fraction of lignocellulosic biomass (agave bagasse) by native microbiota to produce volatile fatty acids (VFA) and hydrogen for energy purposes. Results demonstrated that the nutrients organic nitrogen, calcium ions, and phosphates improved the VFA production and yield by 85 and 92%, respectively, and the soluble chemical oxygen demand by 1.5 times compared to without nutrient addition. Moreover, these nutrients promote the growth of the hydrolytic genera *Cellulomonas*, *Gordonia*, and *Pseudoclavibacter*. Then, the effects of initial pH (5.5 – 6.9) and total solids (TS, 7.8 – 22.1%) on hydrogen production were studied using a response surface methodology. Results showed that initial pH and TS affected two biological processes that occurred in parallel during the solubilization of agave bagasse: i) lactic acid production by lactic acid bacteria and hydrogen production by *Clostridium sensu stricto* 1. While the former acted in the entire pH range studied, the latter performed better at pH > 6.0. Furthermore, higher TS% improved lactic acid formation and, consequently, hydrogen production. The highest butyric acid production at the level of 5.1 g/L and hydrogen production of 4.1 mL H_2/gTS were found at initial pH 6.2 and 22.1% of TS after 48h.

The second experimental part was dedicated to fermenting cellulose into butanol using a butanol-tolerant microbiota. This butanol-tolerant microbiota was obtained previously by adaptive evolution using corn stover as substrate. The aim was to determine the capacity of this butanol-tolerant microbiota for converting the cellulosic fraction into butanol after a long period of storage. Pretreated corn stover and paper filter were used as substrates for comparative purposes. The highest butanol concentration at 23.06 g/L was obtained from corn stover after 120h (productivity

of 0.19 g/L/h). Butanol concentration decreased by 20% using a paper filter as substrate. Instead of acetone and ethanol as co-products, valeric and caproic acids were found at concentrations of 11.02 and 7.07 g/L, respectively, after 168 h from corn stover, and 8.83 and 3.54 g/L, respectively, after 144 h from paper filter. The presence of caproic acid is due to the presence of *Caproiciproducens* in the butanol-tolerant microbiota as a result of chain elongation of butyric acid molecules via the reverse β-oxidation pathway, while valerate is synthesized from propionic acid by the same pathway in the presence of some species of *Clostridium* and *Megasphaera*.

The third experimental part was dedicated to investigating butanol recuperation from a fermentation broth under vacuum distillation in a rotating packed bed. Based on the fermentation broth obtained during consolidated bioprocessing, a synthetic mixture was prepared to investigate butanol recuperation. Firstly, experiments were carried out under total reflux to evaluate the efficiency of the method when thermodynamic equilibrium is reached. Butanol recuperation in the light phase of the top product was found at a concentration of 521.6 g/L, which confirmed the appropriateness of the method for butanol recuperation. Subsequently, experiments with 5% steam stripping were carried out to assess the applicability of the process for commercial use. In the stripping experiment (5%), 126.9 g/L was detected in the light phase, indicating that the method can be used commercially to remove butanol in-situ from fermentation broth. Also, ethanol and furfural were recuperated at high concentrations of 39 and 13 g/L, respectively, during stripping experiments. The butanol-rich phase requires further purification e.g., in a traditional distillation column, to be sold on the market.

The first simulation part aimed to compare the cost-effectiveness of the innovative lignocellulosic biorefinery based on consolidated bioprocesses with a traditional lignocellulosic biorefinery applying a pure culture. Butyric acid was chosen as the main bioproduct and both biorefinery schemes were simulated at plant capacities of 100, 500, and 1000 tonne/d. Results showed that only butyric acid production by innovative biorefineries was economically viable. In the case of traditional biorefineries, the operating costs were 1.2 to 1.5 times higher, while total capital investment was 3-fold higher. This, in turn, resulted in unit production costs 4.7, 5.6, and 7.2 times higher compared to the innovative biorefinery for 100, 500, and 1000 tonne/d plant capacity, respectively. This made no traditional biorefinery plant economically viable. Crucial to the

negative outcome of traditional biorefineries were a high-energy demand sugar concentration stage and expensive materials required for reactor construction.

In the second simulation part, a mathematical optimization model was developed to assess the location of lignocellulose-based biobutanol plants in Mexico. Techno-economic analysis of biobutanol production under the innovative biorefinery was performed for four types of biomass: agave bagasse, corn stover, sugarcane bagasse, and wheat straw at three plant capacities: 500, 1500, and 2400 tonne/d. Additionally, a total Net Present Value (NPV) included biomass supply chain and biobutanol distribution to TAR (from Spanish: Terminales de Almacenamiento y Reparto) of PEMEX. The minimum demand was equal to the amount of biobutanol needed to blend 16% by volume with the gasoline consumed annually in Mexico. While maximum demand was equivalent to the total gasoline consumed in Mexico annually. The mathematical model with an objective function to meet the maximum biobutanol demand equal to the volume of gasoline tanks in 65 TAR suggested the establishment of biorefineries at 13 out of 34 considered locations, which 7 of them processing corn stover at plant capacity of 2400 tonne/d, five sugarcane bagasse at 2400 tonne/d and 1 of wheat straw with a capacity of 1500 tonne/d. The required initial investment was estimated to be $US 5,636,663,000 with a determined NPV income of $US 3,350,387,969. In order to cover the minimum biobutanol demand by 65 TAR of PEMEX, the model specified a minimum investment capital of $US 918,712,000 to establish two biobutanol plants processing corn stover at a plant capacity of 2400 tonnes/d.

1. CHAPTER I: General Introduction

1.1. Basic theoretical concepts

1.1.1. Biorefinery

The main environmental changes arise from human activities transforming materials into products and services to meet socio-economic development. To date, the main source of energy is fossil fuels (coal, oil, natural gas), the combustion of which causes air pollution and greenhouse gas emissions (Perera & Nadeau, 2022). Close to 89% of total CO_2 emissions in 2021 came from energy combustion and industrial processes (IEA, 2022). In Mexico alone, around 418 million tonnes of CO_2 were produced in 2021 (Friedlingstein et al., 2022). The increasing use of fossil fuels, most of which are derived from oil, has been questioned particularly in terms of long-term environmental, energy, and material sustainability. Therefore, it is important to increase and develop knowledge related to the sustainable and energy-efficient production of energy and goods. The biorefinery concept associated with this area is currently being widely studied. A biorefinery is a facility that integrates biomass conversion processes, technology, and equipment for the production of a variety of bioproducts, including biochemicals, biofuels, and biomaterials (Figure 1.1) (Cherubini, 2010). Biorefinery use as an input of renewable organic resources or wastes. The aim of a biorefinery is to maximize the value derived from biomass feedstock by producing multiple products and minimizing waste while reducing environmental impact and promoting sustainability (Barragán-Ocaña et al. 2023).
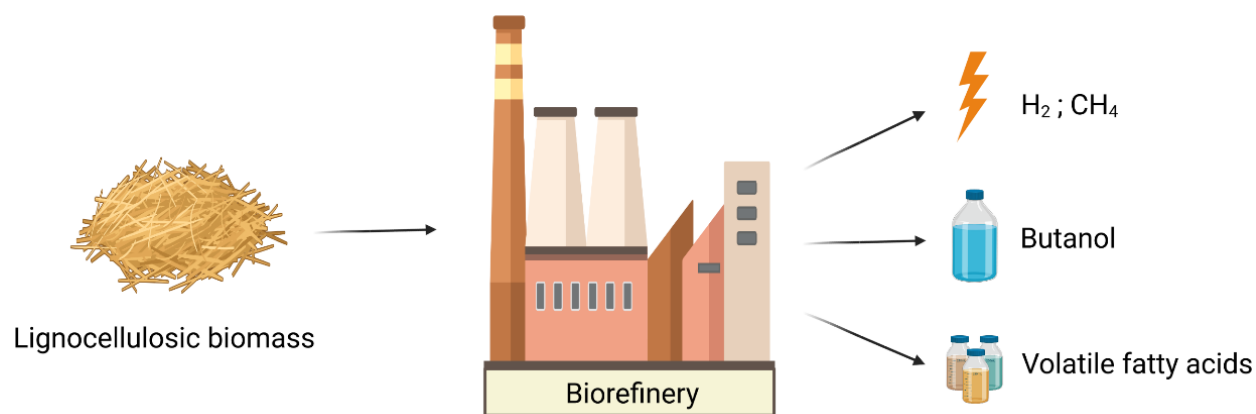
Figure 1.1. A simple visualization of the idea of a biorefinery processing lignocellulosic biomass (created with BioRender.com).

The biorefinery concept is considered an essential part and operation strategy for the circular bioeconomy, which aims to reduce reliance on fossil fuels and move towards a more sustainable, low-carbon economy. Biorefineries can help to create new markets for agricultural and forestry residues, generate employment opportunities in rural areas, and reduce greenhouse gas emissions (Haribabu et al., 2022). They can be categorized based on feedstock input, applied technology, and type of produced bioproducts.

The traditional biorefinery scheme consists of six main stages: *i)* feedstock condition; *ii)* pretreatment of biomass and fraccionation; *iii)* enzymatic hydrolysis *iv)* inoculum growth; *v)* fermentation; *vi)* downstream process; and *vii)* wastewater treatment.

i)   feedstock condition is a preliminary stage in which the biomass matter is ground to reduce particle size and thus increase the contact surface;

ii)   biomass pretreatment stage refers to a chemical process of biomass in the presence of a chemicals (i.e. acids) at high temperature or pressure to destroy the raw structure making it more susceptible to enzymatic hydrolysis;

iii)   enzymatic hydrolysis is a process that uses enzymes to break down complex molecules, such as polysaccharides and proteins, into smaller moleculese;

iv)   inoculum growth stage referes to a small-scale bioreactor used to produce high-quality microorganisms such as bacteria or yeast used to start a fermentation process;

v)   fermentation is a metabolic process carried out by microorganisms that convert the simple sugars released during enzymatic hydrolysis into various bio-products such as VFA, hydrogen, methane, alcohols.

vi)   downstream process is a final stage, where set of methods and techniques is used to purify, concentrate and isolate produced bioproducts.

vii)   wastewater treatment is an additional stage required in a biorefinery where organic matter must to be removed from wastewater to ensure that the production process is sustainable and environmentally friendly.

1.1.2.   Feedstocks

Biorefinery can process a wide range of organic wastes, including agricultural residues such as agave and sugarcane bagasse, corn stover, and wheat straw (Wang et al. 2021). Likewise, energy

crops (switchgrass, miscanthus, willow, and poplar) are typically grown specifically for energy production (Clifton-Brown et al. 2019). Algae, commonly related to fourth-generation biofuels, is composed of proteins (39 – 61%), carbohydrates (10 – 50%), lipids (2 – 38%), and nucleic acid (0 – 6%) (Demirbas and Fatih Demirbas, 2011; Shokravi et al. 2021). Organic Fraction of Municipal Solid Waste (OFMSW) is a complex, variable, and heterogeneous waste from households, restaurants, small businesses, yards, and garden wastes (López-Gómez et al. 2019). In addition, biomass may contain inert materials such as food packaging, plastics, glass, metals, textiles, etc., due to inefficient waste sorting. The challenge is to remove inorganic particles to improve process efficiency (Ponsá et al. 2010). Industrial wastes are another group of organic effluents, such as vinasse, that consists of high chemical oxygen demand (60 – 134 g/L) and biochemical oxygen demands (16 – 96 g/L), and average contents of nitrogen (0.55 – 4.2 g/L), phosphorus (0.13 – 3.03 g/L), and potassium (2 – 17.5 g/L) (Quintero-Dallos et al., 2019) or cheese whey composed by water (93 – 94%), lactose (4.5 – 5%), protein (0.8 – 1%) (Kasapcopur et al. 2021), which can also be processed in a biorefinery.

This dissertation focuses on lignocellulosic biomass of agricultural origin, which is an economical and highly available renewable source for energy production and value-added bioproducts (Rodionova et al., 2022). Its annual global availability is estimated at 181.17 billion tonnes (Ashokkumar et al., 2022). Corn, wheat, and sugar cane, as the three most abundant crops in Mexico, yield approximately 26 million tonnes of dry lignocellulosic biomass per year at strategic locations with the prospect of establishing biorefinery facilities (Dudek et al. 2023mxcad).
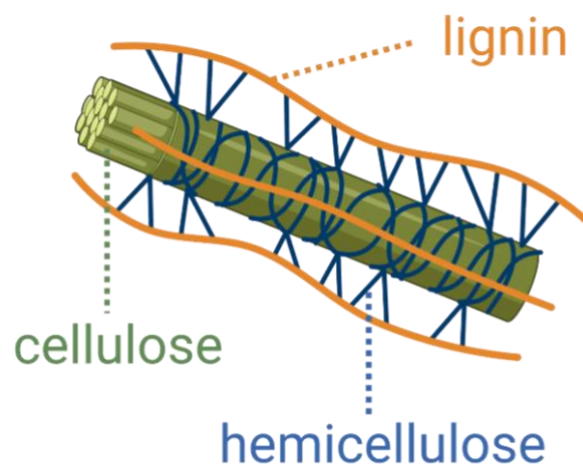
Figure 1.2. Lignocellulosic biomass structure (created with BioRender.com).

Lignocellulosic biomass comprises three polymers: cellulose, hemicellulose, and lignin (Figure 1.2). Cellulose is the main component (9% – 80%), and its fibers consist entirely of glucose. Glucan cellulose chains are linked by hydrogen bonds and van der Waals forces to form long, thread-like crystalline structures called cellulose microfibrils. The shape, size and crystallinity of these microfibrils are important structural parameters that determine the efficiency of the polymer conversion to bioproducts through the biochemical pathway (Rongpipi et al., 2019). Hemicellulose is the second most abundant polymer of lignocellulosic biomass (10% – 50%). Its short, linear, and highly branched heteropolymeric structure is composed of various monomers such as arabinose, galactose, mannose, xylose, 4-O-methylglucuronic and galacturonic acid residues. Lignin (5 – 35%) is a cross-linked phenolic polymer consisting mainly of p-hydroxy- phenyl, guaiacyl and syringyl monomers (Zhou et al., 2016). Its hyper-branched topology without regular repeats and insolubility makes it very difficult to degrade (MekonnenTeto, 2021). This polymer blocks enzymatic digestibility of monosaccharides found in cellulose and hemicellulose (Ji et al., 2022). The ratio of these three monomeric units varies considerably depending on the nature and origin of the biomass (Li et al., 2013).

1.1.3. Products

Depending on the raw material and the technology used, a wide range of biobased products can be obtained within the biorefinery concept. Outbound products can be divided into two main groups. Energy products that include bioethanol, biobutanol, biodiesel, biomethane and other synthetic biofuels, biohydrogen, electricity and heat. While, material products are food, animal feed, fertilizers, glycerine, biomaterials, chemicals and building blocks, polmers and resins (Cherubini et al. 2009).

Lignocellulosic biomass consists of three main polymers that differ in structure and properties. Cellulose and hemicellulose are carbohydrate chains employd for bioenergy production including bioethanol, biobutanol, biohydrogen, biomethane and low molecular organic compounds such as short- and medium-chain volatile fatty acids. The recalcitrant macromolecular lignin component is used in the production of synthetic aromatic polymers such as composite films, polyimides, resins and thermoplastics. The cascade utilisation of biomass, which involves the progressive decomposition of polymers starting with haemicellulose, then cellulose and lignin, followed by a

separation process of the individual components, is the key to effective and highly efficient biomass processing (Ashokkumar et al. 2021).

Biobutanol is an interesting bioproduct due to its properties. It is an organic compound with a four-carbon linear chain (C_4H_9OH), a molecular weight of 74.12 g/mol and a density of 0.81 g/cm3 at 20℃. More details of its physico-chemical properties can be found under CAS number 71-36-3 (Api et al., 2019). Butanol finds an application in the pharmaceutical and cosmetics industry, is used for solvent, eluent, extractant and biofuels production (Talan et al., 2021). Its use as a biofuel ingredient has attracted particular interest recently. Biobutanol has higher energy density then ethanol (36 vs 26.8 MJ/kg) (Rathour et al., 2018), and its lower vapor pressure (0.9 vs 7.9 kPa at 25℃) (Butler et al., 1935; Kretschmer & Wiebe, 1949) improve cold-start conditions. Furthermore, n-butanol has a lower polarity than ethanol (1.66 vs. 1.7) due to the larger carbon chain and this results in a lower importance of the hydroxyl group (-OH), hence, a better stability of n-butanol is observed compared to ethanol blends (Lapuerta et al., 2018). Also, butanol can be mixed with petrol at any concentration without engine modification (Elsemary et al., 2016).

1.1.4. Butanol production

Conventional butanol production takes place in the oil refinery, where oil is processed into a number of marketable products such as chemicals, energy, and fuels. Butanol is formed by processing crude oil through one of three pathways: crotonaldehyde hydrogenation, Reppe synthesis and oxynthesis (hydroformylation) (Abo et al., 2019). The crotonaldehyde hydrogenation occurs at ambient temperature and pressure, involves aldo-condensation of acetaldehyde in the presence of alkaline catalysts, followed by dehydration resulting from the application of acids (acetic or fosforic). Finally, synthesized crotonaldehyde undergoes distillation and hydrogenation in the gas or liquid phase in the presence of a Cu catalyst (Panahi et al. 2019). Butanol production by Reppe synthesis takes place at 100°C and 15 atm. It involves the reaction of propene with carbon monoxide and water in the presence of $Fe(CO)_5$ catalyst. The process has selectivity of 90% and the formed mixture butanol:isobutanol has proportion 85:15 (Liu et al. 2013). Butanol oxosynthesis (hydroformylation) usually require propylene which undergoes hydroformylation to form aldehydes, followed by hydrogenated which gives n-butanol. Another fossil oil derivatives, such as ethylene and triethylthe aluminum can be use for butanol production by oxosynthesis (Patil et al. 2019).

At the beginning of the 20th century, Weizmann discovered the production of biobutanol by acetone-butanol-ethanol (ABE) fermentation (Moon et al., 2016). It is a biphasic bioprocess consisting on acidogenesis where acetic and butyric acids are produced from glucose convertion by acidogenic bacteria. Extracellular pH changes and onset of sporulation results in metabolic shift to solventogenesis, where two alcohols: ethanol from Acetyl-CoA and butanol from Butyryl-CoA together with ketone: acetone from Acetoacetyl-CoA are produced (Buehler and Mesbah, 2016). Factors such as temperature (Sidi Ahmad and Abdul Munaim, 2017), pH (Bahl et al. 1982), nutrient supplementation (McNeil and Kristiansen, 1987), product inhibition (Li et al. 2020) and redox state (Wang et al., 2012) affect ABE fermentation. Species of the Clostridia genus including *Clostridium saccaroper butylacetonicum*, *Clostridium acetobutylicum*, *Clostridium sacharoaceto butylicum* and *Clostridium beijerinckii* are the most efficient in converting glucose into biobutanol (Buehler and Mesbah, 2016; Riaz et al., 2022).

Traditional butanol production from lignocellulosic biomass by ABE fermentation employ pure culture and involves three main stages carry out as a separated units. The process begins with hydrolysis followed by a detoxification step and then fermentation. Due to low yields, genetically modified Clostridium sp. are frequently employed yield (Gao et al., 2014; Guo et al., 2022). Recently, the consolidated bioprocess (CBP) for biobutanol production from lignocellulosic biomass has been developed as an alternative method. The concept of the method focuses on the cooperation of microorganisms to simultaneously degrade the cellulose polymer to glucose and its parallel conversion to biobutanol (Putro et al. 2016).

Biobutanol production at yield of 0.15 g butanol/g biomass, from all available amount of lignocellulosic biomass in Mexico could produced approximately 3.6 million tonnes of biobutanol, which would meet 67% of the total demand for butanol worldwide (Fernández, 2022).

1.1.5. Butanol purification

The butanol purification process can be carried out by various methods including distillation, extraction, adsorption, membrane filtration and crystallization. In distillation process solvents are heated until reached boiling temperature and vaporizate to another stage of distillation column, where condens. The impurities are left behind. The method is based on the physico-chemical properties of the components being separated, specifically the differences in boiling point between

the components. Extraction is another method frequently combined with distillation. It is used as a preliminary step to reduce the volume of liquid to be distilled. Extration involves mixing butanol with a solvent with high selectivity such as mesitylene, followed by further separation of butanol from the solvent. (Sanchez et al., 2017; Valdez-Vazquez and Sanchez, 2018). Butanol can be purified in adsorption process as well. A specific material with a high active surface area and adsorption properties, such as activated carbon, silica gel or zeolite, is used to attract and hold impurities. Mixture is passing through a bed of absorbing material. Pollutants are captured and retained, while butanol passes through (Chiang et al., 2019). Membrane filtration is a process that uses a semi-permeable membrane to separate butanol and solvents sucha as ethanol and acetone from impurities based on size or molecular weight. This method can be used to purify butanol in a continuous process (Knozowska et al., 2021).

The choice of purification method depend on the specific impurities present, the desired purity level, and the economics of the process. So far, distillation is the most commonly used method to purify butanol from ABE fermentation. For most alcohols its direct separation from water by single distillation is impossible due to azeotrope formation. However, in the case of binary water-n-butanol mixture exist miscibility gap for butanol mole fraction (0.02 – 0.45) at boiling point and pressure of 1.013 bar, which separate mixture into a water-rich phase and butanol-rich phase (Card & Farrell, 1982). Therefore, a rotating packed bed (RPB) could be a proper equipment for biobutanol separation from fermentation broth.

The rotating packed bed (RPB) structure consists of a rotating cylindrical bed and a static housing (Figure 1.3). The rotating part is driven by a motor, and the axis of rotation of the motor can be horizontal or vertical. Liquid phase is introduced through the liquid inlet located in the upper centric part of the housing into the rotary packed bed and flows through packing material due to centrifugal forces. Gaseous phase is introduced through the gas inlet located on the edge of the top cover and flows in the opposite direction to the liquid phase and simultaneously interacts with it at the same time (Wang et al., 2019). High gravity (higee) technology by introducing a centrifugal force up to 1000g bypasses the gravitational constraint that limits separation and reaction process. In that way improves heat, momentum transfer, and mass transfer. Therefore, RPB is a promising technology for distillation purpose (Neumann et al., 2018).
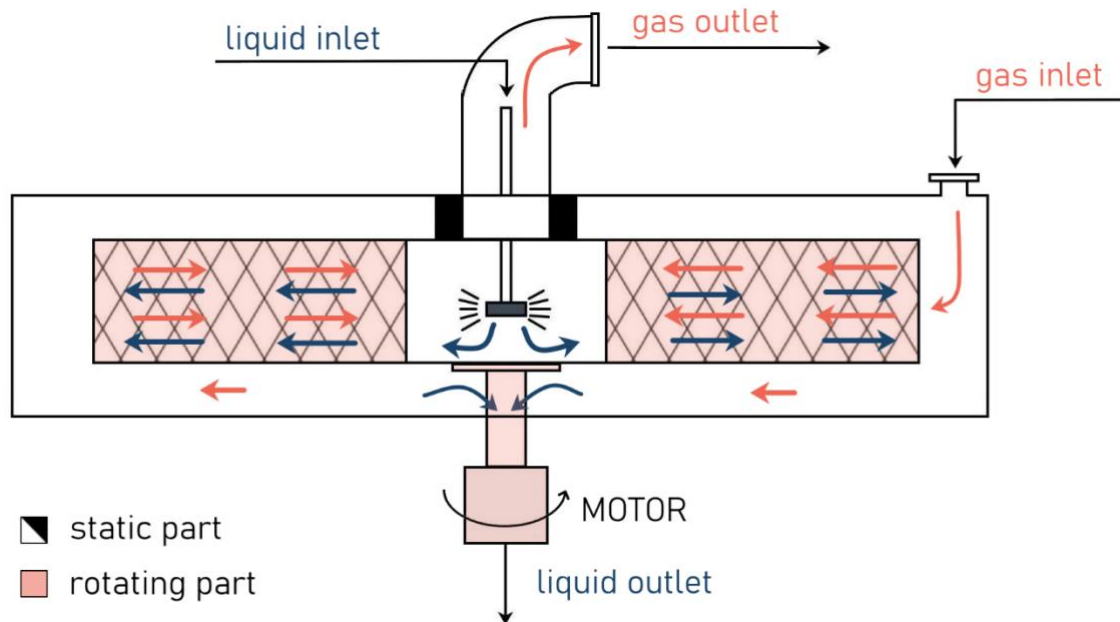
Figure 1.3. Construction of the RPB structure.

1.1.6. Wastewater treatment

Various stages of a traditional biorefinery plant such as biomass pretreatment and fermentation generate wastewater that is characterized by high levels of organic matter such as VFAs (mainly acetic, butyric and propionic acids), as well as nutrients, and suspended solids (Chakhtouna et al., 2022). Their removal from the wastewater is a critical step to minimize a biorefinery impact on the environment and reduce its water consumption. There are several wastewater treatment technologies such as membrane filtration, reverse osmosis, coagulation and flocculation, aerobic treatment, and anaerobic digestion. The last of these is the most promising for lignocellulosic biomass, as biomethane is produced from organic matter, making biorefinery more viable (Srivastava et al., 2018). The potential of biomethan production from lignocellulosic biomass though metabolic pathways varied depending on pretreatment method and type biomass processed (Buitrón et al., 2019).

1.1.7. Economic assessement of biobutanol biorefinery

A techno-economic evaluation of a biorefinery facility is a comprehensive assessment of the used technology for feedstock processing and economic feasibility of energy and material products production from biomass resources. Economic assessment provides a quantitative analysis of the investment capital require for facility establishment, operating costs associated with converting the

input organic material into various bioproducts and the potential revenue from the sale of the products produced by the biorefinery. Techno-economic evaluation involves a detail analysis of feedstock availability and composition, methodology and technology design set for appropriate biomass convertion into desired bio-based products, economic evaluation of required equipment, labor, utilities and operating cost, ending with overall determination of the internal rate of return, net present value (NPV), and payback period. A techno-economic assessment can provide valuable insights to investors and stakeholders interested in developing a sustainable bio-based economy and influence decision-making.

Various methods and tools exist to perform techno-economic assessments and enrich information for decision-making. There are several software program such as SuperPro Designer, BioSTEAM, TEA (Techno Economic Analysis) developed by the National Renewable Energy Laboratory (NREL) that permit simulate technology design, process analysis and optimization on the industrial scale. SimaPro is a life cycle assessment computer program that can be used to evaluate the environmental impacts of biorefinery processes. Methematical optimization model together with commercially available solvers such as CPLEX is an efficient method for decision-making support. More recently, the use of geographic information systems (GIS) software, such as QGIS, has begun to gain importance in facility location decisions-making.

1.1.6.1   SuperPro Designer

SuperPor Designer is a software program developed by Intelligen, Inc. and is designed for development and optimization of batch and continuous bioprocesses. It includes a suits of tools for process modeling, cost analysis, and optimization. It is designed to properly support the development of sustainable biorefineries. The software can be used for modeling biomass condition, biomass pretreatment by physico-chemical or biological methods, enzymatic hydrolysis, fermentation, filtration, seed cultivation, purification, cogeneration stage, among others. Users can create custom models where processes are simulated using data and equipment properties provided by the software developers, as well as properties can be customized to suit specific needs.

The software can be used to estimate the capital and operating costs of a design facility scheme, and to evaluate the economic feasibility of a given process design. The economic analysis can be performed at different levels of detail, from a high-level screening analysis to a detailed project-level analysis. Additionally, the program can be used for sensivity analysis, optimization studies.

The simulations carried out are a source of information that can be used to support decision-making related to process design, technology selection, and investment.

1.1.6.2 Mathematical programming

Mathematical programming refers to mathematical models which manipulating a lot of variables and constraints find solutions to problems such as optimization or decision-making problems (Naud et al., 2020, p. 4). The Linear Programming (LP) attempt to find the feasible area and optimize the solution to obtain the highest (maximization) or the lowest (minimalization) values of the objective function which is subjected to the constraints in the form of linear equations or in the form of linear inequalities (Sierksma et al., 2015). The mathematical problem described requires a solver, i.e. a computer program that interprets the mathematical description as input data and carry out calculation using complex algorithms until the optimal solution of the model is found, giving the output data (Koch et al., 2022). For instance, a simple example of a mathematical problem can be described using linear programming, as shown in the Figure 1.4, while its solution can be found/expressed in graphical from, as depicted in the Figure 1.5.

$$\text{Maximize Profit} = 2A + 8B \qquad \text{Objective function}$$

$$
\left.
\begin{aligned}
5A + B &\leq 21 \\
6A + 3B &\leq 44 \\
2A + 2B &\leq 17 \\
A, B &\geq 0
\end{aligned}
\right\} \text{Constraints}
$$

$$
\left.
\begin{aligned}
A &= ? \\
B &= ?
\end{aligned}
\right\} \text{Variables}
$$

Figure 1.4. Simple mathematical problem description.
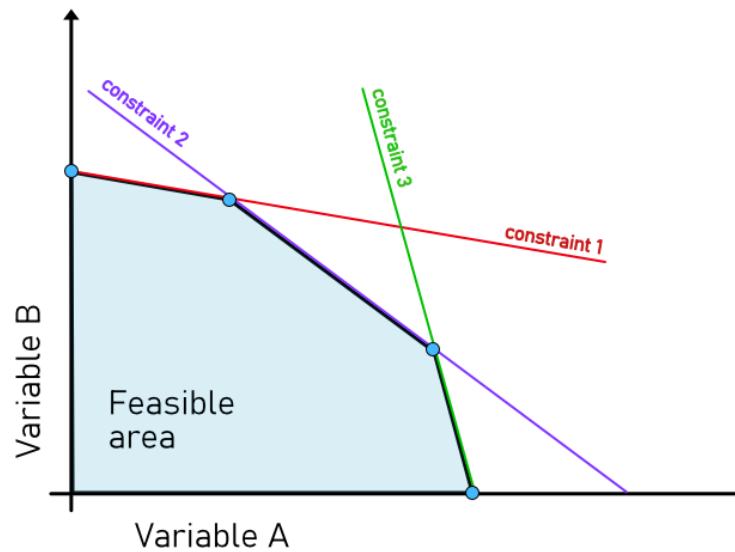
Figure 1.5. Graphical solution of the LP problems.

1.1.6.3 Geographical information system

A geographic information system (GIS) is a useful tool for creates, manages, analyzes, display and store many types of data that are represented spatially or geographically (Lü et al., 2019). GIS connects a data with longitude and latitude to determinate its location on the Earth. This provides a better view on analyzing data and helps users understand patterns, relationships, and geographic context. In recent years, it has been widely used in science and almost every industry because of benefits such as improved communication and efficiency, as well as better management and decision-making (Goodchild, 2018).

In this study, a GIS was used for the economic evaluation of a biorefinery plant in Mexico. Having data related to biomass supplier, road infrastructure, location of industries parks, location of populated area, availability of water and electricity visualized in the map permit in better way suggest the possible location of lignocellulosic-based biorefinery plants.

1.1.8.   References

Abo, B. O., Gao, M., Wu, C., Zhu, W., & Wang, Q. (2019). A review on characteristics of food waste and their use in butanol production. *Reviews on Environmental Health*, *34*(4), 447–457. https://doi.org/10.1515/reveh-2019-0037

Api, A. M., Belmonte, F., Belsito, D., Biserta, S., Botelho, D., Bruze, M., Burton, G. A., Buschmann, J., Cancellieri, M. A., Dagli, M. L., Date, M., Dekant, W., Deodhar, C., Fryer, A. D., Gadhia, S., Jones, L., Joshi, K., Lapczynski, A., Lavelle, M., … Tsang, S. (2019). RIFM fragrance ingredient safety assessment, butyl alcohol, CAS Registry Number 71-36-3. *Food and Chemical Toxicology*, *134*, 111000. https://doi.org/10.1016/j.fct.2019.111000

Ashokkumar, V., Venkatkarthick, R., Jayashree, S., Chuetor, S., Dharmaraj, S., Kumar, G., Chen, W.-H., & Ngamcharussrivichai, C. (2022). Recent advances in lignocellulosic biomass for biofuels and value-added bioproducts—A critical review. *Bioresource Technology*, *344*, 126195. https://doi.org/10.1016/j.biortech.2021.126195

Bahl, H., Andersch, W., Braun, K., & Gottschalk, G. (1982). Effect of pH and butyrate concentration on the production of acetone and butanol by Clostridium acetobutylicum grown in continuous culture. *European Journal of Applied Microbiology and Biotechnology*, 14(1), 17–20. https://doi.org/10.1007/BF00507998

Barragán-Ocaña, Merritt, H., Sánchez-Estrada, O. E., Méndez-Becerril, J. L., & Del Pilar Longar-Blanco, M. (2023). Biorefinery and sustainability for the production of biofuels and value-added products: A trends analysis based on network and patent analysis. *PloS One*, 18(1). https://doi.org/10.1371/journal.pone.0279659

Buehler, A.E., & Mesbah, A. (2016). Kinetic Study of Acetone-Butanol-Ethanol Fermentation in Continuous Culture. *PloS One*, 11(8). https://doi.org/10.1371/journal.pone.0158243

Buitrón, G., Hernández-Juárez, A., Hernández-Ramírez, M. D., & Sánchez, A. (2019). Biochemical methane potential from lignocellulosic wastes hydrothermally pretreated. *Industrial Crops and Products*, *139*, 111555. https://doi.org/10.1016/j.indcrop.2019.111555

Butler, J. A. V., Ramchandani, C. N., & Thomson, D. W. (1935). 58. The solubility of non-electrolytes. Part I. The free energy of hydration of some aliphatic alcohols. *Journal of the Chemical Society (Resumed)*, 280. https://doi.org/10.1039/jr9350000280

Card, J. C., & Farrell, L. M. (1982). Separation of alcohol-water mixtures using salts. *Oak Ridge National Lab., TN (USA)*. https://doi.org/10.2172/5250443

Chakhtouna, H., Benzeid, H., Zari, N., Qaiss, A. el kacem, & Bouhfid, R. (2022). Recent advances in eco-friendly composites derived from lignocellulosic biomass for wastewater treatment. *Biomass Conversion and Biorefinery*. https://doi.org/10.1007/s13399-022-03159-9

Cherubini. F. (2010). The biorefinery concept: Using biomass instead of oil for producing energy and chemicals. *Energy Conversion and Management*, 51(7), 1412–1421. https://doi.org/10.1016/j.enconman.2010.01.015

Cherubini, F., Jungmeier, G., Wellisch, M., Willke, T., Skiadas, I., Van Ree, R., & de Jong, E. (2009). Toward a common classification approach for biorefinery systems. *Biofuels, Bioproducts and Biorefining*, 3(5), 534–546. https://doi.org/10.1002/bbb.172

Chiang, Y., Liang, W., Yang, S., Bond, C. R., You, W., Lively, R. P., & Nair, S. (2019). Separation and Purification of Furans from n-Butanol by Zeolitic Imidazole Frameworks: Multicomponent Adsorption Behavior and Simulated Moving Bed Process Design. *ACS Sustainable Chemistry & Engineering*, 7(19), 16560–16568. https://doi.org/10.1021/acssuschemeng.9b03850

Clifton-Brown, J., Harfouche, A., Casler, M. D., Dylan Jones, H., Macalpine, W. J., Murphy-Bokern, D., Smart, L. B., Adler, A., Ashman, C., Awty-Carroll, D., Bastien, C., Bopper, S., Botnari, V., Brancourt-Hulmel, M., Chen, Z., Clark, L. V., Cosentino, S., Dalton, S., Davey, C., Dolstra, O., Donnison, I., Flavell, R., Greef, J. (2019). Breeding progress and preparedness for mass-scale deployment of perennial lignocellulosic biomass crops switchgrass, miscanthus, willow and poplar. *Global Change Biology - Bioenergy*, 11(1), 118–151. https://doi.org/10.1111/gcbb.12566

Demirbas, A., & Fatih Demirbas, M. (2011). Importance of algae oil as a source of biodiesel. *Energy Conversion and Management*, 52(1), 163–170. https://doi.org/10.1016/j.enconman.2010.06.055

Elsemary, I. M. M., Attia, A. A. A., Elnagar, K. H., & Elaraqy, A. A. M. (2016). Experimental investigation on performance of single cylinder spark ignition engine fueled with hydrogen-

gasoline mixture. *Applied Thermal Engineering*, *106*, 850–854. https://doi.org/10.1016/j.applthermaleng.2016.05.177

Fernández, L. (2022). *Market volume of n-Butanol worldwide from 2015 to 2021, with a forecast for 2022 to 2029*. https://www.statista.com/statistics/1245211/n-butanol-market-volume-worldwide/

Friedlingstein, P., O'Sullivan, M., Jones, M. W., Andrew, R. M., Gregor, L., Hauck, J., Le Quéré, C., Luijkx, I. T., Olsen, A., Peters, G. P., Peters, W., Pongratz, J., Schwingshackl, C., Sitch, S., Canadell, J. G., Ciais, P., Jackson, R. B., Alin, S. R., Alkama, R., … Zheng, B. (2022). Global Carbon Budget 2022. *Earth System Science Data*, *14*(11), 4811–4900. https://doi.org/10.5194/essd-14-4811-2022

Gao, K., Boiano, S., Marzocchella, A., & Rehmann, L. (2014). Cellulosic butanol production from alkali-pretreated switchgrass (Panicum virgatum) and phragmites (Phragmites australis). *Bioresource Technology*, 174, 176–181. https://doi.org/10.1016/j.biortech.2014.09.152

Goodchild, M. F. (2018). Reimagining the history of GIS. *Annals of GIS*, *24*(1), 1–8. https://doi.org/10.1080/19475683.2018.1424737

Guo, Y., Liu, Y., Guan, M., Tang, H., Wang, Z., Lin, L., & Pang, H. (2022). Production of butanol from lignocellulosic biomass: Recent advances, challenges, and prospects. *RSC Advances*, 12(29), 18848–18863. https://doi.org/10.1039/D1RA09396G

Haribabu, K., Sivasubramanian, V., Deepanraj, B., & Ong, H. C. (2022). Thematic issue: Bioenergy and biorefinery approaches for environmental sustainability. Biomass Conversion and Biorefinery, 12(5), 1433–1433. https://doi.org/10.1007/s13399-021-01989-7

IEA. (2022). *Global Energy Review: CO2 Emissions in 2021*. https://www.iea.org/reports/global-energy-review-co2-emissions-in-2021-2

Ji, H., Wang, L., Tao, F., Yao, Z., Li, X., Dong, C., & Pang, Z. (2022). A hydrotrope pretreatment for stabilized lignin extraction and high titer ethanol production. *Bioresources and Bioprocessing*, *9*(1), 40. https://doi.org/10.1186/s40643-022-00530-6

Kasapcopur, E., Mohammed, A. M., & Colakoglu, A. S. (2021). Effects of differences in whey composition on the physicochemical properties of whey butter. *International Journal of Dairy Technology*, 74(3), 535–546. https://doi.org/10.1111/1471-0307.12782

Knozowska, K., Kujawska, A., Li, G., Kujawa, J., Bryjak, M., Kujawski, W., Lipnizki, F., Ahrné, L., Petrinić, I., & Kujawski, J. K. (2021). Membrane assisted processing of acetone, butanol, and ethanol (ABE) aqueous streams. *Chemical Engineering and Processing*, 166, 108462. https://doi.org/10.1016/j.cep.2021.108462

Koch, T., Berthold, T., Pedersen, J., & Vanaret, C. (2022). Progress in mathematical programming solvers from 2001 to 2020. *EURO Journal on Computational Optimization*, *10*, 100031. https://doi.org/10.1016/j.ejco.2022.100031

Kretschmer, C. B., & Wiebe, Richard. (1949). Liquid-Vapor Equilibrium of Ethanol—Toluene Solutions. *Journal of the American Chemical Society*, *71*(5), 1793–1797. https://doi.org/10.1021/ja01173a076

Lapuerta, M., Rodríguez-Fernández, J., Fernández-Rodríguez, D., & Patiño-Camino, R. (2018). Cold flow and filterability properties of n-butanol and ethanol blends with diesel and biodiesel fuels. *Fuel*, *224*, 552–559. https://doi.org/10.1016/j.fuel.2018.03.083

Li, L., Rowbotham, J. S., Christopher Greenwell, H., & Dyer, P. W. (2013). An Introduction to Pyrolysis and Catalytic Pyrolysis: Versatile Techniques for Biomass Conversion. In *New and Future Developments in Catalysis* (pp. 173–208). Elsevier. https://doi.org/10.1016/B978-0-444-53878-9.00009-6

Li, S., Huang, L., Ke, C., Pang, Z., & Liu, L. (2020). Pathway dissection, regulation, engineering and application: lessons learned from biobutanol production by solventogenic clostridia. *Biotechnology for Biofuels*, 13(1), 39–39. https://doi.org/10.1186/s13068-020-01674-3

Liu, H., Wang, G., & Zhang, J. (2013). The Promising Fuel-Biobutanol. In Z. Fang (Ed.), Liquid, Gaseous and Solid Biofuels. *IntechOpen*. https://doi.org/10.5772/52535

López-Gómez, J.P., Latorre-Sánchez, M., Unger, P., Schneider, R., Coll Lozano, C., & Venus, J. (2019). Assessing the organic fraction of municipal solid wastes for the production of lactic acid. *Biochemical Engineering Journal*, 150, 107251. https://doi.org/10.1016/j.bej.2019.107251

Lü, G., Batty, M., Strobl, J., Lin, H., Zhu, A.-X., & Chen, M. (2019). Reflections and speculations on the progress in Geographic Information Systems (GIS): A geographic perspective.

International Journal of Geographical Information Science, *33*(2), 346–367. https://doi.org/10.1080/13658816.2018.1533136

McNeil, B., & Kristiansen, B. (1987). The effect of medium composition on the acetone-butanol fermentation in continuous culture. *Biotechnology and Bioengineering*, 29(3), 383–387. https://doi.org/10.1002/bit.26029031

MekonnenTeto, A. (2021). A Review on Biodegradation and Biological Treatments of Cellulose, Hemicellulose and Lignin. 10(103).

Moon, H. G., Jang, Y.-S., Cho, C., Lee, J., Binkley, R., & Lee, S. Y. (2016). One hundred years of clostridial butanol fermentation. *FEMS Microbiology Letters*, fnw001. https://doi.org/10.1093/femsle/fnw001

Naud, O., Taylor, J., Colizzi, L., Giroudeau, R., Guillaume, S., Bourreau, E., Crestey, T., & Tisseyre, B. (2020). Chapter 4—Support to decision-making. In A. Castrignanò, G. Buttafuoco, R. Khosla, A. M. Mouazen, D. Moshou, & O. Naud (Eds.), *Agricultural Internet of Things and Decision Support for Precision Smart Farming* (pp. 183–224). Academic Press. https://doi.org/10.1016/B978-0-12-818373-1.00004-4

Neumann, K., Gladyszewski, K., Groß, K., Qammar, H., Wenzel, D., Górak, A., & Skiborowski, M. (2018). A guide on the industrial application of rotating packed beds. *Chemical Engineering Research and Design*, *134*, 443–462. https://doi.org/10.1016/j.cherd.2018.04.024

Panahi, K.S., Dehhaghi, M., Kinder, J. E., & Ezeji, T. C. (2019). A review on green liquid fuels for the transportation sector: a prospect of microbial solutions to climate change. *Biofuel Research Journal*, 6(3), 995–1024. https://doi.org/10.18331/BRJ2019.6.3.2

Patil, R. C., Suryawanshi, P. G., Kataki, R., & Goud, V. V. (2019). Chapter 8—Current challenges and advances in butanol production. In M. Rai & A. P. Ingle (Eds.), *Sustainable Bioenergy* (pp. 225–256). Elsevier. https://doi.org/10.1016/B978-0-12-817654-2.00008-3

Perera, F., & Nadeau, K. (2022). Climate Change, Fossil-Fuel Pollution, and Children's Health. *New England Journal of Medicine*, *386*(24), 2303–2314. https://doi.org/10.1056/NEJMra2117706

Ponsá, S., Gea, T., & Sánchez, A. (2010). The effect of storage and mechanical pretreatment on the biological stability of municipal solid wastes. *Waste Management (Elmsford)*, 30(3), 441–445. https://doi.org/10.1016/j.wasman.2009.10.020

Putro, J. N., Soetaredjo, F. E., Lin, S.-Y., Ju, Y.-H., & Ismadji, S. (2016). Pretreatment and conversion of lignocellulose biomass into valuable chemicals. *RSC Advances*, 6(52), 46834–46852. https://doi.org/10.1039/C6RA09851G

Quintero-Dallos, V., García-Martínez, J. B., Contreras-Ropero, J. E., Barajas-Solano, A. F., Barajas-Ferrerira, C., Lavecchia, R., & Zuorro, A. (2019). Vinasse as a Sustainable Medium for the Production of Chlorella vulgaris UTEX 1803. *Water (Basel)*, 11(8), 1526. https://doi.org/10.3390/w11081526

Rathour, R. K., Ahuja, V., Bhatia, R. K., & Bhatt, A. K. (2018). Biobutanol: New era of biofuels. *International Journal of Energy Research*, *42*(15), 4532–4545. https://doi.org/10.1002/er.4180

Riaz, S., Mazhar, S., Abidi, S. H., Syed, Q., Abbas, N., Saleem, Y., Nadeem, A. A., Maryam, M., Essa, R., & Ashfaq, S. (2022). Biobutanol production from sustainable biomass process of anaerobic ABE fermentation for industrial applications. *Archives of Microbiology*, *204*(11), 672. https://doi.org/10.1007/s00203-022-03284-z

Rodionova, M. V., Bozieva, A. M., Zharmukhamedov, S. K., Leong, Y. K., Chi-Wei Lan, J., Veziroglu, A., Veziroglu, T. N., Tomo, T., Chang, J.-S., & Allakhverdiev, S. I. (2022). A comprehensive review on lignocellulosic biomass biorefinery for sustainable biofuel production. *International Journal of Hydrogen Energy*, *47*(3), 1481–1498. https://doi.org/10.1016/j.ijhydene.2021.10.122

Rongpipi, S., Ye, D., Gomez, E. D., & Gomez, E. W. (2019). Progress and Opportunities in the Characterization of Cellulose – An Important Regulator of Cell Wall Growth and Mechanics. *Frontiers in Plant Science*, *9*, 1894. https://doi.org/10.3389/fpls.2018.01894

Sanchez, A., Valdez-Vazquez, I., Soto, A., Sánchez, S., & Tavarez, D. (2017). Lignocellulosic n-butanol co-production in an advanced biorefinery using mixed cultures. *Biomass and Bioenergy*, 102, 1-12. https://doi.org/10.1016/j.biombioe.2017.03.023

Sidi Ahmad, Z., & Abdul Munaim, M. S. (2017). EFFECT OF FERMENTATION TIME, MOISTURE CONTENT, AND TEMPERATURE ON SORBITOL PRODUCTION VIA SOLID STATE FERMENTATION PROCESS. *Journal of Chemical Engineering and Industrial Biotechnology*, 1(1), 64–71. https://doi.org/10.15282/jceib.v1i1.38

Shokravi, Z., Heidarrezaei, M., Ong, H. C., Rahimian Koloor, S. S., Petrů, M., Lau, W. J., & Ismail, A. F. (2021). Fourth generation biofuel from genetically modified algal biomass: Challenges and future directions. *Chemosphere (Oxford)*, 285, 131535–131535. https://doi.org/10.1016/j.chemosphere.2021.131535

Sierksma, G., Sierksma, G., & Zwols, Y. (2015). *Linear and Integer Optimization: Theory and Practice, Third Edition* (0 ed.). Chapman and Hall/CRC. https://doi.org/10.1201/b18378

Srivastava, N., Srivastava, M., Mishra, P. K., Upadhyay, S. N., Ramteke, P. W., & Gupta, V. K. (2018). Integrated Lignocellulosic Biorefinery for Sustainable Bio-Based Economy. In *Sustainable Approaches for Biofuels Production Technologies* (Vol. 7, pp. 25–46). Springer International Publishing AG. https://doi.org/10.1007/978-3-319-94797-6_2

Talan, A., Tiwari, B., Yadav, B., Tyagi, R. D., Wong, J. W. C., & Drogui, P. (2021). Food waste valorization: Energy production using novel integrated systems. *Bioresource Technology*, *322*, 124538. https://doi.org/10.1016/j.biortech.2020.124538

Valdez-Vazquez, I., & Sanchez, A. (2018). Proposal for biorefineries based on mixed cultures for lignocellulosic biofuel production: A techno-economic analysis. *Biofuels, Bioproducts and Biorefining*, 12(1), 56-67. https://doi.org/10.1002/bbb.1828

Wang, F., Ouyang, D., Zhou, Z., Page, S. J., Liu, D., & Zhao, X. (2021). Lignocellulosic biomass as sustainable feedstock and materials for power generation and energy storage. *Journal of Energy Chemistry*, 57, 247–280. https://doi.org/10.1016/j.jechem.2020.08.060

Wang, S., Zhu, Y., Zhang, Y., & Li, Y. (2012). Controlling the oxidoreduction potential of the culture of Clostridium acetobutylicum leads to an earlier initiation of solventogenesis, thus increasing solvent productivity. *Applied Microbiology and Biotechnology*, 93(3), 1021–1030. https://doi.org/10.1007/s00253-011-3570-2

Wang, Z., Yang, T., Liu, Z., Wang, S., Gao, Y., & Wu, M. (2019). Mass Transfer in a Rotating Packed Bed: A Critical Review. *Chemical Engineering and Processing - Process Intensification*, *139*, 78–94. https://doi.org/10.1016/j.cep.2019.03.020

Zhou, X., Broadbelt, L. J., & Vinu, R. (2016). Chapter Two—Mechanistic Understanding of Thermochemical Conversion of Polymers and Lignocellulosic Biomass. In K. M. V. Geem (Ed.), *Thermochemical Process Engineering* (Vol. 49, pp. 95–198). Academic Press. https://doi.org/10.1016/bs.ache.2016.09.002

1.2. Hypothesis

1.2.1. General hypothesis

Innovative biorefinery plant for biobutanol production from lignocellulosic biomass that consists of two cascading consolidated bioprocesses for biological pretreatment of lignocellulosic biomass and acetone-butanol-ethanol (ABE) fermentation from cellulose, is techno-economically viable for establishement in Mexico.

1.2.2. Specific hypothesis

1. Nutrient supplementation improves hemicellulose polymer solubilization, and volatile fatty acids production.
2. During the fermentation of lignocellulosic biomass by its native microbiota pH value close to neutral increases hydrogen production, while its decreases improves the formation of volatile fatty acids.
3. During the fermentation of lignocellulosic biomass by its native microbiota, an increase in total solids content improves biogas and VFA production.
4. Butanol-tolerant mixed culture is an adequate source of microorganisms for efficient butanol production from cellulosic polymer of lignocellulosic biomass during a consolidated bioprocess.
5. Vacuum distillation in a rotating packed bed is an adequate method for the efficient recovery of butanol from synthetic fermentation broth.
6. Lignocellulosic biomass processing within the innovative biorefinery scheme that consists of consolidated bioprocesses using a mixed culture is economically more viable than in a traditional scheme using a pure culture.
7. Given the costs of biobutanol production from lignocellulosic biomass under the innovative biorefinery scheme, the supply chain and distribution of biobutanol to the market allow for the economically viable establishment of a biorefinery in Mexico.

1.3. Objectives

1.3.1. General objective

To assess the cost effectiveness of the innovative biorefinery scheme for biobutanol production from lignocellulosic biomass based on consolidated bioprocessing employing microbial consortia involving biomass supply and biobutanol distribution for its construction in Mexico.

1.3.2. Specific objectives

1. To evaluate nutrients supplementation on solubilization of the hemicellulose fraction, microbial community and volatile fatty acids production during biological pretreatment (acidogenesis) of agave bagasse by its native microbiota with hydraulic retention time and solid retention time decoupled.

2. To assess the effect of pH and total solids on the composition and concentration of volatile fatty acids and hydrogen production from agave bagasse by its native microbial consortia.

3. To assess whether a butanol-tolerant mixed culture is an adequate microorganism source for biobutanol production from biologically pretreated corn stover during a consolidated bioprocess.

4. To evaluate butanol recuperation from a synthetic mixture based on a composition of a real fermentation broth obtained during consolidated bioprocessing of a biologically pretreated corn stover by butanol-tolerant mixed culture using vacuum distillation in a rotating packed bed.

5. To assess the profitability of the innovative biorefinery scheme processing lignocellulosic biomass using mixed culture and compare it with a traditional one employing pure culture.

6. To develop a mathematical model for the optimal location assessment of a lignocellulosic biomass-based biobutanol plant in Mexico, considering supply chain, techno-economic evaluation of biorefinery plant, biobutanol distribution and a limited investment budget.

2. Chapter II: Overall work strategy

An overview on the research activities described in the present doctoral dissertation were visualized on the overall work strategy diagram (Figure 2.1). The work was divided into an experimental and a simulation part. In the experimental part (Chapters III, IV, V, VI), the biological pretreatment of lignocellulosic biomass, production of volatile fatty acids with hydrogen, and subsequent butanol production in consolidated bioprocesses together with its purification were investigated. In the simulation part (Chapters VII and VIII) the collected experimental data was used to assess processes in economic terms on a commercial scale.

Chapter III describes how nutrient supplementation affects the acidogenesis of lignocellulosic biomass, specifically the solubilisation of hemicellulose and evaluate nutrients impact on the microbial environment and the production of volatile fatty acids (Spec. Obj. 1). Chapter IV, on the other hand, is an extension of this, where the effects of pH and total solids on the composition and concentration of volatile fatty acids and hydrogen production are examined (Spec. Obj. 2).

Biologically pretreated lignocellulosic biomass as described in Chapter III, was left with an untreated cellulosic polymer. Chapter V is devoted to the evaluation of an isolated butanol-tolerant mixed culture for production of biobutanol in a consolidated bioprocess from cellulosic fraction of the previously biologically pretreated lignocellulosic biomass (Spec. Obj. 3).

Based on a fermentation broth obtained during biobutanol production from cellulosic fraction of corn stover (biologically pretreated) by a butanol-tolerant mixed culture as described in Chapter V, a synthetic mixture was prepared. The recovery of biobutanol from the synthetic mixture was then investigated in a rotating packed bed under vacuum conditions (Spec. Obj. 4). The experiment and results are described in Chapter VI.

Chapter VII was dedicated to a techno-economic evaluation of the proposed innovative biorefinery scheme which process lignocellulosic biomass in consolidated bioprocess employing native mixed culture (as reported in Chapter III) and compare it with a traditional biorefinery scheme that use pure culture (Spec. Obj. 5).

Finally, Chapter VIII describes studies related to optimal location of lignocellulosic biorefinery for biobutanol production in Mexico. Firstly, economic assessment of technology used in the proposed

innovative biorefinery scheme, where lignocellulosic biomass is converted into biobutanol involving processes described in Chapter III – V, was carried out. Then, optimalization mathematical model was developed to evaluate the optimal plant locations in Mexico, considering techno-economic data of simulated biorefinery, biomass supply chain and biobutanol distribution (Spec. Obj. 6).

Experimental Part

Spec. Obj. 1. Effect of nutrients supplementation on acidogenesis

Acidogenesis of agave bagasse with nutrients supplementation (CH_4N_2O, $CaCl_2$, KH_2PO_4) in semi-continuos reactors (1L)

Innoculum

DNA extraction and sequencing

Bioinformatics analysis

Physico-chemical analysis

Statistical analysis

- pH behavior
- COD soluble
- VFA production and composition
- Biomass degradation
- Microbial diversity
- Effect of nutrients on acidogenesis

Article 1

Spec. Obj. 2. Effect of pH and TS on VFA and H_2 production

Acidogenesis of agave bagasse with nutrients supplementation at different pH and TS% in bath reactors (0.1L)

Cellulose-rich biomass

DNA extraction and sequencing

Bioinformatics analysis

Physico-chemical analysis

Statistical analysis

- pH and TS% effects on:
  -- VFA and H_2 production
  -- Microbial diversity

Submitted Article 4

- fermentation metabolities recovery under vacuum distillation in RPB at different motor speed (rpm)
- fermentation metabolities recovery under total reflux and 5% wt steam

Article 3

Spec. Obj. 3. Biobutanol production by butanol-tolerant mixed culture

Butanol production by butanol-tolerant mixed culture in CBP in batch reactors (0.25L)

Physico-chemical analysis

- Production of butanol and other metabolites
- ABE fermentation kinetics

Fermentation broth composition

Spec. Obj. 4. Biobutanol distillation under vacuum conditions in RPB

RPB vacuum system set-up

Butanol recovery from synthetic fermentation under total reflux

RPB vacuum system modification

Butanol recovery from synthetic fermentation with 5 wt% of steam

Physico-chemical analysis

Statistical analysis

Simulation Part

Spec. Obj. 5. Economic evaluation of the innovative biorefinery scheme

Biorefinery simulation where acidogenesis is carried out by mixed culture and compated with plant using pure culture.

Mass and energy balance

Economic assessment of the technology used

NPV calculation

- unit production cost
- investment costs
- operating costs
- revenue of the plant

Article 2

Spec. Obj. 6. Optimal location of the biobutanol biorefinery in Mexico

Simulation of biobutanol production under the innovative biorefinery scheme, where acidogenesis and ABE fermentation are carried out by a mixed culture in CPB.

Mass and energy balance

Economic assessment of the technology used

NPV calculation

- unit production cost
- investment costs
- operating costs
- revenue of the plant

Economic data collection

Data collection of location and demand of biomass suppliers and biobutanol clients

GIS application for collected data

Optimization mathematical model development for optimal locations of biobutanol biorefinery in Mexico

- locations of established plants with their individual NPV
- number and location of established plants within the budget limit
- sensitivity analysis

Submitted Article 5

Specific Objective | Main activity related to specific objective | Key activity of the specific objective | - obtained results | Published/Submitted Article | - - - - → Imported technology/method

Figure 2.1. Overall work strategy diagram.

3. Chapter III: Nutrient influence on acidogenesis and native microbial community of agave bagasse

Reference to published work:

3.1   Abstract

This study reports the start-up, acclimation, and performance of an acidogenesis process as a biological pretreatment method to solubilize *Agave* bagasse fibers using the native microbiota. The effects of nutrients were evaluated on acidogenesis performance (volatile fatty acid [VFA] production; soluble chemical oxygen demand [sCOD], and VFA yield) in a reactor R(+) supplemented with urea, phosphate salts, and calcium ions and contrasted with a control reactor R(-) containing distilled water. The native microbial lasted ca. 70 days to stabilize the primary technological parameters. Under stable conditions, R(+) improved VFA production by 5 times (101 $\pm$ 12 mg$_{COD}$/g), sCOD by 1.5 times (137 $\pm$ 33 mg$_{sCOD}$/g), and VFA yield by 45 times (634 $\pm$ 54 mg$_{COD}$/g$_{removed}$) compared with R(-). In R(+) nutrient supplementation promoted an alkaline pH due to urea hydrolysis and the major VFA were acetic acid > butyric acid > and propionic acid. In contrast, in R(-) the pH acidified rapidly and the major VFA were acetic acid > butyric acid > and lactic acid. In R(+) thrived *Cellulomonas*, *Gordonia*, and *Pseudoclavibacter*. In contrast, in R(-) pH became rapidly acidic promoting the growth of several bacteria such as *Lactobacillus* and *Beijerinckia* that correlated positively with acid lactic production. In both reactors, *Caproiciproduces* was linked to the production of VFA acetate, propionate, and butyrate. Findings demonstrate that the native microbiota of *Agave* bagasse fibers contained members that depending on the nutrient supplementation solubilized the fibers towards the VFA production with different compositions and yield.

Keywords: biological pretreatment; lactic acid; lignocellulose; urea; volatile fatty acid;

3.2   Introduction

At the start of the 21st century, lignocellulosic biomass fermentation rose to prominent in the energy industry as a promising alternative to conventional energy sources (Sebayang et al. 2017). Many types of lignocellulosic biomasses such as Agave, corn, Miscanthus, poplar, sugarcane and switchgrass have been investigated, among which *Agave* plants have shown particular potential as a bioenergy crop; they can be cultivated in arid or semi-arid soil that is unsuitable for most common energy crops (Escamilla-Treviño 2012). *Agave* plants accumulate soluble nonstructural carbohydrates in plant tissue (Davis et al. 2011), and their processing generates a lignocellulosic bagasse (Hernández et al. 2019). *Agave* may therefore represent a high-quality feedstock for biorefineries, which can obtain numerous valuable products from the soluble sugar fraction and bioenergy from the lignocellulosic fraction.

The chemical composition of *Agave* bagasse ranges from 38 to 53% cellulose, 32-54 % hemicellulose, and 4-14% lignin depending on climate, agronomic practices, harvesting time, and plant age (Hernández et al. 2019). *Agave* bagasse requires pretreatment to modify its complex and recalcitrant structure, which is difficult to ferment (Sebayang et al. 2017). Biological, enzymatic, chemical, and hydrothermal methods have been adopted to solubilize *Agave* fibers, whereas produced hydrolyzates have been used in the subsequent production of hydrogen or methane through dark fermentation or anaerobic digestion, respectively (*e.g.*, Arreola-Vargas et al. 2016; Breton-Deval et al. 2018; Buitrón et al., 2019; Montiel-Corona et al. 2020; Muñoz-Páez et al. 2020; Valdez-Vazquez et al. 2020). A comparison of pretreatment has shown that dilute acid pretreatment solubilizes more carbohydrates than other methods, but the obtained hydrolyzates present problems in inhibition during the anaerobic digestion step (Valdez-Vazquez et al. 2020). Otherwise, biological pretreatments appear to solubilize fewer *Agave* fibers, but the obtained hydrolyzates yield the highest biochemical methane potential. Scholars' clear interest in pretreatment selection is largely due to economic concerns. Chemical pretreatments carry limitations, such as high equipment and operational costs; furthermore, depending on pretreatment conditions, emerging inhibitors can influence subsequent biological conversions (Antizar-Ladislao and Turrion-Gomez, 2008). While biological pretreatments avoid these inhibition problems, a major disadvantage is their long pretreatment times, which are prohibitive for industrial purposes (Amin et al., 2017; Baral and Shah, 2017).

Whereas fungal pretreatments have the longest pretreatment times (*i.e.*, from weeks to months), bacterial pretreatments can reduce the time to several days (Zabed et al. 2019). Of particular interest are microbial consortia, consisting of fungi and bacteria that perform simultaneous tasks to solubilize lignocellulose. Microbial consortia operate under relatively shorter pretreatment times, are more adaptable to new environments and substrates, and they have demonstrated enhanced performance compared with pure cultures (Zabed et al. 2019). The microbial consortia used most frequently to solubilize lignocellulose include ruminal fluids, cattle slurry, manures, compost, and anaerobic sludge, all of which have been used as external inoculants (Amin et al., 2017; Zabed et al. 2019), that is, prior to pretreatment, these microorganisms do not come into contact with the substrate. Microbial ecologists have determined that specific substrates stimulate specialized microbial consortia that possess the enzymatic machinery necessary for their degradation (Reichardt et al., 2018). This phenomenon suggests that not all microbial consortia are appropriate for solubilizing all kinds of substrates, at least without an acclimation process. Interestingly, plant tissues are valuable reservoirs of microbiota that have evolved together over the long term in environments where the plants were cultivated (Compant et al., 2019), as such, these tissues represent a source of specialized lignocellulosic degraders. Native microbial consortia have shortened the time required to solubilize lignocellulosic fibers to less than 4 days with superior fermentation performance over other microbial consortia (Valdez-Vazquez et al., 2017; Valdez-Vazquez et al., 2020). Industrial exploitation of such native microbiotas requires in-depth knowledge to control their behavior in bioreactors, stabilize their activity to ensure a reproducible quality, and maximize their solubilization yields and rates. A previous study reported that the direct conversion of lignocellulosic substrates by their native microbiotas demands essentials nutrients such as urea, $CaCl_2$, KH_2PO_4 that are crucial for cellular activity, growth and metabolism. The C, N and P represent macronutrients and improve synthesis of carbohydrates, lipids, nucleic acids and proteins, while, the K, Ca correspond to micronutrients and are part of enzymes and co-factors (Pérez-Rangel et al., 2020). Nevertheless, that research was limited to batch tests, what did not show a long-term impact of nutrients on acidogenesis and microbial structure. This study reports the start-up of a fermentation process (also referred to as acidogenesis) to solubilize Agave bagasse by its native microbiota (phyllosphere community) with and without nutrient supplementation (urea, $CaCl_2$, KH_2PO_4), evaluates the microbial communities changes in time depending on presence or absence of nutrients and gives details about reactor performance over time until to

observe stable technological parameters (*e.g.*, solubilization, rates, pH, total solids removal [TSrem], and yields). The presented bioreactor operation strategy involves decoupling soluble products from active microorganisms and insoluble fibers (*i.e.*, hydraulic retention time [HRT] < solid retention time [SRT]) to improve the solubilization efficiency (Karthikeyan et al. 2016), a strategy that mimics the ruminal fermentation (Weimer et al., 2009). This study also evaluates the long-term effects of essential nutrients on the technological parameters, as well as the quality and quantity of final products.

3.3   Materials and Methods

3.3.1   Substrate and inoculum

Agave bagasse from the processing of *Agave tequilana* Weber var. azul was delivered from two different tequila producers in Mexico during summer and autumn 2019. Two Agave bagasse batches were used in this study. The first batch, moist Agave bagasse (moisture content: 30%) was taken as the seed inoculum, collected two weeks prior experimentation and stored at 4 ℃.

Table 3.1. Lignocellulosic mass composition of inoculum, substrate, and after acidogenesis by native microbiota in (wt.%). R(+) with nutrient supplementation and R(-) without nutrient supplementation.

	Extactives		Hememicellulose			Cellulose			Lignin	
Inoculum	28.3		21.9			42.4			7.4	
Substrate	20.1		22.6			49.3			8.0	
Reactor			R (+)					R (-)		
Cycle	Ex	Hem	Cell	Lig	WL	Ex	Hem	Cell	Lig	WL
1	14.0	27.8	48.9	9.7	37.6	17.1	26.8	46.8	9.6	28.5
2	-	-	-	-	49.5	-	-	-	-	53.4
3	16.5	27.5	47.3	9.0	13.1	13.8	28.8	49.5	8.3	25.1
4	11.5	30.7	49.7	8.5	13.5	11.2	30.6	50.6	7.9	13.5
5	11.8	29.8	50.7	8.0	13.2	22.4	24.5	44.3	9.0	5.3
6	15.2	28.3	47.5	9.2	24.5	-	-	-	-	-
7	14.3	28.5	44.0	12.2	14.7	-	-	-	-	-
8	18.7	25.3	44.0	12.2	24.9	-	-	-	-	-
9	15.9	27.2	48.0	9.3	23.5	-	-	-	-	-

Notes: wt, weight total. Ex – extractives; Hem – hemicellulose; Cell – cellulose; Lig – Lignin; WL – weight loss (g/100g of dry *Agave* bagasse).

The second batch, air-dried Agave bagasse (5.0% moisture) served as the substrate which was milled to a particle size of less than 5 cm and stored in plastics bags at a room temperature (25 °C on average, 20% humidity) until use. The chemical composition of these two batches was determined one week before starting the experimentation using an automated fiber analyzer (ANKOM 200 Fiber Analyzer, ANKOM Technologies, Macedon, NY) per van Soest et al.'s (1991) recommendation. The chemical compositions were listed in the Table 3.1.

3.3.2   Experimental set-up

Two glass reactors of 1 L with a working volume of 0.75 L were assembled. A single-factor experiment at two levels was conducted to evaluate the effects of nutrient supplementation on *Agave* bagasse solubilization and acclimation time. To do so, at the start of the experiment (Cycle 1), 30 g wet matter of seed inoculum was introduced into each reactor (ca. 3 % of total solids, Pérez-Rangel et al., 2015). One reactor, thereafter called R(+), was filled up to 0.75 L with a culture medium containing essential nutrients for the direct processing of lignocellulosic fibers (1.02 g/L of CH_4N_2O; 0.41 g/L of $CaCl_2$; 0.11 g/L of KH_2PO_4; Pérez-Rangel et al., 2020). The second reactor, hereafter called R(-), was filled up to 0.75 L with distillated water only. The initial pH of both reactors was manually adjusted to 6.5 using 3 M NaOH or 3 M HCl (Pérez-Rangel et al., 2015), after which the reactors were tightly closed with air in the headspace and placed into an incubator with manual shaking once a day (WIS-ML; Wisd Laboratory Instruments, Witeg, Germany) at a temperature of 37 ºC. The pH was not controlled.

After 30 days, it was expected that the microbial activity was stable (Gómez-Guerrero et al., 2019). At the beginning of the second cycle of acclimatization (Cycle 2), 27.1 g and 37.5 g dry matter of substrate were introduced into R(+) and R(-), respectively, with the aim of starting the Cycle 2 with the same bagasse mass in both reactors whereas 7.0 ± 0.7 g dry matter of spent solids (digestate) remained inside each reactor (Cycle 2 with a length of 30 days). In subsequent cycles with a length of 14 days each, both reactors were operated in semi-continuous mode, and the same quantity (19 g dry matter) of substrate was introduced into each reactor; 9.5 ± 0.7 g dry matter of digestates remained inside each reactor, resulting in an average SRT of 20 days. The HRT was adjusted to 6 days, during which 0.25 L was replaced 3 times per week with either fresh culture medium or distillated water with a pH adjusted to 6.5.

3.3.3 Analytical methods

The pH was measured using potentiometer (BACKMAN, 50 pH Meter). Total solids (TS) were determined using standard methods (APHA 2540). Soluble chemical oxygen demand was analyzed in centrifugated supernatants using Hach vials (Method 8000, 0–1,500 mgCOD/L) (Hach Company, Loveland, CO). Carboxylic acids were analyzed using high-performance liquid chromatography (HPLC) with 10 µL sample injection (model 1260 infinity, Agilent Technologies, CA, USA) equipped with Aminex HPX-87H column and Diode-Array Detection (DAD) with detection wavelength of 210 nm. The mobile phase was 0.005 M H2SO4 solution at a flow rate of 0.6 mL/min.

3.3.4 Calculations and statistical analysis

Carboxylic acids were reported as COD using the following stoichiometric factors (Perimenis et al., 2018): 1.067 g_{COD}/g acetic acid, 1.512 g_{COD}/g propionic acid, 1.813 g_{COD}/g butyric acid, and 1.066 g_{COD}/g lactic acid. VFA yield was calculated as the total VFA production expressed as COD per gram of *Agave* fibers removed for each cycle (mg_{COD}/g_{TSrem}). Acidogenesis efficiency was defined as the total VFA production (in COD) per sCOD $\times$ 100 (Kullavanijaya and Chavalparit, 2019). Analysis of variance (ANOVA) was performed to determine significant differences in technology parameters between R(+) and R(-) at a confidence level of 95% using Microsoft Excel 365 ProPlus (Version 1908).

3.3.5 Molecular diversity analysis

Seed inoculum and fermented Agave bagasse solids parts were collected and held in 2 ml plastic Eppendorf with 75 % of humidity in temperature - 20 ℃ to determine the bacterial composition. Wet samples were collected at 0, 67, 81, 95, 106, 131 days for R(+) and R(-) (corresponding to the seed inoculum, and end of cycles 2, 3, 4, 5, and the starvation period). Additional, wet samples were collected at 144, 158, and 187 days for R(+) (corresponding to the end of cycles 6, 7, and 9). Cell pellets were recovered from samples accordingly to Valdez-Vazquez et al. (2019). Genetic DNA was extracted from recovered biomass according to the user´s manual, using the DNeasy PowerSoil Kit (QIAGEN, Germany). Integrity and DNA quality were figured out in an agarose gel dyed with 1 % SYBR Green. The DNA was quantified by spectrophotometry using a NANODrop 2000c (Thermo Scientific, USA). The DNA was submitted to the Research and Testing Laboratory

(RTL, USA) for sequencing using the MiSeq Illumina platform using the primer pair V3-V4 341F (5′-CCTACGGGNGGCWGCAG-3′) and 805R (5′-GACTACHVGGGTATCTAATCC-3′) (Klindworth 2013). Analysis of sequencing was performed according to (Carrillo-Reyes et al., 2021). To compare similarity of community structure among R(+) and R(-), UPGMA (Unweighted Pair Group Method with Arithmetic mean) clustering analysis was performed based on the Bray-Curtis matrix of operational taxonomic units (OTUs) composition at the 95% sequences identity. Associations between bacterial taxa with an abundance >5 %, TS removal, and VFA production were explored using non-parametric Spearman's rank correlation (Spearman's Rho) in PAST software v4.03 (Hammer et al., 2001).

3.4 Results

3.4.1 pH behavior

The pH behavior was the first technological parameter affected by the nutrient supplementation (Figure 3.1a,b). Typically, there are an inverse relationship between the pH and the VFA production in acidogenesis processes (Agematu et al., 2017). However, R(+) underwent an alkalinity process in the course of each cycle, although the average pH tended to decline as the acidogenesis proceeded (Figure 3.1a). Conversely, R(-) experienced a drastic acidification process in each subsequent cycle (Figure 3.1b). Thus, in cycles 3-5, the average pH in R(+) was 7.04 whereas in R(-) was 4.02. The phenomenon of alkalinity in R(+) may be attributed to two reasons. The first is acetogenesis, where acetate is produced either by the reduction of either CO_2 or organic acids (Angelidaki et al. 2011). Dissolved CO_2 forms carbonic acid, which then dissociates to H^+ and decreases pH. The CO_2 consumption in the acetyl-CoA pathway eliminates H^+ in the solution, thereby increasing pH. Second, the addition of urea as a nutrient, and its subsequent hydrolysis by microorganisms, cause alkalinity to increase (Connolly et al. 2015). This reaction results in two ammonium and one bicarbonate ions being formed from each hydrolyzed urea mole. Then, one proton is absorbed, and ammonium is formed, whereby pH increases.

To confirm the effect of nutrients on the alkalization process, after Cycle 5 R(+) was subjected to starvation for three weeks to deplete nutrient and during Cycle 6 it was operated without replacing the culture medium (*i.e.*, HRT was equal to SRT during this cycle). Under such conditions, R(+) experienced the typical acidification process where pH decreased from 7.37 to 4.97 confirming the hypothesis that the addition of urea was responsible for the alkalization process in previous cycles.

In the following Cycles 7-9 when the nutrients were restored, the alkalization phenomenon was again observed.
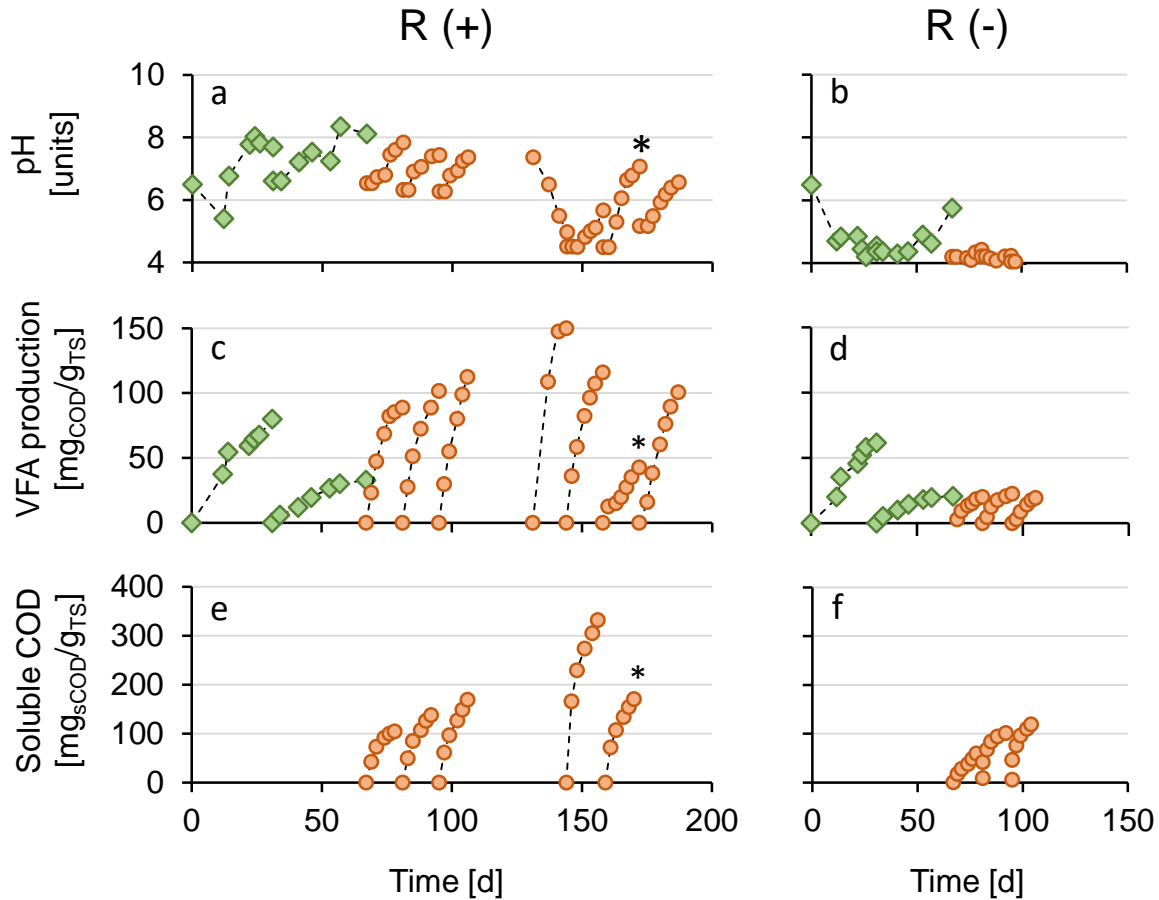
Figure 3.1. Operational progress of reactors with nutrient supplementation [R(+)] and without nutrient supplementation [R(-)]. Green symbols refer to the acclimation period and orange symbols refer to the semi-continuous operation. * refer to operation cycle with washout of suspended cells.

3.4.2   VFA production and soluble chemical oxygen demand

R(+) and R(-) were operated until stabilizing the activity of native microbiota of *Agave* bagasse, and assessing the effects of nutrients on fiber solubilization, measured as VFA production and soluble chemical oxygen demand (sCOD). In Cycle 1, VFA production was 80 and 61 mg_{COD}/g_{TS} for R(+) and R(-), respectively. In Cycle 2, VFA production fell in both reactors due to the addition of air-dried *Agave* bagasse substrate (Figure 3.1c,d). In the following Cycles 3-5, VFA production stabilized with coefficients of variations lower than 10% at 101 ± 12 mg_{COD}/g_{TS} for R(+) and 20 ± 2 mg_{COD}/g_{TS} for R(-). Analysis of variance confirmed a statistical difference in VFA production

between the reactors ($p < 0.001$). Throughout these five operation cycles, the VFA production rate in both reactors increased as follows: from a minimum of 0.95 $mg_{COD}/g_{TS·d}$ for R(+) in Cycle 2 (when the dried *Agave* bagasse was added) to a maximum of 10.03 $mg_{COD}/g_{TS·d}$ in Cycle 5; and from 0.57 $mg_{COD}/g_{TS·d}$ for R(-) in Cycle 2 to 1.85 $mg_{COD}/g_{TS·d}$ in Cycle 5 (Table 3.2).

Table 3.2. Technological parameters during acidogenesis of Agave bagasse by native microbiota. R(+) with nutrient supplementation and R(-) without nutrient supplementation.

Reactor	R (+)		R (-)	
Cycle	VFA production rate [$mg_{COD}/g_{TS}·d$]	VFA yield [mg_{COD}/g_{TSrem}]	VFA production rate [$mg_{COD}/g_{TS}·d$]	VFA yield [mg_{COD}/g_{TSrem}]
1	2.43	212	2.09	10.3
2	0.95	49	0.57	0.8
3	6.48	585	1.37	2.6
4	6.89	625	1.59	5.8
5	10.03	691	1.85	13.1
6	11.94	356	-	-
7	8.05	622	-	-
8	2.88	113	-	-
9	714	271	-	-

Notes: VFA, volatile fatty acid; COD, chemical oxygen demand; TS, total solids; TS_{rem}, total solids removed.

When measured in terms of sCODn *Agave* bagasse solubilization displayed the same behavior as did VFA production. In Cycles 3-5, sCOD averaged 137 ± 33 mg_{sCOD}/g_{TS} for R(+) with an acidogenesis efficiency (η) of 75% and 93 ± 30 mg_{sCOD}/g_{TS} for R(-) with an η value of 24%; both parameters were 30% higher for R(+) than for R(-) ($p < 0.05$; Figure 3.1e,f). However, for both reactors, η value showed a decreasing tendency with each subsequent cycle, likely due to the decoupling of HRT from SRT which resulted in greater oligosaccharide accumulation in the later cycles.

The addition of nutrients during the *Agave* bagasse fermentation over five operation cycles enhanced the solubilization parameters compared with control where these nutrients were omitted. During Cycles 3-5, R(+) overcame R(-) in terms of VFA production and rate, hence why the R(-) reactor's operation completed in the fifth cycle while R(+) continued to operate.

During Cycle 6, when R(+) was operated with SRT equal to HRT, VFA production peaked due to its accumulation in the supernatant. In Cycle 7, the semi-continuous operation with HRT < SRT was restored. Then, in Cycle 8, R(+) suffered a disturbance with the loss of suspended cells (*i.e.*, cell washout), which negatively affected VFA production and VFA yield ($p < 0.05$). Interestingly, sCOD had a concentration of 168 mg$_{sCOD}$/g$_{TS}$, similar to Cycles 3-5. An unforeseen disturbance in R(+) revealed information about the roles of attached and suspended cells in the fermentation process of *Agave* bagasse. At each feeding, digestates were maintained at a constant amount inside the reactor to provide active microorganisms. The similar sCOD value during the cell washout in Cycle 8, compared with previous cycles, suggested that the solubilization activity was unaffected. Conversely, the cell washout of suspended cells negatively affected the fermentation step (low VFA production) and thus led to the lowest η value of 0.28. Based on the results observed during Cycle 8, *Agave* bagasse fermentation also promoted two distinct fiber niches: insoluble fibers, whose attached bacteria contributed to the solubilization of *Agave* bagasse fibers; and suspended cells, which served to convert sugars to VFAs. These two niches could also harbor specific members, for example, fungi and bacteria such as *Clostridium* attach to the insoluble fibers visualized by confocal laser scanning microscopy (Pérez-Rangel et al., 2015; Valdez-Vazquez et al., 2016a), a possibility that calls for further research. In Cycle 9, the disturbance was eliminated, and VFA production recovered.

3.4.3   Total solid removal

TS removal was three-fold higher in the first two cycles than in the following cycles because of the bacteria's contact time with the substrate (Table 3.1). The first two cycles lasted 30 days each one, and each subsequent cycle lasted 14 days. In Cycles 3-5, the TS removal stabilized at $13 \pm 0.25\%$ for R(+); by contrast, TS removal for R(-) declined with each subsequent cycle. The VFA yield, expressed as the total VFA production (in COD) per TS removed, increased for R(+) from 49 mg$_{COD}$/g$_{TSrem}$ in Cycle 2 to a stable value of 634 ± 54 mg$_{COD}$/g$_{TSrem}$ in Cycles 3-5. The VFA yield for R(-) remained below 14 mg$_{COD}$/g$_{TSrem}$ in all cycles (Table 3.2). An analysis of components after acidogenesis shows that the extractive fraction was mainly consumed by microorganisms followed hemicellulose and cellulose (Table 3.1).

3.4.4 VFA composition

VFA composition differed somewhat between reactors. Acetic acid was the most abundant end-product in both, comprising between ca. 50% and 70-80% followed by butyric acid (Figure 3.2). In both reactors, acetic acid peaked when the operation mode was changed from batch mode (the acclimation period) to semi-continuous mode (Cycle 3). These high percentages of acetic acid only were observed in Cycle 3 and could be attributed to stimulation of acetogenic activity, which needs further studies. The third type of VFA differed between reactors: propionic acid was detected in all cycles in R(+), whereas lactic acid progressively increased in R(-). The distinct pH behaviors observed between reactors could explain the selective presence of propionic or lactic acids. Decreasing pH causes acid stress that is unavoidable for bacteria development during fermentation. Low pH promotes the growth of lactic acid bacteria who are acid resistant resulting in the production of lactic acid production (Guan and Liu, 2020). Likewise, propionic acid bacteria keep pH homeostasis under acid stress and change their metabolic to improve propionic acid production (Guan et al., 2016).
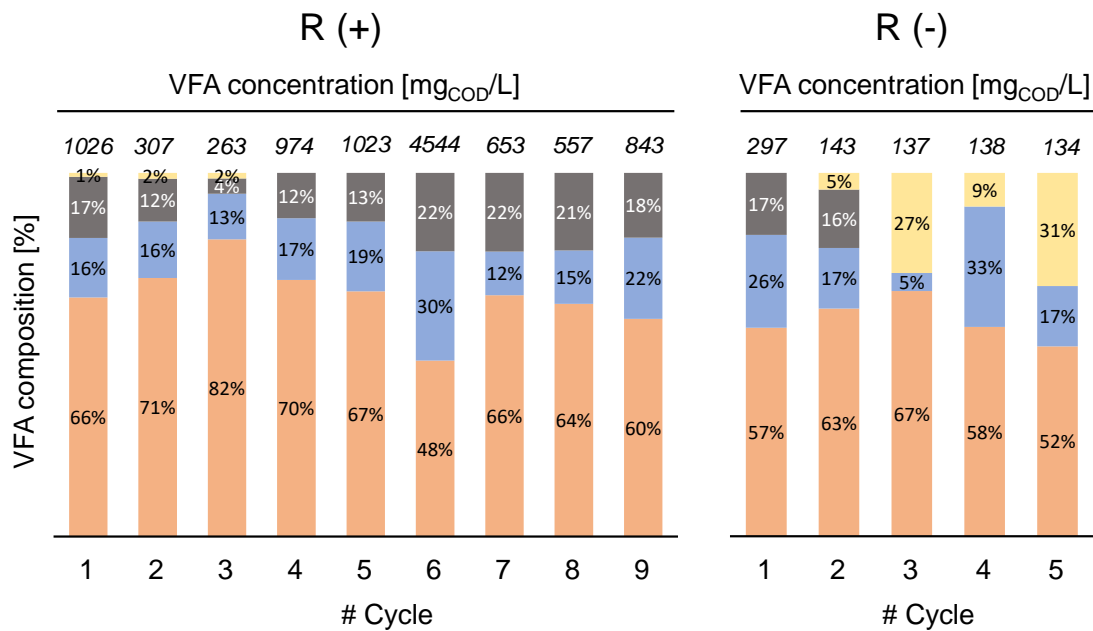
Figure 3.2. VFA composition in reactors with nutrient supplementation [R(+)] and without nutrient supplementation [R(-)]. Legend: ■ acetic acid; ■ butyric acid; ■ propionic acid; and ■ lactic acid.

After the starvation period (Cycle 6), acetic acid recorded its lowest percentage over time while butyric acid increased which could be the result of a change in the microbial community as

discussed below (Figure 3.2). For Cycles 7-9, VFA composition was restored similar to Cycles 3-5.

3.4.5   Microbial diversity over time

The sequencing of 16S rRNA gene amplicons was conducted to describe the bacterial communities change in time, in both reactors, as well as evaluate microbial structure depending on nutrient supplementation. The seed inoculum consisted mainly of *Enterobacter* 36%, *Stenotrophomonas* 16%, *Pantoea* 14%, *Pseudomonas* 5%, *Novosphingobium* 5%, *Sphingobium* 3%, and the rest of other bacteria such as *Kluyvera*, *Sphingomonas*, *Gluconobacter*, *Acetobacter*, *Weissella*, *Komagataeibacter*, *Burkholderia*, and *Leuconostoc*. Many of these genera were previously reported as major genera in phyllosphere of *Arabidopsis thaliana*, soybean, clover and rice (Vorholt 2012). Whereas *Enterobacter*, *Pantoea*, *Kluyvera*, and *Leuconostoc* were common genera found in phyllosphere of wheat (Pérez-Rangel et al. 2021). After the acclimatization period, the microbial structure changed and sixteen OTUs represented the major taxa with microorganism abundances > 5% (Figure 3.3). The microbiota structure after Cycle 2 was principally composed of *Proteiniphilum* (21 %) *Cellulomonas* (17 %), *Gordonia* (13 %) and *Pseudoclavibacter* (7 %) in R(+), while R(-) was consisted of a higher number of microorganisms, among them, the most abundant were: *Bifidobacter*, *Lactobacillus*, *Beijerinckia*, *Clostridium*, *Acetobacter* and Inertae Sedis from *Ethanoligenenaceae* family. The microbial stability with each subsequent cycle was not observed in the reactor R(-), neither, similarity over 80 % between any cycle. In the reactor R(+) the notable changes in microbial structure were observed after starvation period. The Cycles 3 and 4 were similarity in 83 % between itself (Figure 3.3), and their analysis showed decrease in *Cellulomonas* and *Proteiniphilum* and increased in *Gordonia* and *Pseudoclavibacter* genera compared with acclimatization period, with which the similarity was at the level of 65 %. Subsequent analysis of Cycles 5 and a period of 3 weeks of nutrients starvations showed resemblance in 82 % between each other, and in 70 % to Cycles 3 and 4. The most abundant genera were *Gordonia* and *Pseudoclavibacter*. After the Cycle 6, the significant change in microbial community was observed. Therefore, the microbial structure in the reactor R(+) was divided in two subgroups: before and after the starvation period. The first subgroup includes Cycles 1 to 5, and the second subgroup consist of Cycles 6 to 8. In the Cycle 6 the *Caproiciproducens* constituted 49 % of all microorganisms. Then, *Caproiciproducens* bacteria decreased with each subsequent cycle down to 19 % in the Cycle 8. In the Cycles 7 and 8 *Pseudoclavibacter*, *Gordonia* and *Cellulomonas*

disappeared, while *Caproiciproducens* and *Prevotella* were the most abundant. In the Cycles 8 the *Bacteroides* were detected the first time in the reactor R(+) in abundance of 26 %.
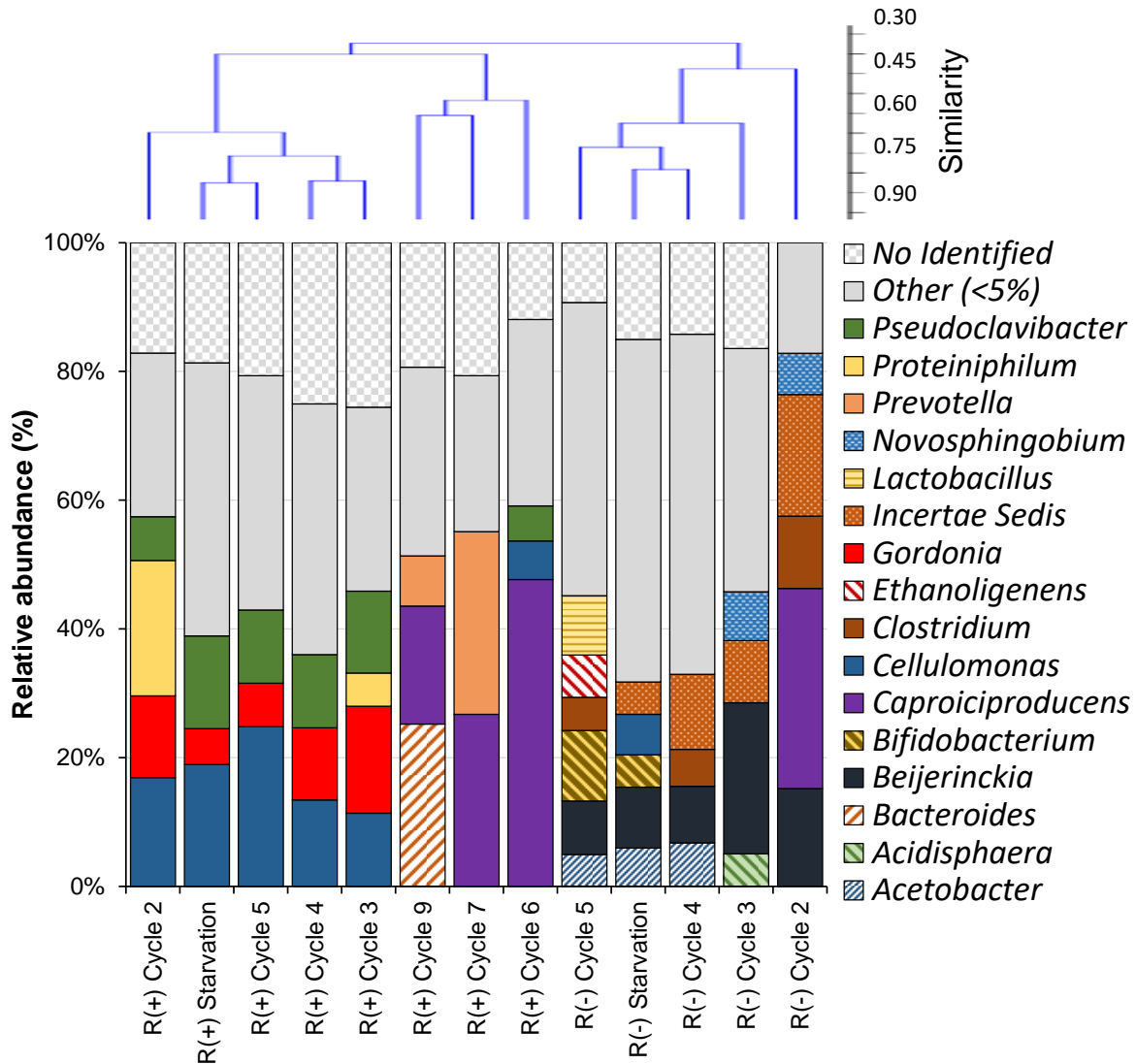
Figure 3.3. UPGMA cluster tree based on the Bray-Curtis matrix obtained at the 95% cutoff value, and bar graph showing relative abundances of bacterial operational taxonomic units of R(+) and R(-) in each operation time.

To better understand the relationships between microbial structure and VFA composition, a heat-plot correlation map was constructed at the genus level (Figure 3.4). Several genera demonstrated a significantly positive correlation ($p < 0.05$) with some acids, among them the *Caproiciproducens* genus with acetate, propionate and butyrate production, whereas, *Acetobacter*, *Acidisphaera*, *Beijerinckia*, *Bifidobacterium*, *Ethanoligenens*, *Lactobacillus* and *Novosphingobium* genera with

lactate formation. The diagram also depicted interesting phenomena of negative correlation between TS removal and *Acetobacter*, *Bifidobacterium*, *Ethanoligenens* and *Lactobacillus* bacteria.
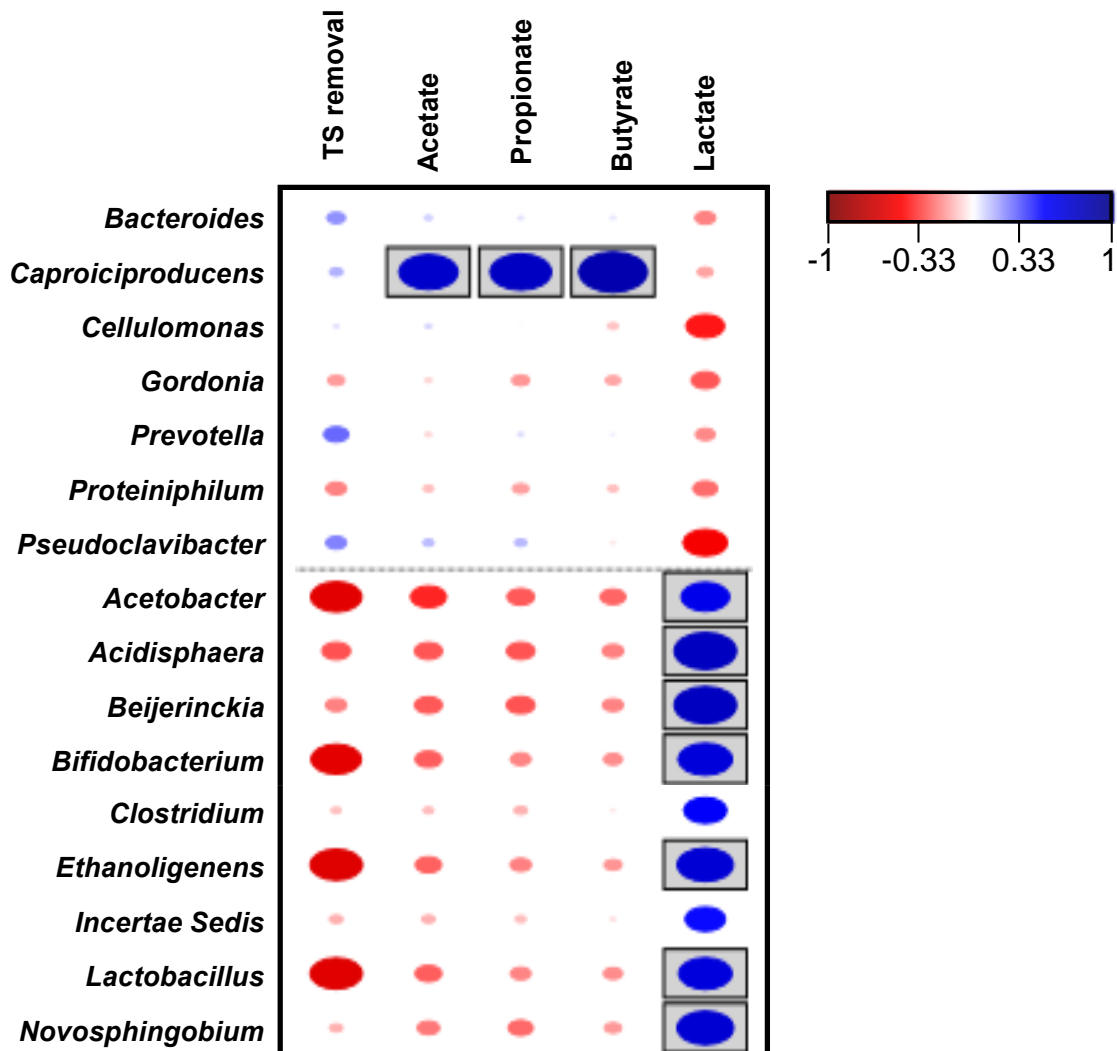
Figure 3.4. Heat-plot of correlation (Pearson's r) between bacterial relative abundance collapsed at the genus level (>5% of community) with total solid removal and volatile fatty acid productions. Values of correlation coefficients are color coded: negative correlation in red and positive correlation in blue. $p <$ 0.05 boxed.

3.5   Discussion

In this research, two batches of *Agave* bagasse fibers were used for the reactor operations. Moisture level was a critical parameter that should be considered during the start-up of bioreactors, since when the dried fibers were fed, microbial activity fell. This pattern is relevant to the industrial

application of native microbiota as degraders of organic material (Fraga et al. 2014); the substrate used as the seed inoculum must contain viable microorganisms (Abraham et al. 2013). Lignocellulosic biomass degradation requires a moisture level above 20% at least, as microbial activity disappears below this threshold (Towey et al. 2019). However, to avoid an uncontrolled fermentation, batches of dried substrate must be prepared for long-term storage. The timespan required to increase and stabilize the microbial activity of native microbiota was longer than the reported timespan of 42 to 51 days for processes of pulp, paper sludge, and food waste fermentation (Lin et al. 2012), and for the anaerobic digestion of food wastes (Zhang et al. 2019). Although these times could still be considered too long for industrial purposes, microorganisms need this time to acclimatize to their new environment. Nevertheless, this acclimation process improved *Agave* bagasse solubilization substantially compared with the first cycle during which the dried *Agave* bagasse was fed. The advantage of using native microbiotas is that each substrate feeding introduces at least a small number of viable microorganisms than can contribute to the stability of the process and render it more economical by eliminating the need for external inoculants.

This study investigated the long-term influence of nutrients on the *Agave* bagasse solubilization by native microbiota in reactors where HRT was decoupled from SRT. In Cycle 1, VFA production was comparable between reactors (Figure 3.1a,b). The fresh raw substrate used as seed inoculum appeared to contain enough nutrients to maintain a similar performance in both reactors, a phenomenon observed in raw food materials in which nutrients are not limited (Wolfe and Dutton 2015). However, VFA production between both reactors in Cycles 3-5 confirmed that nutrients contributed significantly to the process. These nutrients were previously identified as essentials for the direct fermentation of different raw lignocellulosic substrates in batch reactors (Pérez-Rangel et al. 2020). The authors specifically reported improvements in the response variable (hydrogen production) in the order of 1.2- to 3.5-fold times compared to controls with no nutrient addition. However, these authors did not observe the long-term effects of nutrients on the fermentation process. For example, after a 70-days acclimation process, technological parameters were improved in a greater order than those observed in batch reactors. Also, in our study, the nutrient addition promoted a phenomenon of alkalinity that modified VFA production and its composition. According to few published works, nutrients supplementation have a positive impact on acidogenesis by life-sustaining chemical reactions in microorganisms, likewise acting as buffering agents and enzyme components (Pérez-Rangel et al. 2020; Zhang et al., 2020), nevertheless, a

15

negative impacts were observed for VFA production in some cases, due to foster efficiency of the methanogenesis or syntrophic acetate oxidizing microorganisms what results on VFA reduction at a high rates (Nordell et al. 2016; Zieliński et al., 2019). According to the literature, for raw lignocellulosic substrates, the adequate ratio of C/N ranges between 20 and 30 (Wang et al. 2014; Valdez-Vazquez et al. 2016b), the optimum C/P ratio is 700–1000 (Argun et al. 2008; Carosia et al. 2017), and Ca should occur in concentrations between 36 and 400 mg/L (Adhyaru et al. 2014; Cardeña et al. 2018). Decoupling HRT from SRT allows for greater VFA production (Karthikeyan et al. 2016), but low HRTs increase supernatant exchange, and demand more nutrients than those present in the raw substrate.

By decoupling HRT from SRT, it was possible to observe two relevant phenomena. First, TS removal reached up to 50% in Cycle 2 where the substrate remained inside the reactor for longer compared with subsequent cycles. Therefore, future studies should explore the effect of SRT beyond 20 days to improve TS removal. Second, the loss of suspended bacteria in the effluent strongly suggests their particular roles in converting soluble carbohydrates to VFA (as evidenced by data from Cycles 6 and 8). Adequate bioreactor configurations can help preserve all suspended microorganisms together with unfermented fibers as previously pointed out by Karthikeyan et al. (2016).

Compared with previous fermentation studies, VFA production and sCOD for *Agave* bagasse were lower than values reported for other lignocellulosic biomasses (Table 3.3). Kullavanijaya and Chavalparit (2019) performed a fermentation assay under 28-day incubation, resulting in TS removal exceeding 60% and improved VFA production. As discussed earlier, SRT higher than those used in this study could enhance bioreactor performance. Conversely, Murali et al. (2017) reached a VFA production close to the theoretical value considering that the COD of lignocellulosic substrates is near 0.92 g_{COD}/g_{TS} (Kullavanijaya and Chavalparit (2019). However, the investment and operation costs to pretreat the substrate via wet explosion (190 °C/30 min) compared with biological methods warrant further investigation. *Agave* bagasse fibers are more recalcitrant to pretreatment than other biomasses such as corn stover, wheat straw and sugarcane bagasse (Buitrón et al., 2019). This study demonstrated a useful strategy to promote the solubilization of *Agave* bagasse fibers through acclimation of their native microbiota and via supplementation with essential nutrients; both strategies significantly improved the solubilization parameters. However,

other independent variables must be studied to solubilize most present carbohydrates, such as longer SRT, higher organic loading rates, and greater cell retention, among others.

Table 3.3. Fermentation studies of lignocellulosic biomasses by different microbiotas.

Substrate	Inoculum	Type of pretreatment	Bioreactor operation	VFA production (mg$_{COD}$/g$_{TS}$)	sCOD (mg$_{sCOD}$/g$_{TS}$)	η (%)	References
Rice straw	Rumen fluid	Physical: pulverizing	Sequencing batch	310	NR	NR	Agematu et al., (2017)
Pretreated corn stover	Rumen fluid	Wet explosion	Semi-continuous	900	NR	NR	Murali et al., (2017)
Napier grass	Cow manure	None	Batch	182*	392*	62	Kullavanijaya and Chavalparit, (2019)
Crop residues	Rumen fluid	Physical: pulverizing	Continuous	507	1362	37	Nguyen et al., (2020)
Rice straw	Rumen fluid	None	Batch	172**	258	60	Liang et al, (2021)
Agave bagasse	Native microbiota	None	Semi-continuous	101 ± 12	137± 33	73	This study

Notes: VFA, volatile fatty acid; sCOD, soluble chemical oxygen demand; TS, total solids; NR, not reported; η - efficiency; * considering 0.7 gVS/gTS as reported by authors; ** equivalent to acetic acid mg$_{COD}$/g$_{TS}$.

This study confirmed the long-term influence of nutrients on microbial structure changes in both reactors, furthermore, a relationship between microbial communities, acids and TS removal was observed. A positive correlation between *Caproiciproducens* and acetate, propionate and butyrate production, occurs due to ability of this genus to convert acetate or butyrate from the fermentation broth into acetyl-CoA or butyryl-CoA to avoid acidosis. Moreover, these coenzymes are used by the same species to acetate and butyrate formation (Flaiz et al., 2020). Likewise, *Caproiciproducens* strains use lactate as a substrate to produce n-caproate (Contreras-Dávila et al., 2020). A positive significant correlation between some microorganisms and lactate production result from their metabolic pathway. *Lactobacillus* produce lactate as a major product via EMP pathway (Quatravaux et al., 2006). In turn, some species of *Ethanoligenens*, like e.g. *E. harbinense* has genes associated to the lactate dehydrogenase, therefore, can synthesized lactic acid from pyruvate in the presence of NADH (Castro et al., 2013). In the case of *Novosphingobium* genus, its positive correlation is probably related to lactate assimilation by some of their species (Glaeser

et al., 2013; Kämpfer et al., 2015). *Bifidobacteria* bacteria perform fermentation of glucose, xylose, lactose, mannose and galactose, where acetic and lactic acids are the principal bioproducts (Takeuchi et al., 2022; Robinson and Batt, 2014). Is assumed that few species of *Beijerinckia* genus has indirect positive correlation with lactic acid production, e.g. *Beijerinckia indica subsp. indica* contain Bind_3604 gene, that permit secrete malate dehydrogenase, which is source of NAD^+ to lactate dehydrogenase, that convert pyruvate into lactate (Mansouri et al., 2017; COMBREX-DB). It was found that *Acidisphaera* bacteria grow well using lactate as a carbon source (Hiraishi et al., 2000), while *Acetobacter* used lactate as an important source for acetoin and biomass building blocks (Adler et al., 2014).

Pseudoclavibacter, *Prevotella* and *Bacteroides* presented positive correlation with TS removal, it is a result of *Pseudoclavibacter* enzymes activity against α- and β-glucosidase that permit degrade cellulosic polymer (Manaia et al., 2004; Kim and Jung, 2009; Cho et al., 2010;). Similarly, *Bacteroides* are able to degrade cellulose, hemicellulose polymers, pectin, starch and inulin by involved variety of glucosidase activities (Salyers et al., 1977; Dabek et al., 2008). The *Prevotella* has a common ancestor with *Bacteroides* (Ley, 2016). Moreover, when a long-term diet is rich in carbohydrates, especially fiber, predominate *Prevotella*, while grass and proteins are the principal source of diet, *Bacteroides* species dominate. Some species of *Prevotella* genus are able to degrade hemicellulose (Emerson and Weimer, 2017). A negative correlation takes place between TS removal and *Acetobacter*, *Bifidobacterium*, *Ethanoligenens* and *Lactobacillus* genera, however, there was no information found in the literature that confirm that phenomenon. In the case of *Acetobacter* genus can be assumed, that its negative correlation could be an effect of consumption only ethanol and in the case of some their strains sucrose for its growth. Moreover, this genus is not capable of monosaccharides metabolisms (Robinson and Batt, 2014).

3.6 Conclusions

This study demonstrated that *Agave* bagasse fibers were an adequate source of microorganisms for self-fermentation. This native microbiota required two months of acclimation to significantly increase their activity. Nutrient supplementation improved VFA production and VFA yield by 85% and 92%, respectively, compared to control without such supplementation. Moreover, the presence of nutrients, especially urea, promoted the reactor alkalization what affects VFA composition by propionate production, whereas, the lack of nutrients triggered the pH acidification with the

subsequent lactic acid formation. Nutrients selected a specific microbial community, enabling the growth of *Cellulomonas*, *Gordonia*, and *Pseudoclavibacter* genera that were not detected in R(-). The *Caproiciproducens* growth was detected in both reactors.

3.7   References

Abraham, J., Gea, T., Sánchez, A., 2013. Potential of the solid-state fermentation of soy fibre residues by native microbial populations for bench-scale alkaline protease production. Biochem. Eng. J. 74, 15-19. https://doi.org/10.1016/j.bej.2013.02.008

Adhyaru, D., Bhatt, N., Modi, H., 2014. Enhanced production of cellulase-free, thermo-alkali-solvent-stable xylanase from *Bacillus altitudinis* DHN8, its characterization and application in sorghum straw saccharification. Biocatal. Agric. Biotechnol. 3(2), 182-190. https://dx.doi.org/10.1016/j.bcab.2013.10.003

Adler, P., Frey, L. J., Berger, A., Bolten, C. J., Hansen, C. E., Wittmann, C. 2014. The key to acetate: Metabolic fluxes of acetic acid bacteria under cocoa pulp fermentation-simulating conditions. Appl. Environ. Microbiol., 80(15), 4702-4716. https://doi.org/10.1128/AEM.01048-14

Agematu, H., Takahashi, T., Hamano, Y. 2017. Continuous volatile fatty acid production from lignocellulosic biomass by a novel rumen-mimetic bioprocess. J. Biosci. Bioeng., 124(5), 528-533. https://dx.doi.org/10.1016/j.jbiosc.2017.06.006

Amin, F.R., Khalid, H., Zhang, H., Rahman S., Zhang, R., Liu, G., Chen, C., 2017. Pretreatment methods of lignocellulosic biomass for anaerobic digestion. AMB Expr. 7, 72. https://doi.org/10.1186/s13568-017-0375-4

Angelidaki, I., Karakashev, D., Batstone, D., Plugge, C., Stams, A., 2011. Biomethanation and its potential. Method. Enzymol. 494, 327-351. https://doi.org/10.1016/B978-0-12-385112-3.00016-0

Antizar-Ladislao, B., Turrion-Gomez, J.L., 2008. Second-generation biofuels and local bioenergy systems. Biofuel. Bioprod. Biorefin. 2(5), 455-469. https://doi.org/10.1002/bbb.97

Argun, H., Kargi, F., Kapdan, I., Oztekin, R., 2008. Biohydrogen production by dark fermentation of wheat powder solution: Effects of C/N and C/P ratio on hydrogen yield and formation rate. Int. J. Hydrog. Energy. 33(7), 1813-1819. https://doi.org/10.1016/j.ijhydene.2008.01.038

Arreola-Vargas, J., Flores-Larios, A., González-Álvarez, V., Corona-González, R.I., Méndez-Acosta, H.O., 2016. Single and two-stage anaerobic digestion for hydrogen and methane

production from acid and enzymatic hydrolysates of *Agave* tequilana bagasse. Int. J. Hydrog. Energy. 41(2), 897-904. https://doi.org/10.1016/j.ijhydene.2015.11.016

Baral, N.R., Shah, A., 2017. Comparative techno-economic analysis of steam explosion, dilute sulfuric acid, ammonia fiber explosion and biological pretreatments of corn stover. Bioresour. Technol. 232(C), 331-343. https://doi.org/10.1016/j.biortech.2017.02.068

Breton-Deval, L., Méndez-Acosta, H.O., González-Álvarez, V., Snell-Castro, R., Gutiérrez-Sánchez, D., Arreola-Vargas, J., 2018. *Agave* tequilana bagasse for methane production in batch and sequencing batch reactors: Acid catalyst effect, batch optimization and stability of the semi-continuous process. J. Environ. Econ. Manag. 224, 156-163. https://doi.org/10.1016/j.jenvman.2018.07.053

Buitrón, G., Hernández-Juárez, A., Hernández-Ramírez, M., Sánchez, A., 2019. Biochemical methane potential from lignocellulosic wastes hydrothermally pretreated. Ind. Crops. Prod. 139, 111555. https://doi.org/10.1016/j.indcrop.2019.111555

Cardeña, R., Moreno-Andrade, I., Buitrón, G., 2018. Improvement of the bioelectrochemical hydrogen production from food waste fermentation effluent using a novel start-up strategy. J. Chem. Technol. Biotechnol. 93(3), 878-886. https://doi.org/10.1002/jctb.5443

Carosia, M., Dos Reis, C., Sakamoto, I., Varesche, M., Silva, E., 2017. Influence of C/P and C/N ratios and microbial characterization in hydrogen and ethanol production in an anaerobic fluidized bed reactor. Int. J. Hydrog. Energy. 42(15), 9600-9610. https://doi.org/10.1016/j.ijhydene.2017.01.127

Carrillo-Reyes, J., Buitrón, G., Arcila, J. S., López-Gómez, M. O. 2021. Thermophilic biogas production from microalgae-bacteria aggregates: Biogas yield, community variation and energy balance. Chemosphere (Oxford), 129898. https://doi.org/10.1016/j.chemosphere.2021.129898

Castro, J.F., Razmilic, V., Gerdtzen, Z.P. 2013. Genome based metabolic flux analysis of Ethanoligenens harbinense for enhanced hydrogen production. Int. J. Hydrog. Energy, 38(3), 1297-1306. https://doi.org/10.1016/j.ijhydene.2012.11.007

Cho, S., Jung, M.Y., Park, M., Chang, Y., Yoon, J., Myung, S.C., Kim, W. (2010). Pseudoclavibacter chungangensis sp. nov., isolated from activated sludge. International Int. J. Syst. Evol. Microbiol., 60(Pt 7), 1672-1677. https://doi.org/10.1099/ijs.0.015552-0

COMBREX-DB. Online access: 11/02/2021 https://combrex.bu.edu/DAI?command=SciBay&fun=gene&geneID=6201778

Compant, S., Samad, A., Faist, H., Sessitsch A., 2019. A review on the plant microbiome: Ecology, functions, and emerging trends in microbial application. J. Adv. Res. 19, 29-37. https://doi.org/10.1016/j.jare.2019.03.004

Connolly, J.M., Jackson, B., Rothman A.P., Klapper, I., Robin Gerlach., 2015. Estimation of a biofilm-specific reaction rate: Kinetics of bacterial urea hydrolysis in a biofilm. Npj. Biofilms. Microbiomes. 1, 15014. https://doi.org/10.1038/npjbiofilms.2015.14

Contreras-Dávila, C.,A., Carrión, V.,J., Vonk, V. R., Buisman, C. N. J., Strik, D. P. B. T. B. 2020. Consecutive lactate formation and chain elongation to reduce exogenous chemicals input in repeated-batch food waste fermentation. Water Res., 169, 115215. https://dx.doi.org/10.1016/j.watres.2019.115215

Dabek, M., McCrae, S. I., Stevens, V. J., Duncan, S. H., Louis, P. 2008. Distribution of β-glucosidase and β-glucuronidase activity and of β-glucuronidase gene gus in human colonic bacteria. FEMS Microbiology Ecology, 66(3), 487-495. https://dx.doi.org/10.1111/j.1574-6941.2008.00520.x

Davis, S., Dohleman, F., Long, S., 2011. The global potential for *Agave* as a biofuel feedstock. Global Change Biology. Bioenergy, 3(1), 68-78. https://doi.org/10.1111/j.1757-1707.2010.01077.x

Emerson, E. L., Weimer, P. J. 2017. Fermentation of model hemicelluloses by *Prevotella* strains and *Butyrivibrio fibrisolvens* in pure culture and in ruminal enrichment cultures. Appl. Microbiol. Biotechnol., 101(10), 4269-4278. https://dx.doi.org/10.1007/s00253-017-8150-7

Escamilla-Treviño, L., 2012. Potential of plants from the genus *Agave* as bioenergy crops. Bioenergy Res. 5(1), 1-9. https://doi.org/10.1007/s12155-011-9159-x

Flaiz, M., Baur, T., Brahner, S., Poehlein, A., Daniel, R., Bengelsdorf, F. R. 2020. *Caproicibacter fermentans* gen. nov., sp. nov., a new caproate-producing bacterium and emended description

of the genus *Caproiciproducens*. Int. J. Syst. Evol. Microbiol., 70(7), 4269-4279. https://dx.doi.org/10.1099/ijsem.0.004283

Fraga, M., Perelmuter, K., Valencia, M., Martínez, J., Abin-Carriquiry, M., Cajarville, A., Zunino, C., 2014. Evaluation of native potential probiotic bacteria using an in vitro ruminal fermentation system. Ann. Microbiol. 64(3), 1149-1156. https://doi.org/10.1007/s13213-013-0753-3

Glaeser, S. P., Bolte, K., Martin, K., Busse, H., Grossart, H., Kämpfer, P., Glaeser, J. 2013. Novosphingobium fuchskuhlense sp. nov., isolated from the north-east basin of lake grosse fuchskuhle. Int. J. Syst. Evol. Microbiol., 63, 586-592. https://dx.doi.org/10.1099/ijs.0.043083-0

Guan, N., Li, J., Shin, H., Du, G., Chen, J., Liu, L., 2016. Metabolic engineering of acid resistance elements to improve acid resistance and propionic acid production of propionibacterium jensenii. Biotechnol. Bioeng. 113(6), 1294-1304. https://dx.doi.org/10.1002/bit.25902

Guan, N., Liu, L., 2020. Microbial response to acid stress: Mechanisms and applications. Appl. Microbiol. Biotechnol. 104(1), 51-65. https://dx.doi.org/10.1007/s00253-019-10226-1

Gómez, A.V., Valdez-Vazquez, I., Caballero-Caballero, M., Chiñas-Castillo, F., Alavéz-Ramírez, R., Montes-Bernabé, J.L., 2019. Co-digestion of *Agave angustifolia* Haw bagasse and vinasses for biogas production from mezcal industry. Revista Mexicana De Ingeniería Química, 18(3), 1073-1083. https://dx.doi.org/10.24275/uam/izt/dcbi/revmexingquim/2019v18n3/Gomez

Hammer, O., Harper, D.A.T., Ryan, P.D. 2001. PAST: paleontological statistics software package for education and data analysis. Palaeontologia Electronica 4, 9. http://folk.uio.no/ohammer/past/

Hernández, C., Escamilla-Alvarado, C., Sánchez, A., Alarcón, E., Ziarelli, F., Musule, R., Valdez-Vazquez, I., 2019. Wheat straw, corn stover, sugarcane, and *Agave* biomasses: Chemical properties, availability, and cellulosic-bioethanol production potential in Mexico. Biofuel. Bioprod. Biorefin. 13(5), 1143-1159. https://doi.org/10.1002/bbb.2017

Hiraishi, A., Matsuzawa, Y., Kanbe, T., Wakao, N. 2000. Acidisphaera rubrifaciens gen. nov., sp. nov., an aerobic bacteriochlorophyll-containing bacterium isolated from acidic

environments. Int. J. Syst. Evol. Microbiol., 50(4), 1539-1546. https://doi.org/10.1099/00207713-50-4-1539

Kämpfer, P., Martin, K., McInroy, J. A., Glaeser, S. P. 2015. Novosphingobium gossypii sp. nov., isolated from gossypium hirsutum. Int. J. Syst. Evol. Microbiol., 65(9), 2831-2837. https://dx.doi.org/10.1099/ijs.0.000339

Karthikeyan, O., Selvam, A., Wong, J., 2016. Hydrolysis–acidogenesis of food waste in solid–liquid-separating continuous stirred tank reactor (SLS-CSTR) for volatile organic acid production. Bioresour. Technol. 200, 366-373. https://doi.org/10.1016/j.biortech.2015.10.017

Kim, B., Seung Jeon, B., Kim, S., Kim, H., Um, Y., Sang, B. (2015). Caproiciproducens galactitolivorans gen. nov., sp. nov., a bacterium capable of producing caproic acid from galactitol, isolated from a wastewater treatment plant. Int. J. Syst. Evol. Microbiol., 65(12), 4902-4908. https://dx.doi.org/10.1099/ijsem.0.000665

Kim, M. K., Jung, H. (2009). Pseudoclavibacter soli sp. nov., a β-glucosidase-producing bacterium. Int. J. Syst. Evol. Microbiol., 59, 835-838

Klindworth, A., Pruesse, E., Schweer, T., Peplies, J., Quast, C., Horn, M., Glöckner, F.O. 2013. Evaluation of general 16S ribosomal RNA gene PCR primers for classical and next-generation sequencing-based diversity studies. Nucleic Acids Res. 41(1), e1. https://doi.org/10.1093/nar/gks808

Kullavanijaya P, Chavalparit O., 2019. The production of volatile fatty acids from Napier grass via an anaerobic leach bed process: The influence of leachate dilution, inoculum, recirculation, and buffering agent addition. J. Environ. Chem. Eng. 7(6), 103458. https://doi.org/10.1016/j.jece.2019.103458

Ley, R. E. 2016. Gut microbiota in 2015: Prevotella in the gut: Choose carefully. Nature Reviews. Gastroenterology & Hepatology, 13(2), 69-70. https://dx.doi.org/10.1038/nrgastro.2016.4

Liang, J., Zheng, W., Zhang, H., Zhang, P., Cai, Y., Wang, Q., Zhou, Z., Ding, Y. 2021. Transformation of bacterial community structure in rumen liquid anaerobic digestion of rice straw. Environ. Pollut, 269, 116130. https://dx.doi.org/10.1016/j.envpol.2020.116130

Lin, Y., Wang, D., Liang, J., Li, G., 2012. Mesophilic anaerobic co-digestion of pulp and paper sludge and food waste for methane production in a fed-batch basis. Environ. Sci. Technol. 33(23), 2627-2633. https://doi.org/10.1080/09593330.2012.673012

Manaia, C.M., Nogales, B., Weiss, N., Nunes, O.C. (2004). Gulosibacter molinativorax gen. nov., sp. nov., a molinate-degrading bacterium, and classification of 'Brevibacterium helvolum' DSM 20419 as Pseudoclavibacter helvolus gen. nov., sp. nov. Int. J. Syst. Evol. Microbiol., 54(3), 783-789. https://doi.org/10.1099/ijs.0.02851-0

Mansouri, S., Shahriari, A., Kalantar, H., Moini Zanjani, T., Haghi Karamallah, M. 2017. Role of malate dehydrogenase in facilitating lactate dehydrogenase to support the glycolysis pathway in tumors. Biomed. Rep., 6(4), 463. https://dx.doi.org/10.3892/br.2017.873

Montiel-Corona, V., Palomo-Briones, R., Razo-Flores, E., 2020. Continuous thermophilic hydrogen production from an enzymatic hydrolysate of *Agave* bagasse: Inoculum origin, homoacetogenesis and microbial community analysis. Bioresour. Technol. 306, 123087. https://doi.org/10.1016/j.biortech.2020.123087

Muñoz-Páez, K., Alvarado-Michi, E., Moreno-Andrade, I., Buitrón, G., Valdez-Vazquez, I., 2020. Comparison of suspended and granular cell anaerobic bioreactors for hydrogen production from acid *Agave* bagasse hydrolyzates. Int. J. Hydrog. Energy. 45(1), 275-285. https://doi.org/10.1016/j.ijhydene.2019.10.232

Murali, N., Fernandez, S., Ahring, B.K., 2017. Fermentation of wet-exploded corn stover for the production of volatile fatty acids. Bioresour. Technol. 227, 197-204. https://doi.org/10.1016/j.biortech.2016.12.012

Nguyen, A. Q., Nguyen, L. N., Johir, M. A. H., Ngo, H., Chaves, A. V., Nghiem, L. D. 2020. Derivation of volatile fatty acid from crop residues digestion using a rumen membrane bioreactor: A feasibility study. Bioresource Technology, 312, 123571. https://dx.doi.org/10.1016/j.biortech.2020.123571

Nordell, E., Nilsson, B., Nilsson Påledal, S., Karisalmi, K., Moestedt, J., 2016. Co-digestion of manure and industrial waste – The effects of trace element addition. Waste Manag. 47(PA), 21-27. https://doi.org/10.1016/j.wasman.2015.02.032

Pérez-Rangel, M., Barboza-Corona, J., 2020. Essential nutrients for improving the direct processing of raw lignocellulosic substrates through the dark fermentation process. Bioenergy Res. 13(1), 349-357. https://doi.org/10.1007/s12155-019-10083-w

Pérez-Rangel, M., Quiroz-Figueroa, F., Gonzalez-Castaneda, J., Valdez-Vazquez, I., 2015. Microscopic analysis of wheat straw cell wall degradation by microbial consortia for hydrogen production. Int. J. Hydrog. Energy, 40(1), 151-160. https://dx.doi.org/10.1016/j.ijhydene.2014.10.050

Pérez-Rangel, M., Barboza- Corona, J.E., Navarro- Díaz, M., Escalante, A.E., Valdez-Vazquez, I., 2021. The duo *Clostridium* and *Lactobacillus* linked to hydrogen production from a lignocellulosic substrate. Water Sci. Technol. wst2021186. https://doi.org/10.2166/wst.2021.186

Perimenis, A., Nicolay, T., Leclercq, M., Gerin, P., 2018. Comparison of the acidogenic and methanogenic potential of agroindustrial residues. Waste Manag. 72, 178-185. https://doi.org/10.1016/j.wasman.2017.11.033

Quatravaux, S., Remize, F., Bryckaert, E., Colavizza, D., Guzzo, J., 2006. Examination of lactobacillus plantarum lactate metabolism side effects in relation to the modulation of aeration parameters. J. Appl. Microbiol., 101(4), 903-912. https://dx.doi.org/10.1111/j.1365-2672.2006.02955.x

Reichardt, N., Vollmer, M., Holtrop, G., Farquharson, F.M., Wefers, D., Bunzel, M., Duncan, S.H., Drew, J.E., Williams, L.M., Miligan, G., Preston, T., Morrison, D., Flint, H.J., Louis, P., 2018. Specific substrate-driven changes in human faecal microbiota composition contrast with functional redundancy in short-chain fatty acid production. ISME J. 12(2), 610-622. . https://doi.org/10.1038/ismej.2017.196

Robinson, R.K., Batt, C.A. 2014. Encyclopedia of Food Microbiology. Cambridge: Elsevier Science & Technology. ISBN: 9780123847300

Salyers, A. A., Vercellotti, J. R., West, S. E., Wilkins, T. D. 1977. Fermentation of mucin and plant polysaccharides by strains of bacteroides from the human colon. Appl. Environ. Microbiol., 33(2), 319-322. https://doi.org/10.1128/AEM.33.2.319-322.1977

Sebayang, A., Hassan, M., Ong, H., Dharma, S., Silitonga, A., Kusumo, F., Bahar, A., 2017. Optimization of Reducing Sugar Production from Manihot glaziovii Starch Using Response Surface Methodology. Energies. 10(1), 35. https://doi.org/10.3390/en10010035

Tang, J., Yuan, Y., Guo, W., Ren, N. 2012. Inhibitory effects of acetate and ethanol on biohydrogen production of ethanoligenens harbinese B49. Int. J. Hydrog. Energy, 37(1), 741-747. https://dx.doi.org/10.1016/j.ijhydene.2011.04.067

Takeuchi, D.M., Kishino, S., Ozeki, Y., Fukami, H., & Ogawa, J. (2022). Analysis of astragaloside IV metabolism to cycloastragenol in human gut microorganism, bifidobacteria, and lactic acid bacteria. Bioscience, Biotechnology, and Biochemistry, 86(10), 1467–1475. https://doi.org/10.1093/bbb/zbac130

Towey, R., Webster, K., Darr, M., 2019. Influence of storage moisture and temperature on lignocellulosic degradation. J. Agric. Eng. 1(3), 332-342. https://doi.org/10.3390/agriengineering1030025

Vorholt, J. A., 2012. Microbial life in the phyllosphere. Nat. Rev. Microbiol. 10(12), 828-40. https://doi.org/10.1038/nrmicro2910

Valdez-Vazquez, I., Alatriste-Mondragón, F., Arreola-Vargas, J., Buitrón, G., Carrillo-Reyes, J., León-Becerril, E., Weber, B., 2020. A comparison of biological, enzymatic, chemical and hydrothermal pretreatments for producing biomethane from *Agave* bagasse. Ind. Crops. Prod. 145, 112160. https://doi.org/10.1016/j.indcrop.2020.112160

Valdez-Vazquez, I., Castillo-Rubio, L.G., Pérez-Rangel, M., Sepúlveda-Gálvez, A., Vargas, A., 2019. Enhanced hydrogen production from lignocellulosic substrates via bioaugmentation with Clostridium strains. Ind. Crops Prod. 137, 105-111. https://doi.org/10.1016/j.indcrop.2019.05.023

Valdez-Vazquez I., Quiroz-Figueroa F.R., Carrillo-Reyes J., Medina-López A., 2016a. Microscopy Applied In Biomass Characterization. In: Vaz Jr. S. (eds) Analytical Techniques and Methods for Biomass. Springer, Cham. https://doi.org/10.1007/978-3-319-41414-0_7

Valdez-Vazquez, I., Torres-Aguirre, G.J., Molina, C., Ruiz-Aguilar, G.M.L., 2016b. Characterization of a lignocellulolytic consortium and methane production from untreated

wheat straw: dependence on nitrogen and phosphorous content. BioResources. 11(2), 4237-4251. https://doi.org/10.15376/biores.11.2.4237-4251

Valdez-Vazquez, I., Morales, A., Escalante, A., 2017. History of adaptation determines short-term shifts in performance and community structure of hydrogen-producing microbial communities degrading wheat straw. Appl. Microbiol. Biotechnol. 10(6), 1569-1580. https://doi.org/10.1111/1751-7915.12678

Van Soest, P.J., Robertson, J.B., Lewis, B.A., 1991. Methods for dietary fiber, neutral detergent fiber, and nonstarch polysaccharides in relation to animal nutrition. Int. J. Dairy Sci. 10, 3583-3597. https://doi.org/10.3168/jds.S0022-0302(91)78551-2

Wang, X., Lu, X., Li, F., Yang, G., 2014. Effects of temperature and carbon-nitrogen (C/N) ratio on the performance of anaerobic co-digestion of dairy manure, chicken manure and rice straw: Focusing on ammonia inhibition. Plos One, 9(5), E97265. https://doi.org/10.1371/journal.pone.0097265

Weimer, P.J., Russell, J.B., Muck, R.E., 2009. Lessons from the cow: What the ruminant animal can teach us about consolidated bioprocessing of cellulosic biomass. Bioresour. Technol. 100(21), 5323-5331. https://doi.org/10.1016/j.biortech.2009.04.075

Wolfe, B., Dutton, R., 2015. Fermented foods as experimentally tractable microbial ecosystems. Cell. 161(1), 49-55. https://doi.org/10.1016/j.cell.2015.02.034

Zabed, H.M., Suely, A., Yun, J., Zhang, G., Awad, F.N., Qi, X., Sahu, J.N., 2019. Recent advances in biological pretreatment of microalgae and lignocellulosic biomass for biofuel production. Renew.Sust. Energ. Rev. 105, 105-128. https://doi.org/10.1016/j.rser.2019.01.048

Zhang, G.W, Wang, C, Du, H.S, Wu, Z.Z, Liu, Q, Guo, G, Huo, W.J., Zhang, J., Zhang, Y.L., Pei, C.X., Zhang, S.L., 2020. Effects of folic acid and sodium selenite on growth performance, nutrient digestion, ruminal fermentation and urinary excretion of purine derivatives in Holstein dairy calves. Livest. Sci. 231, 103884. https://doi.org/10.1016/j.livsci.2019.103884

Zhang, W., Chen, B., Li, A., Zhang, L., Li, R., Yang, T., Xing, W., 2019. Mechanism of process imbalance of long-term anaerobic digestion of food waste and role of trace elements in maintaining anaerobic process stability. Bioresour. Technol. 275, 172-182. https://doi.org/10.1016/j.biortech.2018.12.052

Zieliński, M., Kisielewska, M., Dębowski, M., Elbruda, K., 2019. Effects of nutrients supplementation on enhanced biogas production from maize silage and cattle slurry mixture. Water Air Soil Pollut. 230(6), 1-7. https://doi.org/10.1007/s11270-019-4162-5

4. Chapter IV: Effects of pH and TS on volatile fatty acids production from agave bagasse by mixed culture

Reference to submitted work:

4.1 Abstract

The objective of the study was to evaluate the effects of pH and total solids (TS) on hydrogen production from agave bagasse by mixed culture. The experimental design was based on a central composite design which consisted of two numeric factors initial pH at 5.7 (low level) and 6.7 (high level) and TS 10% (low level) and 20% (high level) resulting in 13 runs. The pH was maintained using a buffer of two different capacities. The response variable was the accumulation of volatile fatty acids (VFA), where production of butyric acid was considered as an indicator of hydrogen production. The highest concentration of total VFAs (12.1 g COD/L) where butyric acid was produced at the highest ratio was obtained for initial pH 6.2 and TS 22.1%. The VFAs reached maximum titers at different times beginning with lactic, propionic, butyric, and acetic acid at 24, 72, 120 and 120 h, respectively. Statistical analysis showed a significant effect of TS% on butyric acid. At incrasing TS% increasing butyric acid concentration. The changes of the initial pH did not effect its production. In contrary, both studied factors have significan effect on lactic acid production. With an increase in TS%, the production of lactic acid and thus butyric acid and hydrogen increases. The contrary tendency was observed for pH, an its decrease, lactic acid production increases because of its accumulation. The VFAs composition changes over time confirmed hydrogen and butyric acid production via lactate/acetate pathway when pH was about 6.0 or higher.

Keywords: biogas; dark fermentation; lignocellulosic biomass; volatile fatty acids;

4.2   Introduction

Utilization of organic wastes for biofuels and biochemicals production has become one of the most important lines of research in the global transition from fossil fuels to renewable resources. Lignocellulosic biomass being plant waste is an adequate source for the production of energy and value-added bioproducts. Moreover, it is a particularly attractive carbon source because it does not compete with the food industry, and its annual production is estimated at 181.5 billion tons per year (Dahmen et al., 2019). Among many types of lignocellulosic biomass, Agave bagasse from the Tequila and Mezcal industries, is one of the most abundant in Mexican territory and its annual dry weight is estimated at 149,777 tons (Honorato-Salazar et al., 2021). The biomass composition ranges from 38 to 53% cellulose, 32–54% hemicellulose, 4–14% lignin and up to 20% extractives. This wide variability is conditioned by climate cultivation, agronomic practices, harvesting time and plant age (Dudek et al., 2021). Its biodegradability is low and is affected by several factors such as recalcitrant character of the lignocellulosic biomass, polymeric and crystalline degree of cellulose and branching nature of hemicelluloses and lignin polymers (Banu et al., 2021). Therefore, physicochemical or biological pretreatment is required to broke down the complex structure of hemicellulose and cellulose into pentoses (mainly xylose) and glucose, respectively (Jacobsen and Wyman, 2000; Yankov, 2022). Recently, consolidated bioprocessing (CBP) has been widely studied as a biological pretreatment of lignocellulosic biomass due to its advantage of combining three processes occurring at the same site: production of saccharolytic enzymes, hydrolysis of the polysaccharides, and pentose and hexose fermentation (Dudek et al., 2021). Process parameters such as temperature, pH, total solids (TS), solid and hydraulic retention time, nutrients availability, agitation, type of substrate and inoculum, affect final products and process yields (García-Depraect et al., 2021; Motte et al., 2013; Pérez-Rangel et al., 2020; Sarkar et al., 2021; Sun et al., 2021).

Dark fermentation is a suitable intermediate technology, in which several types of bacteria, usually *Clostridium* and *Enterobacter*, can use carbohydrates and other carbon source to produce biohydrogen and organic acids via acidogenic pathways (Cheonh et al., 2022). Theoretically, from 1 g of cellulose can be produced up to 567 ml of hydrogen (Liu et al., 2003). Nevertheless, the experimental yields of direct fermentation of cellulosic materials are very low due to the complex structure of lignocellulose. The CBP carrying out by mixed culture produce volatile fatty acids

(VFA), which being byproducts can be used as precursors to produce liquid biofuels such as butanol, as well as to enhance hydrogen production (Mockaitis et al., 2020). The 2-hydroxypropanoic acid with a molecular formula $CH_3CH(OH)COOH$, better known as a lactic acid (LA) is a potential building block for hydrogen and value-added bioproducts production through metabolic pathways performed by diverse bacteria, mainly *Clostridium spp.* (García-Depraect et al., 2021). Moreover, the organic acids like acetic, butyric, and propionic are utilized by different metabolic pathways during hydrogen generation. The acetic acid is usually the main electron donor (Chen et al., 2011).

In this study the impact of initial pH and TS parameters on VFA production from Agave bagasse var. Azul during CBP by mixed culture was evaluated. Moreover, the impact of pH stability maintained by two different MES buffer capacities on bioproducts, and biogas production were evaluated.

4.3   Materials and methods

4.3.1   Substrate and inoculum

The agave bagasse used for the experiments was collected in mid-February 2022 and delivered from Tequilera Real de Penjamo in Penjamo, Guanajuato, Mexico. The biomass was then sun-dried and stored in a closed plastic container at room temperature. Before its use, the lignocellulosic biomass was milled using an industrial mixer (LI-3A, VECA INTERNATIONAL) and particles between 2 mm and 4 mm size were selected using sieves (Endecotts, London).

The inoculum used was obtained from a reactor that was inoculated with the native microbiota of non-sterile agave bagasse at 80% moisture content and was operated for eight weeks under the following conditions: TS 15%, initial pH of 6.5 which was adjusted at each feeding, 37 °C, and agitation of 150 rpm. The culture medium contained (g/L): 1.02 of CH_4N_2O, 0.41 $CaCl_2$, and 0.11 KH_2PO_4 according to Pérez-Rangel et al., 2020.

4.3.2   Experimental design

The aim of this study was to investigate the effect of pH and TS on the production of VFA from lignocellulosic biomass. To buffer the pH, the 2-(N-morpholino)ethane-sulfonic acid (MES) was chosen due to its advantages such as: high solubility in water, minimal salts impact, and chemical

and enzymatic stability among others (Good et al., 1966). In consequence, the pH range of the experimental design ranged from 5.5 to 6.9. The levels of TS content to be studied were selected based on a literature review (Sun et al., 2021; Yang et al., 2015). The central composite design (CCD) which consisted of two numeric factors at two levels: initial pH at 5.7 (low level) and 6.7 (high level) and TS at 10% (low level) and 20% (high level) was used. In this way, 13 runs were obtained, where eight runs represented the non-center points and five runs the center points (or replicates). The experimental runs were depicted in the Table 4.1.

A quadratic model (equation 1) was used to assess the relationship between the response variable (VFA concentration) and the factors (X_1 - pH, X_2 - TS) based on experimental data.

$$Y_i = \beta_0 + \sum \beta_i X_i + \sum \beta_{ii} X_i^2 + \sum \beta_{ij} X_i X_j \tag{1}$$

Where Y_i is the response variable (VFA concentration expressed in g/L or VFA production in mgCOD/gTS), β_0 is the constant, β_i is the linear coefficient, β_{ii} is the squared coefficient, and β_{ij} is the interaction coefficient. The experimental design, statistical analysis, and construction of 3D response surface plots were prepared using Design Expert v10 (Stat-Ease, Inc., MN, USA).

The experiments were conducted in 250 mL glass flask bottles (Bellco Glass, Shrewsbury, UK), with a working volume of 100 mL. Into each reactor, 10 g of inoculum (85% of moisture) was introduced. The culture medium, TS%, and initial pH varied according to the experimental design. The culture medium contained 100 mM MES buffer and the following nutrients (g/L): 1.02 of CH_4N_2O, 0.41 $CaCl_2$, and 0.11 KH_2PO_4 (Pérez-Rangel et al., 2020). The reactors were sealed tightly and incubated at 37 °C, with agitation of 150 rpm for 5 days. Every 24 h a sample of the fermentation broth was taken while the gases were released to the atmosphere.

4.3.3   Validation experiment

The experimental condition that led to the highest concentration of VFAs and the highest butyric acid ratio to the total VFAs was chosen as optimal condition and validated in an additional set of experiments. The run was as follows: initial pH 6.5, TS 15%, with the above-mentioned composition of the culture medium. Additionally, two different MES buffer capacities of 100 and 400 mM were applied to evaluate their effects on pH stability, hence, VFA concentration. For the MES buffer capacity of 100 mM, 15 identical reactors with pH 6.5 and TS 22.1% were prepared.

For all reactors, every 12 h the gases were measured and then released to the atmosphere. Also, at times 0, 24, 36, 48, and 72 h, three reactors were discarded from the experiment to take liquid and solid samples for further analytical and molecular analyses. Then, the experiment was repeated with 400 mM MES buffer capacity.

4.3.4   Analytical methods

The pH was measured using a potentiometer (BACKMAN, 50 pH Meter). Concentrations of VFAs were analyzed using high-performance liquid chromatography (HPLC) with 10 µL sample injection (model 1260 infinity, Agilent Technologies, CA, USA) equipped with an Aminex HPX-87H column and two detectors: Refractive Index Detector (RID) and Diode-Array Detector (DAD) with detection wavelength of 210 nm. The mobile phase was a 5 mM H_2SO_4 solution at a flow rate of 0.6 mL/min. Biogas composition was analyzed with a gas chromatography (GC) (SRI Instruments Model 8610C, Champaign, IL, USA) equipped with a thermal conductivity detector (TCD) and two steel columns (2 m in length; 0.79 mm in diameter). The injector, column and detector temperatures were 90, 110 and 150 °C, respectively. Nitrogen was used as a carrier gas at a flow rate of 20 mL/min. Gas volume was reported at standard temperature and pressure (0 °C and 1013.25 hPa).

4.3.5   Calculation and statistical análisis

The VFAs productivity was calculated as a VFA concentration expressed as a chemical oxygen demand (COD) per gram of TS of Agave bagasse fibers introduced into reactor (mgCOD/gTS). To convert concentration of VFAs to COD, the following stoichiometric factors were used: 1.067 gCOD/g acetic acid, 1.512 gCOD/g propionic acid, 1.813 gCOD/g butyric acid, and 1.066 gCOD/g lactic acid (Perimenis et al., 2016). Analysis of variance (ANOVA) was performed to determine significant differences between the MES buffer capacity and VFAs, and butyric acid production. Microsoft Excel 365 ProPlus (Version 1908) was used to carried out calculations, and the confidence level was 95%.

4.4   Results and discussion

4.4.1   Effect of pH and TS on VFA production

Both, initial pH and TS affected the total VFA concentration from Agave bagasse during acidogenesis by the mixed culture. The highest VFA concentration of 13.8 g COD/L was achieved

for the reactor with initial pH 6.7 and TS 20%. The lowest VFA concentration at level of 5.8 g COD/L was detected for the reactor operated with initial pH 5.7 and TS 10% (Table 4.1). The most abundant fermentation products formed during consolidated bioprocessing of Agave bagasse were acetic, propionic, and butyric acid, which correspond to the dominant VFA obtained from lignocellulosic biomass by native microbiota reported in the literature (Ayala-Campos et al., 2022; Dudek et al., 2021). The concentration and total production of VFAs showed independent tendencies (Figure 4.1 a, b). Moreover, the production of individual VFA was presented in four graphics since each of the key acids reached its highest concentration at different times (Figure 4.1 c, d, e, f).

Table 4.1. Effect of initial pH and TS on VFA production from Agave bagasse. Reported concentrations correspond to 120h of fermentation.

Run	Initial pH (X_1)	Total solids (%), (X_2)	Total VFA production (mgCOD/gTS)	Total VFA concentration (mg COD/L)	Acetic Acid	Propionic Acid	Butyric Acid	Lactic Acid
					Concentration (mg/L)			
1	5.49	15	633.3	6712.7	3049.0	1432.2	2231.5	0.0
2	5.70	10	750.0	5756.6	3355.8	1200.4	1131.4	0.0
3	5.70	20	760.0	10504.5	4351.3	2248.6	3904.7	0.0
4	6.20	8	996.4	6168.9	3719.3	1297.0	1050.0	0.0
5	6.20	15	946.7	10857.9	6666.6	1941.0	2250.3	0.0
6	6.20	15	826.7	9378.6	5520.6	1713.6	2144.5	0.0
7	6.20	15	840.0	9660.2	5875.1	1732.4	2052.7	0.0
8	6.20	15	840.0	9563.2	5677.7	1718.1	2167.5	0.0
9	6.20	15	800.0	9330.8	5883.2	1676.4	1771.2	0.0
10	6.20	22	792.9	12130.6	5177.3	2151.8	4801.5	0.0
11	6.70	10	1040.0	7947.5	4835.8	1506.4	1605.3	0.0
12	6.70	20	960.0	13780.2	6880.5	2323.3	4576.3	0.0
13	6.91	15	726.7	6139.9	2331.1	1443.6	1998.3	0.0

The highest experimental total VFA concentration of 19200 mgCOD/L was reached at the initial pH 6.7 and TS 10%. The ANOVA of mathematical model of total VFA concentration for the 120 h of fermentation resulted significant ($p = 0.0010$). The quadratic model with the corresponding

power law transformation (λ = -2.77; k = 0) predicted the highest value of 32000 mgCOD/L at initial pH 5.78 and TS 19.9% with a desirability value of 1.00. The kinetics parameters were calculated using the equation 2, where C_{TC} refers to the total VFA concentration of all produced acids (mgCOD/L). The determination coefficient of (R^2) of 0.92 and R^2 adjusted of 0.86 were close which indicate that the model is a good fit of the data. The growing tendency of total VFA concentration was observed when decreasing initial pH till 5.9 and increasing TS % (Figure 1a). The ANOVA of the model of total VFA concentration indicated that pH and TS % affect significantly total VFA concentration (pH: ρ = 0.0203; TS%: ρ = 0.0015).

$$(C_{TC})^{-2.77} = 4.023E^{-12} - 2.06E^{-12}X_1 - 3.482E^{-12}X_2 + 5.485E^{-12}X_1X_2 + 1.683E^{-12}X_1{}^2 + 2.424E^{-12}X_2{}^2 \tag{2}$$

The C_{TP} corresponds to the total acids production expressed in mgCOD/gTS and was calculated according to equation 3, to project mathematical model of kinetics parameters. The ANOVA confirmed the significance of the quadratic model (ρ = 0.0110) with a value of R^2 of 0.84 and R^2 adjusted of 0.72.

$$C_{TP} = 820.08 + 77.50X_1 + 2.42X_2 + 17.50X_1X_2 - 56.63X_1{}^2 + 87.94X_2{}^2 \tag{3}$$

The highest total VFA production was predicted for the TS content of 22% and the initial pH between 6.5 and 6.9, while a point with slightly lower value of total VFA production was observed for the TS content of 7.9% and at initial pH of 6.44. In general, an increasing trend of total VFA production appeared when the TS content increases or decreases from a value of 13% (Figure 4.1 b). Regarding to pH, its increase up to 6.2 was related with accelerated increase of total VFA production, then the VFA production stabilization was observed. Numerical optimization of the response variable predicted the maximal total VFA production of 950.28 mgCOD/gTS at initial pH 6.62 and TS 20%.

Lactic acid was produced at the beginning of the fermentation and the highest experimental concentration was 1.72 g/L after 24 h (Figure 4.1 c).
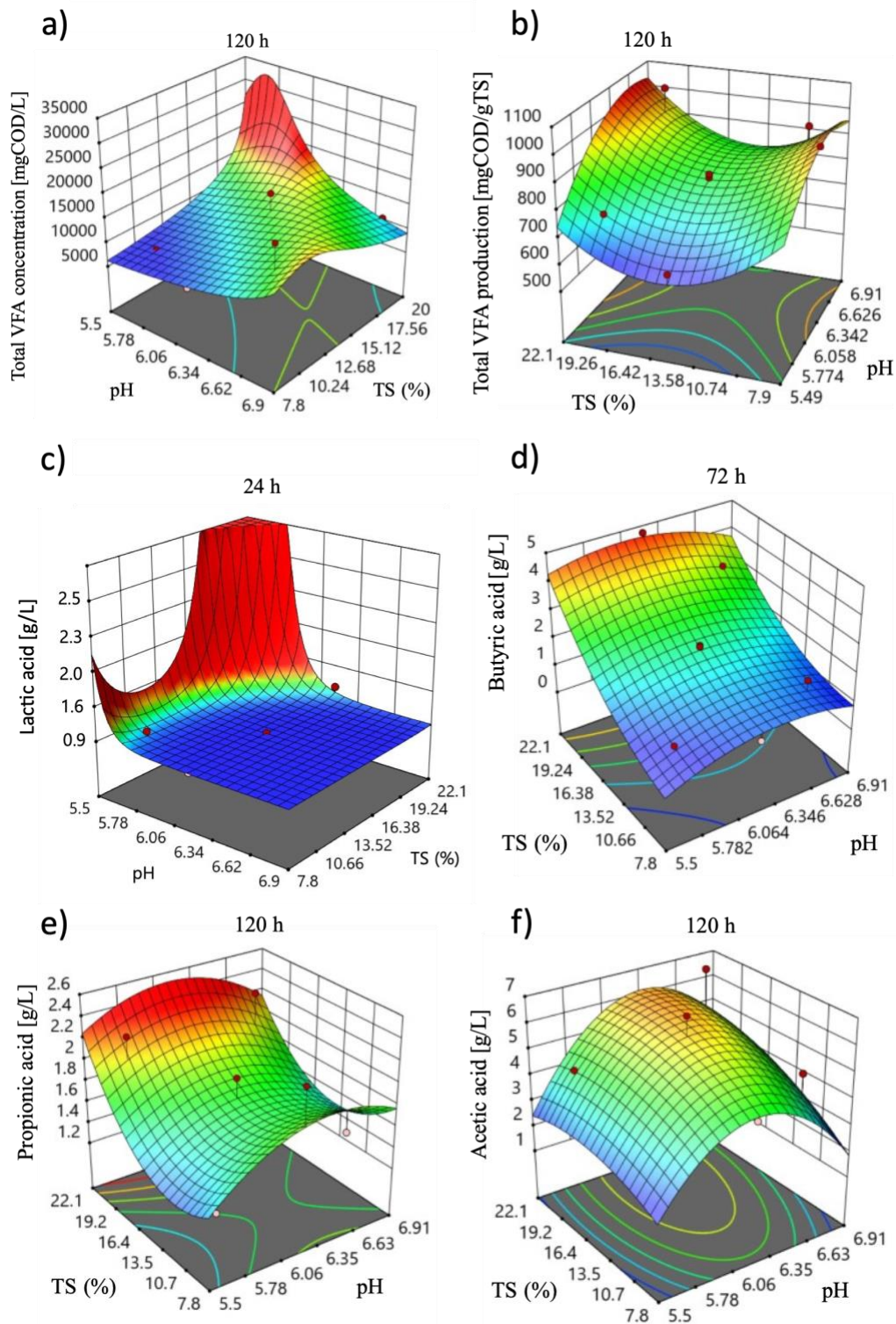
Figure 4.1. Effect of TS and pH on the production of the carboxylic acids: a) lactic acid; b) butyric acid; c) propionic acid; d) acetic acid; obtained during acidogenesis of Agave bagasse by mixed culture.

Its production was probably due to the consumption of xylose, whose concentration at the start was between 1.7 and 3.8 g/L depending on TS content (from 8 to 22%). Lactic acid production increases when pH decreases, and TS increases. As long as the pH was higher than 5.7, the production of lactic acid was completely inhibited, regardless of the TS content. The C_{HLa} refers to the concentration of lactic acid (g/L) calculated according to quadratic equation 4 transformed with natural log (k=0.00176019) to predict the mathematical model of its formation depending on pH and TS. The value of R^2 of 0.91 indicates that the model was an accurate representation of the data. The ANOVA indicated that, both, pH ($\rho = 0.0003$) and TS content ($\rho = 0.0200$) have significance impact on lactic acid production.

The numerical optimization predicted the maximum lactic acid concentration of 1.05 g/L at the initial pH 5.86 and TS content of 20%. The experimental lactic acid production had a R^2 adjusted in 83.5% to its predicted production by the model.

$$Ln\ (C_{HLa} + 0.0017) = -6.09 - 2.71X_1 + 1.26\ X_2 - 0.3158X_1X_2 + 1.48X_1{}^2 + 1.42X_2{}^2 \qquad (4)$$

ANOVA of the transformed quadratic regression model showed to be significant ($\rho = 0.0016$). The highest butyric acid concentration of 4.8 g/L was found at the initial pH 6.2 and TS 22% after 72 h of fermentation (Figure 4.1 d). Its production has a growing tendency, when the TS content increased from 13.52 to 22.1%, butyric acid concentration reached 4 g/L. The optimum initial pH was 6.2, so a lower or a higher pH value was associated with a negative effect on the concentration of butyric acid. A quadratic model for the butyric acid production (C_{HBc}) (equation 5) has a high value of R^2 of 0.96 which is close to the value of R^2 adjusted of 0.94. It is an interesting fact, that only TS affects butyric acid production significantly ($\rho = 0.0001$) while pH was not statistically different ($\rho = 0.8501$). The numerical optimization gave the highest butyric acid concentration of 3.94 g/L for the initial pH 6.19 and TS 20%. The ANOVA also showed that the model was significant ($\rho = 0.0001$).

$$C_{HBc} = 2.24 + 0.0187X_1 + 1.20X_2 - 0.1423X_1X_2 - 0.3170X_1{}^2 + 0.3344X_2{}^2 \qquad (5)$$

After 120 h the most abundant acids detected in the reactor were acetic acid at the highest concentration of 6.9 g/L at initial pH 6.7 and TS 20%, followed by propionic acid with its the

highest concentration of 2.3 g/L at two different initial pH 6.7 and 5.7 and the same TS content of 20% (Figure 4.1 e, f).

For acetic acid, the area in which optimum acetic acid production is expected include the initial pH value between 6.0 and 6.3 and a TS from 15 to 22%. Decreasing or increasing initial pH results in decrease of acetic acid production. A quadratic model, where C_{HAc} corresponds to acetic acid production is shown in equation 6. The value of R^2 was 0.70 and the adjusted R^2 was 0.48 which is not as close as expected. The numerical optimization of the acetic acid concentration found the highest value of 6.2 g/L at the initial pH 6.32 and TS content of 19.9%.

$$C_{HAc} = 16.15 + 1.11X_1 + 2.2X_2 + 0.28X_1X_2 + 12.46X_1{}^2 + 0.63X_2{}^2 \tag{6}$$

The calculated model was not significant ($\rho = 0.0761$). Neither initial pH ($\rho = 0.3225$), nor TS ($\rho = 0.1781$) were significant. In the case of propionic acid, a wide range of pH could be observed at which the production is high. The propionic acid concentration increases when TS increases or decreases from 10%, reaching its maximum value for TS 22% (Figure 4.1 e). For propionic acid, the mathematical model was prepared. The C_{HPr} refers to propionic concentration and was calculated using quadratic equation 7. The ANOVA of the model used showed the value of R^2 of 0.65 and R^2 adjusted of 0.38. The maximal concentration of propionic acid calculated by numerical optimization function was 2.2 g/L for the initial pH 6.19 and TS 20%.

$$C_{HPr} = 1.76 + 0.0494X_1 + 0.2161X_2 - 0.0578X_1X_2 - 0.1578X_1{}^2 + 0.2218X_2{}^2 \tag{7}$$

According to ANOVA the proposed model resulted to be insignificant ($\rho = 0.1330$). Moreover, the initial pH ($\rho = 0.6362$) and TS content ($\rho = 0.0679$) have no significance on propionic acid production. Nevertheless, the lack of fit was significant to the pure error ($\rho < 0.0114$). The negative predicted R^2 (-1.3921) implies that the overall mean may be a better predictor of the response than the current model. The insignificant model, pH and TS contact evaluated by ANOVA, could indicate that for production of acetic and propionic acid, there are other factors that impact their production, however, were not studied in this study, hance, were not considering for mathematical model build. The ANOVA indicated that factors such as the initial pH and TS content are important when lactic acid is a desirable product. On the other hand, when butyric acid is the bioproduct of interest in the fermentation, the key factor is a TS content, while pH value is of minor importance

(statistically irrelevant). For propionic and acetic acids production, it is meaningless what initial pH or TS content is chosen. As mentioned before, possibly there are other factors, not studied in this work that could favor the production of acetic and propionic acids during lignocellulosic biomass fermentation.

The VFA production from lignocellulosic biomass reported in the literature was presented in the Table 4.2. Butyric acid production from different solid substrates by mixed cultures.. The highest concentration of total VFA of 24.3 g/L was obtained by Ai et al. (2016). In their study, the fermentation was carried out in a batch reactor at pH 6.0 stabilized with buffer and TS 10%. Butyric acid was the most abundant acid and accounted for 66% of the total VFA. Acetic acid was found at a concentration of 6.4 g/L. The authors reported that between second and sixth day of fermentation a large amount of hydrogen was generated in the reactor, and at the same time the highest production of butyric acid was registered. Similarly, in this study the highest hydrogen and butyric acid production took place at pH close to 6.0 (Figure 2). Therefore, it can be assumed that in both cases at the mentioned pH the consumption of lactic acid and acetic acid occurred giving biogas and butyric acid. Such a large difference in total VFA concentration compared to the results of the present study was due to the applied NaOH pretreatment of rice straw, which made hemicellulose and cellulose polymers accessible for microbial processing. Ayala-Campos et al. (2022) obtained the concentration total of VFAs of 13 g/L during Agave bagasse fermentation in semi-continuous reactor, operated with initial pH 6.5 buffered with phosphate 40 mM and TS 10%. The principal bioproduct was lactic acid at the concentration of 11.6 g/L followed by acetic acid (3.6 g/L). Butyric and propionic acids were not detected in the fermentation broth at that time. However, the decrease of lactic acid and formation of butyric acid was observed in time. It was related with pH decrease when buffer capacity was not enough to maintain stable pH. After 96 h of fermentation, butyric acid was the most abundant acid (53%), followed by acetic acid (35%). The same authors also processed sugarcane bagasse under the same conditions and obtained total VFA concentration of 13.2 g/L. However, the VFA composition was different. The lactic acid was found at a concentration of 6.3 g/L followed by 3.4 g/L of acetic acid and 0.8 g/L of butyric acid at 24 h. After 96 h, butyric acid formed 57% of total VFA, while acetic acid 27%. In this study the butyric acid concentration at its maximum concentration after 72 h represented 54% of total concentration of VFA. It can therefore be assumed that an interesting phenomenon is occurring. Regardless of the type of biomass, butyric acid at its maximum concentration represents between

50 and 60% of the total amount of acids. While the total VFA concentration depends on the characteristics of the lignocellulosic biomass structure and the number of microorganisms capable of degrading hemicellulose.

Table 4.2. Butyric acid production from different solid substrates by mixed cultures.

Microorganism	Substrate	Mode	pH	TS (%)	T °C	Concentration (g/L)					Reference
						Total VFA	Acetic Acid	Propionic Acid	Butyric Acid	Lactic Acid	
Undefined Mixed Culture	Rice straw [p]	Batch	6.0 [b]	10	35	24.2	6.4	0.83	15.9	0.0	Ai el al. 2016
C. thermocellum ATCC 27405 and *C. thermobutyricum* ATCC 49875	Delignified rice straw	Batch	6.5 [c]	2	55	2.45	0.08	0.0	2.37	0.0	Chi et al. 2018
Native mixed culture	Agave bagasse	Batch	6.5	10	37	4.54	2.18	1.0	1.36	0.0	Dudek et al. 2021
Native mixed culture	Wheat straw	Semi-cont.	6.5	10	37	12.2	3.9	1.5	4.3	0.0	Pérez-Rangel et al. 2021
Native mixed culture	Agave bagasse	Semi-cont.	6.5	10	37	13.0	1.4	0.0	0.0	11.6	Ayala-Campos et al. 2022
	Sugarcane bagasse					13.2	3.7	< 0.2	0.8	6.3	
Mixed culture	Agave bagasse	Batch	6.5	22	37	12.7	3.7	1.6	5.1	0.6	This work

Pérez-Rangel et al. (2021) carried out raw wheat straw fermentation with initial pH 6.5 (without control) and TS 10%. The authors obtained 12.2 g/L of total VFA after 96 h, where butyric acid was found at the highest concentration of 4.3 g/L, then acetic acid and propionic acid at 3.9 and 1.5 g/L, respectively. The lactic acid was not detected. Similarly, to the present study, in the first four days the highest hydrogen production was detected. Additionally, high butyric acid concentration and absence of lactic acid, could indicate that lactic acid was consumed to produce hydrogen and butyric acid. The lower proportion of butyric acid in the total VFA (35%) compared with this work and previously mentioned studies, may indicate that the sample analyzed was not taken at a time when butyric acid concentration was the highest (the authors have been taken samples every 96 h). In addition, the formation of propionic acid is evidenced by pH reduction to

5.2 or lower, as in the present study, at which pH the production of propionic acid began. Moreover, Pérez-Rangel et al. (2021) reported that pH during fermentation varied between 4.58 and 5.16.

4.4.2   Validation experiment

The reactors with MES buffer capacity of 100 and 400 mM produced 11.5 and 12.7 g/L of VFAs, respectively. Analysis of variance disproved a statistical difference in VFAs production between those reactors. Lactic acid reached the highest concentration of 1.7 g/L in the reactor with 100 mM buffer capacity after 24 h, then decreased immediately to 0.4 g/L, producing 3191 cm^3/L of biogas and increasing butyric acid concentration from 0.6 to 2.9 g/L within next 12 h. After 38 h, biogas production decreased over time. Meanwhile, butyric acid achieved a stable production of 4.5 g/L by 72 h (Figure 4.2). In the case of the reactors with 400 mM buffer capacity, lactic acid reached its maximum concentration of 3.4 g/L after 36 h. Thereafter, its amount dropped to 0.1 g/L, producing a maximum volume of 2780 cm^3/L of biogas and increasing butyric acid concentration from 0.2 to 3.1 g/L within next 12 h. Butyric acid production was increasing in time, till reach the highest concentration of 5.1 g/L after 72 h.

Biogas production increasing in time, having a constant level of hydrogen of 15%. In the key moment, when pH dropped below 6.0 and occurred lactic acid to hydrogen conversion, the hydrogen reached its maximum concentration of 35%. In both type of reactors, the volume of gases remained constant after 72 h of fermentation. The v/v hydrogen amount was close to 38% obtained from rice straw waste (Cheng et al., 2016). Meanwhile, Lu et al. (2021) obtained 44% hydrogen content during corn stalk processing.

Analyzing reactors could be concluded that buffer capacity permits for lactic acid production till pH does not drop below 6.0. Therefore, for the lower buffer capacity reactors, culmination biogas production was carried out between 24 and 36 h, while for the stronger buffer capacity reactors its formation was postponed in time and occurred between 36 and 48 h. Also, the acetic acid concentration in time frames mentioned above, was the same. Therefore, it is evidence of hydrogen and butyric acid production from lactic acid.

As for the experiment evaluating the effect of initial pH and TS on VFA production, it is likely that lactic acid was also produced in significant quantities, but due to the CBP its conversion into other bioproducts occurred in parallel. This can be confirmed by the analysis of VFAs profile production

13
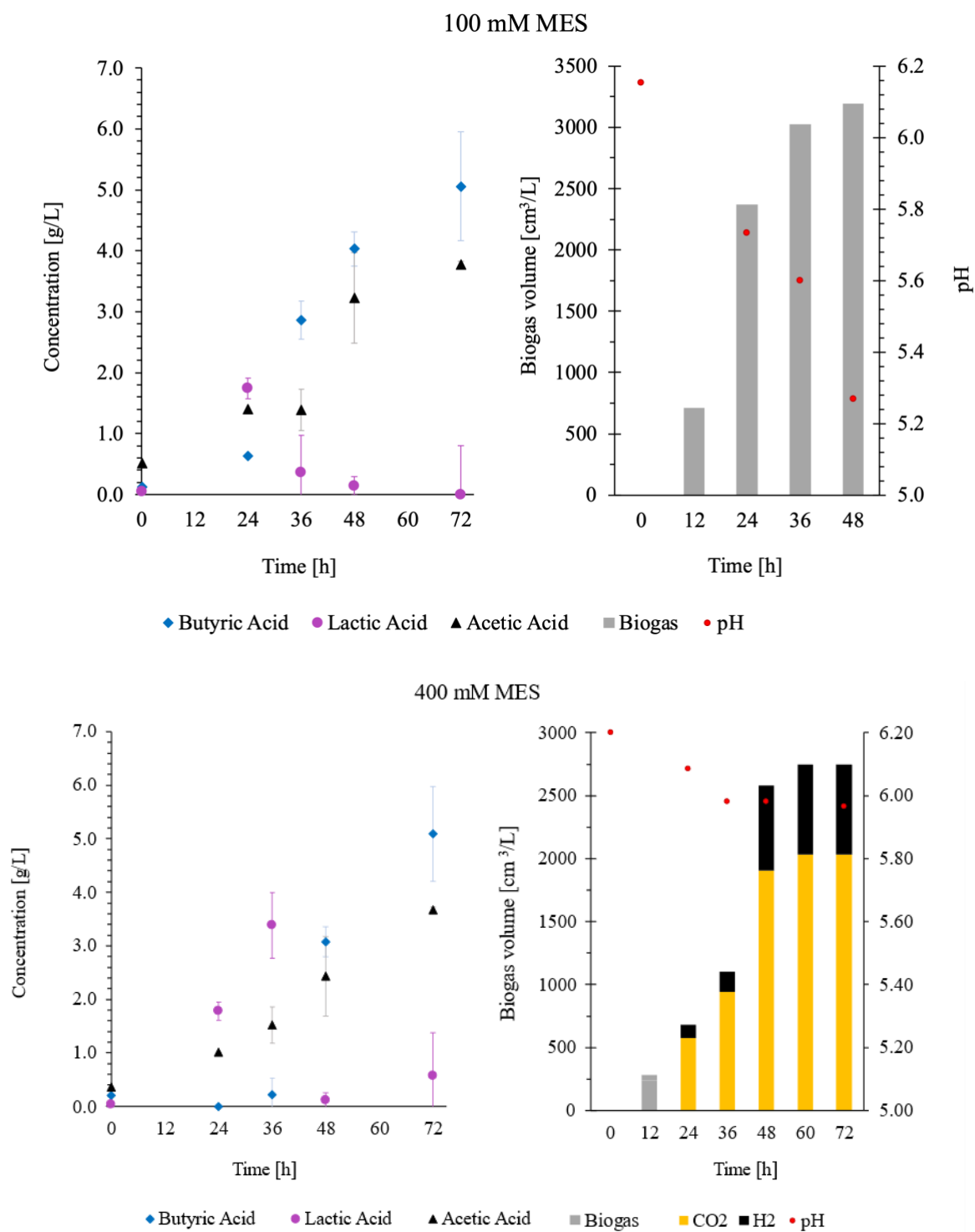
Figure 4.2. Influence of the MES buffer capacity on pH stability, the VFAs and biogas production from Agave bagasse during acidogenesis by mixed culture.

(see Figure 4.1) and a subsequent experiment with different buffer capacity. Noteworthy is the order of VFAs production. Starting fermentation, lactic acid was produced reaching its the highest concentration (1.76 g/L) in the first 24 h. Then, its amount drastically decreases, due to lactic acid decomposition to hydrogen and butyric acid through two major pathways of biochemical metabolism: the acrylate pathway and the pyruvate-ferredoxin oxidoreductase pathway carried out by *Clostridium beijerinckii* and *Clostridium tyrobutryicum* (Bhat and Barker, 1947; Tholozan et al., 1992; Woolford and Sawczyc, 1984). According to García-Depraect et al. (2021), mentioned pathways take place when pH is between 5.5 and 6.0. Therefore, probably at decreasing pH in time, hydrogen together with butyric acid were produced from lactate after 24 h, and the four-carbon acid achieved its maximum concentration (4.8 g/L) after 72 h. Also, the increase of butyric acid concentration and its ratio to acetic acid were observed with the increase of TS content. For the pH levels 6.7, 6.2 and 5.7, increasing TS from 10 to 20% increased butyric acid concentration by 2.9, 2.3 and 3.5 times, respectively. Likewise, the ratio of butyric acid to acetic acid at TS 10 and 20 % was 0.3 and 0.9, respectively. Similarly, Motte et al. (2013) obtained the ratio of butyric to acetic acid of 0.4 for TS of 10%, and from 0.4 to 1 for fermentations with TS content ranges between 19 and 28%.

The literature report lactic acid conversion into propionic and acetic acids in the absence of glucose when NADH is available thought the acrylate pathway by *Propionibacterium* (Rafieenia et al., 2018). Additionally, the optimal pH for propionic acid production by mentioned pathway occurs when pH is between 6.0 to 6.5 (Ranaei et al., 2020). Moreover, the pH ranges from 5.0 to 6.0 led to decrease of butyric acid by its conversion to propionate (Sinha & Kundu, 1998; Sun et al., 2021), which confirms the highest concentration of propionic acid in the reactors with initial pH 6.7, 6.2, and 5.7 after 120 h of acidogenesis.

Acetic acid was produced in all reactors as the most abundant VFA. Its highest concentration was achieved after 120 h of fermentation in the reactor with initial pH 6.7 and TS 20%. The accelerated formation of acetic acid started after 72 h, which may indicate that its production is due to the consumption of hydrogen. It may be assumed, that syntrophic acetate-oxidizing microbes were presented in the reactors. They are able to produce hydrogen but also grow axenically on hydrogen and carbon dioxide to produce acetate (Hattori, 2008). This simple acid is obtained via acetogenesis

though CO_2 and hydrogen reduction by autotrophic acetogens via Wood-Ljungdahl pathway (Valdez-Vazquez and Poggi-Varaldo, 2009).

4.5   Conclusions

The effects of initial pH in the rage between 5.5 to 6.9 and TS between 7.8 to 22.1% on hydrogen production during CBP of agave bagasse were studied using a response surface methodology. Results showed that initial pH and TS content affected two biological processes that occurred in parallel during the solubilization of the biomass. The CBP consisted of lactic acid production by lactic acid bacteria and hydrogen production. The analysis of VFA production at different initial pH of set-up reactors, showed that lactic acid bacteria have wider pH tolerance range (5.5 – 6.9), then hydrogen-producing bacteria (6.0 – 6.9). The experiments confirmed lactic acid conversion though lactate/acetate pathway to hydrogen and butyric acid. Studied factors were only significant for lactic acid production at the beginning of fermentation (first 24 h). The significative impact of TS% ($\rho = 0.0001$) on butyric acid production at 72h was observed. With an increase in TS%, butyric acid concentration increases. This can be related to xylan dissolving bacteria, as well as various hydrogen-producing bacteria that carry out their metabolic pathways, producing hydrogen together with butyric acid, under different conditions.

The highest butyric acid production at the level of 4.8 g/L and hydrogen production of 3.2 mL H_2/gTS were found at initial pH 6.2 and 22.1% of TS after 72 h. The highest biogas volume was obtained after 48 h (3191 cm^3/L, measured at 0°C and 1013.25 hPa), where hydrogen formed 35%. The use of a stronger buffer, buffering the pH at 6.0, prolonged the lactic acid production step (its accumulation was observed) and delayed its conversion to hydrogen and butyric acid. Although similar concentration of butyric acid was obtained in experiments with two different buffer capacities, differences were observed in the volume of biogas produced. This may suggest that lowering the pH < 6.0 improved microbial activity and thus biogas production at reactors with lower buffer capacity. The knowledge and relevant information on bacterial growth conditions can help control fermentation to synthesize hydrogen together with butyric acid. Future research should focus on hydrogen production without the presence of the buffer to assess whether production without a buffer is feasible, thus reducing production costs.

The liquid stream obtained during acidogenesis can be channelled to anaerobic digestion to produce methane, which will then be used to produce energy and thus reduce the operating costs of the biorefinery. The biogas produced can be directly sent to support the cogeneration stage.

4.6   References

Ai, B., Chi, X., Meng, J., Sheng, Z., Zheng, L., Zheng, X., & Li, J. (2016). Consolidated Bioprocessing for Butyric Acid Production from Rice Straw with Undefined Mixed Culture. *Frontiers in Microbiology*, *7*. https://doi.org/10.3389/fmicb.2016.01648

Ayala-Campos, O. R., Sanchez, A., Rebollar, E. A., & Valdez-Vazquez, I. (2022). Plant-associated microbial communities converge in fermentative hydrogen production and form a core microbiome. *International Journal of Hydrogen Energy*, S036031992201727X. https://doi.org/10.1016/j.ijhydene.2022.04.155

Banu J, R., Sugitha, S., Kavitha, S., Kannah R, Y., Merrylin, J., & Kumar, G. (2021). Lignocellulosic Biomass Pretreatment for Enhanced Bioenergy Recovery: Effect of Lignocelluloses Recalcitrance and Enhancement Strategies. *Frontiers in Energy Research*, *9*, 646057. https://doi.org/10.3389/fenrg.2021.646057

Bhat, J. V., & Barker, H. A. (1947). *Clostridium lacto-acetophilum* Nov. Spec. And the Role of Acetic Acid in the Butyric Acid Fermentation of Lactate. *Journal of Bacteriology*, *54*(3), 381-391. https://doi.org/10.1128/jb.54.3.381-391.1947

Chen, C.-Y., Liu, C.-H., Lo, Y.-C., & Chang, J.-S. (2011). Perspectives on cultivation strategies and photobioreactor designs for photo-fermentative hydrogen production. *Bioresource Technology*, *102*(18), 8484-8492. https://doi.org/10.1016/j.biortech.2011.05.082

Cheng, H.-H., Whang, L.-M., Chung, M.-C., & Chan, K.-C. (2016). Biological hydrogen and methane production from bagasse bioethanol fermentation residues using a two-stage bioprocess. *Bioresource Technology*, *210*, 49-55. https://doi.org/10.1016/j.biortech.2015.12.084

Cheonh, P. Y. Y., Kansedo, J., Lau, J. S. Y., & Tan, Y. H. (2022). Renewable Biomass Wastes for Biohydrogen Production. En *Comprehensive Renewable Energy* (pp. 273-298). Elsevier. https://doi.org/10.1016/B978-0-12-819727-1.00091-1

Dahmen, N., Lewandowski, I., Zibek, S., & Weidtmann, A. (2019). Integrated lignocellulosic value chains in a growing bioeconomy: Status quo and perspectives. *GCB Bioenergy*, *11*(1), 107-117. https://doi.org/10.1111/gcbb.12586

Dudek, K., Buitrón, G., & Valdez-Vazquez, I. (2021). Nutrient influence on acidogenesis and native microbial community of Agave bagasse. *Industrial Crops and Products*, *170*, 113751. https://doi.org/10.1016/j.indcrop.2021.113751

García-Depraect, O., Castro-Muñoz, R., Muñoz, R., Rene, E. R., León-Becerril, E., Valdez-Vazquez, I., Kumar, G., Reyes-Alvarado, L. C., Martínez-Mendoza, L. J., Carrillo-Reyes, J., & Buitrón, G. (2021). A review on the factors influencing biohydrogen production from lactate: The key to unlocking enhanced dark fermentative processes. *Bioresource Technology*, *324*, 124595. https://doi.org/10.1016/j.biortech.2020.124595

Good, N. E., Winget, G. D., Winter, W., Connolly, T. N., Izawa, S., & Singh, M. (1966). *Hydrogen Ion Buffers for Biological Research*. *5*(2), 11. https://doi.org/doi.org/10.1021/bi00866a011

Hattori, S. (2008). Syntrophic Acetate-Oxidizing Microbes in Methanogenic Environments. *Microbes and Environments*, *23*(2), 118-127. https://doi.org/10.1264/jsme2.23.118

Honorato-Salazar, J. A., Aburto, J., & Amezcua-Allieri, M. A. (2021). Agave and Opuntia Species as Sustainable Feedstocks for Bioenergy and Byproducts. *Sustainability*, *13*(21), 12263. https://doi.org/10.3390/su132112263

Jacobsen, S. E., & Wyman, C. E. (2000). Cellulose and hemicellulose hydrolysis models for application to current and novel pretreatment processes. *Applied Biochemistry and Biotechnology*, *84*, 16.

Liu, H., Zhang, T., & Fang, H. H. P. (2003). Thermophilic H2 production from a cellulose-containing wastewater. *Biotechnology Letters*, *25*, 365-369. https://doi.org/10.1023/a:1022341113774

Lu, C., Li, W., Zhang, Q., Liu, L., Zhang, N., Qu, B., Yang, X., Xu, R., Chen, J., & Sun, Y. (2021). Enhancing photo-fermentation biohydrogen production by strengthening the beneficial metabolic products with catalysts. *Journal of Cleaner Production*, 12.

Mockaitis, G., Bruant, G., Guiot, S. R., Peixoto, G., Foresti, E., & Zaiat, M. (2020). Acidic and thermal pre-treatments for anaerobic digestion inoculum to improve hydrogen and volatile fatty acid production using xylose as the substrate. *Renewable Energy*, *145*, 1388-1398. https://doi.org/10.1016/j.renene.2019.06.134

Motte, J.-C., Trably, E., Escudié, R., Hamelin, J., Steyer, J.-P., Bernet, N., Delgenes, J.-P., & Dumas, C. (2013). Total solids content: A key parameter of metabolic pathways in dry anaerobic digestion. *Biotechnology for Biofuels*, *6*(1), 164. https://doi.org/10.1186/1754-6834-6-164

Pérez-Rangel, M., Barboza-Corona, J. E., Buitrón, G., & Valdez-Vazquez, I. (2020). Essential Nutrients for Improving the Direct Processing of Raw Lignocellulosic Substrates Through the Dark Fermentation Process. *BioEnergy Research*, *13*(1), 349-357. https://doi.org/10.1007/s12155-019-10083-w

Pérez-Rangel, M., Barboza-Corona, J. E., Navarro-Díaz, M., Escalante, A. E., & Valdez-Vazquez, I. (2021). The duo *Clostridium* and *Lactobacillus* linked to hydrogen production from a lignocellulosic substrate. *Water Science and Technology*, *83*(12), 3033-3040. https://doi.org/10.2166/wst.2021.186

Perimenis, A., van Aarle, I. M., Nicolay, T., Jacquet, N., Meyer, L., Richel, A., & Gerin, P. A. (2016). Metabolic profile of mixed culture acidogenic fermentation of lignocellulosic residues and the effect of upstream substrate fractionation by steam explosion. *Biomass Conversion and Biorefinery*, *6*(1), 25-37. https://doi.org/10.1007/s13399-015-0164-8

Rafieenia, R., Pivato, A., Schievano, A., & Lavagnolo, M. C. (2018). Dark fermentation metabolic models to study strategies for hydrogen consumers inhibition. *Bioresource Technology*, *267*, 445-457. https://doi.org/10.1016/j.biortech.2018.07.054

Ranaei, V., Pilevar, Z., Mousavi Khaneghah, A., & Hosseini, H. (2020). Propionic Acid: Method of Production, Current State and Perspectives. *Food Technology and Biotechnology*, *58*(2), 115-127. https://doi.org/10.17113/ftb.58.02.20.6356

Sarkar, O., Rova, U., Christakopoulos, P., & Matsakas, L. (2021). Influence of initial uncontrolled pH on acidogenic fermentation of brewery spent grains to biohydrogen and volatile fatty acids production: Optimization and scale-up. *Bioresource Technology*, *319*, 124233. https://doi.org/10.1016/j.biortech.2020.124233

Sinha, R., & Kundu, K. K. (1998). Chemical Transfer Energetics of the $-CH_2-$ Group: A Possible Probe for the Solvent Effect on Hydrophobic Hydration and the 3D-Structuredness of

Solvents. *The Journal of Physical Chemistry B*, *102*(35), 6880-6888. https://doi.org/10.1021/jp982281r

Sun, J., Zhang, L., & Loh, K.-C. (2021). Review and perspectives of enhanced volatile fatty acids production from acidogenic fermentation of lignocellulosic biomass wastes. *Bioresources and Bioprocessing*, *8*(1), 68. https://doi.org/10.1186/s40643-021-00420-3

Tholozan, J. L., Touzel, J. P., Samain, E., Grivet, J. P., Prensier, G., & Albagnac, G. (1992). Clostridium neopropionicum sp. Nov., a strict anaerobic bacterium fermenting ethanol to propionate through acrylate pathway. *Archives of Microbiology*, *157*(3), 249-257. https://doi.org/10.1007/BF00245158

Valdez-Vazquez, I., & Poggi-Varaldo, H. M. (2009). Hydrogen production by fermentative consortia. *Renewable and Sustainable Energy Reviews*, *13*(5), 1000-1013. https://doi.org/10.1016/j.rser.2008.03.003

Woolford, M. K., & Sawczyc, M. K. (1984). An investigation into the effect of cultures of lactic acid bacteria on fermentation in silage. 1. Strain selection. *Grass and Forage Science*, *39*(2), 139-148. https://doi.org/10.1111/j.1365-2494.1984.tb01675.x

Yang, L., Xu, F., Ge, X., & Li, Y. (2015). Challenges and strategies for solid-state anaerobic digestion of lignocellulosic biomass. *Renewable and Sustainable Energy Reviews*, *44*, 824-834. https://doi.org/10.1016/j.rser.2015.01.002

Yankov, D. (2022). Fermentative Lactic Acid Production From Lignocellulosic Feedstocks: From Source to Purified Product. *Frontiers in Chemistry*, *10*, 823005. https://doi.org/10.3389/fchem.2022.823005

5. Chapter V: High-efficiency production of biobutanol from lignocellulosic biomass using a butanol-tolerant mixed culture

5.1   Abstract

An alternative for traditional and commonly known biobutanol production from lignocellulosic biomass during acetone-butanol-ethanol (ABE) fermentation is consolidated bioprocessing (CBP). In which, a group of microorganisms with different specialties convert a cellulose polymer into glucose and then produce organic solvents from it. In this work, a butanol-tolerant mixed culture obtained during adaptative evolution was applied for biobutanol production from pretreated corn stover and a cellulosic filter paper (the control reactor) during CBP. Both reactors were loaded with a total solids percentage corresponding to a similar cellulose content and an initial pH was adjusted to 7.5. The highest butanol concentration at a level of 23.06 g/L was found after 120 hours by using pretreated corn stover. In this reactor, valeric and caproic acids were detected also after 168 h of incubation reaching concentrations of 11.02 and 7.07 g/L, respectively. In the control reactor, the highest butanol concentration was 18.54 g/L after 168, with valeric and caproic acids after 144 h of incubation reaching concentrations of 8.83 and 3.54 g/L, respectively.

Keywords: ABE fermentation; consolidated bioprocessing; corn stover; solventogenesis;

5.2   Introduction

Energy is an important factor in the strength of the economy and social development. In an era of climate change, caused by high emissions of greenhouse gases, especially carbon dioxide because of the consumption of fossil fuels such as coal, gasoline and natural gas, energy policy has been tightened in recent years to promote and develop renewable energy sources (Azarpour et al., 2022). As a highly available and economical renewable material, lignocellulosic biomass has been recognized as an attractive feedstock for bioenergy production (Fatma et al., 2018). Its annual global supply, from agricultural and food processing industries, is estimated at 181.5 billion tonnes (Dudek et al., 2022). Therefore, conversion of lignocellulosic materials into biofuel would help mitigate the effects of global warming (Adewuyi, 2022). Biobutanol is a promising compound of renewable fuels due to its superior energy properties such as high energy density (29.2 MJ/L) (Xue & Cheng, 2019), low vapor pressure (0.9 kPa at 25°C) (Butler et al., 1935), total compatibility with vehicles engines (Elsemary et al., 2016), and its production is possibly throughout acetone-butanol-ethanol (ABE) fermentation process of lignocellulosic waste (Gottumukkala et al., 2017). Since 2010, approximately 2570 papers have been published on ABE fermentation research of lignocellulosic biomass (Google Academy, 2023). There are various substrates used for biobutanol production including agave bagasse (Morales-Martínez et al., 2020), corn stover (Lin et al., 2021; Wu et al., 2021), barley straw (Qi et al., 2019), wheat straw, rice straw, rice bran, cassava bagasse, corncob (Huzir et al., 2018). The highest yields of biobutanol production are obtained during glucose processing. The amount of the monosaccharide varies from 340 to 407 g glucose/kg biomass, depending on the type and origin of the biomass, and is encapsulated in cellulose polymer fibers (Riaz et al., 2022). The majority of studies have carried out traditional biobutanol production from lignocellulosic biomass by ABE fermentation, which requires prior hydrolysis, detoxification and very often the use of genetically modified *Clostridium sp.* bacteria to increase the biobutanol yield (Gao et al., 2014; Guo et al., 2022; Ranjan et al., 2013). An alternative is cellulosic biobutanol produced by a consolidated bioprocess (CBP), in which a group of microorganisms break down the cellulose polymer into glucose and simultaneously convert it into biobutanol (Putro et al., 2016). To date, two publications have been published on the high performance of cellulosic biobutanol. Wen et al. (2017) produced 11.5 g/L biobutanol using alkaline extraction as a pretreatment of deshelled corn cob and employing genetically modified *Clostridium cellulovorans* and *Clostridium beijerinckii*. Meanwhile, Valdez-Vazquez et al. (2015) carried out a biological

pretreatment of corn stover using epiphytic strains of *Enterococcus*, followed by CBP using synthetic mixture of *Clostridium beijerinckii 10132* and *Clostridium cellulovorans 35296*, yielding 14.2 g/L. The aim of the present study was to evaluate cellulosic biobutanol production from two sources of cellulose employing a butanol-tolerant mixed culture obtained previously by laboratory adaptive.

5.3   Methodology

5.3.1   Material and methods

Spent solids from an acidogenesis process (a biological pretreatment step), consisting mainly of cellulose and lignin, were rinsed with tap water until the transparent color of the water was observed, in order to eliminate washing substances and remaining microorganisms. Then, the solids were dried to a moisture content of < 5 % and stored in a plastic bag until use. A cellulose filter paper (99.8 % cellulose) was used as substrate in the control reactor. The culture medium had the following composition: 2 g of $CO(NH_2)_2$, 0.5 g of KH_2PO_4, 2.1 g of NaH_2PO_4, 0.2 g of $NiSO_4$, 0.2 g of Na_2SO_4, 0.2 g of $FeCl_3 \cdot 4H_2O$, 0.2 g of $MnCl_2 \cdot 4H_2O$, 0.1 g of $CaCl_2 \cdot 6H_2O$, 0.1 g of $ZnCl_2$, 0.02 g of $CoCl_2$ and 0.01g $NaMo_4 \cdot 2H_2O$. A butanol-tolerant mixed culture obtained by González-Tenorio et al. (2023) was used as the inoculum. This microbial mixed culture is mainly integrated by *Clostridium sensu stricto* 7 as butanol producers and *Caproiciproducens* as n-caproate producer.

5.3.2   Experiment set-up and procedure

Two glass bottles of 0.25 L with working volume of 0.15 L were assembled. The substrate masses were 10 g of the pretreated corn stover and 5 g of the filter paper for the experimental reactor (ER) and control reactor (CR), respectively. Subsequently, 1 g of the inoculum and 135 ml of the medium culture were introduced into both reactors. The initial pH was adjusted manually to 7.5 using 3 M NaOH and 3 M HCl. Finally, both reactors were sealed and placed in an incubator at 35 ℃ with a 150 rpm stirrer (WIS-ML; Wisd Laboratory Instruments, Witeg, Germany). The experiment was prepared in an anaerobic atmosphere generation bag with a atmosphere with CO_2. Due to the limited amount of inoculum, no replicates were prepared.

5.3.3   Analytical methods

Collected samples were analyzed using high-performance liquid chromatography (1260 infinity, Agilent Technologies, CA, USA) equipped with Aminex HPX-87H column, and Diode-Array

Detection with detection wavelength of 210 nm. A solution of 0.005 M H_2SO_4 at a flow rate of 0.6 mL/min was used as the mobile phase.

5.4 Results and discussion

The CR and ER reactors were operated to confirm activity of butanol-tolerant mixed culture previously reported. Produced metabolites and their concentrations were depicted in the Figure 1a, b. No samples were taken from both reactors during the first 72 h, as this was the time for acclimatization and bacterial proliferation. After 120 h, biobutanol was found at 1.76 g/L in the CR and its concentration increased, reaching 18.54 g/L after 168 hours, at the end of the experiment. The first ER taken sample after 96 hours had 7.5 g/L biobutanol. The maximum concentration of 23.03 g/L was reached after 120 hours. Then, a downward trend in biobutanol production was observed until the end of the experiment, and biobutanol concentration was 15 g/L after 168 h.

In the CR, a slow increase in acetic acid was observed from 0.08 at 96 h to 1.97 g/L at 168 h. In contrast, in the ER, acetic acid was detected only in the sample taken after 144 hours at 2.01 g/L.

In the CR, in all samples butyric acid was below 0.5 g/L. Meanwhile, 0.83 and 1.63 g/L of butyric acid was observed in the ER in the samples taken after 120 and 168 hours, respectively. Additionally, in both reactors, valeric and caproic acids were found as the most abundant unexpected products (Figure 1b,d). In the CR, valeric acid was presented at 3.5 g/L after 96 and 120 hours, then reached its maximum of 8.83 g/L at 144 hours, and finally decreased to zero at 168 h. Meanwhile, in the ER, a stable concentration of valeric acid at 10 g/L was detected after 96 and 120 hours. Its concentration reached zero after 144 hours, and suddenly increased to 11.02 g/L at 168 h. Caproic acid trended upwards from 0.22 to 3.16 g/L, between 96 and 144 hours in the CR. It disappeared after 168 hours. While, in the ER its concentration of 5.5 g/L was observed after 96 and 120 hours. Then, after 144 hours it decreased to 1.36 g/L and reached a maximum of 7.5 g/L after 168 hours at the end of the experiment.

5.5 Conclusions

The present study confirmed the activity of a butanol-tolerant mixed culture for the production of biobutanol during CBP from two sources de cellulose after a long period of conservation of inoculum. The highest cellulosic biobutanol of 23.06 g/L was produced after 120 hours from

pretreated corn stover. For filter paper, the highest cellulosic biobutanol of 18.54 g/L was found, but it is very feasible that a longer time is required to observe the higher value. Also, these experiments confirm the production of n-caproate from the elongation of short-chain fatty acids at the end of the fermentation time. Next, continuous reactors should be operated for a long time to verify the stability of the process of butanol production.
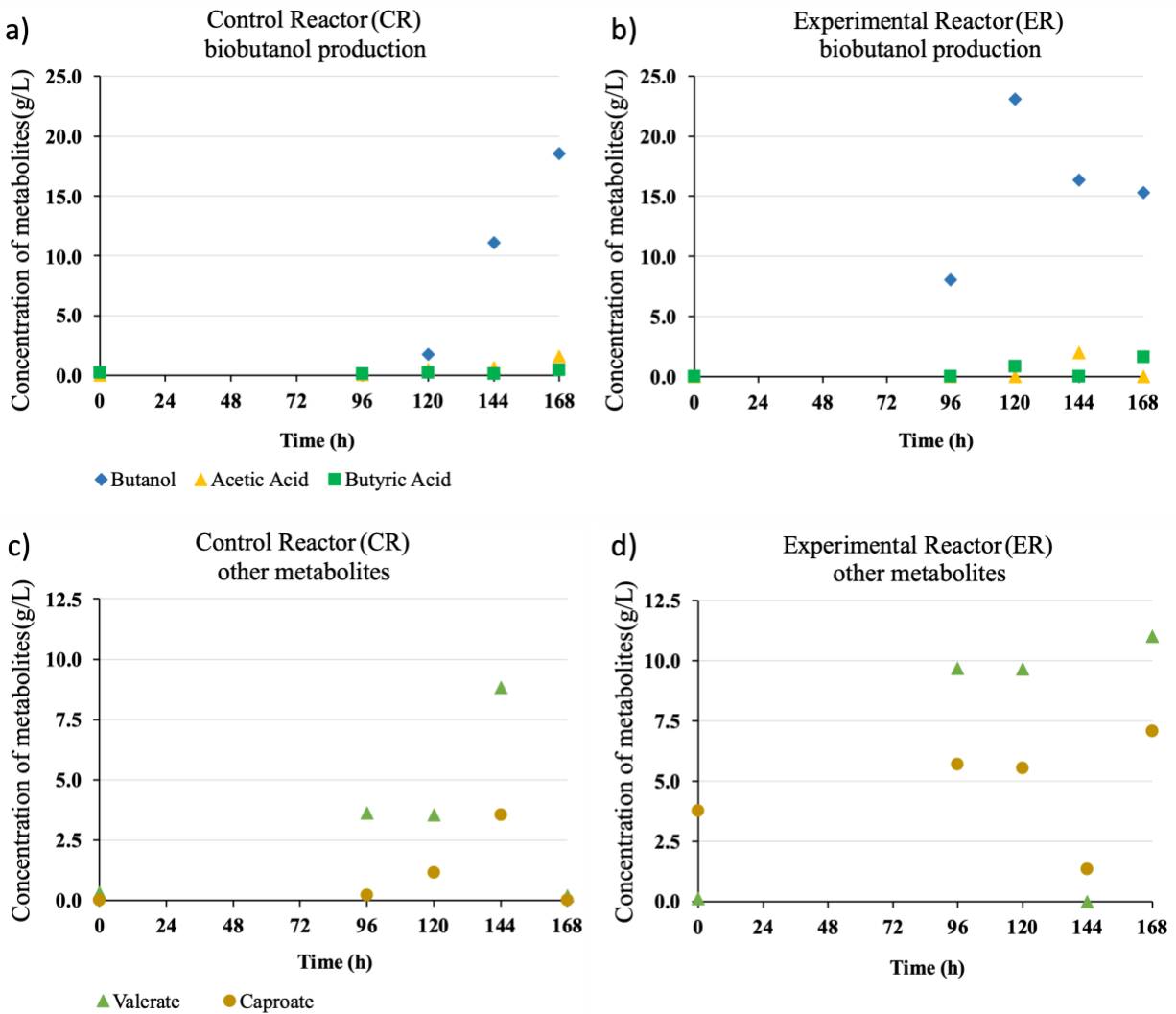
Figure 5.1. Produced biobutanol (a,b) and other metabolites (c,d) during CBP of biologically pretreated corn stover. * results that were detected outside the calibration curve.

5.6   References

Adewuyi, A. (2022). Underutilized Lignocellulosic Waste as Sources of Feedstock for Biofuel Production in Developing Countries. *Frontiers in Energy Research*, *10*, 741570. https://doi.org/10.3389/fenrg.2022.741570

Azarpour, A., Mohammadzadeh, O., Rezaei, N., & Zendehboudi, S. (2022). Current status and future prospects of renewable and sustainable energy in North America: Progress and challenges. *Energy Conversion and Management*, *269*, 115945. https://doi.org/10.1016/j.enconman.2022.115945

Butler, J. A. V., Ramchandani, C. N., & Thomson, D. W. (1935). 58. The solubility of non-electrolytes. Part I. The free energy of hydration of some aliphatic alcohols. *Journal of the Chemical Society (Resumed)*, 280. https://doi.org/10.1039/jr9350000280

Dudek, K., Molina-Guerrero, C. E., & Valdez-Vazquez, I. (2022). Profitability of single- and mixed-culture fermentations for the butyric acid production from a lignocellulosic substrate. *Chemical Engineering Research and Design*, *182*, 558–570. https://doi.org/10.1016/j.cherd.2022.04.018

Elsemary, I. M. M., Attia, A. A. A., Elnagar, K. H., & Elaraqy, A. A. M. (2016). Experimental investigation on performance of single cylinder spark ignition engine fueled with hydrogen-gasoline mixture. *Applied Thermal Engineering*, *106*, 850–854. https://doi.org/10.1016/j.applthermaleng.2016.05.177

Fatma, S., Hameed, A., Noman, M., Ahmed, T., Shahid, M., Tariq, M., Sohail, I., & Tabassum, R. (2018). Lignocellulosic Biomass: A Sustainable Bioenergy Source for the Future. *Protein & Peptide Letters*, *25*(2), 148–163. https://doi.org/10.2174/0929866525666180122144504

Gao, K., Boiano, S., Marzocchella, A., & Rehmann, L. (2014). Cellulosic butanol production from alkali-pretreated switchgrass (Panicum virgatum) and phragmites (Phragmites australis). *Bioresource Technology*, *174*, 176–181. https://doi.org/10.1016/j.biortech.2014.09.152

Google Academy. (2023). Google Academy Browser. Key Words "Lignocellulosic Biomass" and "ABE Fermentation". Access Time: 01/19/2023. https://scholar.google.com

Gottumukkala, L. D., Haigh, K., & Görgens, J. (2017). Trends and advances in conversion of lignocellulosic biomass to biobutanol: Microbes, bioprocesses and industrial viability.

Renewable and Sustainable Energy Reviews, *76*, 963–973. https://doi.org/10.1016/j.rser.2017.03.030

Guo, Y., Liu, Y., Guan, M., Tang, H., Wang, Z., Lin, L., & Pang, H. (2022). Production of butanol from lignocellulosic biomass: Recent advances, challenges, and prospects. *RSC Advances*, *12*(29), 18848–18863. https://doi.org/10.1039/D1RA09396G

Huzir, N. M., Aziz, M. M. A., Ismail, S. B., Abdullah, B., Mahmood, N. A. N., Umor, N. A., & Syed Muhammad, S. A. F. (2018). Agro-industrial waste to biobutanol production: Eco-friendly biofuels for next generation. *Renewable and Sustainable Energy Reviews*, *94*, 476–485. https://doi.org/10.1016/j.rser.2018.06.036

Lin, X., Liu, Y., Zheng, X., & Qureshi, N. (2021). High-efficient cellulosic butanol production from deep eutectic solvent pretreated corn stover without detoxification. *Industrial Crops and Products*, *162*, 113258. https://doi.org/10.1016/j.indcrop.2021.113258

Morales-Martínez, T. K., Medina-Morales, M. A., Ortíz-Cruz, A. L., Rodríguez-De la Garza, J. A., Moreno-Dávila, M., López-Badillo, C. M., & Ríos-González, L. (2020). Consolidated bioprocessing of hydrogen production from agave biomass by Clostridium acetobutylicum and bovine ruminal fluid. *International Journal of Hydrogen Energy*, *45*(26), 13707–13716. https://doi.org/10.1016/j.ijhydene.2019.11.089

Putro, J. N., Soetaredjo, F. E., Lin, S.-Y., Ju, Y.-H., & Ismadji, S. (2016). Pretreatment and conversion of lignocellulose biomass into valuable chemicals. *RSC Advances*, *6*(52), 46834–46852. https://doi.org/10.1039/C6RA09851G

Qi, G., Huang, D., Wang, J., Shen, Y., & Gao, X. (2019). Enhanced butanol production from ammonium sulfite pretreated wheat straw by separate hydrolysis and fermentation and simultaneous saccharification and fermentation. *Sustainable Energy Technologies and Assessments*, *36*, 100549. https://doi.org/10.1016/j.seta.2019.100549

Ranjan, A., Khanna, S., & Moholkar, V. S. (2013). Feasibility of rice straw as alternate substrate for biobutanol production. *Applied Energy*, *103*, 32–38. https://doi.org/10.1016/j.apenergy.2012.10.035

Riaz, S., Mazhar, S., Abidi, S. H., Syed, Q., Abbas, N., Saleem, Y., Nadeem, A. A., Maryam, M., Essa, R., & Ashfaq, S. (2022). Biobutanol production from sustainable biomass process of

anaerobic ABE fermentation for industrial applications. *Archives of Microbiology*, *204*(11), 672. https://doi.org/10.1007/s00203-022-03284-z

Valdez-Vazquez, I., Pérez-Rangel, M., Tapia, A., Buitrón, G., Molina, C., Hernández, G., & Amaya-Delgado, L. (2015). Hydrogen and butanol production from native wheat straw by synthetic microbial consortia integrated by species of Enterococcus and Clostridium. *Fuel*, *159*, 214–222. https://doi.org/10.1016/j.fuel.2015.06.052

Wen, Z., Minton, N. P., Zhang, Y., Li, Q., Liu, J., Jiang, Y., & Yang, S. (2017). Enhanced solvent production by metabolic engineering of a twin-clostridial consortium. *Metabolic Engineering*, *39*, 38–48. https://doi.org/10.1016/j.ymben.2016.10.013

Wu, Y., Wang, Z., Ma, X., & Xue, C. (2021). High temperature simultaneous saccharification and fermentation of corn stover for efficient butanol production by a thermotolerant Clostridium acetobutylicum. *Process Biochemistry*, *100*, 20–25. https://doi.org/10.1016/j.procbio.2020.09.026

Xue, C., & Cheng, C. (2019). Chapter Two—Butanol production by Clostridium. In Y. Li & X. Ge (Eds.), *Advances in Bioenergy* (Vol. 4, pp. 35–77). Elsevier. https://doi.org/10.1016/bs.aibe.2018.12.001

6. Chapter VI: Butanol recovery from synthetic fermentation broth by vacuum distillation in a rotating packed bed

Reference to published work:

6.1   Abstract

The present study was performed to investigate feasibility of butanol recuperation from a synthetic fermentation broth via vacuum distillation in a rotating packed bed (RPB). Unlike in stationary columns, the packing element rotates generating a centrifugal field which exceeds gravity by orders of magnitude. Thereby, the RPB improves the gas-liquid mass transfer by factors of 10 up to 1000, resulting in more efficient compounds separation. The process was performed under reduced pressure to allow temperatures getting closer to the typical fermentation temperature, which is usually between 35 to 37 °C. Therefore, the butanol recuperation can be carried out in-line without bacteria deactivation. The complex mixture used in this study was based on a real fermentation broth obtained during fermentation of cellulosic fraction of lignocellulosic biomass by butanol-tolerant mixed culture. Consequently, the composition of the synthetic fermentation broth as liquid feed stream was as following (g/L): 20 of butanol, 7 of ethanol, 2.5 of acetic acid, 3 of propionic acid, 5.5 of valeric acid, 2.0 of caproic acid, and 3.5 of furfural. Experiments under total reflux and stripping experiments using 5% of steam relative to the fermentation broth feed were performed. In the first case, butanol recuperation in the light phase of the top product reached concentration of 521.6 g/L. For stripping experiments, butanol concentration achieved the concentration at the level of 126.9 g/L in the top product. Ethanol and furfural were also recuperated at high concentrations at 39 and 13 g/L, respectively during stripping experiments. The experiments demonstrated that vacuum distillation in an RPB allows not only for separation of butanol from complex mixture but also for ethanol and furfural recuperation. Nevertheless, a further purification step is needed to achieve a pure product which can be used as an alternative fuel or feedstock substitute for the fossil components.

6.2   Introduction

6.2.1   Butanol production from lignocellulosic biomass

Biofuel production plays a crucial role in developing a sustainable economy, considering current and future economic and social needs (Panwar et al., 2011). Butanol was found as a high potential biofuel due to its properties, such as having a higher heating value than ethanol, less water content and lower volatility, which causes fewer ignition problems (Jin et al., 2011).

Butanol can be formed during fermentation of lignocellulosic biomass (Qureshi, 2009). Usually, its production is conducted via acetone-butanol-ethanol (ABE) fermentation, where mentioned compounds are produced in a ratio of 3:6:1, respectively via solventogenesis. Traditional butanol formation during ABE fermentation consists of separate pretreatment, saccharification and fermentation. However, the pretreatment and saccharification stages contributes 50% to the fixed capital investment (Jang and Choi, 2018). The consolidated bioprocess (CBP) using microbial consortia integrates into a single unit the production of hydrolytic enzymes, saccharification and fermentation. That considerably reduces the fixed capital investment and operating costs (Valdez-Vazquez and Sanchez, 2018). Butanol titers in literature related to butanol production directly from cellulose through CBP do not exceed 11.5 g/L using a co-culture of *Clostridium cellulovorans* with *Clostridium beijerinckii* (Bao et al., 2022). Recently, our Research Group performed the adaptive evolution of an acidogenic mixed culture to the stepwise enrichment of butanol from 2 to 5 g/L for 84 days. After the long-term exposure to butanol, the mixed culture was represented by several fibrolytic bacteria such as *Bacteroides, Dysgonomonas*, *Ruminococcus*, and *Prevotella*, while the fermentative bacteria were represented by *Caproiciproducens, Clostridium, Oscillibacter*, and *Proteiniphilum.* The adaptive evolution increased the butanol production from 1.5 g/L to 13.8 g/L from steam-exploded corn stover. This butanol-tolerant mixed culture was then used to perform a CBP using steam-exploded corn stover as the substrate at 8% of total solids, initial pH 7.5, and incubated for seven days at 35 ℃. The fermentation broth contained as major products butanol (23 g/L), valeric acid (11 g/L), and caproic acid (7 g/L) (Supplementary material: Table A.1).

6.2.2   Butanol separation in RPB

In general, butanol separation from multi-component mixtures can be performed by numerous methods such as membrane adsorption, liquid-liquid extraction, reverse osmosis, gas stripping, or

vacuum pervaporation (Diltz et al., 2007; Grobben et al., 1993; Qureshi and Blaschek, 2001; Stoffers and Górak, 2013). However, the most common technique is distillation due to its advantages, such as: ability to handle a wide range of feed flow rates, separate feed components independently of their concentrations and ability to produce highly purified products (Smith and Jobson, 2000). Moreover, comparing distillation to membrane adsorption, the effect of temperature on separation selectivity is greater for distillation than for membranes, especially in the case of the complex mixture. The main disadvantages of liquid-liquid extraction, especially when used with fermentation broths, are the possibility of emulsion formation and contamination of the extractant. While reverse osmosis requires routine filter changes and maintenance which is related to higher costs compared to the other methods. Gas stripping results in formation of excessive amounts of ammonia in the reactor. Furthermore, it is often required to add an anti-foaming reagent, which can be toxic to bacteria (Kujawska et al., 2015). The main disadvantage of distillation is the high energy demand required in the reboiler. However, the temperature level at which the heat is needed can be reduced by lowering the pressure.

Many alcohol-water mixtures form azeotropes making the separation into pure components impossible by single distillation. However, in the case of the binary water-n-butanol system, the vapor-liquid-liquid-equilibrium (VLLE) exhibits a miscibility gap for butanol mole fractions between 0.02 and 0.45 at boiling temperature and atmospheric pressure (1.013 bar) (Card and Farrell, 1982). That means any water-n-butanol mixture with a butanol mole fraction in the mentioned range spontaneously separates into a water-rich phase and butanol-rich phase (McCabe et al., 2001) (Supplementary material: Figure A.A.1).

Each part of the distillation process, i.e., the column 1 or the column 2 depicted in the Figure 6.1, can be performed in a rotating packed bed (RPB) that is referred to high gravity (Higee) technology (Lin et al., 2010). The rotation of the packing element generates a centrifugal acceleration exceeding gravity by orders of magnitude thereby improving the gas-liquid mass transfer by factors of 10 up to 1000 (Lin et al., 2009). This phenomenon occurs due to thinner liquid films or formation of smaller droplets resulting in an increased contact surface area between gas and liquid (Hilpert et al., 2021). In consequence, process intensification machines like RPBs offer a high effective interfacial area while exhibiting a low footprint. That property makes them a promising alternative for conventional columns in retrofit applications or any circumstance with limited space.

Furthermore, they are capable of handling highly viscous media which makes them perfect for processing fermentation broths. Moreover, Lukin et al. (2021) showed that microorganisms are able to survive the treatment in the RPB, due to the short residence time of the bacteria in the hot zones of the system, in contrast to the traditional distillation.
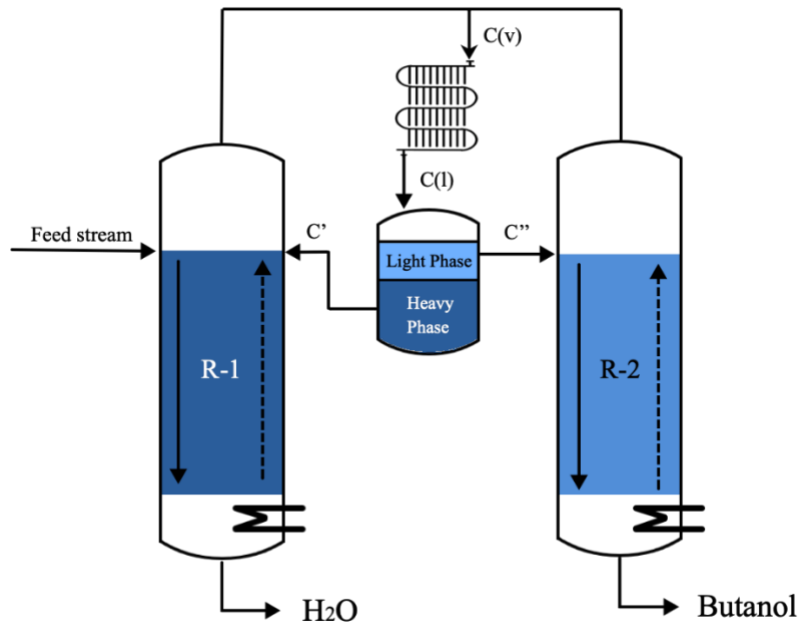
Figure 6.1. Heteroazeotropic distillation of butanol in water-rich (R-1) and butanol-rich (R-2) columns.

6.2.3   Aim of this study

The present study was performed to evaluate butanol recuperation from a complex mixture based on the real fermentation broth via distillation under reduced pressure (where the boiling point of the mixture is close to the fermentation temperature) in an RPB and the subsequent separation phase into an aqueous and an organic phase. The further purification of the organic phase into almost pure butanol was not part of this study since it is not a crucial step for the fermentation.

6.3   Materials and methods

6.3.1   Materials

Butanol, ethanol, acetic acid, propionic acid, valeric acid, caproic acid and furfural were supplied by Merck. The purities of all chemicals exceeded 99 % and were used without further purification.

The water was purified by a Merck MILLI-Q® system equipped with a Millipak® Express 40 filter having a pore size of 0.22 μm resulting in water with a total organic carbon content of less than 5 ppb and an electrical resistance of 18.2MΩcm.

In order to investigate butanol recuperation from a complex mixture, a synthetic fermentation broth was prepared, which closely matched the real fermentation broth of lignocellulosic biomass obtained by the butanol-tolerant mixed culture. The synthetic fermentation broth used in this study had the following composition: 20 g/L of butanol, 7 g/L of ethanol, 2.5 g/L of acetic acid,3 g/L of propionic acid, 5.5 g/L of valeric acid, 2.0 g/L of caproic acid, and 3.5 g/L of furfural.

6.3.1 Experimental set-up

6.3.6.1 Distillation under total reflux

The system used for butanol distillation from binary, ternary and more complex mixtures was assembled from the reboiler, condenser, reflux tank, reflux heater, reflux pump, cold trap, liquid flow meter, vacuum pump, and the RPB itself (Figure 6.2).
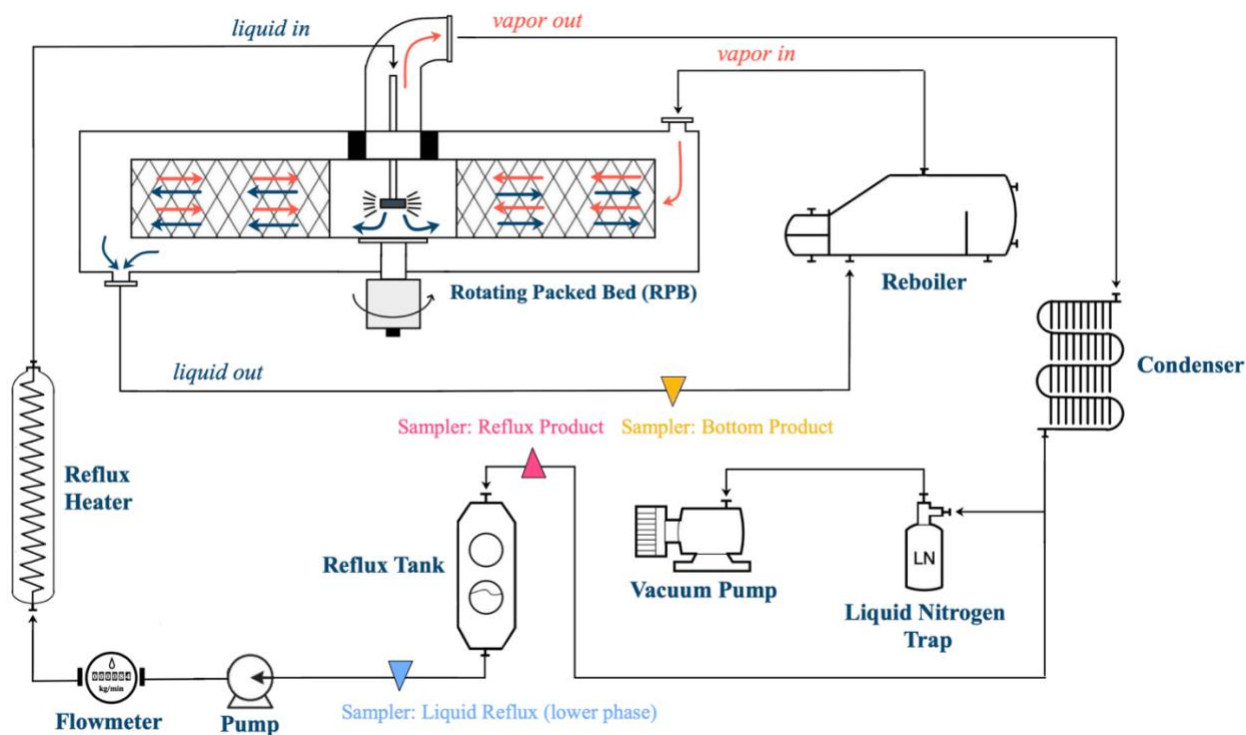
Figure 6.2. System setup for butanol recuperation from binary and ternary mixture as well as synthetic fermentation broth under total reflux.

The reboiler was operated with thermal oil heated by a thermostat (Teco tt, gwk, Germany) and the temperature of the oil was set to 75 °C. In preliminary experiments, it was found that this temperature is sufficient to evaporate the bottom product, but not at a too high temperature to overheat it. The pressure in the eye of the RPB was set to 89 mbar and was regulated with a vacuum controller (Vacuum Controller Vaccu-Select, Vaccubrand) connected to the vacuum pump (TRIVAC D4A, Leybold GmbH). For that pressure, the maximum temperature in the plant was 45°C, which would not kill the bacteria during an in-situ butanol separation (Nguyen et al., 2009). The RPB had a vapor inlet located in the upper section of the casing, the vapor outlet was also in the top, close to the center. The liquid inlet in the RPB's eye consisted of a full jet nozzle directing the liquid flow directly onto the packing material. The liquid outlet was placed in the bottom plate of the casing in the most outer position possible (Figure 6.2). The metal foam (NCX1116, Recemat BV) was used as packing material (Table 6.1). The condenser (AlfaNova 27-18H, Alfa Laval) was operated with tap water and the cold trap was filled with liquid nitrogen, which was protecting the vacuum pump from any vapors that were not condensed in the condenser. From the reflux tank, the liquid was recirculated into the RPB by a gear pump (PUMPdrive PD5230, Heidolph) through a reflux heater bringing the reflux 2 K below its boiling temperature. The reflux flow rate was set to 0.08 kg/min which corresponds to an F-factor of 1.15 Pa^0.5.

Table 6.1. Design specifications of the applied RPB and packing (NCX1116).

Specification	Dimension
RPB casing inner diameter (mm)	355
Rotor outer diameter (mm)	260
Packing inner diameter (mm)	146
Packing outer diameter (mm)	260
Axial height of packing (mm)	10
Number of pores / inches	11 - 16
Average pore Ø (mm)	1.4
Porosity (%)	8

6.3.6.2 Stripping experiments

Another experimental design, being closer to industrial application, referred to stripping experiments with pure water vapor. Based on the liquid feed mass flow, 5% vapor was fed to the

RPB. The system used for butanol distillation from binary and complex mixtures was assembled from the water tank, water pump, reboiler, condenser, reflux tank, product pump, product tank, liquid nitrogen trap, vacuum pump, feed tank, feed pump, flowmeter, feed heater, residue pump, residue tank, and RPB itself (Figure 6.3).
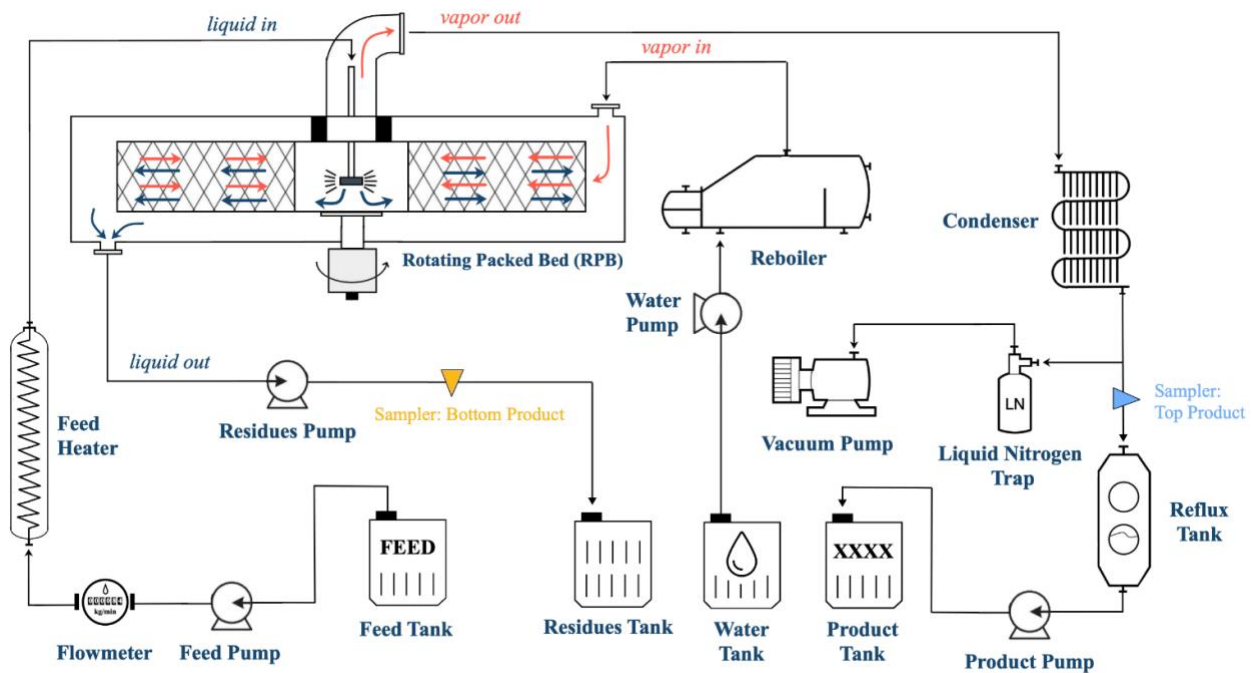
Figure 6.3. Setup for butanol stripping from binary mixture and synthetic fermentation broth with 5 wt.% of steam as a stripping gas.

The condenser, vacuum controller, vacuum pump, feed heater (corresponds to reflux heater from total reflux experiments) have the same settings as for the total reflux experiments. The reboiler was operated with thermal oil heated by a thermostat (Teco tt, gwk, Germany) and the temperature of the oil was set to 65 °C. This temperature was found to be sufficient to evaporate the water at the 89 mbar but did not result in superheated steam. The liquid feed pump (ISM405A, Ismatec) had a flow rate of 200 g/min and was computer controlled. The liquid outlet was conducted to the residues tank by the residues pump (Pumpdrive 5230, Heidolph) with the volume flow controlled manually. The distillated water from the water tank was pumped to the reboiler by a peristaltic water pump (505S, Watson Marlow) at a flow rate of 10 g/min. The collected liquid in the reflux tank was transported to the product tank by the product pump (PUMPdrive PD5230, Heidolph).

6.3.2 Experimental procedure

6.3.6.1 Distillation under total reflux

The design of a distillation column, it is distinguished between the rectifying section and the stripping section which are usually combined in a single conventional distillation column. However, as can be seen in the Figure 6.1, the heavy, i.e., aqueous phase, is returned to the top of the 1st column. As long as there are two phases present in the reflux tank and the process is operated with a butanol-water system, the butanol concentration is dependent on temperature only. The temperature, on the other hand is defined by the pressure (89 mbar). According to literature, the butanol concentration for those conditions is around 65 g/L. In accordance with the VLE data the feed stream from the fermenter would be at stage 1, i.e., top stage, making it unnecessary to distinguish distillation between the rectification and the stripping sections.

To simulate the 1st column of the process depicted in the Figure 6.1 as RPB, the butanol concentration in the synthetic fermentation broth was increased to 60 g/L. Two things were thus ensured: *i)* the plant solution consists of only one phase, *ii)* with that composition it was established a two-phase system being present in the reflux tank during the operation.

For initial testing, experiments were performed with the binary water-butanol system under total reflux. For the same reason as stated above, the plant was filled with a 60 g/L butanol solution.

The rpm levels investigated were 300, 600, 1200, and 2400 rpm. For each rpm setting the process was given 20 min to achieve steady state, then the product samples were taken for analysis. The experiment for each rpm setting was performed twice, the error bars depicted the standard deviation between the experiments.

6.3.6.2 Stripping experiments

For the stripping experiments, the binary water-butanol system mixture and the synthetic fermentation broth as liquid feeds were used together with the stream made from an external source of distilled water. Furthermore, an additional experiment was performed with the addition of polyethylene glycol 10000 (PEG) to the water-butanol binary mixture, to investigate the influence of viscosity on butanol recuperation.

The rpm levels investigated were 600, and 2400 rpm. For each rpm setting, the plant was run for 20 minutes, thereafter product samples were taken for analysis.

6.3.3   Analytical method

Alcohols and carboxylic acids were analyzed using gas chromatography (GC) (model GC-14A, Shimadzu) equipped with the INNOPEG-FFAP capillary column (diameter of 0.32 mm, a length of 25 m and a film thickness of 0.5 μm) and Flame Ionization Detector (FID). The sample injection volume was 5 μL. Helium was used as a carrier gas at a gas velocity of 30 cm/s. The temperature ramp applied was the following: the initial temperature of 135 °C was maintained for 0.3 min, then it ramped up to 210 °C at a rate of 75 °C/min, then it was held for 2.3 min resulting in a total time of around 7.5 minutes.

The viscosity of the real fermentation broth samples was measured in a compact modular rheometer MCR-102 (ANTON PAAR) on a CC27 concentric cylinder system at a strain rate of $12s^{-1}$. The measurement temperature range was from 25 to 90 °C. The viscosity of the binary mixtures and synthetic fermentation broth was measured with a capillary viscosimeter (Schott, K = 0.003163)

6.4   Results and discussion

6.4.1   Distillation under total reflux

The rpm was the first technical parameter to evaluate butanol removal from binary water-butanol system using RPB. Independent on the rotor speed the butanol concentration in top product was similar in all cases (around 63 g/L), while its amount in the bottom product was decreasing, at rpm was increasing (Figure 6.4). The liquid reflux for each rpm was the same as expected, because the composition of 2-phase water-butanol mixture depends on temperature only and in accordance with literature data is 65 g/L for 45 °C (Barton, 1984). Low concentration in the bottom product indicates the high efficiency of butanol recovery from the synthetic fermentation broth using RPB.

High fluctuations at 300 rpm were probably due to the unstable operation of the RPB at that setting. Additionally, the highest butanol concentrations in the bottom product excluded that rpm setting from further experiments. Given that butanol concentrations in the top and bottom products at rotational speeds of 600 and 1200 rpm were quite similar, it was decided to exclude also the 1200 rpm speed from the study. Further experiments were conducted only at 600 and 2400 rpm.
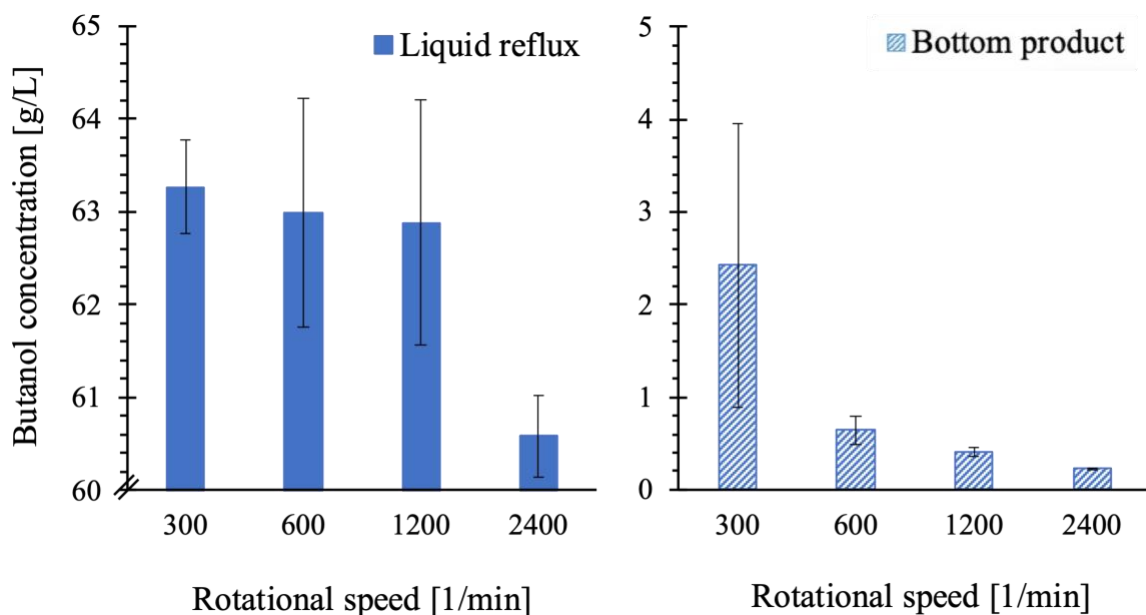
Figure 6.4. Butanol distribution between the liquid reflux and bottom product obtained during distillation under total reflux in the RPB under reduced pressure at different rotational speeds.

For the butanol-water system there are two "specialties" worth mentioning. First, considering the pure component boiling temperatures, water would be the top product, i.e., the distillate, if there was no azeotrope. That means, for a separation of those two components, the water fraction would have to be evaporated which would require a vast amount of energy for highly diluted butanol solutions. However, due to the presence of a boiling point minimum azeotrope and the low amount of butanol in the feed, the top product has a composition closer to the azeotrope. Thus, according to the conditions described, butanol is enriched in the distillate. Second, as mentioned above, it is impossible to cross the azeotropic point with a single distillation process. Fortunately, physicochemical laws create a feature that is built into the butanol-water system that allows azeotrope separation without the additional component of a miscibility gap. For this reason, separation into pure components is possible by performing a heteroazeotropic distillation depicted in the Figure 6.1. The results discussed in this section belong to column R1 and the decanter. The liquid-liquid separation in that plant takes place in the reflux tank acting as a decanter since the reflux is withdrawn at the very bottom. Column R2 is not part of this study as it is not crucial for the fermentation process.

The rpm for butanol recovery from the multicomponent mixture by vacuum distillation in RPB has almost no impact on butanol separation. However, the lowest butanol concentration in the bottom product was observed at 2400 rpm. Comparing the butanol concentration at 600 rpm in liquid reflux to those of the binary system, it slightly decreased (from 63 to 61 g/L). That could be explained by the impact of additional components on the phase system. Nevertheless, butanol remained enriched in the top product (Figure 6.5). Similarly, ethanol was also enriched in the top product as expected, due to its low boiling temperature. Ethanol in-situ removal from fermentation broth by vacuum distillation is an effective method and was already described in literature (Zhang et al., 2017). The interesting phenomena not yet reported, were observed regarding furfural and carboxylic acids. According to the physical properties of volatile fatty acids, their boiling point increases with carbon atoms in the chain. Therefore, it was expected that as the chain increased, a given acid should remain in the bottom product. Nevertheless, the opposite trend has been observed. Short-chain fatty acids, such as acetic (two carbon atoms) and propionic acids (three carbon atoms), were enriched in the bottom product, while longer-chain fatty acids, like valeric (five carbon atoms) and caproic (six carbon atoms) acids, were enriched in the top product. Likewise, furfural, whose pure component data define it as a heavy boiler compound, showed unexpected behavior and was enriched in the top product instead of the bottom product. The reason for the described behavior could be as follows: pure component data are misleading in the present case since every component investigated – except acetic acid – forms a temperature minimum azeotrope with water not only at ambient pressure but also at the conditions of this study. Furthermore, the azeotropes are located at a component concentration higher as in the fermentation broth which leads to the enrichment of those components in the distillate. For the stripping section, the binary data between the respective component and water clearly provide a reasonable explanation for the behavior of the multicomponent mixture. However, interactions between those components might occur with increasing concentration of those components in subsequent separation processes, for example the liquid-liquid separation and the column 2 in the Figure 6.1.

The removal of both, butanol and other bioproducts from the synthetic fermentation broth has two advantages: *i)* VFAs have an inhibitory effect on cell growth (Wambugu et al., 2020), and furfural is highly toxic to bacteria (Becerra et al., 2022), hence, the treated fermentation broth possibly can be recycled to the bioreactor, saving freshwater consumption (this part requires experimental verification); *ii)* other bioproducts may provide additional revenue after separating them. However,

all components present in the top product must be considered in the subsequent purification processes.
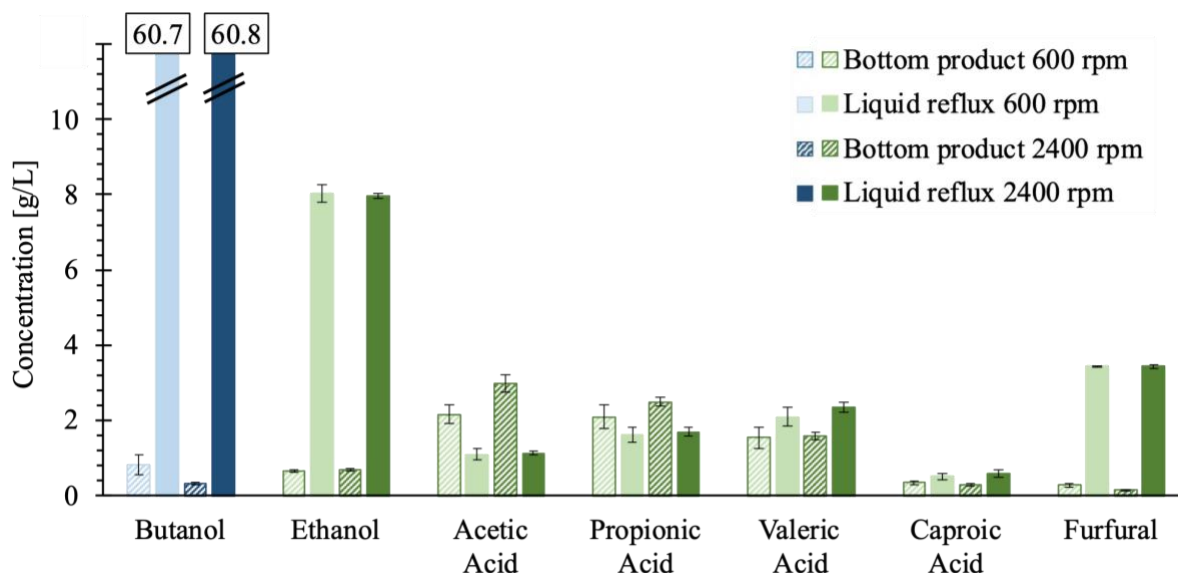
Figure 6.5. Concentration of the synthetic fermentation broth components in the top product and bottom product obtained under total reflux experiments in the RPB under reduced pressure at rotational speed of 600 and 2400 rpm.

The samples of the condensed top product showed butanol concentration in a butanol-rich phase at the level of 521.6 g/L. The composition of the bottom product as well as the top product divided into the light and the heavy phases are presented in the Table 6.2. Transferring those results to operation under finite reflux with the heavy aqueous phase is recycled to the RPB that would result in 3.8 % of the inlet stream leaving the decanter as butanol rich light phase for further purification. Certainly, the separation performance of the RPB needs to be higher to achieve similar concentrations under finite reflux but with some optimizations in the packing size or specific surface area that should be possible.

The literature extensively describes in-situ butanol elimination directly from the bioreactor under reduced pressure (Stoffers et al., 2013; Chen et al., 2018; Grisales Díaz et al., 2019). The reduced pressure is required for in situ separation to reduce the boiling point of butanol or, more precisely, the water-butanol azeotrope. At ambient pressure, the minimum boiling point of the azeotrope is 92.4 °C (Zong et al., 1983), while typical temperature for butanol production during fermentation process usually ranges between 35 and 37 °C (He et al., 2017; Tsai et al., 2020; González-Tenorio

et al., 2020; Bao et al., 2022). When fermentation is performed under reduced pressure, the boiling point of the mixture decreases, enabling in-situ butanol recovery.

Table 6.2. Bottom and top product (heavy and light phase) of rectifying section under total reflux.

Rotational speed 2400 rpm	Bottom product	Top product	
		Heavy phase	Light phase
		g/L	
Butanol	0.3	60.8	521.6
Ethanol	0.7	8.0	21.7
Furfural	0.2	3.4	13.8
Acetic acid	3.0	1.1	4.5
Propionic acid	2.5	1.5	5.3
Valeric acid	1.6	2.4	47.9
Caproic acid	0.3	0.6	36.8

So far, there is a few publications considering direct butanol removal via vacuum distillation at a close temperature to the fermentation temperature. Nguyen et al. (2018) carried out glucose fermentation employing *Clostridium acetobutylicum* CAB1060 (genetically modified strain) that was able to produce up to 10.5 g/L of butanol, as well as ethanol (10 g/L) and acetic acid (1 g/L).

The authors applied in-situ extraction by distillation under low pressure (making boiling temperature close to fermentative temperature) and were able to recuperate butanol, ethanol, and acetic acid at concentrations of 550, 60 and 3.3 g/L, respectively. The reported concentrations of butanol and ethanol were higher than in this work, which may be explained by the fact that the mixture was less complex (four-compounds mixture vs seven-compounds mixture). In this study butanol concentration from binary water-butanol mixture achieved concentration of 545 ± 7.1 g/L, while its concentration decreased to 521.6 g/L (Table 6.2) during butanol recuperation from the complex mixture. That stream must be purified further for use as alternative fuel or feedstock. For a process as depicted in the Figure 6.1, the interaction of the components presented in the complex mixture must be investigated to demonstrate the feasibility of in-line butanol recuperation. The VLLE data are available in the literature for binary and, in some cases, ternary mixtures only. For that reason, the impact of the additional components on the relative butanol volatility is as important as the impact on the miscibility gap since this is the key for the feasibility of the

heteroazeotropic distillation. Du et al. (2021) were able to produce up to 20 g/L of butanol though glucose fermentation by genetically modified *Clostridium* acetobutylicum. Then, by carrying out in situ product recovery via vapor stripping-vapor permeation achieved butanol concentration at the level of 441.9 g/L. The method used applied carbon nanotube (based hybrid materials) in high-performance membrane preparation. As indicated Yang et al. (2018), the metallic impurities and structural defects in the hollow core or at the tips of the carbon nanotubes may block the penetrant molecules through their channels. Moreover, the membrane has high selectivity for alcohols, therefore, VFA or furfural removal probably is not possible or very limited. In contrast, the RPB carries out not only effective alcohol recuperation (butanol and ethanol), but also removed high concentration of furfural and VFA. This possibly allows the aqueous phase to be returned to the fermenter. Moreover, both studies mentioned produced butanol from glucose using genetically modified species. That is more related to scientific developments in genetic modification and the possibilities of bacteria, rather than to the scale-up of the process for commercial application, due to the conflict of interest with the alimentary industry. In this work, the high butanol concentration was obtained from cellulosic fraction of lignocellulosic biomass, a sustainable feedstock. Moreover, the mixed culture does not require sterile conditions and its cultivation is much cheaper than the pure culture. Therefore, further research could lead to the commercialization of this process as a new method of obtaining butanol from renewable energy sources.

Some authors applied vacuum pressure to increase the ABE fermentation component concentrations in the gas phase above the liquid phase inside the reactor (Mariano et al., 2011; Qureshi et al., 2014), which is not a distillation but an evaporation process. However, there are some studies on in situ ethanol recovery by vacuum distillation. For example, Ghose et al. (1984) reached 1.4-fold higher ethanol concentration compared with traditional fermentation by performing in-situ ethanol removal from fermentation broth using vacuum distillation combined with cell recycling.

6.4.1   Stripping experiments

Stripping experiments were performed with 5 wt. % of steam as stripping gas at 600 and 2400 rpm. The butanol in the top-product reached 118 g/L for 2400 rpm (Figure 6.6). That means, according to butanol component balance, after condensation 12.7 % of the inlet stream leaves the column as top product which then separates into a light butanol rich phase and a heavy water rich phase. It

must be considered at this point, the concentration in the liquid reflux is not given, but the composition of the condensed vapor after leaving the top of the column. Since two phases were formed after the condensation, the samples were diluted with water until a single phase for analysis was obtained. The error bars for the top product indicates large fluctuations. This may be due to the sampling method, which required a sufficiently large volume of samples to be taken after condensation to ensure representative amount of the aqueous and the organic phase. However, the concept of the process with the simplified two-phase system is proven. The light organic phase formed after condensation is withdrawn for further purification, and the heavy aqueous phase is mixed with the feed from the fermenter and recycled to the RPB. The bottom product is recycled to fermenter with butanol concentration lower than 10 g/L. Consequently, the stripping synthetic fermentation broth experiments assert that single RPB can be used to operate in the column R-1 in the Figure 6.1.
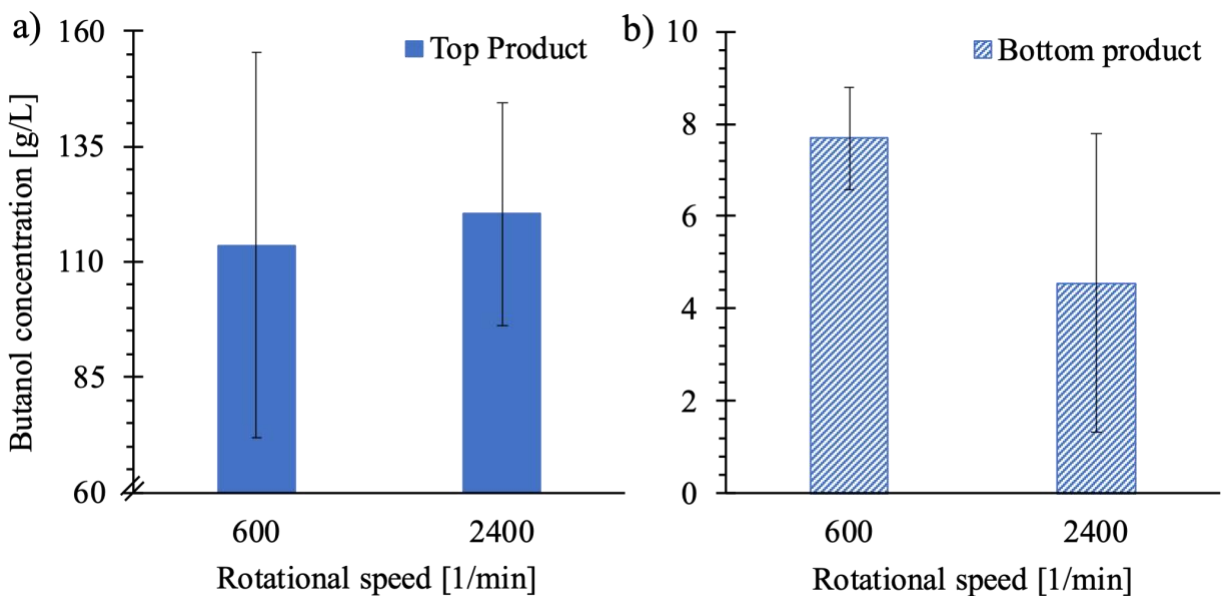
Figure 6.6. Stripping experiments of the water-butanol binary mixture with 5 wt.% of steam as a stripping gas at 600 and 2400 rpm in RPB under reduced pressure; a) butanol concentration in the top product; b) butanol concentration in the bottom product.

The same stripping binary water-butanol mixture experiments with additional 2% of polyethylene glycol 10000 (PEG) were performed. The viscosity of synthetic fermentation broth increased from $\eta = 0.66$ mPa*s to $\eta = 0.99$ mPa*s at 45 °C. For the real fermentation broth supernatant $\eta = 0.56$ mPa*s at 45 °C was determined. However, when the real fermentation broth is processed in the

RPB without any pretreatment, the apparent viscosity might increase. Nonetheless, no impact on mass transfer was detected, the composition of the organic and the aqueous phases were like those depicted in the Figure 6.6. Possibly, it was because the viscosity was not high enough to impact the mass transfer. On the other hand, further increase of viscosity by adding more polymer may affect the VLE, which must be verified beforehand. Future investigation should evaluate the viscosity influence on both butanol and bioproducts separation from fermentation broth.
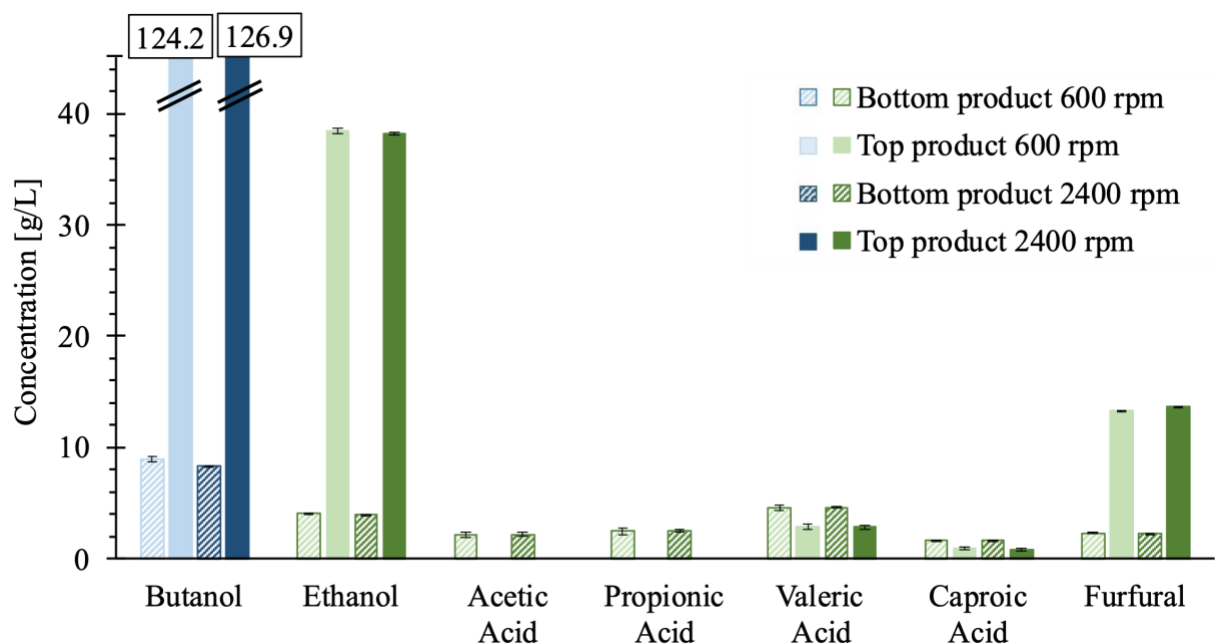
Figure 6.7. Concentrations of the synthetic fermentation broth components in the bottom and the top product obtained during stripping experiments in the RPB under reduced pressure at rotational speed of 600 and 2400 rpm.

During stripping experiments of the synthetic fermentation broth, two liquid phases were observed after condensation, hence, the top product samples were diluted analysis. Butanol removal with 5% of stripping steam resulted in a butanol concentration in the top product up to 126.9 g/L. Thus, when processing the real Fermentation broth, after condensation 9.1% of the inlet stream leaves the column as top product which then separates into a light butanol rich phase and a heavy aqueous phase (data from the Figure 6.7, 2400 rpm). Similarly, ethanol was stripped from the synthetic fermentation broth independent of the rpm (Figure 6.7). Moreover, furfural had a four-times higher concentration in the top product during stripping experiments than under total reflux. An interesting observation was that acetic and propionic acids were not detected in the top product. They were

found in concentrations close to their amounts in the feed stream in the bottom product. Valeric and caproic acids were found in both, top and bottom products. Unlike distillation experiments under total reflux the concentration of VFAs at an increasing carbon chain were slightly lower in the top product. These observations indicate that changes in the reflux ratio in stripping experiments affect the partitioning of individual components.

6.5   Conclusions

Vacuum distillation in the RPB is an adequate method for butanol recuperation from the synthetic fermentation broth. Distillation allows the removal of ethanol, furfural, and carboxylic acids. The liquid-liquid separation of the top product yields two phases: a butanol-rich organic phase, which needs subsequent purification into pure components, and an aqueous phase that can be recycled to the fermenter. Recycling of the depleted bottom product to the fermenter seems reasonable. Nevertheless, its general feasibility regarding by-product accumulation in the fermenter was not demonstrated in this study. What has been demonstrated is the possibility of in-line butanol stripping from the mixture that represents fermentation broth obtained from lignocellulosic waste by mixed culture. Replacing the reboiler with a source of 'open steam' has the advantage of avoiding hotspots or dead zones in the reboiler that may harm or kill the bacteria. Furthermore, it was shown that the liquid-liquid separation, a crucial step towards pure butanol, is possible under presence of numerous side components from fermentation.

Due to the low viscosity of the systems investigated, the impact of rotational speed on the separation was detectible, but not enough to make it excessively important. That raises the question whether an RPB or a conventional column is the machine/apparatus of choice for this specific separation task. The advantage of feeding the RPB with non-pretreated fermentation broth supernatant stands against the simplicity and robustness of a static column. Furthermore, the susceptibility to fouling together with the final composition of the fermentation broth will play a major role in the final decision.

Future investigations should focus on the impact of in-line butanol recovery from the fermentation process and the butanol production rate. Furthermore, the feasibility of recycling the bottom product to the fermenter needs to be verified with special focus on accumulation of side products like acetic or propionic acid. Those are of special interest since they were not separated with the

butanol and might influence the fermentation. Additionally, the impact of the components separated with the butanol on the subsequent butanol purification (Figure 6.1, R-2) needs to be investigated to verify the feasibility of the entire downstream process.

6.6   References

Bao, T., Jiang, W., Ahmad, Q.A., & Yang, S.T. (2022). Consolidated bioprocessing for ethanol and butanol production from lignocellulosic biomass: Recent advances in strain and process engineering. In A-Z of Biorefinery (pp. 473-506). Elsevier. https://doi.org/10.1016/B978-0-12-819248-1.00009-9

Barton, A. F. M. (1984). Solubility data series: Alcohols with Water (First Edition, Vol. 15).

Becerra, M. L., Lizarazo, L. M., Rojas, H. A., Prieto, G. A., & Martinez, J. J. (2022). Biotransformation of 5-hydroxymethylfurfural and furfural with bacteria of bacillus genus. Biocatalysis and Agricultural Biotechnology, 39, 102281. https://doi.org/10.1016/j.bcab.2022.102281

Card, J. C., & Farrell, L. M. (1982). Separation of alcohol-water mixtures using salts. Oak Ridge National Lab., TN (USA). https://doi.org/10.2172/5250443

Chen, H., Cai, D., Chen, C., Wang, J., Qin, P., & Tan, T. (2018). Novel distillation process for effective and stable separation of high-concentration acetone–butanol–ethanol mixture from fermentation–pervaporation integration process. Biotechnology for Biofuels, 11(1), 286. https://doi.org/10.1186/s13068-018-1284-8

Diltz, R. A., Marolla, T. V., Henley, M. V., & Li, L. (2007). Reverse osmosis processing of organic model compounds and fermentation broths. Bioresource Technology, 98(3), 686-695. https://doi.org/10.1016/j.biortech.2006.01.022

Du, G., Zhu, C., Xu, M., Wang, L., Yang, S.T., & Xue, C. (2021). Energy-efficient butanol production by Clostridium acetobutylicum with histidine kinase knockouts to improve strain tolerance and process robustness. Green Chemistry, 23(5), 2155-2168. https://doi.org/10.1039/D0GC03993D

Dudek, K., Molina-Guerrero, C. E., & Valdez-Vazquez, I. (2022). Profitability of single- and mixed-culture fermentations for the butyric acid production from a lignocellulosic substrate. Chemical Engineering Research and Design, 182, 558-570. https://doi.org/10.1016/j.cherd.2022.04.018

Ghose, T. K., Roychoudhury, P. K., & Ghosh, P. (1984). Simultaneous saccharification and fermentation (SSF) of lignocellulosics to ethanol under vacuum cycling and step feeding. Biotechnology and Bioengineering, 26(4), 377-381. https://doi.org/10.1002/bit.260260414

González-Tenorio, D., Muñoz-Páez, K. M., & Valdez-Vazquez, I. (2020). Butanol production coupled with acidogenesis and CO2 conversion for improved carbon utilization. Biomass Conversion and Biorefinery. https://doi.org/10.1007/s13399-020-00805-y

Grisales Díaz, V. H., von Stosch, M., & Willis, M. J. (2019). Butanol production via vacuum fermentation: An economic evaluation of operating strategies. Chemical Engineering Science, 195, 707-719. https://doi.org/10.1016/j.ces.2018.10.016

Grobben, N. G., Eggink, G., Petrus Cuperus, F., & Huizing, H. J. (1993). Production of acetone, butanol and ethanol (ABE) from potato wastes: Fermentation with integrated membrane extraction. Applied Microbiology and Biotechnology, 39(4-5), 494-498. https://doi.org/10.1007/BF00205039

He, C.R., Kuo, Y.Y., & Li, S.Y. (2017). Lignocellulosic butanol production from Napier grass using semi-simultaneous saccharification fermentation. Bioresource Technology, 231, 101-108. https://doi.org/10.1016/j.biortech.2017.01.039

Hilpert, M., Calvillo Aranda, G. U., & Repke, J.U. (2021). Experimental analysis and rate-based stage modeling of multicomponent distillation in a Rotating Packed Bed. Chemical Engineering and Processing - Process Intensification, 108651. https://doi.org/10.1016/j.cep.2021.108651

Jang, M.O., & Choi, G. (2018). Techno-economic analysis of butanol production from lignocellulosic biomass by concentrated acid pretreatment and hydrolysis plus continuous fermentation. Biochemical Engineering Journal, 134, 30-43. https://doi.org/10.1016/j.bej.2018.03.002

Jin, C., Yao, M., Liu, H., Lee, C. F., & Ji, J. (2011). Progress in the production and application of n-butanol as a biofuel. Renewable and Sustainable Energy Reviews, 15(8), 4080-4106. https://doi.org/10.1016/j.rser.2011.06.001

Kujawska, A., Kujawski, J., Bryjak, M., & Kujawski, W. (2015). ABE fermentation products recovery methods - A review. Renewable and Sustainable Energy Reviews, 48, 648-661. https://doi.org/10.1016/j.rser.2015.04.028

Lin, C.C., Lin, Y.C., Chen, S.C., & Hsu, L.J. (2010). Evaluation of a rotating packed bed equipped with blade packings for methanol and 1-butanol removal. Journal of Industrial and Engineering Chemistry, 16(6), 1033-1039. https://doi.org/10.1016/j.jiec.2010.09.002

Lin, C.C., Lin, Y.C., & Chien, K.S. (2009). VOCs absorption in rotating packed beds equipped with blade packings. Journal of Industrial and Engineering Chemistry, 15(6), 813-818. https://doi.org/10.1016/j.jiec.2009.09.005

Lukin, I., Gładyszewski, K., Skiborowski, M., Górak, A., & Schembecker, G. (2021). Aroma absorption in a rotating packed bed with a tailor-made archimedean spiral packing. Chemical Engineering Science, 231, 116334. https://doi.org/10.1016/j.ces.2020.116334

Mariano, A. P., Qureshi, N., Filho, R. M., & Ezeji, T. C. (2011). Bioproduction of butanol in bioreactors: New insights from simultaneous in situ butanol recovery to eliminate product toxicity. Biotechnology and Bioengineering, 108(8), 1757-1765. https://doi.org/10.1002/bit.23123

McCabe, W. L. (2001). Unit operations of chemical engineering. Sixth edition. Boston: McGraw Hill. https://search.library.wisc.edu/catalog/999954470702121

Nguyen, N.P.T., Raynaud, C., Meynial-Salles, I., & Soucaille, P. (2018). Reviving the Weizmann process for commercial n-butanol production. Nature Communications, 9(1), 3682. https://doi.org/10.1038/s41467-018-05661-z

Nguyen, V.D., Kosuge, H., Auresenia, J., Tan, R., & Brondial, Y. (2009). Effect of Vacuum Pressure on Ethanol Fermentation. Journal of Applied Sciences, 9(17), 3020-3026. https://doi.org/10.3923/jas.2009.3020.3026

Panwar, N.L., Kaushik, S.C., & Kothari, S. (2011). Role of renewable energy sources in environmental protection: A review. Renewable and Sustainable Energy Reviews, 15(3), 1513-1524. https://doi.org/10.1016/j.rser.2010.11.037

Qureshi, N. (2009). Solvent Production. En M. Schaechter (Ed.), Encyclopedia of Microbiology (Third Edition) (pp. 512-528). Academic Press. https://doi.org/10.1016/B978-012373944-5.00160-7

Qureshi, N., & Blaschek, H. P. (2001). Recovery of butanol from fermentation broth by gas stripping. Renewable Energy, 22(4), 557-564. https://doi.org/10.1016/S0960-1481(00)00108-7

Qureshi, N., Singh, V., Liu, S., Ezeji, T. C., Saha, B. C., & Cotta, M. A. (2014). Process integration for simultaneous saccharification, fermentation, and recovery (SSFR): Production of butanol from corn stover using Clostridium beijerinckii P260. Bioresource Technology, 154, 222-228. https://doi.org/10.1016/j.biortech.2013.11.080

Smith, R., & Jobson, M. (2000). DISTILLATION. In I. D. Wilson (Ed.), Encyclopedia of Separation Science (pp. 84-103). Academic Press. https://doi.org/10.1016/B0-12-226770-2/00041-7

Stoffers, M., & Górak, A. (2013). Continuous multi-stage extraction of n-butanol from aqueous solutions with 1-hexyl-3-methylimidazolium tetracyanoborate. Separation and Purification Technology, 120, 415-422. https://doi.org/10.1016/j.seppur.2013.10.016

Stoffers, M., Heitmann, S., Lutze, P., & Górak, A. (2013). Integrated processing for the separation of biobutanol. Part A: Experimental investigation and process modelling. Green Processing and Synthesis, 2(2). https://doi.org/10.1515/gps-2013-0009

Tsai, T.Y., Lo, Y.C., Dong, C.D., Nagarajan, D., Chang, J.S., & Lee, D.J. (2020). Biobutanol production from lignocellulosic biomass using immobilized Clostridium acetobutylicum. Applied Energy, 277, 115531. https://doi.org/10.1016/j.apenergy.2020.115531

Valdez-Vazquez, I., & Sanchez, A. (2018). Proposal for biorefineries based on mixed cultures for lignocellulosic biofuel production: A techno-economic analysis. Biofuels, Bioproducts and Biorefining, 12(1), 56-67. https://doi.org/10.1002/bbb.1828

Wambugu, C. W., Eldon, R. R., Van de Vossenberg, J., Dupont, C., & van Hullebusch, E. D. (2020). Waste Biorefinery Integrating Biorefineries for Waste Valorisation: Chapter 8—Biochar from various lignocellulosic biomass wastes as an additive in biogas production from food waste. Elsevier. https://doi.org/10.1016/B978-0-12-818228-4.00008-3

Yang, D., Tian, D., Xue, C., Gao, F., Liu, Y., Li, H., Bao, Y., Liang, J., Zhao, Z., & Qiu, J. (2018). Tuned Fabrication of the Aligned and Opened CNT Membrane with Exceptionally High Permeability and Selectivity for Bioalcohol Recovery. Nano Letters, 18(10), 6150-6156. https://doi.org/10.1021/acs.nanolett.8b01831

Zhang, J., Lei, C., Liu, G., Bao, Y., Balan, V., & Bao, J. (2017). In—Situ Vacuum Distillation of Ethanol Helps To Recycle Cellulase and Yeast during SSF of Delignified Corncob Residues. ACS Sustainable Chemistry & Engineering, 5(12), 11676-11685. https://doi.org/10.1021/acssuschemeng.7b03084

Zong, Z.L., Yang, X.H., & Zheng, X.Y. (1983). Determination and correlation of vapor-liquid equilibria of alcohol solutions. Journal of Chemical Engineering of Japan, 16(1), 1-6. https://doi.org/10.1252/jcej.16.1

7. Chapter VII: Profitability of single- and mixed-culture fermentations for the butyric acid production from a lignocellulosic substrate

Reference to published work:

7.1   Abstract

Butyric acid (BA) is one of the most promising precursors for pharmaceutical and plastic manufacturers, as well as for fuel butanol production. Lignocellulosic biomass can be used as an adequate source for BA production due to its low prices and widespread abundance. The conversion of lignocellulosic biomass into BA requires different steps depending on the type of inoculum. Pure cultures, which produce high amounts of BA, demand sequential processing of lignocellulosic substrates. In contrast, mixed cultures, which produce a lower amount of BA, work as a consolidated bioprocess, therefore, some processing steps occur simultaneously. It is unknown which of these two schemes for BA production is more profitable yet. The following study presents a review about the most recent advances about BA production from lignocellulose by pure and mixed cultures. In addition, a techno-economic analysis for BA production is considered for each type of inoculum and different plant capacities. The pure strain scheme involves seven stages, while the mixed culture scheme involves only four. Both schemes include the final product purification through membranes where the purity of BA was 99.8%. The mixed culture scheme is more profitable than the pure strain one, with Total Production Costs of 3.2, 1.3, and 0.9 US$/kg for plant capacities of 100, 500, and 1000 tons/day, respectively. With respect to the pure strain scheme, the Total Production Costs are 15.1, 7.3, and 6.5 US$/kg for plant capacities of 100, 500, and 1000 tons/day, respectively. The operating costs in the pure culture plants are 30.4, 81.7, and 145.2 million US$/year for the plant capacities of 100, 500, and 1000 tons/day, respectively. These operating costs are between 1.2 to 1.5 times higher compared with the mixed culture plants. Also, the Total Capital Investment is three times higher with the pure strain scheme.

Keywords: consolidated bioprocess; process simulation; techno-economic analysis; total production cost;

7.2 Introduction

Butyric acid (BA), a four-carbon short-chain fatty acid is commercially obtained from petroleum through the oxidation of butyraldehyde, either derived from the oxosynthesis or hydroformylation of propylene (Dwidar et al., 2012; Baroi et al., 2017). BA is used for food and pharmaceutical industries (Merklein et al., 2014), the manufacture of biodegradable plastics, and also for the treatment for hemoglobinopathies, cancer, and gastrointestinal diseases (Canani et al., 2011). Recent analyses indicate that BA production will be increased at an annual growth rate of 8.5% between 2020-2027. In addition to this, it is expected that its market value will reach USD 944,785 million by 2027 (Data Bridge Market Research, 2020). Considering environmental pollution and the negative impacts of petroleum-derived products for human health, BA formation during fermentation has become an attractive alternative (Wainaina et al., 2019).

What it is known at present is that BA production through fermentation is still much more expensive than through chemical synthesis due to the low yields and productivities (Luo et al., 2018). Therefore, past investigations were focused on improving the economic feasibility of BA production through engineering strategies (Fu et al., 2017; Suo et al., 2018; He et al., 2020), consolidated bioprocessing (Ai et al., 2016; Chi et al., 2018; Pérez-Rangel et al., 2021; Ayala-Campos et al., 2022) and the optimization of the fermentation processes (Huang et al., 2016; Xiao et al., 2018).

Lignocellulosic biomass is one of the most promising carbon sources for BA production due to its abundance and low cost (Anwar et al., 2014). Every year, 181.5 billion tons of lignocellulosic biomass are produced worldwide, but only 8.2 billion tons are further processed (Dahmen et al., 2019). In Mexico, the availability of the lignocellulosic biomass generated only from four types of agricultural activities reaches more than 22.9 million tons, concentrated in 34 centroids equivalent to plant capacities between 100,000 to 660,000 ton/year (Hernández et al. 2019). In South America, harvesting and processing of agricultural goods generate up to 500 million tons of lignocellulosic biomass annually. The two largest manufactures are Brazil, where corn, sugarcane and soybean are the most abundant crops, and Argentina with corn, soybean, and wheat which accounts for more than 87 % of the total amount of lignocellulosic biomass (Magalhães et al., 2019). Most of this biomass is burning in boilers and used for electricity generation. Nevertheless, this purpose is not

always economically favorable, especially when biomass has a high moisture content and a low heating value.

Lignocellulosic biomass processing to produce BA can use pure strains, genetically modified strains, or mixed cultures. Each type of inoculum affects the biorefinery design due to the different steps that it requires to process the biomass. As it is claimed that, until now there are no studies that evaluate the impacts of the type of inoculum on the profitably of BA production from lignocellulosic biomass. In this context, the present study was divided into two main objectives: firstly, to analyze the key factors that influence single- and mixed-culture fermentations, discuss the advantages and disadvantages from a technical point of view, and identify significant steps forward in this field. Secondly, to present a techno-economic analysis for comparing the profitability of BA production from single- and mixed-culture fermentation using a model of lignocellulosic biomass.

7.3   BA production by single-culture fermentation

Clostridium spp. including *Clostridium tyrobutyricum, Clostridium butyricum,* and *Clostridium thermobutyricum* are the main bacteria employed for BA production.

Table 7.1. Butyric acid production from lignocellulosic hydrolysates by pure cultures.

Microorganism	Type of hydrolysate	Operating mode	pH	T °C	Butyric acid				References
					Productivity (g/L*h)	Concentration (g/L)	Yield (g/g)	Selectivity (%)	
C. SP1	Softwood	Batch	6.0	37	0.66	21.2	0.47	100	Kim et al. (2016)
C. tyrobutyricum	Oilseed rape straw	Batch, FBB	6.0	37	0.85	21.5	0.45	86	Huang et al. (2016)
C. tyrobutyricum Ct-pTBA	Soybean hull	Batch	6.0	37	0.15	15.3	0.43	48	Fu et al. (2017)
C. tyrobutyricum	Corn husk	Batch, FBB	6.0	37	0.39	21.8	0.39	83	Xiao et al. (2018)
C. tyrobutyricum ATCC 25755/sdr+groESL	Corncob	Batch	6.0	37	0.29	32.8	0.36	94	Suo et al. (2019)
C. tyrobutyricum ATCC 25755/kept	Spent coffee grounds	Batch, FBB	6.0	37	0.36	34.3	0.37	85	He et al. (2020)

Note: FBB –Fibrous bed bioreactor for cell immobilization.

3

These bacteria display high yields and selectivity for BA production, resistance to high concentrations of BA and acetic acid (Jiang et al., 2011), and some of them metabolize simultaneously hexose and pentose sugars released from lignocellulosic biomass (Zhang et al., 2009; Dwidar et al., 2012). For example, *C. tyrobutyricum* produced 13.6 g/L of BA from an oilseed rape straw hydrolysate (Huang et al., 2016) and 21.8 g/L from a corn husk acid hydrolysate (Xiao et al., 2018). When the simultaneous conversion of glucose and mannose occurred, *Clostridium* sp. S1 produced 21.2 g/L of BA (Kim et al., 2016). Through genetic engineering, He et al. (2020) reported the simultaneous consuming of glucose and galactose by the engineered *C. tyrobutyricum* ATCC 25755/kept resulting in 34.3 g/L of BA. Also, the engineered *C. tyrobutyricum* Ct-pTBA simultaneously consumed glucose and xylose reaching 42.6 g/L (Fu et al., 2017) and 32.8 g/L of BA (Suo et al., 2019). The data of production, productivity, yield, and selectivity of BA production by pure strains from lignocellulosic biomass were presented in the Table 7.1.

7.3.1   Type of substrate and pretreatment

Lignocellulosic biomass mainly composed by cellulose, hemicellulose, and lignin (Tayyab, 2018), requires a pretreatment to modify its complex and recalcitrant structure, which is difficult to be fermented directly by pure cultures. Since lignocellulosic composition, especially the lignin content which reduces the enzyme accessibility of polysaccharides, varies depending on type of biomass (Table 7.2), the nature of pretreatment and selection of parameters will depend on the specific type of lignocellulosic biomass (Aftab et al., 2018).

Diluted acids and bases are mainly used as pretreatments according to the published literature. For example, Kim et al. (2016) applied 75 wt% of H_2SO_4 at 30°C for 30 min to hydrolyze Japanese larch and produced 21.2 g/L of BA. Similarly, Fu et al. (2017) hydrolyzed separately various lignocellulosic biomasses, soybean hull, corn fiber, wheat straw, rice straw, and sugarcane bagasse with diluted acid at 121°C for 30 min. The engineered *Clostridium tyrobutyricum* Ct-pTB produced the highest amount of BA (42.6 g/L) from sugarcane bagasse hydrolysate. Additionally, He et al. (2020) hydrolyzed spent coffee grounds by using 0.04 M H_2SO_4 at a solid-liquid ratio of 10% (w/v), 121°C for 40 min and produced 34.3 g/L of BA. Whereas Huang et al. (2016) removed lignin, acetyl, and uronic substitutes by applying a NaOH pretreatment at 121 °C for 40 min and produced 21.5 g/L of BA in the further fermentation.

Table 7.2. Composition of lignocellulosic biomass commonly used for butyric acid production.

Lignocellulosic biomass	Hemicellulose (%)	Cellulose (%)	Lignin (%)	Ash (%)	Reference
Corn stover	26	36	21	17	Ayala-Campos et al., (2022)
Corn husk	45	40	7	3	Xiao et al., (2018)
Agave	21 - 23	42 - 49	7 - 8	20 - 28	Dudek et al., (2021)
Rice straw	24.8	39.7	15.3	20.2	Ai et al., (2016)
Softwood	13.0	58.6	20.1	8.3	Kim et al., (2016)
Wheat straw	28	38	22	12	Ayala-Campos et al., (2022)
Sugarcane bagasse	27	44	18	11	

7.3.2   Toxicity and detoxification

When pure cultures carried out the BA production from lignocellulosic biomass, the pretreatment stage is mandatory to release soluble sugars which are then fermented. However, chemical and physicochemical pretreatments of lignocellulosic biomass form inhibitors most of the time such as weak acids, furan derivatives, phenolics, and aromatic compounds during the degradation of biopolymers into soluble sugars. These undesirable products have an impact on cell membranes, enzyme activity, gene expression, cell growth, and metabolite production (Chandel et al., 2013; Jonsson et al., 2013; Monnappa et al., 2013). Since pure cultures require equipment sterilization, detoxification after treatment, and exogenous enzymes for biopolymer solubilization, the overall process tends to be more expensive (Tajarudin et al., 2018; Xiao et al. 2018).

The type and quantity of formed inhibitors depend on the composition of feedstock and type of pretreatment (Kim, 2018). Literature reports some efficient removal methods of inhibitors. For example, Lee et al. (2015) applied the electrochemical detoxification and removed 71% of the total phenolic compounds from rice straw hydrolysate without any sugar loss. Xiao et al. (2018) utilized the microporous activated carbon detoxification according with Cantarella et al. (2004) to detoxify corn husk hydrolysate resulting in 51% removal of HMF and losing only 8% of total sugars. On the other hand, each microorganism has different toxin resistance. For example, HMF caused prolongation of the lag phase, a decrease in xylose consumption, and BA production by *C.*

tyrobutyricum; nevertheless, these negative effects did not happen when the concentration of HMF was below 0.6 g/L (Liu et al., 2017). There are also some modified chemical pretreatments that decrease the formation of inhibitors compared with conventional methods. Huang et al. (2016) performed a novel stepwise pretreatment relying on alkali deacetylation combined with liquid hot water pretreatment to hydrolyze oilseed rape straw. Glucose yields as high as 53 % and low concentrations of furfural and HMF at the levels of 0.011 g/L and 0.003 g/L were achieved, respectively. In other studies, the detoxification stage was not required when adapted or engineered bacteria were used. The one-year adaptation of *C. tyrobutyricum* to increasing concentrations of wheat straw hydrolysate (from 40% to 80% v/v) resulted in an increase in the BA yield ranging from 0.06 g/g to 0.48 g/g sugar (Baroi et al., 2015). Meanwhile, Suo et al. (2019) carried out co-expression of furfural and phenolic tolerance-related genes, obtaining the engineered *C. tyrobutyricum* ATCC 25755/sdr+groESL that produced 28 % more BA from undetoxified corncob acid hydrolysate, compared with the wild strain. Some authors described genetic overexpression of oxidoreductases as a factor to enhance the tolerance to furfural derivatives (Wang et al., 2013; Chung et al., 2015; Kim et al., 2017).

7.3.3 Cultivation pH

Most investigations related to BA production by pure strain performed the fermentation processes at pH 6.0. It is possible to assume that there is a very narrow pH range that permits obtaining optimal efficiency. Zhu and Yang (2004) assessed different pH values (5.0, 5.3, 5.7, 6.0, 6.3) for BA production by *C. tyrobutyricum*, the highest concentration of 57.9 g/L was obtained at pH 6.3. However, lactic and acetic acids were the most abundant byproducts at pH values below 6.0. Similar results were reported by Chong et al. (2009), who evaluated the influence of three pH levels (5.0, 5.5, 6.0) on BA production from glucose by *C. butyricum* EB6. The highest BA concentration (12.51 g/L) and selectivity were observed at pH 6.0. Only acetic acid was detected together with BA. Drahokoupil and Patáková (2020) assessed BA production from glucose by *C. beijerinckii* NRRL B-598 at five pH values (6.0, 6.5, 7.0, 7.5, 8.0). Results showed that the highest BA concentration of 11.49 g/L was obtained at pH 7.0, in the presence of low concentrations of acetic and lactic acids (below 4 g/L). The highest BA to acetic acid ratio occurred at pH 6.5. To summarize, *C. tyrobutyricum* and *C. butyricum* presented a higher BA selectivity than *C. beijerinckii*.

7.3.4 Cultivation temperature

Mesophilic and thermophilic fermentative bacteria have optimal growth temperatures ranging between 20 to 45 °C and 50 to 80 °C, respectively (Willey et al., 2017). Most of the reviewed studies carried out single-culture fermentation processes under mesophilic temperatures, particularly at 37 °C. This mesophilic temperature is considered optimal for the growth of *C. butyricum* and *C. tyrobutyrium* to produce BA (Zigova et al., 1999; Ruusunen et al., 2012). On the other hand, thermophilic microorganisms, *e.g*., the co-culture *Clostridium thermocellum* ATCC 27405 and *C. thermobutyricum* ATCC 49875 produced the highest BA concentration of 33.9 g/L at 55 °C (Chi et al., 2018).

7.3.5 Reactor configuration

BA production has been usually performed by using different batch reactor configurations. Until now, the traditional vessel configuration is the most used for single-culture fermentations (Kim et al. 2016; Fu et al. 2017; Suo et al. 2019). Traditional suspended cell fermentation is associated with a low cell density per reactor volume, which extends the lag phase resulting in a low product concentration and a decrease in productivity (Duarte et al., 2013). Notwithstanding, the process was improved by applying a fibrous bed bioreactor (FFB). This type of reactor immobilizes cells with low cell growth rates, reduces the reaction time, and increases the substrate conversion, which allows the process to achieve a higher productivity and product yield (Kim et al., 2016; Zhu and Yang, 2003; Duarte et al., 2013; Wang et al., 2016). For instance, Huang et al. (2016) reported 16%, 165% and 17% increase in BA yield, productivity, and final concentration, respectively when using an FFB compared with the suspended cell fermentation. In addition to this, Xiao et al. (2018) evaluated BA formation from glucose in two different reactors and achieved 53% more BA in an FBB compared to the suspended cell fermentation.

7.4 BA production by mixed-culture fermentation

Besides pure strains, mixed cultures also produce BA. Herein, more than one type of microorganism collaborates with each other and shares the available sources (Brenner et al., 2008). Mixed cultures include co-cultures of at least two different microorganisms and microbial communities where the identity of their members may or may not be fully characterized. In both cases, their members simultaneously perform the production of hydrolytic enzymes,

saccharification, and fermentation (Lynd et al., 2005), an integrated process called consolidated bioprocess (CBP). In mixed cultures, one type of microorganism (or group of them) produces enzymes responsible for the saccharification of lignocellulosic biomass to monosaccharides, while other microorganism (or group of them) transforms these monosaccharides (hexose or/and pentose sugars) into different bioproducts. What is a fact that when the mixed cultures produce the hydrolytic enzymes, it could decrease the total production costs. Nevertheless, it is important to note that CBP could present some of the following disadvantages: low cell density, bacterial competition for resources, and mainly a low product yield because of the concurrent formation of several byproducts (Chen and Blaschek, 1999; Michel-Savin et al., 1990a; Michel-Savin et al., 1990b). Maiti et al. (2016) reported that small changes in pH and temperature in a CBP favor the establishment of undesired microorganisms that could produce unwanted byproducts.

Ai et al. (2016) used an undefined mixed culture derived from cattle manure, pig manure compost, corn field soil, and rotten wood. This undefined mixed culture produced 15.6 g/L of BA from rice straw in a semi-continuous fermentation. Other volatile fatty acids (VFAs) were also produced, 6.6 g/L of acetic acid, and propionic, valeric, caproic acids at concentrations below 0.9 g/L. Chi et al. (2018) utilized a co-culture of *C. thermocellum* ATCC 27405 (the hydrolytic bacterium) and *C. thermobutyricum* ATCC 49875 (the fermentative bacterium) to produce 2.4 g/L of BA from delignified rice straw. More recently, Perez-Rangel et al. (2021) produced 4.5 g/L of BA and 7.6 g/L of other VFAs directly from wheat straw. The native microbiota of substrate was used as inoculum, which was composed mainly by *Lactobacillus* and *Clostridium*. Dudek et al. (2021) produced 1.4 g/L of BA and 2.7 g/L of acetic and propionic acids directly from Agave bagasse. The inoculum consisted of the native microbiota of substrate where *Caproiciproducens* was linked to the BA production while *Bacteroides* and *Prevotella* were associated to the substrate hydrolysis. Ayala-Campos et al. (2022) succeeded in producing 4.3 g/L of BA and 4 g/L of other VFAs directly from Agave bagasse by changing the operation mode from batch to semicontinuous and by using an organic loading rate of 5.7 g/L-d. *Lactobacillus* and *Clostridium* together with other microorganisms integrated the native microbiota that was used as inoculum. These previous studies demonstrated that native microbiotas of lignocellulosic substrates are successful in performing a CBP and producing similar concentration of VFAs to those reported by pure cultures. However, future studies should focus on controlling the operating conditions to favor the BA ratio over the

other VFAs. Studies where mixed cultures produce BA production from lignocellulosic biomass were resumed in the Table 7.3.

Table 7.3. Butyric acid production from different lignocellulosic biomasses by mixed cultures.

Microorganism	Substrate	Mode	pH	T °C	Butyric acid				References
					Productivity (g/L/h)	Concentration (g/L)	Yield[a] (g/g)	Selectivity (%)	
Undefined Mixed Culture	Rice straw	Batch	6.0[b]	35	0.09	16.2	0.17	61	Ai el al., (2016)
C. thermocellum ATCC 27405 and *C. thermobutyricum* ATCC 49875	Delignified rice straw	Batch	6.5[b]	55	0.04	2.4	0.14	59	Chi et al., (2018)
Native mixed culture	Agave bagasse	Batch	6.5	37	0.01	1.4	0.07	30	Dudek et al., (2021)
Native mixed culture	Wheat straw	Batch	6.5	37	0.03	4.5	-	40	Pérez-Rangel et al., (2021)
Native mixed culture	Agave bagasse Sugarcane bagasse	Semi-cont.	6.5	37	0.03	4.3	-	25 30	Ayala-Campos et al., (2022)

[a] – Yield (g/g biomass fed). [b] – with pH control.

7.4.1   Type of substrate

So far, there are few publications that employed mixed cultures to produce BA from lignocellulosic biomass through CBP (Table 7.3). From them, Ai et al. (2014, 2016) used a delignified rice straw obtained by soaking the substrate in 1% NaOH, at 50°C for 72 h, which removed 66% of lignin, and retained 84% of cellulose and 71% of hemicellulose. The delignified rice straw allows the undefined mixed culture to produce 10 times more BA compared with the untreated rice straw. Lately, native microbiotas of lignocellulosic substrates have proved to produce high amounts of VFAs directly from untreated substrates (Dudek et al. 2020; Pérez-Rangel 2021; Ayala-Campos et al., 2022). These native microbiotas have hydrolyzed and fermented almost 50% of the hemicellulosic fraction of Agave bagasse (Dudek et al. 2020), and up to 60% of the hemicellulosic fraction of wheat straw, corn stover, Agave bagasse and sugarcane bagasse (Pérez-Rangel 2021; Ayala-Campos et al., 2022). These native microbiotas are specialists in consuming the hemicellulosic fraction leaving relatively unfermented the cellulosic fraction for further processing.

7.4.2 Cultivation pH

Reviewed literature shows that pH range between 6.0 and 7.2 is suitable for the optimal BA production from lignocellulose during mixed-culture fermentation (Table 7.3). Ai et al. (2014) evaluated the BA production from alkali pretreated rice straw by an undefined mixed culture at different pH values (5.0, 5.5, 6.0, 6.5, and 7.0). The highest BA concentration of 6.7 g/L was achieved at pH values between 6.0 to 6.5. Also, Chi et al. (2018) investigated the effects of four different pH values (5.5, 6.0, 6.5, and 7.0) on BA production by the thermophilic co-culture of *C. thermocellum* ATCC 27405 and *C. thermobutyricum* ATCC 49875. The pH 6.5 was found as the most suitable pH for BA production by this thermophilic co-culture. Ai et al. (2014) and Blanco et al. (2019) reported that the initial pH in the mixed-culture fermentations determines the metabolic pathways and the bacterial communities present in the system; therefore, its control is decisive to obtain the desired fermentation products.

7.4.3 Cultivation temperature

Most studies about BA production by mixed cultures reported mesophilic temperatures, particularly between 35 and 37 °C. Only Chi et al. (2018) reported a thermophilic co-culture incubated 55 °C for BA production (Table 7.3). So far, there are not enough information to conclude if the temperature affects the BA production. However, thermophilic temperatures increase the enzymatic hydrolytic of lignocellulosic substrates, therefore, it could be expected that BA production increase (Kozuchowska and Evison, 1995; Jiang et al., 2016).

7.5 Summary of single- and mixed-culture fermentations for BA production

Up to now, there are only a few research focused on BA production as the main product from lignocellulosic biomass (Thanakoses et al., 2003; Merklein et al., 2014; Ai et al., 2014; Dudek et al., 2021). Pure cultures achieve the highest concentrations at the level of 34.3 g/L (He et al., 2020) and 32.8 g/L (Suo et al., 2019), nonetheless only from hydrolysates. This implies the necessity of pretreatments which most of them release inhibitors (Xiao et al., 2018), having as a consequence the requirement of an additional stage, the detoxification stage.

These two steps require additional equipment made of durable and highly resistant to aggressive compounds materials, which may turn the process to be more expensive. In contrast, mixed cultures have been used to ferment lignocellulosic biomass directly, but the achieved concentrations have

not exceeded 7.6 g/L (Ai et al., 2014). However, mixed cultures have the advantage of performing a CBP, which, according to Lynd et al. (2005), could reduce the cost of production.

The first part of this paper presents a literature overview on BA production from lignocellulosic biomass during fermentation carried out by pure and mixed cultures. Against this background, the next part of this work presents a techno-economic evaluation of BA production using: (a) a pure culture where the substrate is pretreated with diluted acid; and (b) a mixed culture, where the substrate is directly fermented during CBP.

7.6   Techno-economic evaluation of BA production

The BA production from lignocellulosic biomass was modeled and evaluated by using SuperPro Designer v11.2 (SPD) (Intelligen, Inc., Scotch Plains, NJ, USA) in the two different configurations of plants (Figure 7.1): (a) a plant design based on a single-culture fermentation where the engineered *Clostridium tyrobutyricum* produced BA from an undetoxified lignocellulosic acid hydrolysate (Suo et al. 2019); and (b) a plant configuration based on a mixed-culture fermentation where a mixed culture produced BA from an untreated lignocellulosic substrate (Ai et al. 2016; Pérez-Rangel et al., 2021; Ayala-Campos et al., 2022).

7.6.1   Feedstock

The simulation of both types of plants considered a lignocellulosic feedstock model with 70 % of polysaccharides and the following composition: 40 % of cellulose, 30 % of hemicellulose, 20 % of lignin, and 10 % of ash in dry basis. This lignocellulosic feedstock model was based on the composition of corn residues whose worldwide production was about 360.25 million metric tons in 2020/2021 (Shahbandeh, 2021).

7.6.2   Description of plant configurations

7.6.6.1   BA plant based on single-culture fermentation

The BA plant based on a single-culture fermentation considered six main stages: *i)* feedstock conditioning; *ii)* acid pretreatment; *iii)* inoculum preparation; *iv)* fermentation; *v)* product purification; and *vi)* cogeneration of steam and power.

(a) In ton/day

Biomass **500.0**
   hemicellulose **165.3**
   cellulose **220.4**
   lignin **110.2**

biomass → Grinding

5544 water

H_2SO_4

Pretreatment

Seed reactor

glucose **24.3**
xylose **71.3**
water **4426.7**

water **3497.1**

glucose **24.3**
xylose **71.3**
water **929.7**

Centrifugation — supernatant → Evaporation — concentrated sugars → Fermentation → Downstream process → butyric acid **27.5**

hemicellulose **84.3**
cellulose **192.9**
lignin **110.2**
water **1106.7**

nutrients

air

solids → Co-generation

wastewater → butyric acid **3.2**
acetic acid **9.6**
water **231.5**

electricity

steam

(b) In ton/day

Biomass **500.0**
   hemicellulose **165.3**
   cellulose **220.4**
   lignin **110.2**

biomass → Grinding

water **2083.4**

4950 water → Consolidated bioprocessing

butyric acid **81.8**
acetic acid **18.7**
water **3454.2**

Centrifugation — supernatant → Downstream process → butyric acid **73.6**

hemicellulose **66.1**
cellulose **159.2**
lignin **110.2**
water **1480.4**

solids → Co-generation

air

wastewater → butyric acid **8.2**
acetic acid **18.7**
water **1370.8**

electricity

steam

Figure 7.1. Mass balance for the a) pure and b) mixed culture plants.

7.6.2.1.1 Feedstock conditioning

The lignocellulosic feedstock entered to a grinding system to reduce the particle size to 4 mm.

7.6.2.1.2 Pretreatment

The lignocellulosic feedstock was introduced into a blending storage system at a solid/liquid ratio of 1:11. Subsequently, the material was treated with 0.1 M H_2SO_4 at 121 °C for 30 min to convert 52.0 % of hemicellulose and 12.3 % of cellulose giving a concentration of 15.0 g/L and 5.1 g/L of xylose and glucose, respectively (Chen et al., 2017; Suo et al., 2019). Then, the slurry was conducted to a stirred reactor, cooled down and neutralized to pH 7.0 with 2M NaOH. Subsequently, the supernatant was obtained after the centrifugation stage and then concentrated to 90 g/L of total sugars using a Flash Drum (Suo et al., 2019). Finally, the concentrated hydrolysate was directed to the fermentation process. The solid part, which was composed mainly of lignin and unconverted cellulose and hemicellulose, was transferred to the cogeneration stage.

7.6.2.1.3 Inoculum preparation

The engineered *C. tyrobutyricum* ATCC 25755/*sdr+gro*ESL was employed as inoculum due to its resistance to furan derivatives and phenolic compounds (Suo et al., 2019). The microorganism was anaerobically cultivated at 37 °C in Clostridial Growth Medium (CGM) that contained (g/L): 50 glucose, 2 yeast extract, 4 tryptone, 2 $(NH_4)_2SO_4$, 1 $K_2HPO_4 \cdot 3H_2O$, 0.5 KH_2PO_4, 0.1 $MgSO_4$, 0.1 $MgSO_4 \cdot 7H_2O$, trace elements, and 30 µg/mL of thiamphenicol (Suo et al., 2017).

7.6.2.1.4 Fermentation

A CSTR fermentation reactor, which is made of sterilizable stainless steel, was inoculated with 5 % v/v and operated at 37 °C, 150 rpm, and a hydraulic retention time of 112 h. The hydrolysate was used without detoxification. The chemical reactions, stoichiometry and the conversion efficiencies were presented in the Table 7.4. Glucose and xylose were consumed simultaneously with an efficiency of 100 and 89 %, respectively resulting in a BA production of 32.8 g/L (Suo et al., 2019). Two streams left out from the reactor: *i)* fermentation gases, mainly CO_2 and H_2, and *ii)* the fermentation broth that was subjected to reverse electro enhanced dialysis (REED) with anion-exchange membrane and electrodialysis with bipolar membrane (EDBM), where the separation process occurred into two new streams: *iii)* the BA flow with a concentration of 110 g/L, which was sent to the purification stage; and *iv)* the effluent that contained byproducts and small quantities of unfermented monosaccharides.

13

Table 7.4. Stoichiometry and conversion efficiency assumed for the different plant models.

Reactions	Fraction (%) converted to products	
	Pure culture	Mixed culture
Pretreatment		
Cellulose + Water → 1.1 Glucose	12.3	27.8
Hemicellulose + Water → 1.32 Xylose	52.0	60.0
Fermentation		
Glucose → Butyric acid + 2 CO_2 + 2 H_2	20.6	95
1.2 Glucose → 2 Acetic acid + 2 CO_2 + 4 H_2	79.4	5
3 Xylose → 2.5 Butyric acid + 5 CO_2 + 5 H_2	89	80.8
3 Xylose → 5 Acetic acid + 3 CO_2 + 9 H_2	-	15.2

[a] – values represent the conversion of each compound set in the simulation program to obtain the products concentrations given by the authors.

7.6.2.1.5 Downstream process

The stream containing BA was introduced into mixer-settler extraction, where BA was extracted from water by 1-octanol. That organic solvent was used due to the high difference of partition co-efficient between BA and acetic acid, 6.17 and 0.68, respectively. Moreover, the solubility of 1-octanol in water and vice versa was 0.01 g/L (Baroi et al., 2017). Extracted BA was transferred to a distillation column containing 45 theoretical stages. The 1-octanol was recuperated and recycled for further liquid-liquid extraction. The lost part of organic solvent was supplemented according to a concentration sensor. The BA was purified to 99.8 %.

7.6.2.1.6 Co-generation stage

Steam and power were generated in the cogeneration stage by burning cellulose and lignin, which were introduced as a solid waste stream. The mass balance of the 500 ton/day plant capacity for the pure and mixed cultures was illustrated in the Figure 7.1. Generated steam had a temperature and pressure of 255 °C and 45 bar, respectively, and was partly used for the heat-exchange system. When the final temperature and pressure were 224 °C and 45 bar, respectively, the steam was conducted to a straight-flow steam turbine-generator to produce electricity.

7.6.6.2 BA plant based on mixed-culture fermentation

The BA plant based on mixed-culture fermentation involved four main stages: *i)* feedstock conditioning; *ii)* CBP; *iii)* downstream process; and *iv)* cogeneration stage.

7.6.2.2.1 Feedstock conditioning

This stage was performed by using the same process described in the Section 3.6.2.1.1.

7.6.2.2.2 Pretreatment

Mixed culture performed as a CBP, therefore the pretreatment stage as a separate unit was omitted in the simulation.

7.6.2.2.3 Inoculum preparation

The BA-producing mixed culture was derived from cattle manure, pig manure compost, corn field soil and rotten wood, and prepared according to Ai et al. (2016). The acclimation stage was skipped in the simulation.

7.6.2.2.4 CBP reactor

The CBP reactor was fed with untreated lignocellulosic feedstock with a total solid content of 10% w/v (Pérez-Rangel et al., 2021). The CBP reactor was an anaerobic digester made of concrete and operated at 37 °C with mechanical agitation with a hydraulic retention time of 168 h (Ayala-Campos et al., 2022). The mixed culture carried out the hemicellulose solubilization (60 % of conversion; Ayala-Campos et al., 2022) and the sugar fermentation to produce BA and acetic acid at the concentrations of 15.6 and 3.3 g/L, respectively (Table 7.4; Ai et al., 2016). Other VFAs were omitted in the simulation due to their low concentration. Two streams came out from the CBP reactor: *iii)* fermentation gases, mainly CO_2 and H_2, *iv)* the slurry fraction composed of fermentation broth, as well as a solid part, which was mainly consisted of cellulose, lignin, and hemicellulose residues. The stream *iv)* was centrifuged. The solid phase was sent to the cogeneration stage, while the liquid phase was directed to the membrane separation system with *in-situ* removal according to Baroi et al. (2017). Effluent was reacted with aqueous NaOH to remove organic acids from the broth, followed by REED with EDBM. The process separated the fermentation broth into two streams: *vi)* recovered BA and acetic acid with the efficiency of 90 and 91%, respectively, and *vii)* water with remaining compounds. The stream *vi)* was sent to the purification stage, while *vii)* being recycled into the CBP reactor.

7.6.2.2.5 Downstream process

This stage was performed as described in the Section 3.6.2.1.5.

7.6.2.2.6   Co-generation stage

This stage was performed as described in the Section 3.6.2.1.6.

7.6.3   Financial investment and assumptions

The Total Production Cost (TPC) of BA refers to the cost of raw materials, the purchase and the maintenance of the equipment needed for its processing, utilities, and the costs of human labor necessary to produce 1 kg of the final product. This variable is based on Dynamic Cash Flow Analysis (DCFA) which determines a working capital. In other words, the amount of money available to start-up a plant and complete its transactions. The DCFA evaluates if the enterprise will be able to pay its bills and generate enough cash to continue operating with profit. The DCFA uses calculations which based on the Net Present Value (NPV) method. The NPV determinates the current value of all future cash flows generated by the plants, including the initial capital investment. This methodology of economic evaluation was used by SuperPro Designer v11 and was extensively described by Sanchez et al. (2017).

Each plant configuration was operated for 330 days over a year considering three plant capacities: 100, 500, and 1000 ton/day. The construction of the plant and plant-life period were fixed at 2.5 and 15 years, respectively, with an interest rate of 7 % and equity of 70 % with the investor's back-payment starting in year 3, these economics parameters have been used typically in previous lignocellulosic plant (Sanchez et al., 2013). The interest rate indicates the costs of loans and should be carefully selected considering the financial security of the plant. An interest rate between 3 and 9 % is suggested according to previous studies related with biomass processing to make a plant profitable (González-Arias et al., 2022). Considering license for the patented strain application, the patents royalties were established as 5 % of the Gross Operating Cost (GOC) for the BA plant to employ the engineered strain. The federal taxes were fixed at 40 % of profit (Sanchez et al., 2013). The lignocellulosic feedstock price was fixed at US$ 65 per ton according to local agricultural selling prices. The reagent costs used for the formulation of the culture medium were considered for both BA plants as well (Alibaba.com, 2021a). The utility prices for electricity, low-pressure stream, high-pressure steam, and cooling water were US$ 0.1 per 0.1 kW-h, US$ 12 per 1 ton, US$ 20 per 1 ton, and US$ 0.05 per 1 ton, respectively, and their values were based on the rates of the Federal Electricity Commission of Mexico (Comisión Federal de Electricidad, 2020).

7.7 Results and discussion

7.7.1 Economic summary of plant with pure and mixed cultures

The economic analysis for BA production from lignocellulosic biomass using pure and mixed cultures at plant capacities of 100, 500, and 1000 tons/d was investigated. The resulting BA yields in the pure and mixed culture plants were 0.06 and 0.15 ton per ton of feedstock, respectively (Figure 7.1). In both simulations, the BA purity was 99.8 %. The Total Capital Investment (TCI) was 3.5 times lower for the mixed culture plant than for the pure culture one independently of the plant capacity (Table 7.5). The Operating Costs in the mixed culture plant decreased by 50, 57, and 62 % for plant capacities of 100, 500, and 1000 ton/day respectively, compared with the pure culture plant.

Moreover, the savings were two times higher for the pure culture plant compared to the mixed culture plant due to the power production in the cogeneration stage. The quantity of solids burned in both BA plants was similar (385 ton/d and 335 ton/d for the pure and mixed culture plants, respectively), however, the pure culture plant had a higher energy consumption. Consequently, the savings were higher.
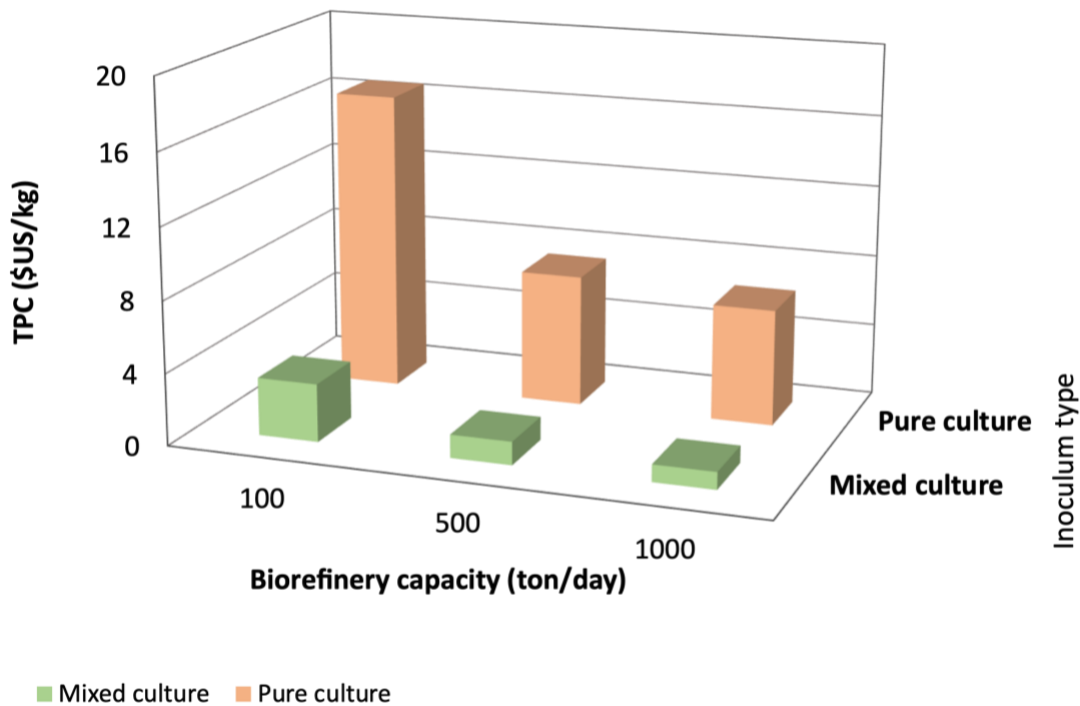
Figure 7.2. TPC of BA depending on the inoculum type and the plant capacity.

Table 7.5. Summary of the economic analysis and energy requirements for butyric acid production depending on inoculum type and plant capacity under the proposed plant models.

	Pure culture			Mixed culture			
Plant capacity (ton/day):	100	500	1000	100	500	1000	**Unit**
Total Capital Investment	61.6	188.7	340.2	17.8	61.9	98.6	million $
Operating Costs	30.4	81.7	145.2	15.4	35.0	55.5	million $/yr
Credits	1.7	8.7	17.3	0.8	4.0	7.9	million $/yr
Savings (due to Power Recycled)	1.2	6.5	12	0.4	2.5	5.4	million $/yr
Net Operating Cost	27.4	66.5	115.9	14.2	28.5	42.2	million $/yr
Cost Basis Annual Rate	1820	9077	17890	4423	22059	44108	tons MP/yr
Total Production Cost	16.7	9.0	8.1	3.5	1.6	1.3	$/kg MP
Efficiency (MP / feedstock)		5.4			13.4		
Power (electricity demand)	22,075	81,699	163,149	12,108	39,295	64,523	MW-h/yr
Net stream (high P) demand	253717	1268582	2537163	1943	9687	19360	tons/yr
Cooling Water	2176	9988	19118	170320	848754	1696492	tons/yr
Chilled Water	622502	3030968	5979087	666159	3327902	6654995	tons/yr
			Data for revenue of 2.9 US$				
Revenues	5.3	26.3	51.8	12.8			million $/yr
Gross Margin	-420	-153	-124	-11	55	67	%
Return On Investment	-27	-12	-10	1	43	61	%
Payback Time	N/A	N/A	N/A	160.92	2.32	1.64	years
IRR (After Taxes)	N/A	N/A	N/A	N/A	25.27	37.6	%
NPV (at 7.0% Interest)	-202.7	-452.2	-762.8	-27.6	72.9	213	million $/yr

MP - butyric acid as the main product; IRR - Internal Rate of Return; NPV - Net Present Value; N/A – not applicable.

The pure culture plant resulted in Total Production Costs of 15.1, 7.3, and 6.5 US$/kg for the plant capacities of 100, 500 and 1000 ton/day, respectively (Figure 7.2). In the case of the mixed culture plant, the Total Production Costs were 3.2, 1.3, and 0.9 US$/kg for the plant capacities of 100, 500 and 1000 ton/day, respectively. Current selling market price of BA varies between 1.8 and 2.9 US$ for industrial grade, and 3.2 US$ for food grade (Alibaba.com, 2021b). Considering these market prices, the mixed culture plants with capacities of 500 and 1000 ton/day were profitable. On the other hand, because of its purity > 99 %, the produced BA could be sold at the highest market price of 3.2 US$ per kg. Opposite, the pure culture plants resulted unprofitable.
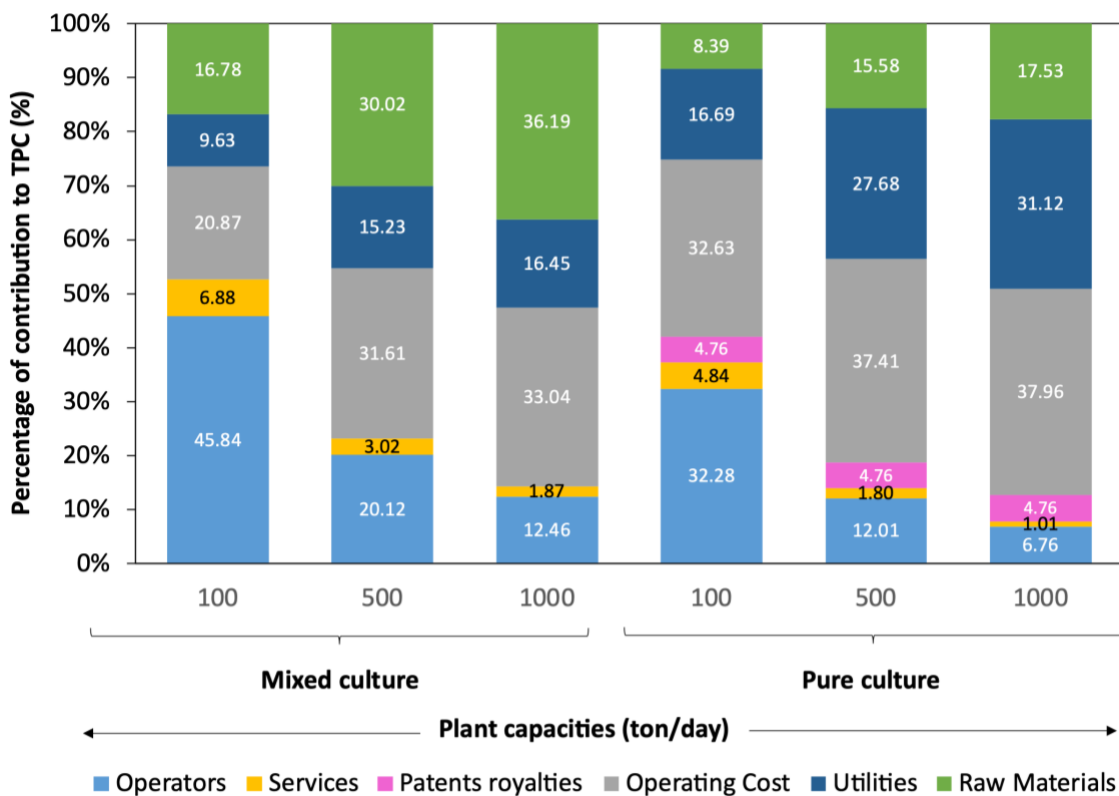
Figure 7.3. Distribution costs in the butyric acid production.

7.7.2   Distribution of operating costs

The distribution of total production costs (TPC) that includes operators, services, patents royalties, operating cost utilities, and raw material varied depending on the type of inoculum type and the plant capacity (Figure 7.3). The costs of raw materials were 16.8, 30.0, and 36.2 % for the mixed culture plant with capacities of 100, 500, and 1000 ton/day, respectively. In contrast, the same quantity of feedstock in the pure strain plant contributed to the total costs being two times less

expensive, due to an increase in the contribution of utilities. This happened because the pretreatment and inoculum preparation stages in the pure culture plant required five-times more energy input. For the largest plant capacity of 1000 ton/d, the differences in the operating cost parameters between both plants almost disappear. The operating costs in the pure culture plant were 1.5, 1.2, and 1.2 times higher for the plant capacities of 100, 500, and 1000 ton/day, respectively, compared with the mixed culture plants. These higher costs were due to a more expensive equipment, associated maintenance, and the need for more qualified personnel.
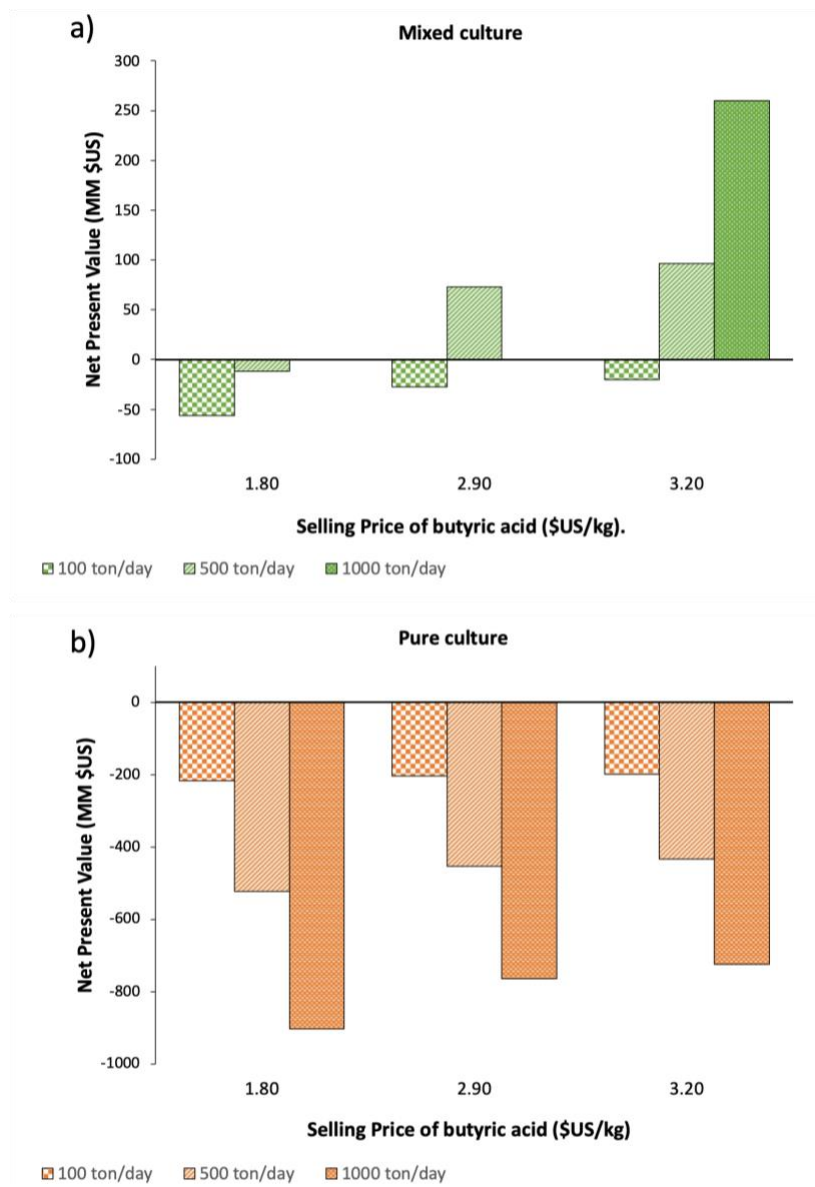
Figure 7.4. Effect of selling price of butyric acid on Net Present Value for different plant capacities. . (a) mixed culture and (b) pure culture.

In the case of the mixed culture plants, the lowest plant capacity of 100 ton/day resulted in debt regardless the selling price. For the middle capacity of 500 ton/day, the mixed culture plant was profitable for selling prices of 2.9 and 3.2 US$/kg. Whereas for the highest plant capacity of 1000 ton/day, NPV turned into a more positive result for selling prices ranging from 1.8, 2.9, to 3.2 US$/kg with values of 40, 213, and 260 million US$, respectively. Furthermore, the NPV increased by 81 % when the plant capacity increased from 100 to 500 ton/day, and by 18 % when the plant capacity increased from 500 to 1000 ton/day. In contrast, for the pure culture plant, the NPV presented a negative result for all the plant capacities and selling prices. In addition, its value became more unfavorable as the plant capacity increased. This phenomenon occurred because of the higher plant capacities which involved increments in the equipment costs that were much higher than the revenues.

7.7.3   Analysis of Total Production Cost using the Net Present Value (NPV)

The Net Present Value (NPV) was used to evaluate the profitability of both BA plants. NPV describes annual cash flow considering initial investment based on an interest rate and repayment period. A plant design is considered profitable when NPV > 0. On the contrary, when its value is < 0, the plant is not cost-effective. The NPV for both type of BA plants varied depending on the BA revenue (**Error! Reference source not found.**).

7.8   Discussion

In comparison with the mixed culture plant, the pure culture plant was unprofitable despite of obtaining a higher BA concentration in the fermentation stage. Higher TPCs resulted from the pretreatment and inoculum preparation stages that required more expensive equipment and higher energy inputs. These two stages demanded higher capital investments, for example, the pure culture plant of 1000 ton/day was 3.5 more expensive than the mixed culture plant. In contrast, the mixed culture plant resulted to be cost-effective, being able to compete with actual market prices of oil-derived BA. The TPCs of BA for the mixed culture plant were more than six times lower as compared with the pure culture plant. These results were possible because the CBP omitted the energy-demanding, expensive pretreatment stage, the pH neutralization stage that requires high amounts of bases, the inoculum preparation that requires very costly reagents, as well as the maintenance of sterile conditions. Moreover, the CBP reactor could be 7.5 times larger than the CSTR used for the pure culture fermentation. Additionally, it is worth noting that the CBP reactor

was made of concrete, which had a price 8 times lower than that of the stainless steel required that it required for the pure culture fermentation.

Baroi et al. (2017) carried out a techno-economic evaluation of BA production from wheat straw by a pure culture and a plant capacity of 30 ton/day. The Total Production Cost of BA was 2.75 $US/kg and 3.31 $US/kg for purities of 89 and 99 %, respectively. Baroi et al. (2017) reduced unit production cost by 16 % due to electricity and steam generation. Meanwhile in this study, cogeneration stage and heat exchange system, achieved to reduce unit production cost up to 60 %. Moreover, the lignocellulosic biomass cost per ton was 5-fold more expensive as compared to feed stock in the simulation performed by Baroi et al. (2017), what should be considerate as a significant impact on TPC. Likewise, Sanchez et al. (2013) performed simulation of ethanol production from lignocellulosic waste at different plant capacities and types of feedstocks. In that study, the enzymatic hydrolysis stage was the most expensive. The separation stage was much cheaper compared to the BA purification, because of the lower boiling point of ethanol than BA. That involves lower energy input in the purification step. Also, the authors indicated that the type of feedstock significantly impact TPC, because lignocellulosic biomass composition may increase TPC by up to 20%. According to Sanchez et al. (2013), the plant capacity of 300 and 600 ton/day were found as the most suitable plant size, owing to final unit production costs and a raw material demand. Similarly, Molina-Guerrero et al. (2021) carried out the economic analysis of butanol production from apple pomace by a mixed culture at different plant capacities. The results showed that CBP causes slowly TPC change for different plant configuration (between 140 to 153 Million$US) compared to standard fermentation by pure strain in CSTR (range from 193 to 1200 Million$US) for processing capacities of 2000 ton/day. That small costs differences were attributed to the less inversion to the reactor technology. Moreover, the CBP reduced the TPCs and operating costs since the hydrolysis and fermentation stages occurred simultaneously.

Nevertheless, the published literature on which this paper was based on provided fermentation results at the laboratory scale only. It is mandatory to investigate and collect data about the performance and stability of mixed cultures in larger CBP reactors. In addition, the BA plants described in this study did not consider the influence of the plant location and biomass supply on the TPCs. Providing biomass to the BA plant is certainly significant that since high amounts of lignocellulosic biomass are required for daily processing (between 500 and 1000 ton/day), the

pathway to build a biorefinery could be long and requires a significant amount of complementary simulation and experimental research.

7.9 Conclusions

The impact of inoculum type on the profitability of BA production from lignocellulose was evaluated at three plant capacities (100, 500 and 1000 ton/day). Results showed that only the mixed culture plant was profitable at plant capacities higher than 500 ton/day and a BA spelling price not lower than $US 2/kg. Despite of having a better performance in fermentation, the pure culture plant was unprofitable due to expensive construction materials, the fact that high number of reactors were required in the fermentation stage and high operating costs and energy consumption in the pretreatment and sugar concentration stages. Increasing the plant capacity had a positive effect on revenues and profits only for the mixed culture plant.

In the present study, the simulation of the mixed culture plant considered a high BA selectivity of 80%. However, past studies indicate that the BA selectivity in mixed cultures is easily affected by the operating conditions, for instance, pH and the total solid content. Therefore, future simulation studies could conduct a sensitivity analysis to estimate how BA selectivity affects the TPC. For the pure culture plant, future simulation studies should focus on reducing the energy requirements, mainly in the pretreatment stage. In this study, the pretreatment was carried out at 121 °C for 30 min. Hence, it would be interesting to simulate how pretreatments that work at lower temperatures (but with comparable efficiency) affect the plant profitability. An engrossing scenario for the pure culture plant and reducing its energy requirements would be to omit the stage of sugar concentration and determine its effect on the TPC. Another direction for future simulation studies is how to replace expensive culture media that contain salts like potassium phosphate or nitrogen sources like yeast extract, with inexpensive compounds, for instance, agro-industrial residues. The use of co-substrates could reduce the TPC.

7.10 References

Aftab, M. N., Iqbal, I., Riaz, F., Karadag, A., Tabatabaei, M. (2018). Biomass for Bioenergy - Recent Trends and Future Challenges: Different Pretreatment Methods of Lignocellulosic Biomass for Use in Biofuel Production. http://dx.doi.org/10.5772/intechopen.84995

Ai, B., Chi, X., Meng, J., Sheng, Z., Zheng, L., Zheng, X., Li, J. (2016). Consolidated bioprocessing for butyric acid production from rice straw with undefined mixed culture. Frontiers in Microbiology, 7, 1648. http://dx.doi.org/10.3389/fmicb.2016.01648

Ai, B., Li, J., Chi, X., Meng, J., Jha, A. K., Liu, C., Shi, E. (2014). Effect of pH and buffer on butyric acid production and microbial community characteristics in bioconversion of rice straw with undefined mixed culture. Biotechnology and Bioprocess Engineering: BBE, 19(4), 676-686. http://dx.doi.org/10.1007/s12257-013-0655-z

Akinosho, H., Yee, K., Close, D., Ragauskas, A. (2014). The emergence of Clostridium thermocellum as a high utility candidate for consolidated bioprocessing applications. Frontiers in Chemistry, 2, 66. http://dx.doi.org/10.3389/fchem.2014.00066

Alibaba.com (2021a). Accessed 12 March 2021. https://www.alibaba.com/

Alibaba.com (2021b). Looked for: "butyric acid", "industrial grade", "food grade". Accessed 15 March 2021. https://www.alibaba.com/

Anwar, Z., Gulfraz, M., Irshad, M. (2014). Agro-industrial lignocellulosic biomass a key to unlock the future bio-energy: A brief review. Journal of Radiation Research and Applied Sciences, 7(2), 163-173. http://dx.doi.org/10.1016/j.jrras.2014.02.003

Ayala-Campos, O.R., Sanchez, A., Rebollar, E.A., Valdez-Vazquez, I. (2022). Plant-associated microbial communities converge in fermentative hydrogen production and form a core microbiome. International Journal of Hydrogen Energy. In press.

Baroi, G.H., Westermann, P., Skiadas, I. (2017). Fermentative production of butyric acid from wheat straw: Economic evaluation. Industrial Crops and Products, 104, 68–80. https://doi.org/10.1016/j.indcrop.2017.04.008

Baroi, G.H. (2015). Butyric acid fermentation from pretreated and hydrolysed wheat straw by an adapted Clostridium tyrobutyricum strain. Microb Biotechnol 8(5):874-82

Blanco, V.M.C, Oliveira, G.H.D, Zaiat, M. (2019). Dark fermentative biohydrogen production from synthetic cheese whey in an anaerobic structured-bed reactor: Performance evaluation and kinetic modeling. Renewable Energy, 139, 1310-1319. http://dx.doi.org/10.1016/j.renene.2019.03.029

Brenner, K., You, L., Arnold, F.H. (2008). Engineering microbial consortia: a new frontier in synthetic biology. Trends in Biotechnology, 26, 483-489. http://dx.doi.org/10.1016/j.tibtech.2008.05.004

Canani, R. B., Costanzo, M. D., Leone, L., Pedata, M., Meli, R., Calignano, A. (2011). Potential beneficial effects of butyrate in intestinal and extraintestinal diseases. World Journal of Gastroenterology, 17(12), 1519-1528. http://dx.doi.org/10.3748/wjg.v17.i12

Cantarella, M., Cantarella, L., Gallifuoco, A., Spera, A., Alfani, F. (2004). Comparison of different detoxification methods for steam-exploded poplar wood as a substrate for the bioproduction of ethanol in SHF and SSF. Process Biochemistry, 39(11), 1533-1542. http://dx.doi.org/10.1016/S0032-9592(03)00285-1

Chong, M., Rahman, N. A., Yee, P. L., Aziz, S. A., Rahim, R. A., Shirai, Y., Hassan, M. A. (2009). Effects of pH, glucose and iron sulfate concentration on the yield of biohydrogen by Clostridium butyricum EB6. International Journal of Hydrogen Energy, 34(21), 8859-8865. http://dx.doi.org/10.1016/j.ijhydene.2009.08.061

Comisión Federal de Electricidad (2020). In: https://app.cfe.mx/Aplicaciones/CCFE/Tarifas/TarifasCREIndustria/Tarifas/DemandaIndustrialTran.aspx

Chandel, A., Silva, S., Singh, O. (2013). Detoxification of lignocellulose hydrolysates: biochemical and metabolic engineering toward white biotechnology. Bioenergy Research 6, 388–401. https://doi.org/10.1007/s12155-012-9241-z

Chen, C. K., Blaschek, H. P. (1999). Effect of acetate on molecular and physiological aspects of Clostridium beijerinckii NCIMB 8052 solvent production and strain degeneration. Applied and Environmental Microbiology, 65(2), 499-505. http://dx.doi.org/10.1128/AEM.65.2.499-505.1999

Chen, T., Zhang, L., Luo, G., Yuan, W. (2017). Butyric acid production by Clostridium tyrobutyricum in Sugar Mixtures and Corncob Hydrolysate Containing Arabinose. BioResources 12(4), 7931-7942

Chi, X., Li, J., Antwi, P., Wang, X., Zhang, Y. (2018). Hyper-production of butyric acid from delignified rice straw by a novel consolidated bioprocess. Bioresource Technology, 254, 115-120. http://dx.doi.org/10.1016/j.biortech.2018.01.042

Chung, D., Verbeke, T. J., Cross, K. L., Westpheling, J., Elkins, J. G. (2015). Expression of a heat-stable NADPH-dependent alcohol dehydrogenase in Caldicellulosiruptor bescii results in furan aldehyde detoxification. Biotechnology for Biofuels, 8, 102. http://dx.doi.org/10.1186/s13068-015-0287-y

Drahokoupil M, Patáková P. (2020). Production of butyric acid at constant pH by a solventogenic strain of Clostridium beijerinckii. Czech J. Food Sci., 38: 185-191. https://doi.org/10.17221/95/2020-CJFS

Dahmen, N., Lewandowski, I., Zibek, S., Weidtmann, A. (2019). Integrated lignocellulosic value chains in a growing bioeconomy: Status quo and perspectives. Global Change Biology.Bioenergy, 11(1), 107-117. http://dx.doi.org/10.1111/gcbb.12586

Data Bridge Market Research, (2020). Global Butyric Acid Market – Industry Trends and Forecast to 2027. https://www.databridgemarketresearch.com/reports/global-butyric-acid-market

Duarte, J. C., Rodrigues, J. A., Moran, P. J. S., Valenca, G. P., Nunhez, J. R. (2013). Effect of immobilized cells in calcium alginate beads in alcoholic fermentation. AMB Express, 3(1), 1-8. http://dx.doi.org/10.1186/2191-0855-3-31

Dudek, K., Buitrón, G., Valdez-Vazquez, I. (2021). Nutrient influence on acidogenesis and native microbial community of Agave bagasse. Industrial Crops and Products, 170, 113751. https://dx.doi.org/10.1016/j.indcrop.2021.113751

Dwidar, M., Lee, S., Mitchell, R. J. (2012). The production of biofuels from carbonated beverages. Applied Energy, 100, 47-51. https://dx.doi.org/10.1016/j.apenergy.2012.02.054

Fu, H., Yang, S.T., Wang, M., Wang, J., Tang, I.C. (2017). Butyric acid production from lignocellulosic biomass hydrolysates by engineered Clostridium tyrobutyricum

overexpressing xylose catabolism genes for glucose and xylose co-utilization. Bioresource Technology, 234, 389-396. https://doi.org/10.1016/j.biortech.2017.03.073

González-Arias, J., Sánchez, M. E., Cara-Jiménez, J. (2022). Profitability analysis of thermochemical processes for biomass-waste valorization: A comparison of dry vs wet treatments. Science of the Total Environment, 811 http://dx.doi.org/10.1016/j.scitotenv.2021.152240

He, F., Qin, S., Yang, Z., Bai, X., Suo, Y., Wang, J. (2020). Butyric acid production from spent coffee grounds by engineered Clostridium tyrobutyricum overexpressing galactose catabolism genes. Bioresource Technology, 304, 122977. http://dx.doi.org/10.1016/j.biortech.2020.122977

Hernández, C., Escamilla-Alvarado, C., Sánchez, A., Alarcón, E., Ziarelli, F., Musule, R., Valdez-Vazquez, I. (2019). Wheat straw, corn stover, sugarcane, and Agave biomasses: Chemical properties, availability, and cellulosic-bioethanol production potential in Mexico. Biofuels, Bioproducts & Biorefining, 13(5), 1143-1159. https://dx.doi.org/10.1002/bbb.2017

Huang, J., Zhu, H., Tang, W., Wang, P., Yang, S. (2016). Butyric acid production from oilseed rape straw by Clostridium tyrobutyricum immobilized in a fibrous bed bioreactor. Process Biochemistry (1991), 51(12), 1930-1934. http://dx.doi.org/10.1016/j.procbio.2016.08.019

Jiang, L., Wang, J., Liang, S., Cai, J., Xu, Z., Cen, P., Yang, S., Li, S. (2011). Enhanced butyric acid tolerance and bioproduction by Clostridium tyrobutyricum immobilized in a fibrous bed bioreactor. Biotechnology and Bioengineering, 108(1), 31-40. http://dx.doi.org/10.1002/bit.22927

Jiang, W., Xu, J. (2016). A novel stepwise pretreatment on corn stalk by alkali deacetylation and liquid hot water for enhancing enzymatic hydrolysis and energy utilization efficiency. Bioresource Technology, 209, 115-124. http://dx.doi.org/10.1016/j.biortech.2016.02.111

Jonsson, L. J., Alriksson, B., Nilvebrant, N. (2013). Bioconversion of lignocellulose: Inhibitors and detoxification. Biotechnology for Biofuels, 6(1), 16. http://dx.doi.org/10.1186/1754-6834-6-16

Kim, D. (2018). Physico-chemical conversion of lignocellulose: Inhibitor effects and detoxification strategies: A mini review. Molecules (Basel, Switzerland), 23(2). http://dx.doi.org/10.3390/molecules23020309

Kim, S., Groom, J., Chung, D., Elkins, J., Westpheling, J. (2017). Expression of a heat-stable NADPH-dependent alcohol dehydrogenase from Thermoanaerobacter pseudethanolicus 39E in Clostridium thermocellum 1313 results in increased hydroxymethylfurfural resistance. Biotechnology for Biofuels, 10. http://dx.doi.org/10.1186/s13068-017-0750-z

Kim, M., Han, M. W., Ki-Yeon, K., Lee, K. M., Min-Kyu Oh, Youn, S. H., Lee, S., Um, Y. (2016). Butyric acid production from softwood hydrolysate by acetate-consuming Clostridium sp. S1 with high butyric acid yield and selectivity. Bioresource Technology, 218, 1208-1214. http://dx.doi.org/10.1016/j.biortech.2016.07.073

Kozuchowska, J., Evison, L. M. (1995). VFA production in pre-acidification systems without pH control. Environmental Technology, 16(7), 667-675

Lee, K. M., Han, M. W., Ki-Yeon, K., Min, K., Choi, O., Han, S. O., Kim, Y., Um, Y. (2015). Electrochemical detoxification of phenolic compounds in lignocellulosic hydrolysate for clostridium fermentation. Bioresource Technology, 187, 228-234. http://dx.doi.org/10.1016/j.biortech.2015.03.129

Liu, Y., Geng, Y., Zhou, Q., Yuan, W. (2017). The effect of furfural and 5-hydroxymethyl furfural on butyric acid fermentation by Clostridium tyrobutyricum. Journal of Chemical Technology and Biotechnology 1986, 93(3), 849-854. http://dx.doi.org/10.1002/jctb.5439

Luo, H., Yang, R., Zhao, Y., Wang, Z., Liu, Z., Huang, M., Zeng, Q. (2018). Recent advances and strategies in process and strain engineering for the production of butyric acid by microbial fermentation. Bioresource Technology, 253, 343-354. http://dx.doi.org/10.1016/j.biortech.2018.01.007

Lynd, L. R., van Zyl, W.,H., McBride, J. E., Laser, M. (2005). Consolidated bioprocessing of cellulosic biomass: An update. Current Opinion in Biotechnology, 16(5), 577-583. http://doi.org/10.1016/j.copbio.2005.08.009

Magalhães, A. I., Jr, de Carvalho, J. C., Gilberto Vinícius de, M. P., Karp, S. G., Marcela Candido Câmara, Coral Medina, J. D., Soccol, C. R. (2019). Lignocellulosic biomass from agro-

industrial residues in South America: Current developments and perspectives. Biofuels, Bioproducts & Biorefining, 13(6), 1505-1519. http://dx.doi.org/10.1002/bbb.2048

Maiti, S., Buelna, G., Gallastegui, G., Verma, M., Drogui, P., Brar, S. K., Sarma, S.J. Bihan, Y. L. (2016). A re-look at the biochemical strategies to enhance butanol production. Biomass and Bioenergy, 94, 187-200. http://dx.doi.org/10.1016/j.biombioe.2016.09.001

Merklein, K., Fong, S. S., Deng, Y. (2014). Production of butyric acid by a cellulolytic Actinobacterium thermobifida fusca on cellulose. Biochemical Engineering Journal, 90, 239-244. http://dx.doi.org/10.1016/j.bej.2014.06.012

Michel-Savin, D., Marchal, R., Vandecasteele, J. P. (1990a). Control of the selectivity of butyric acid production and improvement of fermentation performance with Clostridium tyrobutyricum. Applied Microbiology and Biotechnology, 32(4), 387-392

Michel-Savin, D., Marchal, R.,Vandecasteele, J. P. (1990b). Butyrate production in continuous culture of Clostridium tyrobutyricum : Effect of end-product inhibition. Applied Microbiology and Biotechnology, 33(2), 127-131

Molina-Guerrero, C.E., Valdez-Vazquez, I., Macías-Mora, M., León-Pérez, K., Ibarra-Sánchez, J., Alcántara-Avila, J. (2021). Development of a bidimensional analysis approach for n–butanol and electricity production in apple pomace biorefineries in a Mexican context. Biomass Conversion and Biorefinery. https://doi.org/10.1007/s13399-021-01472-3

Monnappa, A.K., Lee, S., Mitchell, R.J. (2013). Sensing of plant hydrolysate-related phenolics with an aaeXAB::luxCDABE bioreporter strain of Escherichia coli. Bioresource Technology 127, 429–434. https://doi.org/10.1016/j.biortech.2012.09.086

Pérez-Rangel, M., Barboza-Corona, J., Navarro-Díaz, M., Escalante, A., Valdez-Vazquez, I. (2021). The duo Clostridium and Lactobacillus linked to hydrogen production from a lignocellulosic substrate. Water Science and Technology, 83(12), 3033-3040. http://dx.doi.org/10.2166/wst.2021.186

Ruusunen, M., Surakka, A., Korkeala, H., Lindström, M. (2012). Clostridium tyrobutyricum strains show wide variation in growth at different NaCl, pH, and temperature conditions. Journal of Food Protection, 75(10), 1791-1795. http://dx.doi.org/10.4315/0362-028X.JFP-12-109

Sanchez A, Sevilla-Güitrón V, Magaña G, Gutierrez L. (2013). Parametric analysis of total costs and energy efficiency of 2G enzymatic ethanol production. Fuel, 113, 165-179. http://dx.doi.org/10.1016/j.fuel.2013.05.034

Sanchez, A., Soto, A., Tavarez, D., Valdez-Vazquez, I., Sánchez, S. (2017). Lignocellulosic n-butanol co-production in an advanced biorefinery using mixed cultures. Biomass and Bioenergy, 102, 1-12. https://dx.doi.org/10.1016/j.biombioe.2017.03.023

Shahbandeh, M. (2021). Corn production worldwide 2020/2021, by country. The Statistics Portal. Revied July 27, 2021. https://www.statista.com/statistics/254292/global-corn-production-by-country

Suo, Y., Liao, Z., Qu, C., Fu, H., Wang, J. (2019). Metabolic engineering of Clostridium tyrobutyricum for enhanced butyric acid production from undetoxified corncob acid hydrolysate. Bioresource Technology, 271, 266-273. http://dx.doi.org/10.1016/j.biortech.2018.09.095

Suo, Y., Luo, S., Zhang, Y., Liao, Z., Wang, J. (2017). Enhanced butyric acid tolerance and production by class I heat shock protein-overproducing Clostridium tyrobutyricum ATCC 25755. Journal of Industrial Microbiology and Biotechnology, 44(8), 1145-1156. https://dx.doi.org/10.1007/s10295-017-1939-7

Suo, Y., Ren, M., Yang, X., Liao, Z., Fu, H., Wang, J. (2018). Metabolic engineering of Clostridium tyrobutyricum for enhanced butyric acid production with high butyrate/acetate ratio. Applied Microbiology and Biotechnology, 102(10), 4511-4522. http://dx.doi.org/10.1007/s00253-018-8954-0

Tajarudin, H., Zacharof, M., Ratanapongleka, K., Williams, P., Lovitt, R. (2018). Intensive Production of Carboxylic Acids Using C. butyricum in a Membrane Bioreactor (MBR). Fermentation (Basel), 4(4), 81. http://dx.doi.org/10.3390/fermentation4040081

Tayyab, M. (2018). Bioethanol production from lignocellulosic biomass by environment-friendly pretreatment methods: A review. Applied Ecology and Environmental Research, 16(1), 225-249. http://dx.doi.org/10.15666/aeer/1601_225249

Thanakoses, P., Mostafa, N. A., Holtzapple, M. T. (2003). Conversion of sugarcane bagasse to carboxylic acids using a mixed culture of mesophilic microorganisms. Applied Biochemistry and Biotechnology, 105 -108, 523-546. http://doi.org/10.1385/ABAB:107:1-3:523

Wainaina, St., Lukitawesa, K. A., Mukesh, T., Mohammad J. (2019). Bioengineering of anaerobic digestion for volatile fatty acids, hydrogen or methane production: A critical review. Bioengineered, 10(1), 437-458. http://dx.doi.org/10.1080/21655979.2019.1673937

Wang, J., Lin, M., Xu, M., Yang, S. (2016). Anaerobic fermentation for production of carboxylic acids as bulk chemicals from renewable biomass. Advances in Biochemical Engineering/Biotechnology, 156, 323-361. http://dx.doi.org/10.1007/10_2015_5009

Willey, J. (2017). Prescott's Microbiology. Columbus: McGraw-Hill US Higher Ed USE. ISBN13: 9781259281594

Wang, X., Yomano, L. P., Lee, J. Y., York, S. W., Zheng, H., Mullinnix, M. T., Shanmugam, K. T., Ingram, L. O. (2013). Engineering furfural tolerance in Escherichia coli improves the fermentation of lignocellulosic sugars into renewable chemicals. Proceedings of the National Academy of Sciences of the United States of America, 110(10), 4021-4026. http://dx.doi.org/10.1073/pnas.1217958110

Xiao, Z., Chu, C., Bao, T., Liu, L., Wang, B., Tao, W., Pei, X., Yang, S., Wang, M. (2018). Production of butyric acid from acid hydrolysate of corn husk in fermentation by Clostridium tyrobutyricum: kinetics and process economic analysis. Biotechnology for Biofuels, 11 http://dx.doi.org/10.1186/s13068-018-1165-1

Zhang, C., Yang, H., Yang, F., Ma, Y. (2009). Current progress on butyric acid production by fermentation. Current Microbiology, 59(6), 656-663. http://dx.doi.org/10.1007/s00284-009-9491-y

Zigova, J., Sturdik, E., Vandak, D., Schlosser, S. (1999). Butyric acid production by Clostridium butyricum with integrated extraction and pertraction. Process Biochemistry, 34(8), 835-843. http://dx.doi.org/10.1016/S0032-9592(99)00007-2

Zhu, Y., Yang, S. (2003). Adaptation of Clostridium tyrobutyricum for enhanced tolerance to butyric acid in a fibrous-bed bioreactor. Biotechnology Progress, 19(2), 365-372. http://dx.doi.org/10.1021/bp025647x

Zhu, Y., Yang, S. (2004). Effect of pH on metabolic pathway shift in fermentation of xylose by Clostridium tyrobutyricum. Journal of Biotechnology, 110(2), 143-157. http://dx.doi.org/10.1016/j.jbiotec.2004.02.006

8. Chapter VIII: Optimalization model for strategic location of the biorefinery for biobutanol production from lignocellulosic biomass in Mexico

Reference to submitted work:

Dudek, K., Rahmani, K., Aghamohamadi, S., Valdez-Vazquez, I., Sowlati, T. (2023). Optimalization model for strategic location of lignocellulosic biorefinery for biobutanol production in Mexico. *Computers and Chemical Engineering*.

8.1 Abstract

Biobutanol is one of the most desirable biofuels because of its high energy density, ability to be blended with gasoline up to 16% by volume, and can be produced from lignocellulosic biomass during acetone-ethanol-butanol (ABE) fermentation. The obtained biobutanol concentration at a level of 23 g/L on the laboratory scale has sparked interest in the techno-economic evaluation of the process on an industrial scale to determine its cost-effectiveness. This study aimed to carry out a techno-economic assessment and develop a mathematical model to find the optimal strategic location of biorefinery plants for the production of biobutanol from agave bagasse, corn stover, sugarcane bagasse, and wheat straw in Mexico, taking into account the supply chain and demand for biobutanol by PEMEX.

The simulated innovative biorefinery scheme for biobutanol production from lignocellulosic biomass resulted in positive net present value (NPV) for all studied crops and plant capacities. The techno-economic assessment of the biorefineries gave the highest total production cost (TPC) of 1.93 $US/kg for wheat straw and plant capacity of 500 tonne/d due to the highest biomass purchase cost (US$ 60) compared to the other biomass (US$ 40-50). The lowest TPC ($US 1.50) was obtained for corn stover and sugarcane bagasse at a plant capacity of 2400 tonne/d. The mathematical optimization model developed suggested setting up biorefineries at a plant capacity of 2400 tonne/d in 13 locations out of 34 considered to meet PEMEX's total butanol demand (118,793 tonne/year). The required initial investments to cover the establishment costs were $US 5,636,663,000, resulting in a positive NPV of $US 3,350,387,969.

Keywords: economic feasibility; goal programming; lignocellulosic biomass; optimalization; supply chain;

8.2   Introduction

Carbon dioxide is the most important greenhouse gas (GHG) affecting long-term climate change due to its properties of absorbing the sun's rays and radiating heat (Manabe, 2019). According to the IEA (2022), nearly 89% of total CO_2 released to the atmosphere in 2021 came from fossil fuels combustion and industrial process. Based on the IPCC WG1 AR6 assessment (*Climate Change 2021: The Physical Science Basis*, 2021), the global warming increased around 1.2 °C by 2020 compared to the Earth's temperature in the 1850-1900 period (Meinshausen et al., 2022). In addition, increasing dioxide carbon concentration decreases the pH of the earth's waters impacting stratification and currents, affecting sea ice, ice shelves, marine ecosystems, as well as plays a role in sea level changes (Garcia-Soto et al., 2021). From 1770 to 2000, the pH of the oceans dropped from 8.2 to 8.1 (Jiang et al., 2019) and scientific forecasts predict the pH of the oceans at 7.7 by 2100 if carbon dioxide is released at current levels (Findlay & Turley, 2021). Therefore, it is necessary to take measures to reduce CO_2 emissions. As of October 2022, around 140 countries have committed to achieving carbon neutrality by 2050 (Zerotracker, 2022). Therefore, scientists and private institutes make efforts to solve the climate crisis in many ways. Amid sustainable transition, bioenergy production has drawn much attention as it plays a key role in climate change mitigation and environment protection (Seo et al., 2022). Lignocellulosic biomass is one of the most promising sources for biofuels production, thereby fossil fuel replacement, due to its consistency, high availability, and low costs (Clauser et al., 2021). Its annual global production is estimated at 181.5 billion tonnenes (Ashokkumar et al., 2022). Currently, only 0.045% of this amount is used mainly for composting, and recently it has been gaining popularity as a feedstock for bioenergy production (Singh et al., 2022). Butanol is one of the biofuels of high interest because of its favorable thermodynamic properties compared to ethanol (Iliev, 2021), such as higher energy density (19.5 vs 29.2 MJ/L)(Xue & Cheng, 2019), lower Reid vapor pressure (16 vs 5 kPa) (Andersen et al., 2010), which means lower volatility and evaporative emissions. Butanol can be mixed with gasoline up to 16% by volume (Green, 2011; Lapuerta et al., 2018). In addition, its blends reduce particulate emissions by up to 58% when blended with diesel-butanol in a 10:1 ratio (Tipanluisa et al., 2022). According to a research study published by Fernández (2022) the global market for butanol is estimated to increase from 5.4 million tonnes in 2022 to about 6.7 million tonnes by 2029.

Butanol is produced commercially from fossil fuels (Kolesinska et al., 2019). Given the environmental impact of petroleum products, the production of biobutanol (due to its biological origin) from lignocellulosic biomass by acetate-ethanol-butanol (ABE) fermentation, has become an attractive alternative (Mondal et al., 2022; Rezaei et al., 2021; Sanchez et al., 2017; Tri & Kamei, 2020). Advances in converting cellulose into biobutanol by divers' bacteria during ABE fermentation (Mahalingam et al., 2022; Veza et al., 2021) or consolidated bioprocessing (CBP) (Olguin-Maciel et al., 2020; Zhao et al., 2019) are leading to increasing yields, up to 14.2 g/L of cellulosic biobutanol produced from steam-explosion pretreated corn stover by synthetic consortium of *Clostridium sp.* (Valdez-Vazquez et al., 2015). This, in turn, spark interest in techno-economic evaluation of the process on an industrial scale to determine its profitability.

Most papers on the economic evaluation of biobutanol plants from lignocellulosic waste uses concentrated or diluted acid for feedstock pretreatment . It involves the purchase of more expensive reactors because of the acid-resistant materials. Moreover, the ABE fermentation was carried out by pure culture or co-fermenting bacteria, what required handling of inoculum growth, reactors sterilization and cleaning-in-place, which incurred additional operating costs. So far, there are few publications related to biobutanol production from cellulosic part of lignocellulosic biomass during CBP by mixed culture, where at least two microorganisms combine cellulolytic and solventogenic activities making possible to deploy the cellulose polymer into glucose and convert it into biobutanol at the same site (Sanchez et al., 2017; Valdez-Vazquez & Sanchez, 2018). In such cases, the researchers used co-cultures to create synthetic mixed culture composed of *Clostridium beijerinckii* and *Clostridium cellulovorans* (Valdez-Vazquez et al., 2015; Wen et al., 2014b, 2017) or *Clostridium beijerinckii* and *Clostridium thermocellum* (Wen et al., 2014a), reaching between 8.3 and 14.2 g/L of cellulosic biobutanol from lignocellulosic biomass. In contrast to aforementioned works, González-Tenorio and Valdez-Vazquez (2023) carried out laboratory adaptative evolution and isolated butanol-tolerant mixed culture from native microbiota of corn stover capable to produced up to 13.6 g/L of biobutanol. In the present study, corn stover waste was first subjected to a biological pretreatment according to Dudek et al. (2021), in which the hemicellulose was converted to VFAs and hydrogen, while the cellulose polymer remained available. The isolated butanol-tolerant mixed culture by González-Tenorio and Valdez-Vazquez (2023), then was used for cellulosic biobutanol production from obtained solids parts reaching its

concentration at a level of 23 g/L (Dudek et al., 2022). The used culture also produced valeric and caproic acids at 11.02 and 7.07 g/L, respectively.

Usually, the techno-economic reports of lignocellulosic butanol production are incomplete, which does not allow a project to be implemented. These reports did not contain information on where to open a plant due to the availability of feedstock, whether the cost of supply chain does not unduly increase the price, making the plant unprofitable. It is also rare to present the market for the produced bioproduct.

The literature includes 95 published papers between 2009 and 2021 on strategic decision-making regarding biorefinery location. The papers studied the choice of biomass type and cultivation area, selection of location, capacity, technology, and number of facilities. Most of the works only assesses the strategic location of the facility and capacity (Chávez et al., 2018; Galanopoulos et al., 2020; Ganev et al., 2021; Jonker et al., 2016; Park et al., 2019), some of them additionally considers a technology selection (Gilani & Sahebi, 2021; Heidari et al., 2019; Kang et al., 2020; Murele et al., 2020) or biomass type (Fattahi et al., 2021; Fattahi & Govindan, 2018; Gao et al., 2019; Saghaei et al., 2020). Barely a few papers consider the biomass cultivation area. Furthermore, in most cases they are presented as lands rather than specific biomass collection points, which does not allow the calculation of the exact distance from the biomass supplier to the facility. In our work the real biomass supplier's geographical location has been taken into account. In addition, the paper presents the availability of biomass in Mexico taking into account the standard deviation of the biomass variation over 17 the years for corn stover, wheat straw and agave bagasse and a 10-year period for sugarcane bagasse.

A GIS is a valuable analytical tool for collecting and storing data related to positions on Earth´s surface. The system helps manage, analyze, and display geographical data making better understand of spatial patterns and relationships. It can be integrated with mathematical modeling for process optimalization and decision making (Chang, 2017). Only 6 out of 95 articles applied GIS to identify and assess candidate sites for the facility location of the entities in the biomass supply chain . None of the publications included all four selection criteria in the optimization model: type of biomass, biomass suppliers' location, facility location and capacity. Moreover, according to our best knowledge this paper as a first one performed strategic decision-making for

location of biorefinery producing biobutanol from lignocellulosic biomass without using hazardous chemicals or physico-chemical pretreatment.

The aim of this study was to develop a mathematical optimalization model in terms of NPV for strategic location of innovative biorefinery plants producing lignocellulosic biobutanol for study case in Mexico. The mathematical model involves *(i)* techno-economic assessment of biorefinery processing one of the four biomass types at different capacities; *(ii)* the biomass supply and biobutanol distribution chain costs, taking into account the exact distance between the real location of biomass suppliers and biobutanol customers, as well as the suggested location of biorefinery plants based on GIS; *(iii)* strategic location decision-making within a limited budget.

8.3   Materials and methods

8.3.1   Case study

Mexico's Ministry of Energy (SENER), due to its international commitments to climate change and greenhouse gas emission reductions, issued the Energy Transition Law on December 24, 2015, with the goal of increasing the share of clean energy in electricity generation (*DOF*, 2015).

Since then, efforts have been made to promote science, technology, and engineering toward the reindustrialization of the country, where energy production comes from renewable resources such as lignocellulosic biomass.

Hernández et al. (2019) carried out an assessment of the availability of lignocellulosic biomass waste in Mexico for four crops: corn stover, sugarcane and wheat straw which account for 83% of the total agricultural crops produced in the country, and for agave due to its growing global market (Market Data Forecast, 2022). The purpose of the study was to evaluate the possible locations of biomass suppliers considering a type of lignocellulosic source and its annual availability to produce bioethanol. In addition, using the gravity center method, the possible locations of biorefinery plants were evaluated along with possible suppliers within a 50 km radius. Nevertheless, the study does not provide information on which potential biorefinery location could be advantageous, considering all industrial stages, such as: biomass availability and supply chain of a feedstock, raw material processing, and the final product sale to the market.

Based on the procedure described by (Valdez-Vazquez et al., 2010), a nationwide inventory of lignocellulosic biomass waste was performed using data published by the Mexican Government Department SIAP (abbreviation from Spanish: Servicio de Información Agroalimentaria y Pesquera) from 2003 to 2020 for corn stover, wheat straw and agave bagasse, and from 2010 to 2021 for sugarcane bagasse (SIAP, 2021). Microsoft Excel v16.65 was used to compile the data.

The previous study (Dudek et al., 2022) reported the laboratory adaptive evolution of a fermentative microbial that was able of producing up to 23 g/L of biobutanol directly from corn stover cellulose. According to an techno-economic evaluation of biofuel production, this concentration of biobutanol obtained on the laboratory scale would be high enough to make the plant profitable (Sanchez et al., 2017).

The above-mentioned factors prompted an industrial-scale economic evaluation of the lignocellulosic biomass conversion to biobutanol, to assess the viability of its technology for the four types of biomasses (agave bagasse, corn stover, sugarcane bagasse and wheat straw) at different plant capacities.

The potential biorefinery locations published by Hernández et al. (2019) were adjusted using GIS on an intuitive manner considering the location along a major road, distance to potential biomass suppliers, distance to cities or significant villages, access to water, energy, industrial waste collectors, transportation infrastructure, and location of industrial parks (IGISMAP, 2021; Instituto Mexicano del Transporte, 2021; OpenStreetMap, 2022). The location of potential biobutanol customers – PEMEX Logistic's Storage and Distribution Centers (PEMEX, 2022)

were not considered in a location proposal of the biobutanol plants. All data were processed and visualized using QGIS v3.26.3-Buenos Aires. Subsequently, the distance from biomass providers to potential plants location and from potential plants location to customers were calculated using Python programming language with the Google Cloud API service, compiled in Jupiter Notebook 6.4.12.

8.3.2   Biomass availability in Mexico

The biomass resources database for biomass suppliers described by Hernández et al. (2019) has been updated and reported as the average biomass availability from 2003 to 2020 for agave bagasse,

corn stover and wheat straw and from 2013 to 2021 for sugarcane bagasse (Supplementary material: Table A.2).

8.3.3   Geographic information system

The map of Mexico showed 33 possible biorefinery locations for 10 agave bagasse, 43 corn stover, 30 sugarcane bagasse and 14 wheat straw providers. Modification of biobutanol biorefinery plants locations suggested by (Hernández et al., 2019) were depicted in the Supplementary material: Table A.3. The 65 warehousing and distribution centers of PEMEX have been distributed across the country (Figure 8.1). Based on the GIS method, as well as the road transportation network the shortest path was calculated using Google Cloud API for each pair biomass provider-biorefinery location and biorefinery location-PEMEX terminal. The calculated distance was used in Mixed Integer Linear Programming (MILP).
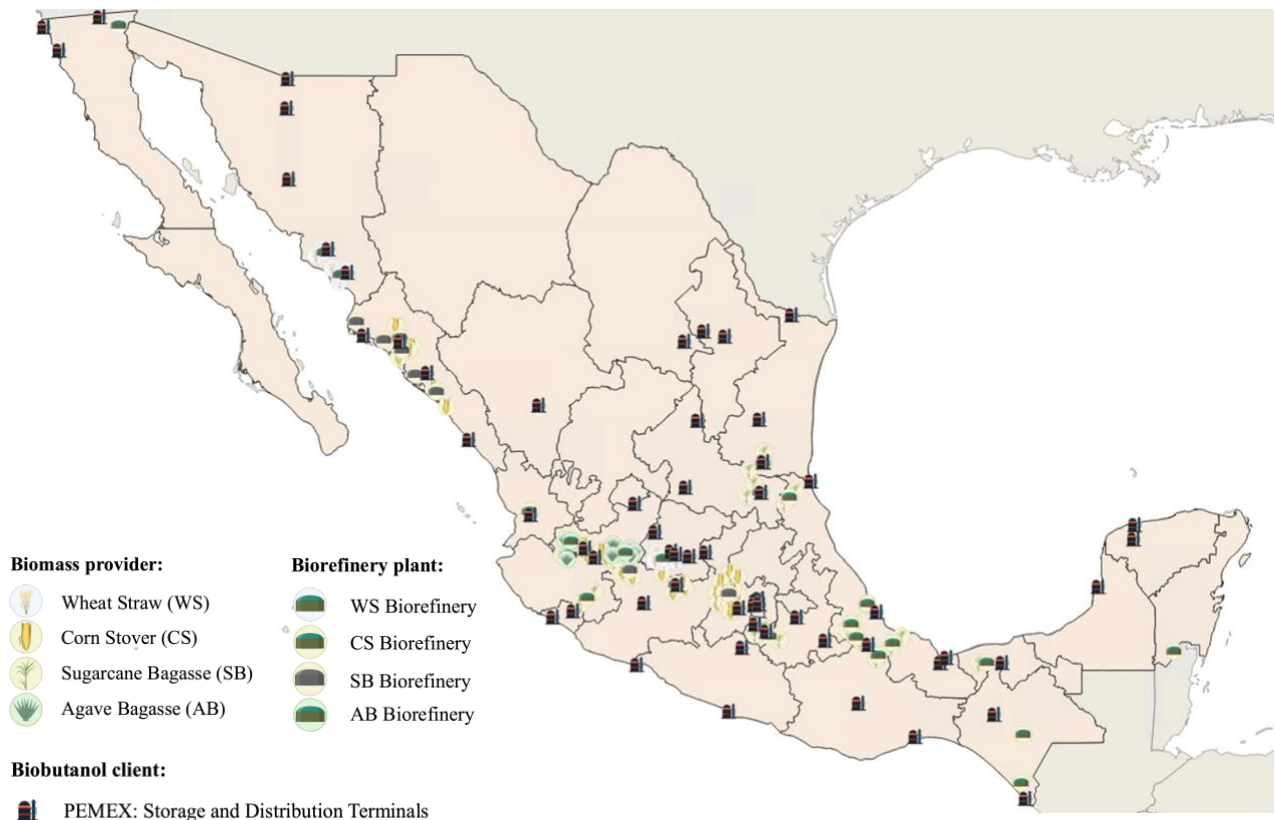
Figure 8.1. Distribution of possible biorefinery location, biomass supplier and PEMEX warehousing and distribution centers in Mexico using GIS.
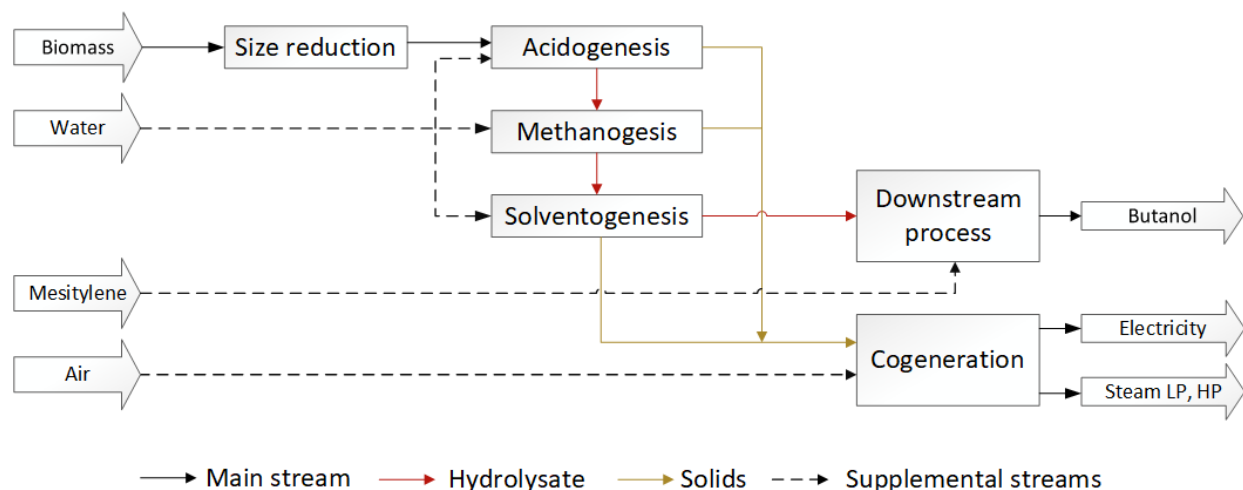
Figure 8.2. Configuration of a biorefinery plant for biobutanol production from lignocellulosic biomass.

8.3.4   Techno-economic assessment of biorefinery

The design of a biorefinery plant for biobutanol production from lignocellulosic biomass was modeled for techno-economic evaluation using the SuperPro Designer v11.2 (SPD) software (Intelligen, Inc., Scotch Plains, NJ, USA) according to the configuration depicted in the Figure 8.2.

8.3.6.1 Feedstock

The simulation of the proposed biorefinery scheme was carried out for the four different lignocellulosic biomasses differing in composition (Table 8.1). On the laboratory scale during fermentation of different raw lignocellulosic biomasses, 65% of hemicellulose was converted to acetic and butyric acids (Ayala-Campos et al., 2022; Dudek et al., 2021), and 50% of cellulose to butanol yielding a concentration of 22.3 g/L (Dudek et al., 2022). These conversions levels of polymers were applied for all types of studied lignocellulosic biomasses to simplify the analysis.

Table 8.1. Lignocellulosic biomass composition (%) in dry basis.

Lignocellulosic biomass	Hemicellulose	Cellulose	Lignin	Ash	References
Agave	22	45	8	25	Dudek et al., (2021)
Corn stover	26	36	21	17	
Sugarcane bagasse	27	44	18	11	Ayala-Campos et al., (2022)
Wheat straw	28	38	22	12	

8.3.6.2 Plant capacity

Based on the current annual biomass availability from suppliers, it was assumed that the established plant at a potential plant location can process only one type of biomass and the assigned suppliers should not be located further than 50 km away. In this way 16 possible plant capacities were obtained. It was decided to choose the highest (2400 t/day) and the lowest (500 t/day) possible plant capacity and a medium size (1500 t/day) that would approximate the size of the most frequently repeated capacities. Therefore, simulations were performed considering three plant capacities (500, 1500 and 2400 tonnes/day).

8.3.6.3 Plant configuration description

Proposed biorefinery plant design consists of six principal stages: *i)* size reduction; *ii)* acidogenesis; *iii)* methanogenesis; *iv)* solventogenesis; *v)* downstream process; and *vi)* cogeneration stage (Figure 8.2). The mass balance is shown in the Table 8.4.

i) *Size reduction.* The lignocellulosic biomass enters a grinding system to reduce the particle size to 4 mm. The biomass grinding energy demand is based on the literature (Anukam et al., 2016; González-Arias et al., 2022; Mani et al., 2004).

ii) *Acidogenesis.* The shredded lignocellulosic biomass was introduced into a digestion reactor at a solid/liquid ratio 1:10, which was operated at 37°C and working volume of 90% with retention time of 12h. The 65% of the hemicellulose fraction was converted into xylose, which was subsequently transformed to acetic acid and butyric acids at concentrations of 8.5 g/L and 3.7 g/L, respectively, by native microbiota of processed biomass (Ayala-Campos et al., 2022; Dudek et al., 2021). The slurry was conducted to centrifugation stage. The obtained supernatant was used for methanogenesis reactor while solid part was conducted to solventogenesis stage.

iii) *Methanogenesis.* Volatile fatty acids (VFAs) obtained in the previous step were converted to methane with an efficiency of 95% for acetic acid and 90% for butyric acid. The reactor was operated at temperature of 37°C, working volume of 75% and the liquid retention time of 10h according to previously described operation conditions by Valdez-Vazquez and Sanchez (2018). The produced gas has been diverted to the cogeneration stage.

iv) *Solventogenesis.* Before introducing the solid portion from acidogenesis into the reactor, water was added to obtain a stream with a TS (total solid) content of 10%. The reactor was operated with 90% of volume, temperature of 37°C, and retention time of 120h. Cellulose was converted to glucose at 50%, which was then used to produce butanol by a butanol-tolerant mixed culture, yielding a concentration of 22.3 g/L (Dudek et al., 2022). In addition, a further 45% of the cellulose fibers were converted to hexanoic and pentanoic acids with concentrations of 11 and 7 g/L, respectively. However, only the production of biobutanol was considered as the main product in this study. The slurry coming out of the reactor went through vacuum filtration. The liquid phase, rich in butanol, was transferred to a further purification stage, while the solids were transported to the cogeneration stage for electricity and steam production.

v) *Downstream process.* The biorefinery plant only simulated butanol separation using mesitylene, according to the processes previously reported by (Sanchez et al., 2017; Valdez-Vazquez & Sanchez, 2018).

vi) *Cogeneration stage.* Steam and electricity were generated in the cogeneration stage by burning residual hemicellulose, cellulose, and lignin, which were not converted into any bioproduct. The resulting steam with a temperature of 255 °C and a pressure of 45 bar was used in the heat exchange system. The steam with a temperature and pressure of 224 °C and 45 bar was used to generate electricity in a steam turbine.

8.3.6.4 Financial investment model

Construction schedule and unit costs of utilities of the proposed biorefinery scheme for the four types of biomasses and the three different capacities were depicted in the **Error! Reference source not found.**

Table 8.2. Biorefinery scheme construction assumptions.

	Values	Ref.
Scheduled operation (d/yr)	330	-
Maintenance and training (d/yr)	35	-
Construction time (yr)	3	-
Life-plant (yr)	20	-
Interest rate (%)	10	González-Arias et al., 2022

Federal taxes (%)	35		Prodecon, 2015
Biomass purchase (US$/tonne)	wheat straw: sugarcane bagasse: corn stover: agave bagasse:	60 60 50 40	local agricultures and tequila industry contacts
Utilities (US$/unit)	electricity (kW-h) LP stream (tonne) HP stream (tonne) cooling water (tonne)	0.1 12 20 0.05	Comisión Federal de Electricidad, 2022
Reagents Prices	mesitylene		Alibaba.com, 2022

Table 8.3. Relevant process features (equipment and utilities) for corn stover plant at capacity of 500 tonne/day.

Equipment	Name	Units	Material	Unit capacity	Power [kW/Unit]	Steam HP (242°C) [MT/h]	Steam (152°C) [MT/h]	Cooling water (25°C) [MT/h]	Chilled water (5°C) [MT/h]	Equipment cost (kUS$/Unit)
Size reduction										
Shredding	SR-101	2	CS	50 MT/h	350	-	-	-	-	282
Vibrating Screen	VSCR-101	2	CS	50 MT/h	15	-	-	-	-	18
Grinding	GR-101	1	CS	98.5 MT/h	631.6	-	-	-		484
Vibrating Screen	VSCR-102	1	CS	98.5 MT/h	29.6	-	-	-	-	26
Pneumatic Conveying	PC-101	1	CS	14.8 MT/h	6.8	-	-	-	-	59
Screw Conveyor	SC-103	4	CS	26.2 m3/h	1.8	-	-	-	-	28
Acidogenesis										
Screw Conveyor	SC-101	4	CS	26.2 m3/h	1.8	-	-	-	-	28
Heat Exchanger	HX-109	1	CS	20 m2	-	-	-	-	-	20
Anaerobic digestor	AD-101	1	Concrete	10095 m3	541	-	42	-	-	6,161
Rotary Vacuum Filter	RVF-104	1	CS	340 m2	749.6	-	-	-	-	536
Methanogenesis										
Anaerobic Digestor	AD-102	1	Concrete	8885.1 m3	399.8	-	-	277.4	-	5,605
Gas Compression	G-101	1	CS	7661.3 m3/h	659.5	-	-	101.1	-	804
Rotary Vacuum Filter	RVF-101	1	CS	336.3 m2	739.8	-	-	-	-	532
Solventogenesis										
Screw Conveyor	SC-102	1	CS	122 m3/h	7.7	-	-	-	-	176
Heat Exchanger	HX-108	1	CS	82.7 m2	-	-	-	-	-	159
Heat Exchanger	HX-103	1	CS	14 m2	-	-	4.2	-	-	19
Anaerobic Digestor	AD-103	5	Concrete	13690.3 m3	664.9		-	10544	-	7,442
Rotary Vacuum Filter	RVF-101	1	CS	300.3 m2	660.6	-	-	-	-	497
Screw Conveyor	SC-102	2	CS	33.8 m3/h	3.3	-	-	-	-	50
Downstream Process										
Centrifugal pump	PM-102	1	SS316	587.1 m3/h	23.3	-	-	-	-	73
Heat Exchanger	HX-106	16	CS	197.1 m2	-	-	-	-	-	104
Heat Exchanger	HX-101	1	CS	65.8 m2	-	-	-	-	-	51
Heat Exchanger	HX-107	1	CS	4.6 m2	-	-	0.8	-	-	9
Heat Exchanger	HX-102	1	CS	238.1 m2	-	-	-	-	-	117
Differential Extraction	DX-101	1	SS304	1548.3 m3	-	-	-	-	-	1,035
Heat Exchanger	HX-111	1	CS	9.5 m2	-	-	-	-	-	14
Heat Exchanger	HX-105	1	CS	103.4 m2	-	-	-	-	821.7	68
Decanter Tank	V-101	1	CS	483.9 m3	-	-	-	-	-	511
Heat Exchanger	HX-110	1	CS	118.2 m2	-	-	-	-	-	74
Distillation	C-101	1	CS	23 m3	-	20720.9	-	1688.8	-	87
Distillation	C-102	1	CS	0.5 m3	-	-	1.8	-	-	20

Heat Exchanger	HX-112	1	CS	16.7	m2	-	-	-	-	-	21
Cogeneration											
Heat Exchanger	HX-104	1	CS	178.9	m2	-	-	-	-	-	97
Steam Generator	SG-101	1	CS	152.6	MT/h	-	-	-	-	-	1,373
Steam Expansion	T-101	1	CS	24729.3	kW	-	-	-	1644.5	-	3,979
Steam Expansion	T-102	1	CS	3997.5	kW	-	-	-	-	-	996
Steam Expansion	T-103	1	CS	4492.3	kW	-	-	-	-	-	1,089

The Total Plant Cost (TPC) included direct costs composed of equipment purchase cost, installation, process piping, instrumentation, insulation, electrical, buildings, yard improvement and auxiliary facilities, as well as indirect cost consisting of engineering and construction. Relevant process features (equipment and utilities) for a plant capacity of 500 t/day were depicted in the Table 8.3.

Table 8.4. Mass balance for the corn stover plant at capacity of 500 tonne/day.

	S-120	S-144	S-109	S-121	S-114	S-110	S-179	S-142	S-141	S-107	P-53
Ash	79.05	0.79	-	0.79	-	-	0.79	-	0.79	-	-
Cellulose	167.40	165.73	-	165.73	-	-	165.73	-	8.29	-	-
Lignin	97.65	97.65	-	97.65	-	-	97.65	-	97.65	-	-
Hemicellulose	120.90	119.69	-	53.86	-	-	53.86	-	53.86	-	-
Water	35.00	2895.18	2721.99	158.64	2721.99	0.25	2913.39	2810.40	105.06	99.03	0.03
Acetic Acid	-	1.31	26.97	1.55	1.31	-	1.55	1.50	0.05	-	-
Butyric Acid	-	0.82	11.70	0.67	0.82	-	0.67	0.65	0.02	-	-
Xylose	-	131.05	132.19	7.59	132.19	-	7.59	7.32	0.27	-	-
Biomass	-	-	-	-	-	0.39	1.34		1.39	-	-
Butanol	-	-	-	-	-	-	-	68.05	2.49	0.03	66.05
Glucose	-	-	-	-	-	-	-	3.33	0.12	-	-
Mesitylene	-	-	-	-	-	-	-	-	-	-	0.29

The Direct Fixed Capital Cost representing the TPC was expanded by contractor's fee and contingency. The used utilities were standard power, steam, high pressure steam, cooling water and chilled water. The annual operating cost consists of raw material cost, labor dependent, facility dependent and utilities. The facility dependent costs were calculated on base of 6% of equipment value, as well as insurance, local taxes factory expenses that correspond to 1, 2 and 5% of direct fixed capital cost, respectively. Transportation costs were calculated basing on diesel combustion per kilometer by trailers of 20t for biomass and 36000L truck-volume for biobutanol transportation obtained from the transportation report published by Mexican Institute of Transportation (Osorno et al., 2022). Considering the biomass density (Kestur G. et al., 2013; Oliveira et al., 2016; Saad, 2012; Y. Zhang et al., 2012) the transportation cost was 0.077, 0.137, 0.171, 0.342 US$ per tonne per km for agave bagasse, wheat straw, sugarcane bagasse and corn wastes, respectively.

8.3.5 Mathematical modeling

8.3.6.1 Problem description

The mathematical model developed in the study addresses a strategic location of biorefinery plant which produces biobutanol from agricultural biomass in Mexico based on a feedstock-chain supply and biofuel distribution to the customer. The schematic design of the biorefinery supply chain is depicted in the Figure 8.3.
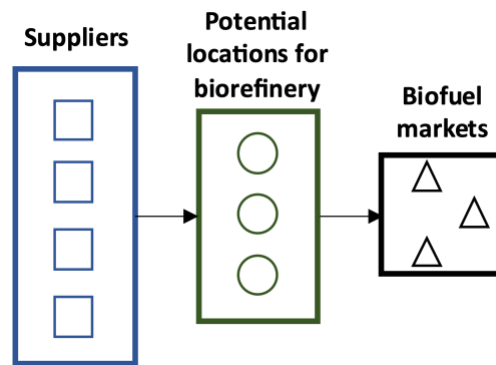
Figure 8.3. Schematic design of biorefinery supply chain.

The supply chain consists of a set of biomass supply sources, potential locations for biobutanol plant and market for the biofuel. The mathematical model is programed to take a biomass from biomass supply sources and deliver it to a potential plant location. The biomass, processed into biobutanol, is then distributed to consumers. The lifetime of each established plant at each capacity is set for 15 years and is divided into equal billing sub-periods of 1 year.

8.3.6.2 Model description

The model proposed in this study is a multi-period mixed-integer linear programming model. The sets, parameters, and variables used in the model are described in the Table 8.5.

Table 8.5. Sets, parameters, and variables in the mathematical model.

Elements	Description
Sets	
$s \in S$	Set of biomass supply sources.
$j \in J$	Set of potential locations for biorefinery plants.

$r \in R$	Set of markets (PEMEX Logistic) for biofuel.
$m \in M$	Set of biomass types.
$b \in B$	Set of material type produced at biorefinery.
$t \in T$	Set of time periods.
$c \in C$	Set of biorefinery plant capacity.

Parameters

β_{mst}	Available biomass m at supply source s in period t (MT).
γ_{bm}	Quantity of biofuel b (biobutanol) that can be produced from processing a unit of biomass m (MT).
D_{brt}	Minimum demand for biofuel b (biobutanol) at market r in period t (MT).
D'_{brt}	Maximum demand for biofuel b (biobutanol) at market r in period t (MT).
η_{sj}	Distance from biomass supply source s to bio-refinery's potential location j (km).
η'_{jr}	Distance from bio-refinery's potential location j to market r (km).
μ	Interest rate.
π_{cm}	Establishment cost of bio-refinery with capacity of c to process biomass m.
λ_{mt}	Cost of purchasing a unit of biomass m per period t ($/MT of product).
α_m	Cost of transporting a unit (MT) of biomass m per km.
α'_b	Cost of transporting a unit (MT) of biofuel b (biobutanol) per km.
τ_{mcj}	Variable cost of processing a unit of biomass m at the bio-refinery plant j with capacity c ($/MT).
θ_{mc}	Fixed cost of processing biomass m at a bio-refinery plant with capacity c ($/year).
ρ_{brt}	Price of biofuel b at market r in period t ($/MT).
φ	A large number.
Q_c	Biomass processing capacity of a plant with capacity of c.

Decision variables

y_{mcsjt}	The quantity of biomass m procured from the biomass supply source s to bio-refinery's potential location j with capacity c in period t (MT).
w_{bjt}	The quantity of biofuel b (biobutanol) produced at bio-refinery's potential location j in period t (MT).
z_{bjrt}	The quantity of biofuel b (biobutanol) transported from bio-refinery's potential location j to be sold at market r in period t (MT).
v_{mcjt}	Amount of biomass m processed at bio-refinery's potential location j with capacity c in period t (MT).
x_{cmj}	1 if bio-refinery plant with capacity c is established to process biomass m at potential location j; 0 otherwise.

8.3.6.3 Objective function

The objective function of this model is to design the biorefinery supply chain in a way that the NPV of the whole investment is maximized. The NPV is calculated by subtracting total costs from total revenues (Equation 1).

$$Max \ NPV \ = Max \left(\sum_t \frac{1}{(1+\mu)^t} (TR_t - TotalCost_t) - EC \right) \tag{1}$$

The revenue of an established plant in each period is generated from the sale of biobutanol to customers (Equation 2).

$$TR_t = \sum_b \sum_j \sum_r (\rho_{brt} \times z_{bjrt}) \qquad \forall t \in T \tag{2}$$

Total costs of the project are divided into one-time and periodical costs. Establishment costs (EC) only occur at the beginning of the project time horizon and hence is not dependent on time (Equation 3). The period costs (PC) come from the cost function and were calculated according to Equation 4. The PC consider the cost of purchasing biomass, raw material transportation cost, fixed biomass processing cost, variable biomass processing cost, and biobutanol distribution costs.

$$EC = \sum_m \sum_c \sum_j (\pi_{mc} \times x_{cmj}) \tag{3}$$

27

$$PC_t = \sum_m \sum_c \sum_s \sum_j (\lambda_{mt} \times y_{mcsjt}) + \sum_m \sum_c \sum_s \sum_j (\alpha_m \times \eta_{sj} \times y_{mcsjt})$$

$$+ \sum_m \sum_c \sum_j (\theta_{mc} \times x_{mcj}) + \sum_m \sum_c \sum_j (\tau_{mcj} \times v_{mcjt}) \tag{4}$$

$$+ \sum_b \sum_j \sum_r (\alpha'_b \times z_{bjrt} \times \eta'_{jr}) \qquad \forall t \in T$$

8.3.6.4   Model constraints

The constraints form the model's feasible region. The mathematical model is required to satisfy the constraints imposed to find a realistically optimal location for the biorefinery. For the strategic location model 9 constraints were established (Equations 5 to 13). The constraint 1 (Equation 5) limits the number of established biorefinery plants with specific capacity and type of biomass that can be processes at each potential location to at most one. The constraint 2 (Equation 6) restrict that the procured biomass from each biomass supply source to potential plant locations cannot exceed the available biomass at that source. The constraint 3 (Equation 7) calculates the amount of biomass of each type that will be process at each plant location and make it equal to all biomass that is sent from one or several sources of biomass supply to a potential plant location. The constraint 4 (Equation 8) makes limitation that biomass can be only processed at potential plant location if a plant is established. Additionally, it limits the amount of the processed biomass at each plant to the maximum processing capacity of the established plant at that location. The constraint 5 (Equation 9) ensure that the amount of biobutanol produced at an established plant is equal to the amount that should be produced according to the efficiency assumption of converting one unit of each type of biomass into biobutanol. The constraint 6 (Equation 10) forces the amount of biobutanol sold to different customers from each established plant location to be equal to the biobutanol produced at each plant. The constraint 7 (Equation 11) determines the extent of demand at each customer. According to this constraint, biobutanol that is sent from all established plant to each costumer satisfy the minimum demand of the whole market. The last constraints 8 and 9 (Equations 12 and 13) specify the domain of continuous and binary variables.

$$\sum_m \sum_c x_{mcj} \leq 1 \qquad \forall j \in J \tag{5}$$

$$\sum_j y_{mcsjt} \le \beta_{mst} \qquad \forall m \in M, s \in S, t \in T, c \in C \tag{6}$$

$$\sum_s y_{mcsjt} = v_{mcjt} \qquad \forall m \in M, j \in J, t \in T, c \in C \tag{7}$$

$$v_{mcjt} \le Q_c x_{mcj} \qquad \forall m \in M, j \in J, t \in T, c \in C \tag{8}$$

$$w_{bjt} = \sum_m \sum_c \gamma_{bm} v_{mcjt} \qquad \forall b \in B, j \in J, t \in T \tag{9}$$

$$\sum_r z_{bjrt} = w_{bjt} \qquad \forall b \in B, j \in J, t \in T \tag{10}$$

$$D_{brt} \le \sum_j z_{bjrt} \le D'_{brt} \qquad \forall b \in B, r \in R, t \in T \tag{11}$$

$$y_{mcsjt}, v_{mcjt}, w_{bjt}, z_{bjrt} \ge 0 \qquad \forall m \in M, s \in S, j \in J, b \in B, r \in R, t \in T, c \in C \tag{12}$$

$$x_{cmj} \in \{0,1\} \qquad \forall c \in C, m \in M, j \in J \tag{13}$$

8.4   Results and discussion

8.4.1   Economy summary

The economy aspects of biobutanol production from lignocellulosic biomass under innovative biorefinery scheme (Figure 8.2) at different plant capacity were investigated. Due to a biomass limitation, a techno-economic assessment of the biorefinery processing agave bagasse was carried out only for plant capacity of 500 tonnes/d, for wheat straw for 500 and 1500 tonnes/d, while for corn stover and sugarcane bagasse were performed for all three plant capacities (500, 1500 and 2400 tonnes/d). The biobutanol yields were 0.124, 0.137, 0.14 and 0.144 tonne of biobutanol per tonne of agave bagasse, corn stover, wheat straw, and sugarcane bagasse, respectively. In all cases the purity of obtained biobutanol was 99.5%. The estimated total capital investment (TCI), operating costs (OC) and biobutanol total production costs (TPC) varied depending on biomass type and plant capacity (Figure 8.4). Within the same plant capacity, the highest TCI around 139 MUS$ for plant capacity of 500 tonne/d was found for wheat straw and sugarcane bagasse, being

14 and 19% higher compared to corn stover and agave bagasse, respectively. This is because the volume of total solids at concentration of 100 g/L introducing into anaerobic digestor (AD-103, Figure 8.2) exceeds the maximum possible volume of the reactor (15000m3), requiring the construction of 2 instead of 1 reactor, what increase the equipment and construction costs. More equipment impact operation costs due to higher utilities demand and maintenance costs. The lowest OC was estimated for agave bagasse-based biorefinery plant due to the lowest feedstock price – 33.3% less compared to corn stover and sugarcane bagasse, and 20% less compared to wheat straw.

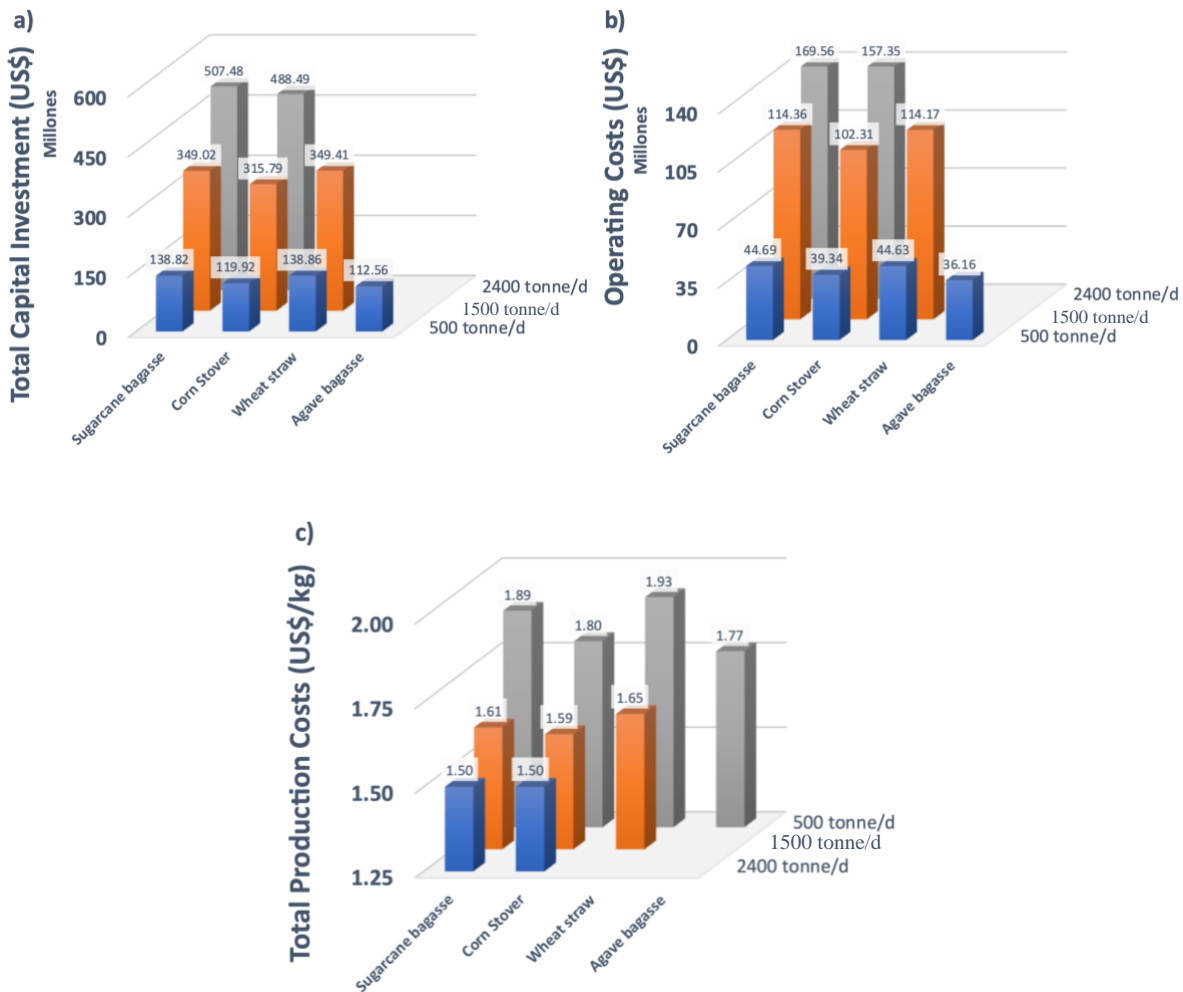Figure 8.4. Techno-economic analysis of biobutanol biorefinery plant a) TCI; b) OC; c) TPC; depending on biomass type and plant capacity.

The TPC is changing depending on biomass type and plant capacity. In the case of a biorefinery processing 500 tonne/d of feedstock, the lowest TPC was found for agave bagasse due to the lowest raw material costs. The wheat straw because of its high biomass purchase (US$ 60) and lower yield

by 0.03 and 0.07 biobutanol unit per biomass unit compared to corn stover and sugarcane bagasse, respectively, makes its TPC the highest (US$ 1.93) out of all studied types of biomasses. The plant scaling up from 500 to 1500 tonne/d decreased the TPC by 15% for sugarcane bagasse and wheat straw and by 13% for corn stover.
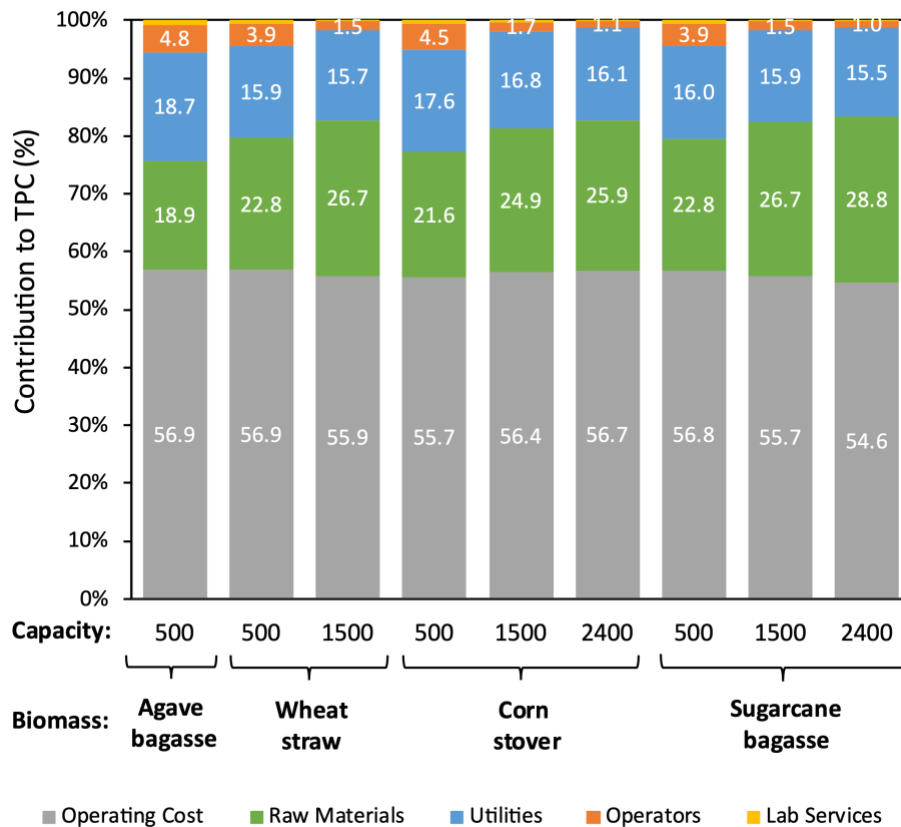
Figure 8.5. Distribution of Total Production Costs (TPC) depending on biomass type and plant capacity.

The estimated TPC for 2400 tonne/d plant capacity for sugarcane bagasse and corn stover was the same 1.5 US$. This is because lower corn stover feedstock price meet balance with higher biobutanol unit produced per feedstock of sugarcane bagasse compared to corn stover (0.14 vs 0.144). Distribution of TPC (Figure 8.5) indicate that for all biomass types and plant capacities, the operating costs account for more than 55% of TPC. Its contribution decreases slightly (=< 1%) for wheat straw and sugarcane bagasse with plant capacity increase, while for corn stover its value slightly increases (=< 1%). Independent on a feedstock price the biomass contribution on TPC increase at increase of plant capacity. However, the utility and operating costs decrease at increase of plant capacity.

The NPV for each biorefinery processing different types of biomasses at different capacities was positive, it means that all simulations in the technology assessment are cost-effective.

The obtained techno-economic data were used in the mathematical optimization model, to extend the construction and operation costs with supply chain depending on the plant location and evaluate new NPV.

8.4.2 Mixed Integer Linear Programming

This section considers three different variants of the proposed mathematical model and examines the corresponding results. These variants are: single objective model without budget constraint, single objective model with budget constraint, and goal programming model considering budget and NPV as the objectives. The mathematical model was ran using AIMMS software and CPLEX 20.1 solver on a desktop computer with Intel ® Core (TM) i7-11700 @ 2.50 GHz processor and 16.0 GB RAM.

8.4.6.1 Single objective model without budget constraint (base case)

The results reported in this section are from the main mathematical programming model proposed in section 8.3.5. The planning horizon of 20 years was considered with interest rate of 10% to solve the model for the case study.

Table 8.6. Separate NPV value of bio-refinery plants.

Plant locations	NPV value (USD)
Atotonilco el Alto	119,433,055
Rancho Viejo del Refugio, Ocotlán	268,299,071
Santa Ana La Ladera, Ixtlahuaca	217,501,801
El cerro de abajo, Angostura	107,154,462
Guadalupe Victoria, Culiacán	277,143,539
Castro Urdiales, Teuchitlán	305,816,863
Estación Refugio	367,319,244
La Coma, El Mante	327,025,053
Gral. Miguel Alemán, Atoyac	141,857,456
Úrsulo Galván, La Antigua	324,241,843
Texas, Cosamaloapan de Carpio	372,531,619
El Molino, Pánuco	237,545,113
Ciudad Obregón	284,518,848

The objective function of the model resulted in a positive NPV with value of $US 3,350,387,969, which indicate that establishment of biorefinery plant considering applied technology, supply chain and distribution of biobutanol makes the case study economically feasible. The required initial investments to cover the establishment costs in order to maximize the project's NPV is $US 5,636,663,000. The individual NPV values associated with each plant can be found in the Table 8.6.
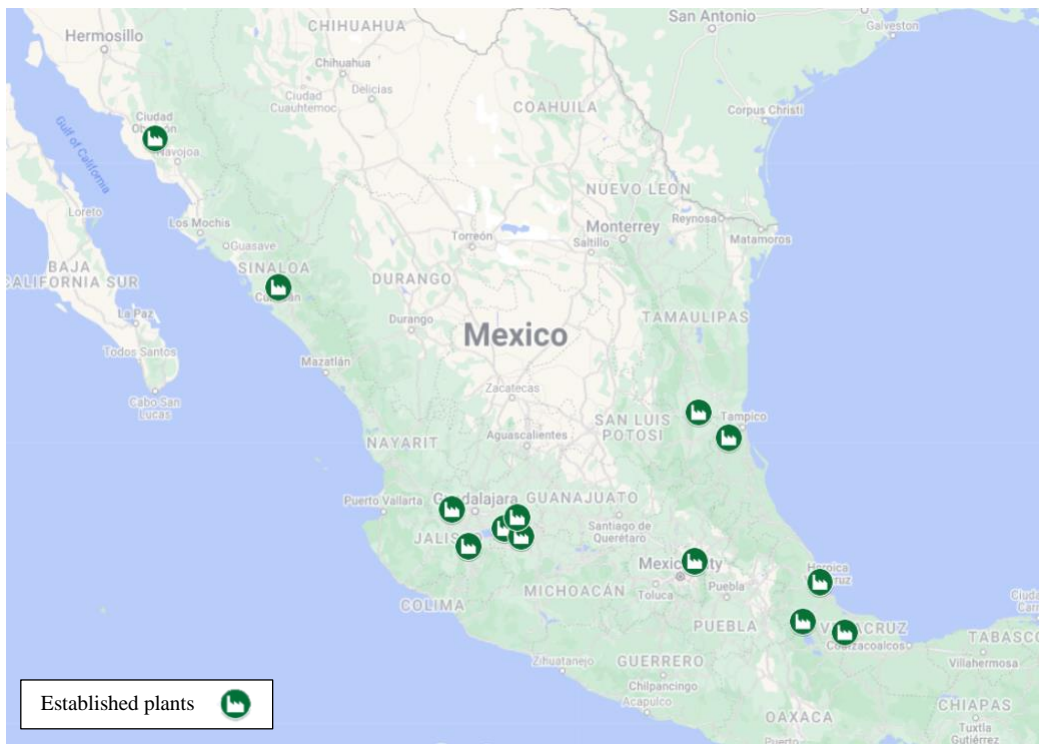
Figure 8.6. Suggested locations for biorefinery plants establishment by the model.

Results of the model suggested establishing biobutanol production plants (i.e., biorefinery plants) at 13 locations from the 34 potential locations that were considered. Most of the selected locations are in central Mexico, as can be seen in the Figure 8.6. 10 biobutanol production plants are suggested to be established with annual biomass processing capacity of 792,000 tonnes, which is the highest level of capacity considered in the case study (2400 tonnes/d). The other three plants are suggested to be established with capacity of 495,000 tonnes of biomass, which is the medium capacity considered (1500 tonnes/d). No plant is suggested to be established with the lowest capacity (165,000 tonnes/yr – 500 tonnes/d). Based on the results of mathematical model optimization, it is suggested that seven plants be set up with sugarcane bagasse and five with corn

stover. Only one plant (established at Ciudad Obregón), which is located in the northwest of the country, is suggested to be established with wheat straw as the input biomass.

The amount of biomass processed at each biorefinery plant remains the same during the planning horizon (Figure 8.7). With the exception of the plant established in El Molino and Pánuco, the capacity the plants is fully utilised, meaning that the amount of biomass processed at these plants is equal to the maximum capacity of the plant.
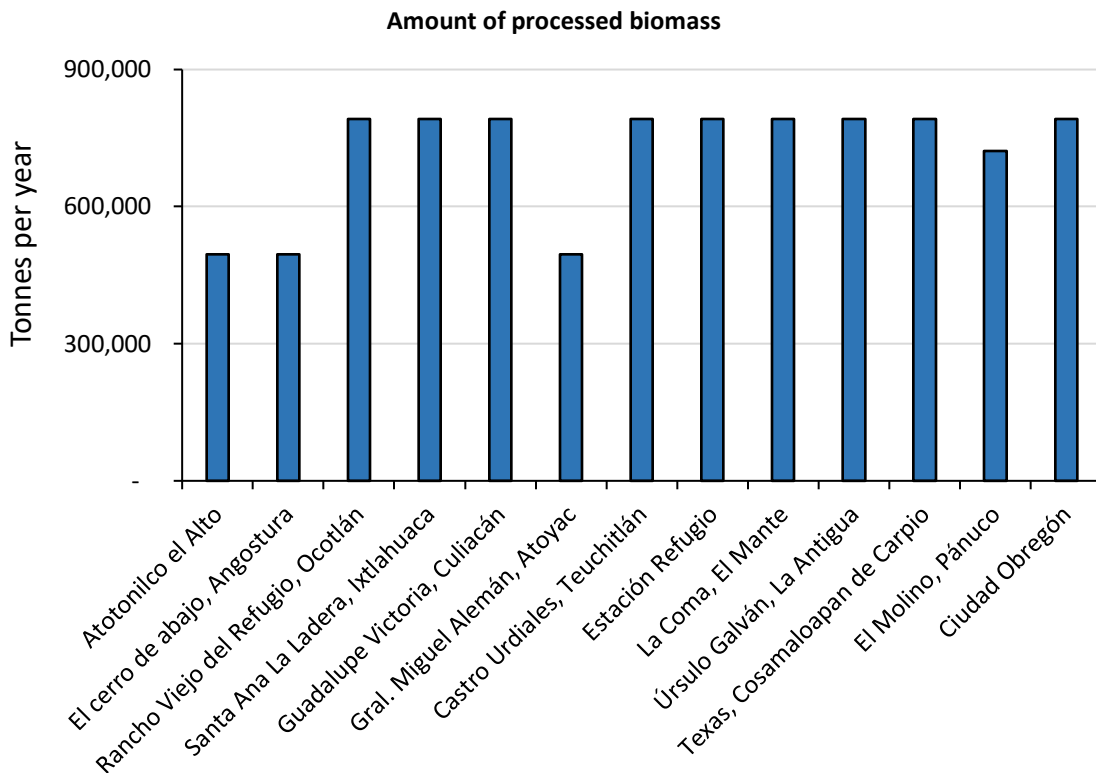
Figure 8.7. Amount of processed biomass at each biorefinery plant.

The amount of produced biobutanol during the processing lignocellulosic biomass under proposed biorefinery scheme for the 13 established plants were depicked in the Figure 8.8. The level of production remains the same for the entire planning horizon. The amount of biobutanol sent to each demand market (i.e., customer) can be found in the Figure 8.9. The amount of biobutanol sold to each customer is equal to the its maximum demand, what means that the established plants have the production capacity to meet the maximum demand of all the customers.
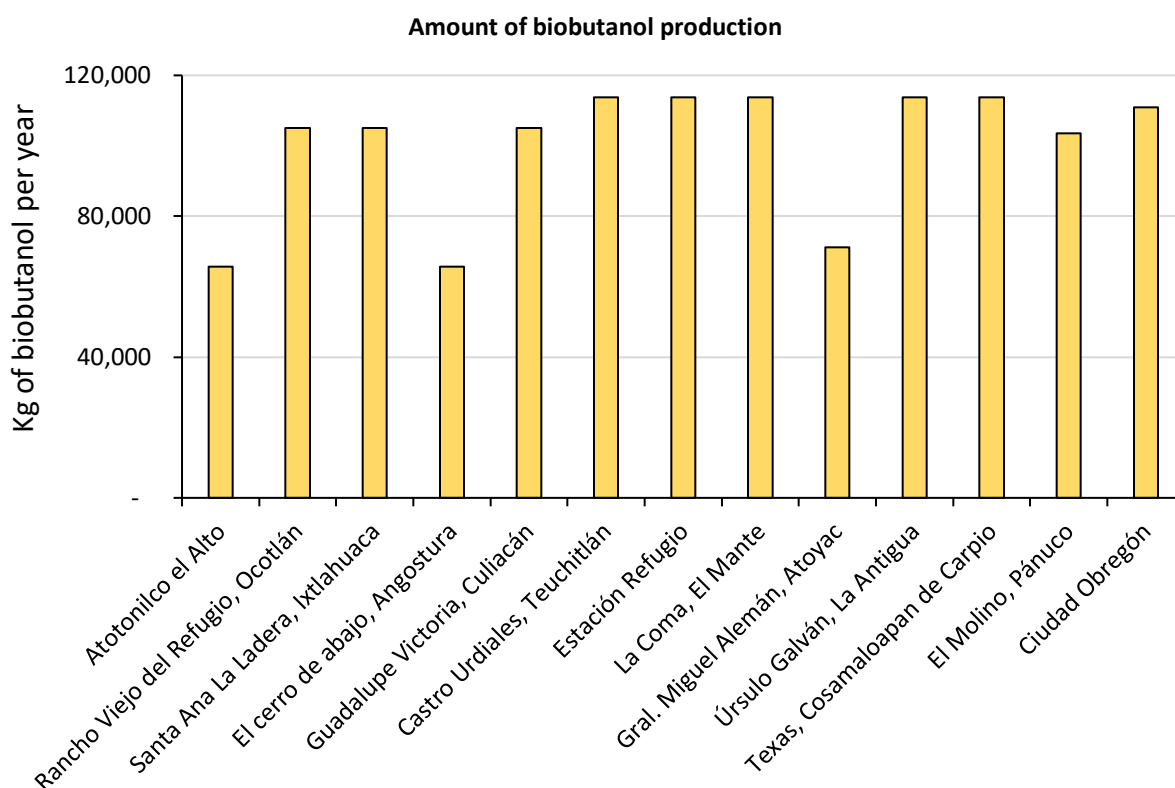
Figure 8.8. Amount of biobutanol production at each biorefinery plant.

8.4.2.1.1 Analysis on demand

The construction of any production facility is highly dependent on market demand. Without a substantiated demand for a particular product, investment in its production is unjustified. Therefore, given the uncertain nature of biobutanol demand in the future, a scenario analysis was carried out to show how the NPV of the project and decisions regarding the establishment of the biorefinery could potentially change the project's performance. For this purpose, four scenarios were defined, which change the minimum and maximum demand in the base case by factors of 0.5, 1.5 and 2.

As seen in the Table 8.7, when the maximum demand increases, total NPV increases as well. Also, a greater number of plants are suggested to be established. However, changing the minimum demand does not affect the results, which shows that the NPV of the project and plant establishments are not limited by the minimum demand. Therefore, it is more economical for the plants to produce biobutanol up to the maximum available demand.

Figure 8.9. The amount of sold biobutanol to each customer from all the established biorefinery plants.

Table 8.7. Total NPV and the number of established plants for scenarios of maximum and minimum demand.

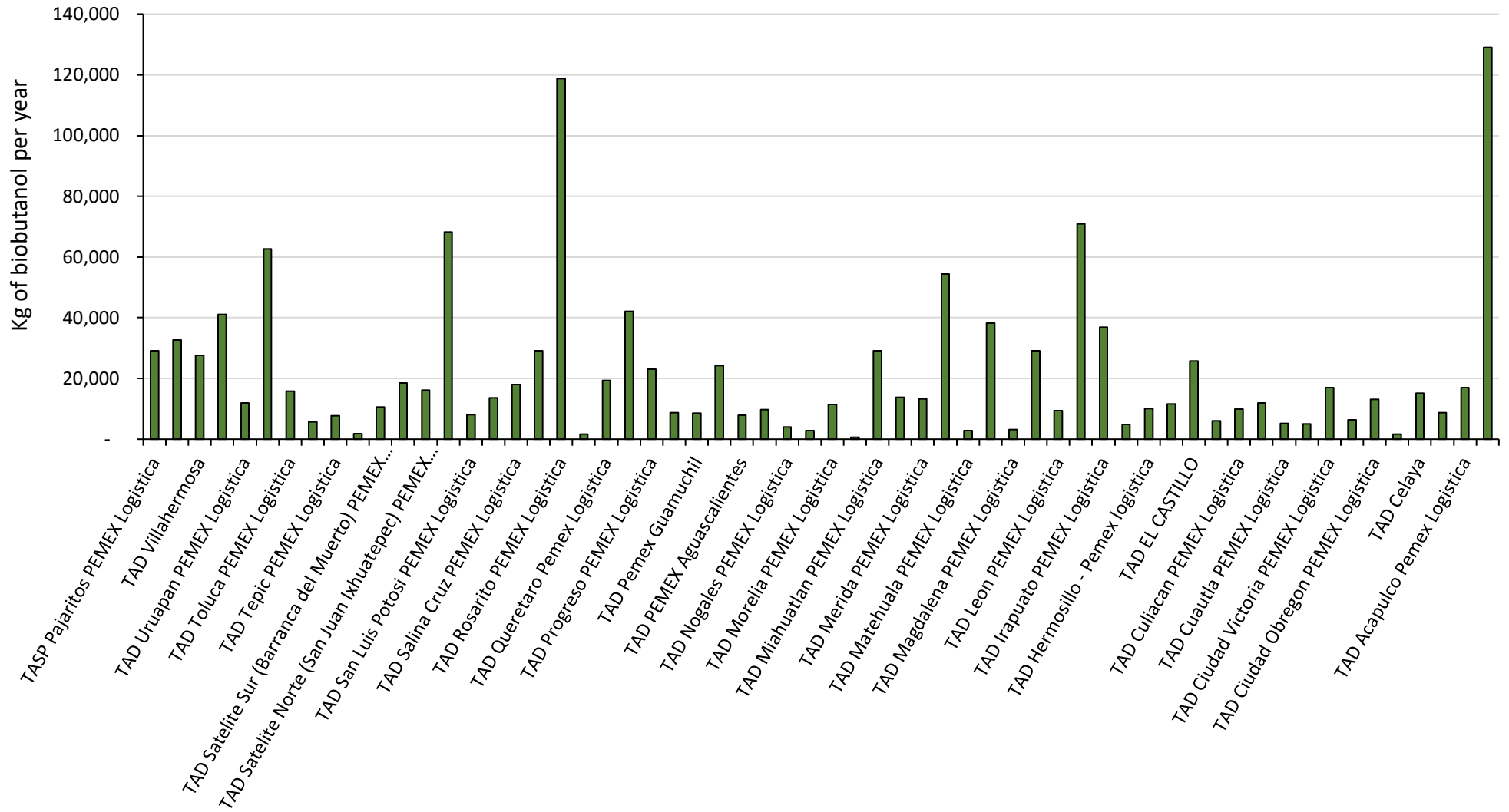| Maximum demand	Total NPV (USD)	Number of established plants	Minimum demand	Total NPV (USD)	Number of established plants
0.5 D_{max}	1,844,509,469	6	0.5 D_{min}	3,350,387,969	13
D_{max} (Base case)	3,350,387,969	13	D_{min} (Base case)	3,350,387,969	13
1.5 D_{max}	4,395,500,492	21	1.5 D_{min}	3,350,387,969	13
2 D_{max}	4,634,851,398	26	2 D_{min}	3,350,387,969	13

8.4.2.1.2 Analysis on interest rate

Interest rate is an important factor that affect the results and NPV of the study case. Due to uncertain nature of this parameter because of global economy in the last years, the effect of changing interest rate on the NPV were presented in this section. Higher interest rate levels lead to lower NPVs and fewer assumed biorefineries (Table 8.8).

Table 8.8. Total NPV and the number of established plants for scenarios of interest rates.

Interest rate (%)	Total NPV (USD)	Number of established plants
0	15,530,119,500	13
5	7,524,474,560	13
10	3,350,387,967	13
15	1,001,910,704	11
20	530,549.76	3

8.4.2.1.3 Analysis on biobutanol price

Table 8.9 shows the effect of biobutanol selling price on the NPV and the number of established plants in the study case. If the selling price of biobutanol falls by half of the estimated market price for the base case (USD 1,200/tonne), the NPV of the study case becomes negative making the investition economically infeasible. In that scenario, only two plants were suggested to be established in order to satisfy the minimum demand of the costumers. For the scenarios where biobutanol selling price increase 1.5 or 2 times compare with the base case, also increase in NPV was observed. Nevertheless, the number of established plants, their capacities, and amount tof biobutanol production remain the same. The explication of this phenomenon is that the maximum

demand of all customers are met considering the biobutanol selling price in the base case. Thus, there is no need to establish more plants. However, the NPV increases as income as a function of NPV increases by the increase in the selling price of biobutanol (Table 8.9).

Table 8.9. Effects of biobutanol's selling price on the project's NPV and the number of established plants.

Biobutanol selling price	Total NPV (USD)	Number of established plants
$0.5\,\rho_{brt}$	-1,564,733,387	2
ρ_{brt} (Base case)	3,350,387,969	13
$1.5\,\rho_{brt}$	16,644,816,352	13
$2\,\rho_{brt}$	29,939,244,740	13

8.4.2.1.4   Analysis on establishment costs

As the set-up costs increase, the NPV decreases and when it doubles, the NPV becomes negative and the project becomes economically unfeasible. At double the establish costs, two plants would be built just to meet the minimum customer demand included in the model (Table 8.10).

Table 8.10. Effects of establishment costs on the project's NPV and the number of established plants with each capacity size

Establishment costs	Total NPV (USD)	Number of established plants (capacity)
$0.5\,\pi_{cm}$	6,183,524,984	13
π_{cm} (Base case)	3,350,387,969	13
$1.5\,\pi_{cm}$	705,683,729	9
$2\,\pi_{cm}$	-247,621,767	2

8.4.2.1.5   Analysis on operating costs (fixed and variable)

Similar to the trend observed for establishment costs, an increase in operating costs, including both fixed and variable costs, resulted in a decrease in NPV. If operating costs increase by 50%, the study case becomes economically unfeasible (Table 8.11).

Table 8.11. Effects of operating costs on the project's NPV and the number of established plants.

Operating costs	Total NPV (USD)	Number of established plants (capacity)
0.5 $(\tau_{mcj}, \theta_{mc})$	9,432,494,588	14
$(\tau_{mcj}, \theta_{mc})$ (Base case)	3,350,387,969	13
1.5 $(\tau_{mcj}, \theta_{mc})$	-322,733,056	2
2 $(\tau_{mcj}, \theta_{mc})$	-1,322,820,790	2

8.4.6.2 Single objective model with budget constraint

In this section, was assumed that exist a specific initial budget for the study case that limits the investment costs (Equitation 3) that can be spend on facilities establishement. In order to address the budget limit, constraint set (14) needs to be added to the main model which is proposed in section 8.3.5.

$$\sum_m \sum_c \sum_j \left(\pi_{mc} \times x_{cmj} \right) \leq Budget \tag{14}$$

In order to obtain the estimated budget, the model proposed in Section 8.3.5 was once again solved by changing the objective function of the model (Section 8.3.5: Equation 1) to Equation 15, which shows the minimisation of establishment cost. The constraints Equations 5-13 remain the same.

$$Min\ EC = \sum_m \sum_c \sum_j \left(\pi_{mc} \times x_{cmj} \right) \tag{15}$$

The obtained budget with this approach was equal to 918,712,000 (USD). Below this budget, the minimum demands of biobutanol customers cannot be met. Therefore, this budget was considered as the minimum required investment ammount to implement the biobutanol production in Mexico. Within the proposed budget, only two biorefinery plants were suggested to be established to process corn stover at plant capacity of 2400 tonnes/d. The individual NPV and amount of produced biobutanol for each plant proposed to be established was was depicked in the Table 8.12. The amount of produced biobutanol remains the same for the entire planning horizon.

Table 8.12. Separate NPV value of biorefinery plants and their biobutanol production amount.

Plant locations	NPV value (USD)	Annual production of biobutanol (tonnes)
Rancho Viejo del Refugio, Ocotlán	257,051,354	105,134
Guadalupe Victoria, Culiacán	256,216,626	105,134

8.4.2.2.1 Analysis on the budget

The initial budget that can be allocated to a case study is of great importance and can significantly affect the results. The impact of the budget on the results was presented in the Table 8.13. A larger budget allows more biorefineries to be established, resulting in a higher NPV. However, when the budget covers the construction of enough biorefinery plants to meet the maximum demand for biobutanol (3,350,387,969 USD), its increase does not affect the NPV, as the NPV value is no longer dependent on budget constraints.

Table 8.13. Effects of budget on the project's NPV and the number of plants established

Amount of budget (USD)	NPV value (USD)	Total number of established biobutanol production plants
Base budget (918,712,000)	513,267,980	2
1.5 × base budget	863,125,450	3
2 × base budget	1,220,705,261	4
2.5 × base budget	1,546,404,493	5
10 × base budget	3,350,387,969	13
20 × base budget	3,350,387,969	13

8.4.6.3 Goal programming model with budget and NPV goals

Goal Programming (GP) belonging to Multi-Criteria Decision Making (MCDM) and allows decisions to be made in the presence of multiple conflicting objectives, moreover, pave the way for striking a balance between different objectives and finding a compromise solution (Jayaraman et al., 2017). A standard GP is not able to provide high-quality Pareto solutions. Therefore, Weighted Goal Programming (WGP) in which decision-makers can specify the importance of the

objectives according to their preferences and is applied in a specific cases. The WGP method can be formulated as follows:

$$Minimize\ Z = \sum_{i=1}^{p} W_i^+ D_i^+ + W_i^- D_i^- \tag{16}$$

Subject to

$$\sum_{t} \frac{1}{(1+\mu)^t} (TR_t - TotalCost_t) \qquad \text{i= 1,2,..., P} \tag{17}$$

$$X \in \Omega \tag{18}$$

$$D_i^-, D_i^+ \geq 0 \qquad \text{i= 1,2,..., P} \tag{19}$$

In the above-mentioned model, Ω is the set of feasible areas, X_i is decision variables, A_{ij} is the coefficient of decision variables in constraints, D_i^- and D_i^+ are the deviations from the determined goal values, and W_i^+ and W_i^- are the important factors (weights) for deviations. The above-mentioned model aims to reduce the total deviations of the decision variables from their determined goals by considering the importance of each goal. In some cases, one of the negative or positive deviations should be considered in the objective function and the related constraint. As an example, some goals are related to the total profit of the problem and negative deviations from the determined goal are not desirable.

The multi-objective version of the above-mentioned problem considers two conflicting objectives simultaneously. The first objective function maximizes the profits of the system excluding EC and the second objective function minimizes the EC. Focusing on establishment cost of biorefinery centers as a separate objective function might affect transportation costs or revenues reversely, and that justifies applying a goal programming method to find a compromised solution for the model. Equation (20) is designed to minimize the summation of deviations as an objective function. Constraint sets (21) and (22) show how the deviations are added to the model. In constraint set (21), negative deviations from the total profits are considered. Positive deviations from the establishment costs are embedded in the constraint (22). Constraint (23) specifies the sign of

deviations. Each objective function is solved separately, and the result is considered as goal for the related constraint.

$$Minimize\ Z = \ d_1 + \ d_2 \tag{19}$$

Subjected to

$$\sum_t \frac{1}{(1+\mu)^t}(TR_t - TotalCost_t) + \ d_1 \geq 3350387969 \qquad \forall\ t \in T \tag{20}$$

$$EC - \ d_2 \ \leq \ 918712000 \tag{21}$$

$$d_1, d_2 \geq 0 \tag{22}$$

After solved the model, the solver reports the objective function value as 2,679,297,736 USD. The solver sets the establishment cost equal to 953,352,000 USD and assummes two biorefinery plants at Estación Refugio and Texas, Cosamaloapan de Carpio with 340,999,848.4 and 364,730,384.2 USD of NPV, respectively.

8.4.2.3.1   Analysis on the goal budget

Sensitivity analysis was conducted on the budget goal (BG) to assess the behavior of the multi-objective version of model under different circumstances. Decreasing the budget goal had no effect on the total NPV and the number of established plants. However, increasing the BG has a direct impact on the total NPV and the number of established plants (Table 8.14).

Table 8.14. Effects of budget goal on the project's NPV and the number of plants established

Budget Goal	Total NPV (USD)	Number of established plants
0.5 *BG*	705,730,233	2
BG (Base case)	705,730,233	2
1.5 *BG*	1,071,040,272	3
2 *BG*	1,404,413,866	4

8.5   Discussion

Under proposed biorefinery scheme all simulated plant capacities independent on biomass type makes biobutanol production viable, given the actual market price of butanol of 2400 US$/tonne.

Biobutanol production is the most profitable when produced at plant capacity of 2400 tonne/d from sugarcane bagasse or corn stover. The TPC fluctuation decreased as the size of the plant increased. This was due to the decreasing importance of global equipment and construction costs and an increasing importance of a raw material price and a process efficiency, which mainly determined the final unit price of biobutanol.

Since 2015, there are few papers in literature related to techno-economic assessment of biobutanol production from lignocellulosic biomass (The mathematical programming model determined the maximum NPV that could be achieved under the case study conditions. The objective function of the model resulted in a positive NPV of $US 3,350,387,969, indicating that the project is economically viable. The initial investment required to maximize the NPV is $US 5,636,663,000.

Table 8.15). Given an interest rate of 10% and actual butanol market price(1.94 US$/L, 2.40 US$/kg), the biorefinery schemes suggested by (Baral & Shah, 2016; Dalle Ave & Adams, 2018; Jang & Choi, 2018; Sanchez et al., 2017; Valdez-Vazquez & Sanchez, 2018), are not suitable for construction in 2022 due to the used technology that would made biobutanol highly expensive to produce. The plant design for biobutanol production proposed by (Carmona-Garcia et al., 2019; Mailaram & Maity, 2022; Molina-Guerrero et al., 2021), technologically are viable to build. Nevertheless, the costs of the biomass supply and distribution chains for biobutanol should be calculated to define the viability of the installation. Molina-Guerrero et al. (2021) obtained for a plant capacity of 2200 tonnes/d lower production costs than in the present work (1.10 US$/L for the capacity of 2200 tonnes/d vs 1.22 US$ for the capacity of 2400 tonnes/d), probably due to the shorter ABE fermentation time (74h vs 120h) and a high yield of 19.4 g/L.

Most works applied chemical pretreatment of biomass and pure culture for ABE fermentation (Carmona-Garcia et al., 2019; Dalle Ave & Adams, 2018; Mailaram & Maity, 2022). These factors required the purchase of additional reagents and an additional bacterial cultivation step, making the process more expensive. Besides, Baral and Shah (2016), and Jang and Choi (2018) used genetically modified species, which involves a patent royalty fee that was not included in the TPC, but it affects the final price of the product. In the present study, the production of biobutanol is highly competitive due to its high yield and the absence of other organic solvents, such as acetone or ethanol, whose presence increases the cost of biobutanol purification.

The mathematical programming model determined the maximum NPV that could be achieved under the case study conditions. The objective function of the model resulted in a positive NPV of $US 3,350,387,969, indicating that the project is economically viable. The initial investment required to maximize the NPV is $US 5,636,663,000.

Table 8.15. Comparison of TPC of biobutanol from lignocellulosic biomass.

Ref.	Year of calculation	Feedstock	Plant Cap [MT/day]	Pretreatment	Inoculum	Reactor type	Yield [*gn-BuOH /gfstck*]	TPC / TPC 2022* [$/L]
Baral et al. 2016	2015	Corn Stover	2211	DAP	*C. beijerinckii 8052*	Batch	0.13	1.76/3.42
Valdez-Vazquez and Sanchez, 2017	2016	Wheat Straw	1000	Biological: *Enterococcus* genus	Co-culture of *C. cellulovorans and C.beijerinckii*	Batch	0.17	1.27/2.25
Sanchez et al. 2017	2016	Wheat Straw	2000	Biological: *Enterococcus* genus	Co-culture of *C. cellulovorans and C. beijerinckii*	Batch	0.06	1.37/2.43
Dalle Ave & Adams, 2017	2017	Switchgrass	2486	DAP	*C. Acetobutylicum*	Batch	0.09	1.58/2.54
Oh Jang et al. 2018	2017	Model BS[c]	1028	CAP	*C. Acetobutylicum ATCC 824*	Fed-Batch	0.12	1.45/2.34
Carmona-Garcia et al. 2019	2018	Coffee Cut Stems	1920	DAP	*C. Acetobutylicum*	Batch	0.08	1.10/1.61
Molina-Guerrero et al., 2021	2019	Wheat Straw	2200	Biological: Rumen microbial consortium	Co-culture of *C. cellulovorans and C. beijerinckii P260*	Batch	0.17	0.83/1.10
Mailaram and Maity, 2022	2021	Birchwood	750	DAP	Co-culture: *C. Acetobutylicum and C. beijerinckii*	Batch	0.15	1.44/1.58
This work	2022	Corn Stover	2400	Biological: native microbiota	BRMC	Batch	0.20	1.22
			1500					1.29
			500					1.49

CAP – concentrated acid pretreatment; DAP – dilute acid pretreatment; Model BSc - 42.5% (w/w) cellulose, 19.3% (w/w) hemicellulose, 25.3% (w/w) lignin, and 12.9% (w/w) other. BRMC – butanol-tolerant mixed culture. * - the NPV calculation of TPC for 2022 considered 10% of interest rate. MT – metric tonne.

The model suggests setting up biobutanol production plants at 13 out of 34 potential locations, meeting the maximum demand of all PEMEX costumers. The sensitivity analysis of the various parameters gave an insight into how these parameters might affect the results. The analysis on demands showed that the NPV and plant establishments are not dependent on the minimum

demand, but higher maximum demands lead to higher NPV values. The analysis of interest rates showed a correlation between higher interest rates and a decrease in both NPV values and the number of established bio-refinery plants. If the biobutanol selling price decreased, the NPV became negative, making the project economically infeasible. Only two plants would be established to fulfill the minimum customer demand in this scenario. As the selling price increases, the NPV also increases. However, the number, plant capacity, and production of established plants stay the same, as the maximum customer demand is already met based on the base case selling price. The economic viability of the project is highly sensitive to changes in both establishment and operating costs. When doubling the establishment costs, the NPV of the study case becomes negative, making the investment uneconomic. A 50% increase in operating costs will also lead to a negative NPV and make the project economically infeasible.

The role of budget was also investigated in forms of a goal in goal programming along the project's NPV and a constraint added to the main model. Larger budget as a constraint leads to the establishment of more plants and higher NPV values. However, once the maximum NPV of $US 3,350,387,969 is reached, further budget increases have no impact as the maximum demands are already met and the results are not limited by the budget constraint. Considering the budget as a goal helps to satisfy both NPV and budget goals to some extends. When $US 918,712,000 was considered as the budget goal, the total NPV was $US 705,730,233. While when it was considered under the budget constraint, the NPV was $US 513,267,980. Aditionally, the analysis on the budget goal indicated that an increase in the budget goal has a direct impact on both the total NPV and the number of established plants, but decreasing the budget goal does not affect the results.

8.6   Conclutions

Performed economy assessment of technology under proposed biorefinery scheme for biobutanol production from lignocellulosic biomass with biobutanol production at 22.3 g/L is economically feasible for all four studied biomasses: agave bagasse, corn stover, sugarcanebagasse and wheat straw, as well as for all three studied plant capacities: 500, 1500 and 2400 tonne/d. For the plant capacity of 500 tonne/d the biobutanol TPC has the following tendency agave bagasse < corn stover < sugarcane bagasse < wheat straw. The same tendency was observed for plant capacity of 1500

tonne/d, while for plant capacity of 2400 tonne/d, biobutanol production from sugarcane bagasse and corn stover resulted in the same TPC (1.50 $US/kg).

The mathematical model with objective function to meet the minimum biobutanol demand by 65 TAR of PEMEX (for blending with gasoline at 16% by volume) specified a minimum investment capital of $US 918,712,000 to allow establish two biorefinery plants processing corn stover at plant capacity of 2400 tonnes/d in Rancho Viejo de Refugio, Ocotlán and Guadalupe Victoria, Culiacán. According to the optimization model, it is possible to cover the total demand for biobutanol of 65 TAR of PEMEX. For that, its required initial investments of $US 5,636,663,000 to cover the establishment costs of biorefineries at 13 locations out of 34 considered. 10 biorefineries were suggested to be established with plant capacity of 2400 tonne/d, the other three plants with capacity of 1500 tonne/d. The model suggest to process sugarcane bagasse in 7 of them, and corn stover at 5 locations. Only one plant in Ciudad Obregón were suggested to be established with wheat straw as the input biomass.

The mathematical model only accounts for 65 TAR of PEMEX demand for biobutanol. Further research into biobutanol demand in the Mexican market could expand the model to include a proposal to build more lignocellulose-based biobutanol plants, which could make the country independent or significantly reduce biobutanol imports from abroad.

8.7   References

Andersen, V. F., Anderson, J. E., Wallington, T. J., Mueller, S. A., & Nielsen, O. J. (2010). Vapor Pressures of Alcohol−Gasoline Blends. Energy & Fuels, 24(6), 3647-3654. https://doi.org/10.1021/ef100254w

Anukam, A., Mamphweli, S., Reddy, P., Meyer, E., & Okoh, O. (2016). Pre-processing of sugarcane bagasse for gasification in a downdraft biomass gasifier system: A comprehensive review. Renewable and Sustainable Energy Reviews, 66, 775-801. https://doi.org/10.1016/j.rser.2016.08.046

Ashokkumar, V., Venkatkarthick, R., Jayashree, S., Chuetor, S., Dharmaraj, S., Kumar, G., Chen, W.-H., & Ngamcharussrivichai, C. (2022). Recent advances in lignocellulosic biomass for biofuels and value-added bioproducts—A critical review. Bioresource Technology, 344, 126195. https://doi.org/10.1016/j.biortech.2021.126195

Ayala-Campos, O. R., Sanchez, A., Rebollar, E. A., & Valdez-Vazquez, I. (2022). Plant-associated microbial communities converge in fermentative hydrogen production and form a core microbiome. International Journal of Hydrogen Energy, 47(46), 20049-20063. https://doi.org/10.1016/j.ijhydene.2022.04.155

Baral, N. R., & Shah, A. (2016). Techno-Economic Analysis of Cellulosic Butanol Production from Corn Stover through Acetone–Butanol–Ethanol Fermentation. Energy & Fuels, 30(7), 5779-5790. https://doi.org/10.1021/acs.energyfuels.6b00819

Carmona-Garcia, E., Ortiz-Sánchez, M., & Cardona Alzate, C. A. (2019). Analysis of the Coffee Cut Stems as Raw Material for the Production of Sugars for Acetone–Butanol–Ethanol (ABE) Fermentation: Techno-Economic Analysis. Waste and Biomass Valorization, 10(12), 3793-3808. https://doi.org/10.1007/s12649-019-00632-x

Chang, K.-T. (2017). Geographic Information System. En D. Richardson, N. Castree, M. F. Goodchild, A. Kobayashi, W. Liu, & R. A. Marston (Eds.), International Encyclopedia of Geography: People, the Earth, Environment and Technology (pp. 1-9). John Wiley & Sons, Ltd. https://doi.org/10.1002/9781118786352.wbieg0152

Charnes, A., and Cooper, W. W. (1957). Management models and industrial applications of linear programming. Management science, 4(1), 38-91.

Chávez, M. M. M., Sarache, W., & Costa, Y. (2018). Towards a comprehensive model of a biofuel supply chain optimization from coffee crop residues. Transportation Research Part E: Logistics and Transportation Review, 116, 136-162. https://doi.org/10.1016/j.tre.2018.06.001

Clauser, N. M., González, G., Mendieta, C. M., Kruyeniski, J., Area, M. C., & Vallejos, M. E. (2021). Biomass Waste as Sustainable Raw Material for Energy and Fuels. Sustainability, 13(2), 794. https://doi.org/10.3390/su13020794

Climate Change 2021: The Physical Science Basis. (2021). 2409.

Dalle Ave, G., & Adams, T. A. (2018). Techno-economic comparison of Acetone-Butanol-Ethanol fermentation using various extractants. Energy Conversion and Management, 156, 288-300. https://doi.org/10.1016/j.enconman.2017.11.020

Dudek, K., Buitrón, G., & Valdez-Vazquez, I. (2021). Nutrient influence on acidogenesis and native microbial community of Agave bagasse. Industrial Crops and Products, 170, 113751. https://doi.org/10.1016/j.indcrop.2021.113751

Dudek, K., Valdez-Vazquez, I., & Koop, J. (2022). Butanol recovery from synthetic fermentation broth by vacuum distillation in a rotating packed bed. Separation and Purification Technology, 297, 121551. https://doi.org/10.1016/j.seppur.2022.121551

Fattahi, M., & Govindan, K. (2018). A multi-stage stochastic program for the sustainable design of biofuel supply chain networks under biomass supply uncertainty and disruption risk: A real-life case study. Transportation Research Part E: Logistics and Transportation Review, 118, 534-567. https://doi.org/10.1016/j.tre.2018.08.008

Fattahi, M., Govindan, K., & Farhadkhani, M. (2021). Sustainable supply chain planning for biomass-based power generation with environmental risk and supply uncertainty considerations: A real-life case study. International Journal of Production Research, 59(10), 3084-3108. https://doi.org/10.1080/00207543.2020.1746427

Fernández, L. (2022). Market volume of n-Butanol worldwide from 2015 to 2021, with a forecast for 2022 to 2029. https://www.statista.com/statistics/1245211/n-butanol-market-volume-worldwide/

Findlay, H. S., & Turley, C. (2021). Chapter 13—Ocean acidification and climate change. En T. M. Letcher (Ed.), Climate Change (Third Edition) (Third Edition, pp. 251-279). Elsevier. https://doi.org/10.1016/B978-0-12-821575-3.00013-X

Galanopoulos, C., Giuliano, A., Barletta, D., & Zondervan, E. (2020). An integrated methodology for the economic and environmental assessment of a biorefinery supply chain. Chemical Engineering Research and Design, 160, 199-215. https://doi.org/10.1016/j.cherd.2020.05.016

Ganev, E., Ivanov, B., Vaklieva-Bancheva, N., Kirilova, E., & Dzhelil, Y. (2021). A Multi-Objective Approach toward Optimal Design of Sustainable Integrated Biodiesel/Diesel Supply Chain Based on First- and Second-Generation Feedstock with Solid Waste Use. Energies, 14(8), 2261. https://doi.org/10.3390/en14082261

Gao, C., Qu, D., & Yang, Y. (2019). Optimal Design of Bioenergy Supply Chains Considering Social Benefits: A Case Study in Northeast China. Processes, 7(7), 437. https://doi.org/10.3390/pr7070437

Garcia-Soto, C., Cheng, L., Caesar, L., Schmidtko, S., Jewett, E. B., Cheripka, A., Rigor, I., Caballero, A., Chiba, S., Báez, J. C., Zielinski, T., & Abraham, J. P. (2021). An Overview of Ocean Climate Change Indicators: Sea Surface Temperature, Ocean Heat Content, Ocean pH, Dissolved Oxygen Concentration, Arctic Sea Ice Extent, Thickness and Volume, Sea Level and Strength of the AMOC (Atlantic Meridional Overturning Circulation). Frontiers in Marine Science, 8, 642372. https://doi.org/10.3389/fmars.2021.642372

Gilani, H., & Sahebi, H. (2021). A multi-objective robust optimization model to design sustainable sugarcane-to-biofuel supply network: The case of study. Biomass Conversion and Biorefinery, 11(6), 2521-2542. https://doi.org/10.1007/s13399-020-00639-8

González-Arias, J., Baena-Moreno, F. M., Pastor-Pérez, L., Sebastia-Saez, D., Gallego Fernández, L. M., & Reina, T. R. (2022). Biogas upgrading to biomethane as a local source of renewable energy to power light marine transport: Profitability analysis for the county of Cornwall. Waste Management, 137, 81-88. https://doi.org/10.1016/j.wasman.2021.10.037

González-Tenorio, D., & Valdez-Vazquez, I. (2023). High butanol production through consolidated bioprocess after adaptive evolution to a fermentative microbial community. Energy Advances, 34.

Green, E. M. (2011). Fermentative production of butanol—The industrial perspective. Current Opinion in Biotechnology, 22(3), 337-343. https://doi.org/10.1016/j.copbio.2011.02.004

Heidari, R., Yazdanparast, R., & Jabbarzadeh, A. (2019). Sustainable design of a municipal solid waste management system considering waste separators: A real-world application. Sustainable Cities and Society, 47, 101457. https://doi.org/10.1016/j.scs.2019.101457

Hernández, C., Escamilla-Alvarado, C., Sánchez, A., Alarcón, E., Ziarelli, F., Musule, R., & Valdez-Vazquez, I. (2019). Wheat straw, corn stover, sugarcane, and Agave biomasses: Chemical properties, availability, and cellulosic-bioethanol production potential in Mexico. Biofuels, Bioproducts and Biorefining, 13(5), 1143-1159. https://doi.org/10.1002/bbb.2017

IEA. (2022). Global Energy Review: CO2 Emissions in 2021. https://www.iea.org/reports/global-energy-review-co2-emissions-in-2021-2

IGISMAP. (2021). Mexico Industrial Landuse Polygon. https://map.igismap.com/gis-data/mexico/industrial_landuse_polygon

Iliev, S. (2021). A Comparison of Ethanol, Methanol, and Butanol Blending with Gasoline and Its Effect on Engine Performance and Emissions Using Engine Simulation. Processes, 9(8), 1322. https://doi.org/10.3390/pr9081322

Instituto Mexicano del Transporte. (2021). Red Nacional de Caminos. http://rnc.imt.mx/recursos/ShapeFiles/Red_Nacional_de_Caminos_2021.zip

Jang, M.-O., & Choi, G. (2018). Techno-economic analysis of butanol production from lignocellulosic biomass by concentrated acid pretreatment and hydrolysis plus continuous fermentation. Biochemical Engineering Journal, 134, 30-43. https://doi.org/10.1016/j.bej.2018.03.002

Jayaraman, R., Colapinto, C., La Torre, D., and Malik, T. (2017). A Weighted Goal Programming model for planning sustainable development applied to Gulf Cooperation Council Countries. Applied Energy, 185, 1931-1939.

Jiang, L.-Q., Carter, B. R., Feely, R. A., Lauvset, S. K., & Olsen, A. (2019). Surface ocean pH and buffer capacity: Past, present and future. Scientific Reports, 9(1), 18624. https://doi.org/10.1038/s41598-019-55039-4

Jonker, J. G. G., Junginger, H. M., Verstegen, J. A., Lin, T., Rodríguez, L. F., Ting, K. C., Faaij, A. P. C., & van der Hilst, F. (2016). Supply chain optimization of sugarcane first generation and eucalyptus second generation ethanol production in Brazil. Applied Energy, 173, 494-510. https://doi.org/10.1016/j.apenergy.2016.04.069

Kang, S., Heo, S., Realff, M. J., & Lee, J. H. (2020). Three-stage design of high-resolution microalgae-based biofuel supply chain using geographic information system. Applied Energy, 265, 114773. https://doi.org/10.1016/j.apenergy.2020.114773

Kanzian, C., Kühmaier, M., Zazgornik, J., & Stampfer, K. (2013). Design of forest energy supply networks using multi-objective optimization. Biomass and Bioenergy, 58, 294-302. https://doi.org/10.1016/j.biombioe.2013.10.009

Kestur G., S., Flores-Sahagun, T. H. S., Dos Santos, L. P., Dos Santos, J., Mazzaro, I., & Mikowski, A. (2013). Characterization of blue agave bagasse fibers of Mexico. Composites Part A: Applied Science and Manufacturing, 45, 153-161. https://doi.org/10.1016/j.compositesa.2012.09.001

Kolesinska, B., Fraczyk, J., Binczarski, M., Modelska, M., Berlowska, J., Dziugan, P., Antolak, H., Kaminski, Z., Witonska, I., & Kregiel, D. (2019). Butanol Synthesis Routes for Biofuel Production: Trends and Perspectives. Materials, 12(3), 350. https://doi.org/10.3390/ma12030350

Lapuerta, M., Ramos, Á., Barba, J., & Fernández-Rodríguez, D. (2018). Cold- and warm-temperature emissions assessment of n-butanol blends in a Euro 6 vehicle. Applied Energy, 218, 173-183. https://doi.org/10.1016/j.apenergy.2018.02.178

Ley de Transición Energética. (2015). https://dof.gob.mx/nota_detalle.php?codigo=5421295&fecha=24/12/2015#gsc.tab=0

Mahalingam, L., Abdulla, R., Sani, S. A., Sabullah, M. K., Faik, A. A. M., & Misson, M. (2022). Lignocellulosic Biomass – A Sustainable Feedstock for Acetone-Butanol-Ethanol

Fermentation. Periodica Polytechnica Chemical Engineering, 66(2), 279-296. https://doi.org/10.3311/PPch.18574

Mailaram, S., & Maity, S. K. (2022). Dual liquid–liquid extraction versus distillation for the production of bio-butanol from corn, sugarcane, and lignocellulose biomass: A techno-economic analysis using pinch technology. Fuel, 312, 122932. https://doi.org/10.1016/j.fuel.2021.122932

Manabe, S. (2019). Role of greenhouse gas in climate change. Tellus A: Dynamic Meteorology and Oceanography, 71(1), 1620078. https://doi.org/10.1080/16000870.2019.1620078

Mani, S., Tabil, L. G., & Sokhansanj, S. (2004). Grinding performance and physical properties of wheat and barley straws, corn stover and switchgrass. Biomass and Bioenergy, 27(4), 339-352. https://doi.org/10.1016/j.biombioe.2004.03.007

Market Data Forecast. (2022, enero). Agave Market Size, Growth, Forecast (2022-2027). 10044. https://www.marketdataforecast.com/market-reports/agave-nectar-market

Meinshausen, M., Lewis, J., McGlade, C., Gütschow, J., Nicholls, Z., Burdon, R., Cozzi, L., & Hackmann, B. (2022). Realization of Paris Agreement pledges may limit warming just below 2 °C. Nature, 604(7905), 304-309. https://doi.org/10.1038/s41586-022-04553-z

Molina-Guerrero, C. E., Valdez-Vazquez, I., Sanchez, A., Vázquez-Castillo, J. A., & Vazquez-Nuñez, E. (2021). A biorefinery based on the biomechanical configuration of the digestive system of a ruminant for ABE production: A consolidated bioprocessing approach. Biomass Conversion and Biorefinery, 11(5), 2079-2088. https://doi.org/10.1007/s13399-020-00620-5

Mondal, S., Santra, S., Rakshit, S., Kumar Halder, S., Hossain, M., & Chandra Mondal, K. (2022). Saccharification of lignocellulosic biomass using an enzymatic cocktail of fungal origin and successive production of butanol by Clostridium acetobutylicum. Bioresource Technology, 343, 126093. https://doi.org/10.1016/j.biortech.2021.126093

Murele, O. C., Zulkafli, N. I., Kopanos, G., Hart, P., & Hanak, D. P. (2020). Integrating biomass into energy supply chain networks. Journal of Cleaner Production, 248, 119246. https://doi.org/10.1016/j.jclepro.2019.119246

Olguin-Maciel, E., Singh, A., Chable-Villacis, R., Tapia-Tussell, R., & Ruiz, H. A. (2020). Consolidated Bioprocessing, an Innovative Strategy towards Sustainability for Biofuels Production from Crop Residues: An Overview. Agronomy, 10(11), 1834. https://doi.org/10.3390/agronomy10111834

Oliveira, S. L., Mendes, R. F., Mendes, L. M., & Freire, T. P. (2016). Particleboard Panels Made from Sugarcane Bagasse: Characterization for Use in the Furniture Industry. Materials Research, 19(4), 914-922. https://doi.org/10.1590/1980-5373-MR-2015-0211

OpenStreetMap. (2022). Planet dump retrieved from https://planet.osm.org. https://www.openstreetmap.org

Osorno, J. A. A., González, G. C., García, S. H., & Hernández, G. A. (2022). Costos de operación base de los vehículos representativos del transporte interurbano 2022. Instituto Mexicano del Transporte, 699, 96.

Park, Y. S., Szmerekovsky, J., & Dybing, A. (2019). Optimal Location of Biogas Plants in Supply Chains under Carbon Effects: Insight from a Case Study on Animal Manure in North Dakota. Journal of Advanced Transportation, 2019, 1-13. https://doi.org/10.1155/2019/5978753

PEMEX. (2022). Logística: Almacenamiento. (Accessed 18 July 2022). (Spanish). https://www.pemex.com/nuestro-negocio/logistica/almacenamiento/Paginas/infraestructura.aspx

Razm, S., Dolgui, A., Hammami, R., Brahimi, N., Nickel, S., & Sahebi, H. (2021). A two-phase sequential approach to design bioenergy supply chains under uncertainty and social concerns. Computers & Chemical Engineering, 145, 107131. https://doi.org/10.1016/j.compchemeng.2020.107131

Rezaei, M., Amiri, H., & Shafiei, M. (2021). Aqueous pretreatment of triticale straw for integrated production of hemicellulosic methane and cellulosic butanol. Renewable Energy, 171, 971-980. https://doi.org/10.1016/j.renene.2021.02.159

Saad. (2012). PHYSICAL PROPERTIES OF WHEAT STRAW VARIETIES CULTIVATED UNDER DIFFERENT CLIMATIC AND SOIL CONDITIONS IN THREE CONTINENTS. American Journal of Engineering and Applied Sciences, 5(2), 98-106. https://doi.org/10.3844/ajeassp.2012.98.106

Sacchelli, S., Bernetti, I., De Meo, I., Fiori, L., Paletto, A., Zambelli, P., & Ciolli, M. (2014). Matching socio-economic and environmental efficiency of wood-residues energy chain: A partial equilibrium model for a case study in Alpine area. Journal of Cleaner Production, 66, 431-442. https://doi.org/10.1016/j.jclepro.2013.11.059

Saghaei, M., Dehghanimadvar, M., Soleimani, H., & Ahmadi, M. H. (2020). Optimization and analysis of a bioelectricity generation supply chain under routine and disruptive uncertainty and carbon mitigation policies. Energy Science & Engineering, 8(8), 2976-2999. https://doi.org/10.1002/ese3.716

Sanchez, A., Valdez-Vazquez, I., Soto, A., Sánchez, S., & Tavarez, D. (2017). Lignocellulosic n-butanol co-production in an advanced biorefinery using mixed cultures. Biomass and Bioenergy, 102, 1-12. https://doi.org/10.1016/j.biombioe.2017.03.023

Seo, J. Y., Tokmurzin, D., Lee, D., Lee, S. H., Seo, M. W., & Park, Y.-K. (2022). Production of biochar from crop residues and its application for biofuel production processes – An overview. Bioresource Technology, 361, 127740. https://doi.org/10.1016/j.biortech.2022.127740

SIAP. (2021). Datos abiertos: Estadística de Producción Agrícola from 2003 to 2021. (Accessed 10 July 2022). (Spanish). http://infosiap.siap.gob.mx/gobmx/datosAbiertos.php

Singh, B., Korstad, J., Guldhe, A., & Kothari, R. (2022). Editorial: Emerging Feedstocks & Clean Technologies for Lignocellulosic Biofuel. Frontiers in Energy Research, 10, 917081. https://doi.org/10.3389/fenrg.2022.917081

Singlitico, A., Goggins, J., & Monaghan, R. F. D. (2020). Life cycle assessment-based multiobjective optimisation of synthetic natural gas supply chain: A case study for the Republic of Ireland. Journal of Cleaner Production, 258, 120652. https://doi.org/10.1016/j.jclepro.2020.120652

Tipanluisa, L., Thakkar, K., Fonseca, N., & López, J.-M. (2022). Investigation of diesel/n-butanol blends as drop-in fuel for heavy-duty diesel engines: Combustion, performance, and emissions. Energy Conversion and Management, 255, 115334. https://doi.org/10.1016/j.enconman.2022.115334

Tri, C. L., & Kamei, I. (2020). Butanol production from cellulosic material by anaerobic co-culture of white-rot fungus Phlebia and bacterium Clostridium in consolidated bioprocessing. Bioresource Technology, 305, 123065. https://doi.org/10.1016/j.biortech.2020.123065

Valdez-Vazquez, I., Acevedo-Benítez, J. A., & Hernández-Santiago, C. (2010). Distribution and potential of bioenergy resources from agricultural activities in Mexico. Renewable and Sustainable Energy Reviews, 14(7), 2147-2153. https://doi.org/10.1016/j.rser.2010.03.034

Valdez-Vazquez, I., Pérez-Rangel, M., Tapia, A., Buitrón, G., Molina, C., Hernández, G., & Amaya-Delgado, L. (2015). Hydrogen and butanol production from native wheat straw by synthetic microbial consortia integrated by species of Enterococcus and Clostridium. Fuel, 159, 214-222. https://doi.org/10.1016/j.fuel.2015.06.052

Valdez-Vazquez, I., & Sanchez, A. (2018). Proposal for biorefineries based on mixed cultures for lignocellulosic biofuel production: A techno-economic analysis. Biofuels, Bioproducts and Biorefining, 12(1), 56-67. https://doi.org/10.1002/bbb.1828

Veza, I., Muhamad Said, M. F., & Latiff, Z. A. (2021). Recent advances in butanol production by acetone-butanol-ethanol (ABE) fermentation. Biomass and Bioenergy, 144, 105919. https://doi.org/10.1016/j.biombioe.2020.105919

Wen, Z., Minton, N. P., Zhang, Y., Li, Q., Liu, J., Jiang, Y., & Yang, S. (2017). Enhanced solvent production by metabolic engineering of a twin-clostridial consortium. Metabolic Engineering, 39, 38-48. https://doi.org/10.1016/j.ymben.2016.10.013

Wen, Z., Wu, M., Lin, Y., Yang, L., Lin, J., & Cen, P. (2014a). A novel strategy for sequential co-culture of Clostridium thermocellum and Clostridium beijerinckii to produce solvents from alkali extracted corn cobs. Process Biochemistry, 49(11), 1941-1949. https://doi.org/10.1016/j.procbio.2014.07.009

Wen, Z., Wu, M., Lin, Y., Yang, L., Lin, J., & Cen, P. (2014b). Artificial symbiosis for acetone-butanol-ethanol (ABE) fermentation from alkali extracted deshelled corn cobs by co-culture of Clostridium beijerinckii and Clostridium cellulovorans. Microbial Cell Factories, 13(1), 92. https://doi.org/10.1186/s12934-014-0092-5

Xue, C., & Cheng, C. (2019). Chapter Two—Butanol production by Clostridium. En Y. Li & X. Ge (Eds.), Advances in Bioenergy (Vol. 4, pp. 35-77). Elsevier. https://doi.org/10.1016/bs.aibe.2018.12.001

Zerotracker. (2022). Net Zero Numbers. (Accessed 5 October 2022) https://zerotracker.net/

Zhang, F., Wang, J., Liu, S., Zhang, S., & Sutherland, J. W. (2017). Integrating GIS with optimization method for a biofuel feedstock supply chain. Biomass and Bioenergy, 98, 194-205. https://doi.org/10.1016/j.biombioe.2017.01.004

Zhang, Y., Ghaly, A. E., & Li, B. (2012). Physical Properties of Corn Residues. American Journal of Biochemistry and Biotechnology.

Zhao, T., Tashiro, Y., & Sonomoto, K. (2019). Smart fermentation engineering for butanol production: Designed biomass and consolidated bioprocessing systems. Applied Microbiology and Biotechnology, 103(23-24), 9359-9371. https://doi.org/10.1007/s00253-019-10198-2

Conclusions and perspectives

Biological pretreatment studies have shown that the native microbiota of bagasse agave is a suitable source of microorganisms to carry out a consolidated bioprocess in which the hemicellulosic polymer is hydrolysed and VFAs production occurs simultaneously. Nutrient supplementation (CH_4N_2O, $CaCl_2$, KH_2PO_4) improves hemicellulose degradation and thus, enhancing VFA production and yield. Also, nutrients affect the microbial community over time.

The consolidated bioprocess experiments also confirmed that initial pH and TS% had an influence on hydrogen production and VFAs. The production of hydrogen and butyric acid via lactic/acetic acid consumption pathways was confirmed. Statistical analysis affirmed the significant effect of TS% on butyric ($\rho < 0.0001$) and lactic acid ($\rho < 0.0200$) production. The pH was a crucial factor affecting metabolic pathways of lactic acid formation ($\rho < 0.0003$). Lactic acid was produced at all studied initial pH range (5.5 – 6.9). The experiments with initial pH between 6.0 and 6.9 gave hydrogen production together with butyric acid, therefore lactic acid was not detected because of its consumption. At TS% increase, increases lactic acid formation, hence, butyric acid and hydrogen production, however, only in the initial pH range between 6.0 to 6.91. The highest butyric acid production at a level of 4.8 g/L was found for the initial pH of 6.2 and TS 22.1%. It is needed to analyze interactions between presented microorganisms and their correlation with produced bioproducts. This knowledge and relevant information on bacterial growth conditions can help control fermentation to synthesize hydrogen together with butyric acid.

The use of butanol-tolerant mixed culture resulted in high butanol production (up to 23 g/L) after 120 hours of consolidated bioprocessing of cellulosic fraction of pretreated corn stover. Moreover, employed butanol-mixed culture produced high concentrations of nonconventional subproducts – valeric and caproic acids, up to 11.0 and 7.1 g/L, respectively.

Vacuum distillation in the RPB is an adequate method for butanol recuperation from the synthetic fermentation broth at temperature near to fermentation temperature (37°C). The method with 5% steam stripping achieved butanol concentrations of up to 126.9 g/L in the top product, making the method attractive for commercial application. Moreover, distillation in RPB removes ethanol, furfural and carboxylic acids. Therefore, the obtained butanol-rich light phase of top product required further purification into pure components in a traditionl destilation column.

Techno-economic assessment of the proposed innovative biorefinery scheme for lignocellulosic biomass processing by mixed culture resulted economically viable. In contrary, a traditional plant using pure culture has resulted in a completely negative economic outcome. The key factors contributing to the plant's unprofitability were the use of a sugar concentration stage, which proved to be highly energy-demand, and the need to purchase expensive reactors due to the materials required for physical and chemical pretreatment, which uses acids and high temperatures and pressures.

Techno-economic evaluation of biobutanol production from lignocellulosic biomass under proposed innovative biorefinery scheme, where acidogenesis and ABE fermentation occurs as two CBPs, resulted economically viable for all simulated biomass (agave bagasse, corn stover, sugarcane bagasse and wheat straw) and all three plant capacities (500, 1500, 2400 tonne/d). The obtained economic data including investment costs, technology, utilities and operating costs, as well as external data such as biomass availability at suppliers in Mexico, butanol demand in the mexican market, road infrastructure, distance from populated areas, availability of water, electricity in geographical location, were used to develop mathematical model for optimal establishment of biobutanol biorefinery in Mexico.

The mathematical model with objective function to meet the minimum biobutanol demand by 65 TAR of PEMEX (for blending with gasoline at 16% by volume) specified a minimum investment capital of $US 918,712,000 to establish two biorefinery plants processing corn stover at plant capacity of 2400 tonnes/d in Rancho Viejo de Refugio, Ocotlán and Guadalupe Victoria, Culiacán. According to the optimization model, the initial investment of $US 5,636,663,000 allows establish biorefineries at 13 locations out of 34 considered, hence cover total biobutanol demand by 65 TAR of PEMEX. 10 biorefineries were suggested to be established with plant capacity of 2400 tonne/d, the other three plants with capacity of 1500 tonne/d. The model suggest to process sugarcane bagasse in 7 of them, and corn stover at 5 locations. Only one plant in Ciudad Obregón was suggested to be established with wheat straw as the input biomass.

Future perspectives of this study should include research on metabolic pathways of bacteria to find the reasons why the growth of some microorganisms is favoured by the addition of nutrients and not others. Also, from an economic point of view, the future simulations of the process, should replace expensive culture media containing salts (potassium phosphate) or nitrogen sources (yeast

extract) by cheaper agro-industrial residues. This could reduce operating costs and thus the unit cost of bioproduct production.

The fact that hydrogen production occurs from lactic acid results in the accumulation of butyric acid, which is beneficial since it can be supplemented for ABE fermentation to improve butanol production during solventogenesis, as reported in the literature. It should be investigated if obtained butanol-tolerant mixed culture also takes advantage of the presence of butyric acid. Moreover, the reactors should be conducted in semi-continous or continuous operation mode to assess the stability of the butanol-tolerant mixed culture for biobutanol and other bioproducts production over time.

Obtained butanol-rich light phase of top product during butanol recuperation from ferementation broth in RPB required further purification in a traditionl destilation column. Therefore, the impact of the components separated with the butanol on the subsequent butanol purification stage needs to be investigated to verify the feasibility of the entire downstream process. The method with 5% of steam stripping should be investigated using real supernatant to evaluate the method impact on microorganisms. Future investigations should be also focued on in-line butanol recovery from the fermentation process and the butanol production rate. Furthermore, the feasibility of recycling the bottom product to the fermenter, in order to reduce water consumption in the process, needs to be verified with special focus on accumulation of side products like acetic or propionic acid. Those are of special interest since they were not separated with the butanol and might influence the fermentation. Finally, since distillation is the stage with the highest energy consumption in the biorefinery scheme, an assessment of the energy efficiency of the method should be carried out to know its cost-effectiveness and be able to compare it with traditional distillation.

Appendix: Tables

Table A.1. Composition of fermentation broth obtained during CBP of cellulosic paper and corn stover by butanol-tolerant mixed culture at 120h. Values in the bracket represent concentrations at the end of the fermentation at 160h.

	Concentration (g/L)		
	cellulose paper	biologically pretreated corn stover	synthetic fermentation broth for experiments
Butanol	0.0 (18.5)	23.1 (15.3)	20
Ethanol	0.0 (0.0)	0.0 (0.0)	7
Acetic Acid	0.5 (1.6)	0.0 (0.0)	2.5
Propionic Acid	0.0 (2.0)	0.0 (0.0)	3
Valeric Acid	3.5 (0.2)	9.7 (11.0)	5.5
Caproic Acid	1.2 (0.0)	5.5 (7.1)	2
Furfural	1.3 (3.9)	0.0 (0.9)	3.5

Table A.2. Average biomass availability from 2003 to 2020 for agave bagasse, corn stover and wheat straw and from 2013 to 2021 for sugarcane bagasse with average yearly availability (AVG.) and standard deviation (SD) between each year.

State	Average biomass (tonne/year)	Standard deviation between years (%)
Corn stover		
Jalisco	1,004,662	0.18
Michoacan	320,884	0.18
Mexico	719,606	0.18
Sinaloa	4,030,341	0.21
Sugarcane bagasse		
Jalisco	843,898	0.11
Chiapas	419,210	0.09
Morelos	260,422	0.09
Puebla	257,046	0.10
Nayarit	323,135	0.08
Oaxaca	156,387	0.07
Veracruz	2,818,830	0.06
Quintana Roo	220,019	0.06
San Luis Potosi	743,145	0.09
Tamaulipas	251,418	0.10
Tabasco	197,060	0.10
Wheat straw		
Baja California	457,592	0.23
Guanajuato	199,420	0.54
Sonora	1,033,199	0.33
Agave Bagasse		
Jalisco	170,335	0.43

Table A.3. Possible locations of lignocellulosic-based biorefinery plants proposed by Hernández et al. (2019) modified with GIS.

	Hernández et al. (2019)		This work	
Corn Stover	Latitude	Longitude	Latitude	Longitude
Ahuisculco, Tala	20.5623	-103.7298	-103.7298	-103.7298
Rancho Viejo del Refugio, Ocotlán	20.4423	-102.643	-102.643	-102.643
Ixtlán de los Hervores, Ecuandureo	20.1825	-102.3472	-102.3472	-102.3472
El curiro, Tarímbaro	19.8488	-101.1898	-101.1898	-101.1898
Santa Ana La Ladera, Ixtlahuaca	19.6299	-99.8621	19.6299	-99.8621
El cerro de abajo, Angostura	25.2057	-108.0272	25.2817	-108.0727
Las Cabezas, Salvador Alvarado	25.5557	-108.1345	25.5557	-108.1345
Ahome	25.9231	-109.2078	25.9231	-109.2078
Guadalupe Victoria, Culiacán	24.3256	-107.2168	24.3256	-107.2168
Guasave	25.5079	-108.5402	25.5079	-108.5402
Navolato	24.7252	-107.7458	24.7252	-107.7458
Sugarcane bagasse				
Castro Urdiales, Teuchitlán	20.3176	-103.8309	20.5674	-103.8617
Atenquique, Tuxpan	19.5334	-103.4132	19.5334	-103.4132
Huixtla	15.1377	-92.4659	15.0977	-92.4999
Venustiano Carranza	16.3394	-92.5632	16.2752	-92.4562
Tepalcingo	18.6189	-98.8435	18.6189	-98.8435
Estación Refugio	18.5917	-96.6606	18.5917	-96.6606
Tepic	21.5532	-104.8486	21.5868	-104.8467
Othon P. Blanco	18.5002	-88.2961	18.2655	-88.6767
La Gloria, Ciudad Valles	22.0511	-99.2224	22.0176	-99.0682
La Coma, Antiguo Morelos	22.7119	-99.1372	22.6867	-98.9823
Cárdenas	18.0012	-93.3732	18.0012	-93.3732
Gral. Miguel Alemán, Atoyac	18.8447	-96.7927	18.905	-96.78
Úrsulo Galván, La Antigua	19.3917	-96.3673	19.3917	-96.3673
Texas, Cosamaloapan de Carpio	18.1713	-96.1391	18.1708	-96.0891
Tesechoacan, Amatitlán	18.4545	-95.6824	18.4509	-95.7372
El Molino, Pánuco	21.9001	-98.325	21.9001	-98.325
Atencingo	18.5206	-98.5782	-	-
San Miguel del Naranjo	22.5313	-99.3372	-	-
Wheat Straw				
Nuevo León, Mexicali	32.4094	-115.1948	32.4094	-115.1948
Abasolo	20.4711	-101.5004	20.4365	-101.7031
Ciudad Obregón	27.4911	-110.0206	27.5218	-110.0078
Las Playitas, Etchojoa	26.9913	-109.6154	26.9192	-109.6491
Agave Bagasse				
Atotonilco el Alto	20.6102	-102.4407	20.6102	-102.4407
Ahualulco de Mercado	20.7918	-103.8149	20.8789	-103.8166

Proposed new locations are highlighted in orange. The absence of color symbolizes locations according to Hernández et al. (2019).
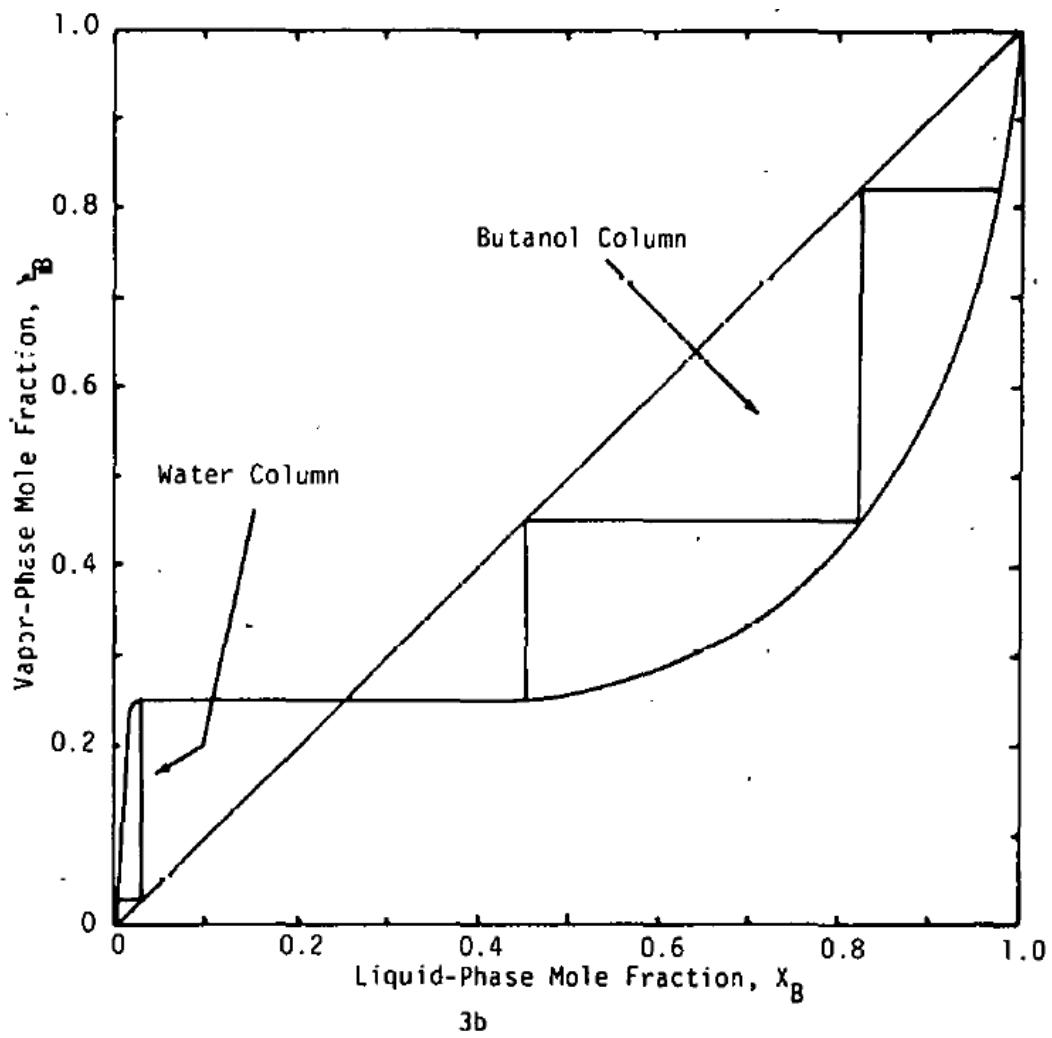
Appendix: Figures

Figure A.A.1. **VLLE of water-butanol binary system** (image from Card and Farrell, 1982), x_B represents the butanol mole fraction.

Dissertation achievements

Published articles:

Dudek, K., Buitrón, G., & Valdez-Vazquez, I. (2021). Nutrient influence on acidogenesis and native microbial community of Agave bagasse. *Industrial Crops and Products*, *170*, 113751. https://doi.org/10.1016/j.indcrop.2021.113751

Dudek, K., Molina-Guerrero, C. E., & Valdez-Vazquez, I. (2022). Profitability of single- and mixed-culture fermentations for the butyric acid production from a lignocellulosic substrate. *Chemical Engineering Research and Design*, 182, 558-570. https://doi.org/10.1016/j.cherd.2022.04.018

Dudek, K., Valdez-Vazquez, I., & Koop, J. (2022). Butanol recovery from synthetic fermentation broth by vacuum distillation in a rotating packed bed. *Separation and Purification Technology*, *297*, 121551. https://doi.org/10.1016/j.seppur.2022.121551

Submitted:

Dudek, K., Alvarez-Guzmán, C.L., Valdez-Vazquez, I. (2023). Influence of initial pH and total solids on hydrogen production via the lactate/acetate pathway through consolidated bioprocessing of agave bagasse.

Dudek, K., Rahmani, K., Aghamohamadi, S., Valdez-Vazquez, I., Sowlati, T. (2023). Optimalization model for strategic location of lignocellulosic biorefinery for biobutanol production in Mexico.

Dudek, K., Valdez-Vazquez, I. (2023). High-efficiency production of biobutanol from lignocellulosic biomass using a butanol-tolerant tolerant mixed culture.

Conference participation:

1. Dudek K., Valdez-Vazquez I. Effect of pH and total solids on the composition of volatile fatty acids produced from untreated Agave bagasse by mixed culture. Simposio Ambiente y Bioenergía 2022, 30 november and 1-2 december, 2022.

2. Dudek K., Rahmani K., Aghamohamadi S., Valdez-Vazquez I., Sowlati T. Optimalization model for strategic location of the lignocellulosic biorefinery plants for biobutanol production in Mexico. Simposio Ambiente y Bioenergía 2022, 30 november and 1-2 december, 2022.

3. Dudek, K., Valdez-Vazquez, I. Effect of pH and total solids on the composition of volatile fatty acids produced from untreated Agave bagasse by a microbial community. XXII International Congress of Mexican Hydrogen Society. 28-30 september, 2022.

4. Dudek, K., Valdez-Vazquez, I., Koop, J. Butanol recovery from a synthetic fermentation broth by vacuum distillation in rotating packed bed for improving the water reuse. 6th Conference IWA-Mexico Young Water Professionals 2022. 25-27 may, 2022.

5. Dudek, K., González-Tenorio, D., Amaya Delgado, L., Valdez-Vazquez, I. Biobutanol production from lignocellulosic waste by hyper butanol tolerant mixed culture. 63rd General Meeting of the Polish Chemical Society. 13-16 september, 2021.

6. Dudek, K., Molina, C., Valdez-Vazquez, I. Butyric acid production from agricultural residues: determination of profitable strategy. XXXVII Virtual Inter-American Congress on Sanitary and Environmental Engineering. 12-15 april, 2021.

7. Dudek, K., Buitrón, G., Valdez-Vazquez, I. Start-up of agave bagasse fermentation process using its native microbiota for volatile fatty acids production. Latin American Meetings on Anaerobic Digestion (Four Sessions). 22 and 29 october, 5 and 12 november, 2020.

8. Dudek, K., Buitrón, G., Valdez-Vazquez, I. Start-up of agave bagasse fermentation process using its native microbiota for volatile fatty acids production. Simposio Ambiente y Bioenergía 2020. 17 - 18 september, 2020.